

UNCLASSIFIED

AD 295 159

*Reproduced
by the*

ARMED SERVICES TECHNICAL INFORMATION AGENCY
ARLINGTON HALL STATION
ARLINGTON 12, VIRGINIA



UNCLASSIFIED

NOTICE: When government or other drawings, specifications or other data are used for any purpose other than in connection with a definitely related government procurement operation, the U. S. Government thereby incurs no responsibility, nor any obligation whatsoever; and the fact that the Government may have formulated, furnished, or in any way supplied the said drawings, specifications, or other data is not to be regarded by implication or otherwise as in any manner licensing the holder or any other person or corporation, or conveying any rights or permission to manufacture, use or sell any patented invention that may in any way be related thereto.

63-2-3

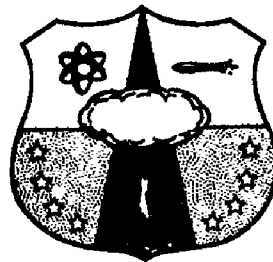
AFSWC-TDR-62-83

SWC
TDR
62-83

FLIGHT TEST CRITERIA FOR
RE-ENTERING NAP SYSTEM

TECHNICAL DOCUMENTARY REPORT NUMBER AFSWC-TDR-62-83

November 1962



Development Directorate
AIR FORCE SPECIAL WEAPONS CENTER
Air Force Systems Command
Kirtland Air Force Base
New Mexico

Project No. 1831, Task No. 183103

(Prepared under Contract No. AF 29(601)-
5104 by Advanced Systems, North American
Aviation, Inc., Space and Information Sys-
tems Division, Downey, California.)

295 159
CATALOGED BY ASIIA
AS AD No. 295159

**HEADQUARTERS
AIR FORCE SPECIAL WEAPONS CENTER
Air Force Systems Command
Kirtland Air Force Base
New Mexico**

When Government drawings, specifications, or other data are used for any purpose other than in connection with a definitely related Government procurement operation, the United States Government thereby incurs no responsibility nor any obligation whatsoever; and the fact that the Government may have formulated, furnished, or in any way supplied the said drawings, specifications, or other data, is not to be regarded by implication or otherwise as in any manner licensing the holder or any other person or corporation, or conveying any rights or permission to manufacture, use, or sell any patented invention that may in any way be related thereto.

This report is made available for study upon the understanding that the Government's proprietary interests in and relating thereto shall not be impaired. In case of apparent conflict between the Government's proprietary interests and those of others, notify the Staff Judge Advocate, Air Force Systems Command, Andrews AF Base, Washington 25, DC.

This report is published for the exchange and stimulation of ideas; it does not necessarily express the intent or policy of any higher headquarters.

Qualified requesters may obtain copies of this report from ASTIA. Orders will be expedited if placed through the librarian or other staff member designated to request and receive documents from ASTIA.

FOREWORD

This is an Interim Report for Phase A of the Flight Test Criteria Study for Re-entering Nuclear Auxiliary Power Systems, Contract AF 29(601)-5104.

This study is one of several in an overall program being conducted by the Air Force Special Weapons Center as a part of Program Task 183103, Nuclear Auxiliary Power System Re-entry and Disposal Phenomena.

A B S T R A C T

This interim report covers Phase A of the Flight Test Criteria Study which will determine criteria that can be used as guidelines in setting up a flight test program or in judging one that has been proposed. This study is intended to be universal in application to NAP re-entry phenomena. The SNAP 10A was designated to provide a representative system for study. The various parameters considered and topics discussed in this report include orbital decay and thermodynamic data, scaling, instrumentation, launch vehicles and sites, and reliability. Significant among the interim conclusions reached is the determination that a 300,000-foot re-entry altitude can be used.

PUBLICATION REVIEW

This report has been reviewed and is approved.



M. E. SORTE
Colonel USAF
Director, Development Directorate



JOHN J. DISHUCK
Colonel USAF
DCS/Plans & Operations

CONTENTS

	Page
INTRODUCTION	1
OBJECTIVE OF FLIGHT TEST CRITERIA STUDY	3
Flight Test Criteria	3
Design of the Experiments	4
Assurance of Safety	9
REPRESENTATIVE SYSTEM FOR STUDY	12
Spacecraft	12
Snap 10A System	12
ORBITAL DECAY	16
Significant Parameters	16
Decay Trajectory and Heat Pulse	17
THERMODYNAMIC DATA	37
Requirements	37
Predicted Failure of Components	38
Heat Required to Ablate Fuel Rod and Cladding	41
Required Heat Flux to Supply Heat Necessary for Fuel Element Ablation	42
Heat Transfer Within the Fuel Element	44
Conclusions	46
Thermodynamic Test Criteria	46
SCALING	49
Approximate Scaling Effects	49
Scaling Investigation Using the IBM 7090 Computer	56
Possible Limits to Simulate Actual Re-Entry Environment	78
INSTRUMENTATION	80
Instrumentation Data Required	80
Reference Data Required	81
Telemetry System Nap Re-Entry Flight Tests	83
RF Blackout	83
System Description	85
Available Instrumentation Methods	89
Possible Systems	93
GOSS Requirements	99

	Page
LAUNCH VEHICLES	102
Possible Booster Systems	102
Guidance and Control Requirements	104
Payload Requirements	104
Cost Analysis	110
Typical Trajectory for Blue Scout and Thor/Able-Star	
Booster Systems	110
Proposed Launch Vehicle	116
LAUNCH SITES	117
Available Range Sites	117
Range Requirements for Tests	127
Possible Range Utilization	131
RELIABILITY OF TEST RESULTS	134
Overall Reliability	134
Confidence of Design Analysis	134
Trajectory Parameters	138
Reliability of Test Results	139
Confidence of Test Simulation	139
SUMMARY	140
Interim Conclusions	140
Flight-Test Considerations	141
REFERENCES	142
BIBLIOGRAPHY	143
APPENDIX A - SYMBOLS	A-1

ILLUSTRATIONS

Figure		Page
1	Logic Diagram	6
2	Cumulative Probability and Individual Events	7
3	Orbiting Spacecraft Study Model	13
4	SNAP 10A Study Model Design	14
5	SNAP 10A Reactor Vessel and Fuel Element Data	15
6	Orbital Decay Trajectory of Tumbling Spacecraft, Flight-Path Angle Zero Degrees	18
7	Orbital Decay Trajectory of Tumbling Spacecraft, Flight-Path Angle Minus 0.05 Degree	19
8	Orbital Decay Trajectory of Tumbling Spacecraft, Flight-Path Angle Minus 0.1 Degree	20
9	Orbital Decay Trajectory of Axial or Tumbling Reactor Vessel, Flight-Path Angle Zero Degrees	21
10	Orbital Decay Trajectory of Tumbling Fuel Element Ejected From Reactor Vessel at 400,000 Feet	22
11	Orbital Decay Trajectory of Tumbling Fuel Element Ejected From Reactor Vessel at 300,000 Feet	23
12	Orbital Decay Trajectory of Tumbling Fuel Element Ejected From Reactor Vessel at 250,000 Feet	24
13	Orbital Decay Trajectory of Tumbling Fuel Element Ejected From Reactor Vessel at 200,000 Feet	25
14	Heat-Transfer Rate Versus Time for Spacecraft Tumbling in Trajectory, Flight-Path Angle Zero Degrees	26
15	Heat-Transfer Rate Versus Time for Spacecraft Tumbling in Trajectory, Flight-Path Angle Minus 0.1 Degree	27
16	Heat-Transfer Rate Versus Time for Reactor Vessel Tumbling in Trajectory, Flight-Path Angle Zero Degrees	28
17	Heat-Transfer Rate Versus Time for Fuel Element Tumbling in Trajectory, Flight-Path Angle Zero Degrees.	29
18	Heat-Transfer Rate Versus Time for Fuel Element After Ejection From Reactor Vessel	30
19	Total Heat Input to Fuel Element During Re-Entry at Stagnation Point	31
20	Variation of Fuel Element Re-Entry Range With Entry Velocity and Flight-Path Angle Variations	32

Figure		Page
21	Heat-Transfer Rate Versus Time for Exposed Reactor Vessel Attached to Spacecraft in Axial Entry	34
22	Altitude Deficiency for Fuel-Element Burnup	39
23	Fuel Element Aerodynamic Heating at Stagnation Point Versus Time	40
24	Heat Input Required for Fuel-Element Heating and Ablation Versus Diameter	45
25	Fuel Element Stagnation-Point Temperature Versus Time	47
26	Re-Entry Trajectory of Tumbling Fuel Element, Flight-Path Angle Zero Degrees, V_E/V_C Equals 0.8	57
27	Re-Entry Trajectory of Tumbling Fuel Element, Flight-Path Angle Minus 5 Degrees, V_E/V_C Equals 0.8	58
28	Re-Entry Trajectory of Tumbling Fuel Element, Flight-Path Angle Minus 10 Degrees, V_E/V_C Equals 0.8	59
29	Re-Entry Trajectory of Tumbling Fuel Element, Flight-Path Angle Minus 15 Degrees, V_E/V_C Equals 0.8	60
30	Re-Entry Trajectory of Tumbling Fuel Element, Flight-Path Angle Minus 5 Degrees, V_E/V_C Equals 1	61
31	Re-Entry Trajectory of Tumbling Fuel Element, Flight-Path Angle Minus 10 Degrees, V_E/V_C Equals 1	62
32	Re-Entry Trajectory of Tumbling Fuel Element, Flight-Path Angle Minus 15 Degrees, V_E/V_C Equals 1	63
33	Re-Entry Trajectory of Tumbling Fuel Element, Flight-Path Angle Minus 5 Degrees, V_E/V_C Equals 1.2	64
34	Re-Entry Trajectory of Tumbling Fuel Element, Flight-Path Angle Minus 10 Degrees, V_E/V_C Equals 1.2	65
35	Re-Entry Trajectory of Tumbling Fuel Element, Flight-Path Angle Minus 15 Degrees, V_E/V_C Equals 1.2	66
36	Heat-Transfer Rate Versus Time for Tumbling Fuel Element in Trajectory, Flight-Path Angle Zero Degrees, V_E/V_C Equals 0.8	67
37	Heat Transfer Rate Versus Time for Tumbling Fuel Element in Trajectory, Flight-Path Angle Minus 5 Degrees, V_E/V_C Equals 0.8	68
38	Heat-Transfer Rate Versus Time for Tumbling Fuel Element in Trajectory, Flight-Path Angle Minus 10 Degrees, V_E/V_C Equals 0.8	69
39	Heat-Transfer Rate Versus Time for Tumbling Fuel Element in Trajectory, Flight-Path Angle Minus 15 Degrees, V_E/V_C Equals 0.8	70
40	Heat-Transfer Rate Versus Time for Tumbling Fuel Element in Trajectory, Flight-Path Angle Minus 5 Degrees, V_E/V_C Equals 0.999.	71

41	Heat-Transfer Rate Versus Time for Tumbling Fuel Element in Trajectory, Flight-Path Angle Minus 10 Degrees, V_E/V_C Equals 0.999.	72
42	Heat-Transfer Rate Versus Time for Tumbling Fuel Element in Trajectory, Flight-Path Angle Minus 15 Degrees, V_E/V_C Equals 0.999.	73
43	Heat-Transfer Rate Versus Time for Tumbling Fuel Element in Trajectory, Flight-Path Angle Minus 5 Degrees, V_E/V_C Equals 1.2	74
44	Heat-Transfer Rate Versus Time for Tumbling Fuel Element in Trajectory, Flight-Path Angle Minus 10 Degrees, V_E/V_C Equals 1.2	75
45	Heat-Transfer Rate Versus Time for Tumbling Fuel Element in Trajectory, Flight-Path Angle Minus 15 Degrees, V_E/V_C Equals 1.2	76
46	Maximum Duration of VHF Radio Frequency Blackout, Time as a Function of Re-Entry Angle.	84
47	Typical Telemetry System for NAP Re-Entry Flight Tests	86
48	Residue Particle Range and Density	98
49	Instrumentation-System Test Range-Support Requirements	101
50	Comparison of Booster Payload Capability	103
51	Variation of Altitude and Range With Re-Entry Velocity and Flight-Path Angle	105
52	Representative Re-Entry Test Telemetry and Radar- Beacon Module	106
53	Representative Re-Entry Test Launch Vehicles and Payloads	107
54	Typical Blue Scout Boost Trajectory	113
55	Typical Thor/Able-Star Boost Trajectory	114
56	Altitude-Range Profile for Typical Flight Tests.	115
57	Atlantic Missile Range	118
58	Atlantic Missile Range Stations, Cape Canaveral to Antigua Vicinity.	119
59	Pacific Missile Range	122
60	Range Utilization With Wallops Island Launch	125
61	Weapons Research Establishment, Australia	126
62	Horizontal Distance Traveled From 300,000-Foot Re-Entry	129
63	Required Instrumentation Coverage During Re-Entry	130
64	Possible Range Profiles	132
65	Fuel Element Temperature Distribution With Front Surface at Ablation Temperature	137

TABLES

Table		Page
1	Re-Entry Ballistic Coefficients	17
2	Variations in Radiant Heat Loss	43
3	Characteristic Data Sources for NAP Re-Entry Flight Tests	88
4	Event Instrumentation	91
5	Fuel-Element Burnup Experiments	92
6	Optical and Infrared Instrumentation Requirement for Free-Flight Burnup Experiment	94
7	Launch Vehicle Cost Estimate Breakdown	110
8	Blue Scout Weight and Motor Data	111
9	Thor/Able-Star Weight and Motor Data	111
10	Atlantic Missile Range Down-Range Instrumentation	120
11	Pacific Missile Range Down-Range Instrumentation	123
12	Range Capabilities	128
13	Material Properties of Fuel Elements	135

INTRODUCTION

The Nuclear Auxiliary Power (NAP) System Disposal Safety Program has a clear objective - that of assuring freedom from hazard in the employment of nuclear-fueled units on Air Force space missions. A complete hazards analysis for the spectrum of Air Force missions must involve all phases of such missions - from pre-launch through launch, mission execution, and final phase. The present series of studies is concerned only with the final phase.

There are various ways of attaining safe disposal of a reactor at the end of its mission. Some of these are listed in order to give perspective to the requirements for the present re-entry study and the initial conditions to be assumed. The simplest disposal is, of course, for the reactor to stay in orbit after shut-down until the fission products have decayed to a non-hazardous level. This situation, which will be achieved for orbits with a mean altitude above about 500 miles, has been analyzed elsewhere.

Among other disposal concepts that have been proposed are those to destroy the reactor while it is still in orbit by breaking it into pieces which will be burned up in the atmosphere when they re-enter. One concept is that, if control still exists at the end of the mission, the reactor be deliberately sent on an excursion which will destroy it, in part at least. Such an excursion would have the favorable feature of greatest effect on the fuel elements and would tend to remove the volatile fission fragments. However, it presumes an end of mission while the reactor is still operative - an unlikely situation.

Another concept is to blow up the reactor by on-board explosives. This action could be taken either on command from the ground, or automatically by sensing loss of heat or of electric power from the nuclear power system. A problem, of course, is the survival of the destructive agent in the radiation flux until it is needed. Potentially, ways might be found around this problem - use of exploding wires, thermite-type devices, gases which can be mixed and detonated, or shaped-charge explosives placed at some distance from the reactor are among the possibilities.

A possibility of a different type is that the reactor and its spacecraft be used as a practice target for an anti-satellite or anti-ICBM missile whose nuclear warhead could completely vaporize the reactor.

Some of these concepts may prove feasible and may be used for low-altitude flights providing the present study and the actual tests show the reactor will not safely be destroyed automatically by atmospheric re-entry. Even if they are feasible, they do not eliminate the need for the re-entry study except in the case of the nuclear warhead, because essentially they result only in breaking the reactor into smaller pieces which must then re-enter.

Therefore, the case which prompts the present study is that in which the reactor is employed in relatively low-altitude orbits. It further will be assumed that the reactor has run for as long as a year and that it may re-enter at any time after that. Under such conditions, the criterion has been set that the fuel elements should be dispersed into particle sizes of the order of a micron by the time they reach 100,000 feet altitude.

The purpose of the re-entry study program is to see if the reactor will be safely destroyed solely from exposure to the heat occurring during a normal orbital decay and atmosphere re-entry. Therefore, one of the ground rules assumed is that there exists no control of the reactor or spacecraft from the ground.

The present study program is to derive results which, as well as possible, can be applied to evaluate the re-entry burnup of any nuclear auxiliary power unit. However, prime emphasis is given to reactor-type units, and, specifically, the SNAP 10A design as it now exists is used as the example, and it is assumed to be attached to the spacecraft configuration which includes the Agena B vehicle.

OBJECTIVE OF FLIGHT-TEST CRITERIA STUDY

The present study is to find criteria that can be used as guidelines in setting up a flight test program or to judge one that has been proposed. This interim report covers Phase A of the study. In Phase B the main objective will be to evaluate the implications of associated studies in the present program as to further definition of experiments which should be carried out in a flight-test program, or in preceding ground tests.

A program in which the end result must be to establish freedom from hazard, flight tests will be performed to prove, i. e., to validate, conclusions already made from analyses or ground tests. It is not a program of research to probe under what conditions burnup will occur and the nature of the phenomena involved. That could be a far more extensive program than one to give assurance of freedom from hazard. Flight tests may be used, however, under certain circumstances, to establish specific facts regarding re-entry which, if they were known, could be analyzed to give a definite answer regarding safety.

FLIGHT TEST CRITERIA

Flight test is expensive. It should be the final phase of an overall test program. It should not be carried out without careful analysis beforehand of the technical points to be verified, and careful planning of the experiments to verify them. Emphasis must be placed both on the reliability of receiving the data and on getting data which, as a minimum, will answer yes or no to the conclusions from analysis.

The desirable situation would be that in which analysis indicates the reactor will be safely destroyed during re-entry and the flight test verifies the conclusion. However, for an already established piece of hardware, analysis may indicate that burnup will probably not occur; in this case the flight test should still be designed to confirm immediately the conclusions, but with the added requirement that if a modification has been suggested by analysis or laboratory tests which offer hope of removing the reason for non-burnup, the flight test be designed to probe such modification of design or conditions.

Alternatives to proof of safe disposal which can be weighed against the delay and cost of modification, including possible compromise of the reactor and an additional testing program, are either to "red-line" the reactor for

use in orbits below 500 miles or to accept the possible hazard if the military situation warrants.

DESIGN OF THE EXPERIMENTS

Flight test experiments cannot exactly reproduce true re-entry conditions. First, it would not be permissible to test a reactor which has been run, although prior operation might affect the freedom with which the fuel elements emerge from the reactor vessel or alter the fuel burnup characteristics. However, it should be permissible to use fuel elements actually containing uranium-enriched zirconium hydride. Second, the practical limits for flight-test re-entry angle and range length will not allow reproduction of actual orbital decay since the re-entry must take place over a specified limited region where proper instrumentation can be provided. Third, the test capsule must be of a size compatible with a reasonably economical launch vehicle.

As a result of the last two requirements above, scaling becomes an important part of the design of a flight-test program. The scaling applies not only to a change of physical dimensions of the test specimens, but to a change of the conditions of re-entry environment. It is necessary to analyze how the parameters of importance for burnup during true orbital decay vary as the conditions are modified and what parameters must be reproduced, and how.

Other factors to be resolved in the design of the flight-test experiments are (1) what is the best sequence of experiments in the flights, (2) how many flights are required, and (3) how is assurance of reactor burnup obtained?

To accomplish the re-entry burnup of NAP units, a sequence of interdependent events must take place. The tests must establish if these do take place. However, the sequence of tests need not follow the sequence of events. The actual grouping of tests will depend on the payload capacity of the launch vehicle and, hence, of what may best be grouped in one test capsule configuration. For instance, the reactor re-entry orientation, plumbing burn-off, reflector retaining-band separation, reactor-can lid-lip burnoff, and emergence of fuel elements may well be grouped in one scaled design.

There are several guidelines in the grouping of tests. The reasoning behind them depends on the technical requirements imposed by different tests, the cost of tests, the predicted probability of a favorable result, and, particularly, on the objective of the tests. As explained above, a safety assurance flight-test program pertinent to a restricted class of missions seems to have a more reasonable basis as a proof of something which, from analysis, design, and ground testing, is believed already to exist, rather

than as an analytic research tool. Therefore, looking at the *a priori* expected cost of the total flight program (which depends on the estimated probability of a favorable answer for any given step or set of steps times the cost for making that test), if the prediction is favorable through all the steps, and if there is no great jump in cost of testing with some particular step, the final favorable answer should be sought at once.

Unfortunately, the situation just described will often be modified. The extent of modification need not be evaluated precisely to permit development of a favorable plan for the tests. One of the first modifications is that usually more than one test will be required to cover all the details on which favorable answers are desired, even though an overall favorable result appears probable. Second, the probability of successful execution of a certain step in the sequence may be estimated as poor, rather than good. Under such a condition, the flight test would not ordinarily be undertaken unless the prediction is disputed or the flight test is needed as an analytic tool to resolve a question on which theory and calculations are uncertain. Third, the cost of testing can take an abrupt jump at a certain step. Fourth, provision for repetition of tests must be included in planning - both to take care of flight failures and to give statistical verification to results in critical areas.

In order to be more specific as to the effect on test plans, consider a system such as the SNAP 10A, and suppose the following situation exists. A sequence of events must occur for satisfactory burnup. Designate them as:

p = proper orientation of reactor in re-entry

q = accessory burnoff (pump, plumbing, reflector retaining band, etc)

r = reactor-lid lip burnoff

s = fuel-element emergence

t = fuel-element disintegration or ablation

u = fuel element burnup to one micron size at 100,000-feet altitude

The final desired answer is u. Preliminary analysis indicates that each step implies, in the sense of mathematical logic, the preceding one; that is,

$$u \rightarrow t \rightarrow s \rightarrow r \rightarrow q \rightarrow p$$

If u occurs, then t must have occurred, etc. Or, in other words, the cases where t happens contains the set of cases where u happens (but note that t can

happen and u fail to happen), i. e. $t \supset u$ where \supset symbolizes "contains", as in the logic diagram Figure 1.

That is, $p \supset q \supset r \supset s \supset t \supset u$.

The cumulative probability P of a favorable answer through any one of these steps may be written as:

P_p , the *a priori* estimate of the probability of p

$$P_q = P_p \times P_{q/p}$$

where $P_{q/p}$ is a conditional probability, the probability of q , given that p occurred.

$$P_r = P_p \times P_{q/p} \times P_{r/q}, \text{ etc.}$$

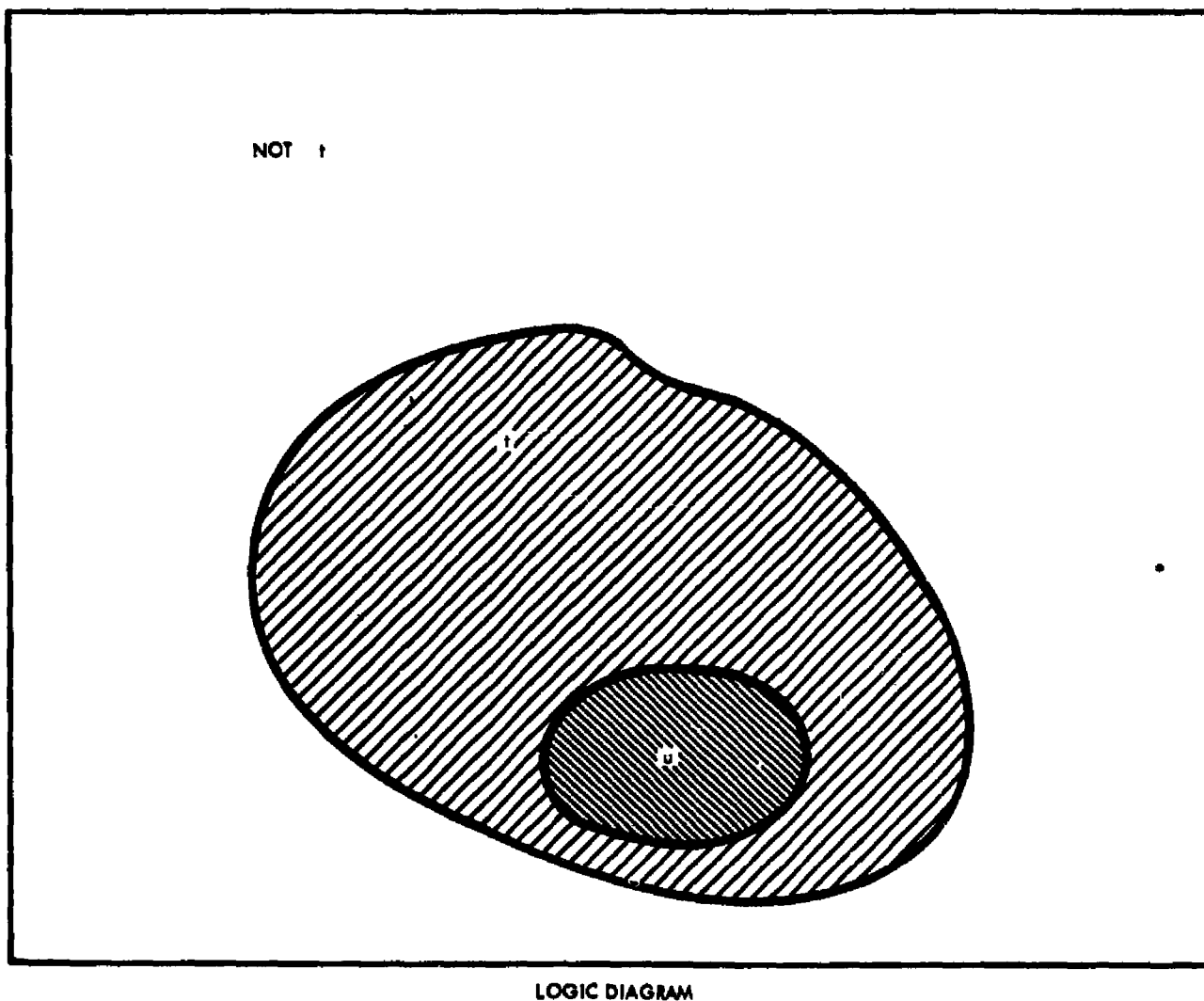


Figure 1. Logic Diagram

Suppose the successive probabilities are plotted as in Figure 2, where the ordinate P is the cumulative a priori estimated probability of a favorable result. On the same chart a rough estimate of cost for testing each event (non-cumulative) might also be plotted.

If a grouping of tests is unavoidable because of payload limitations and different natures of the tests, then, even in the case of a favorable prediction, it is best to see that the cheap tests come out well before carrying out any expensive test (assuming that a subsequent event is not tested if an unfavorable result occurs on a preceding event).

If the probability prediction is unfavorable at any point, as assumed at s above, the first grouping should try to include testing for that event. There is more than one reason for this decision. First, if diagnosis of a problem is expected to be necessary for a design modification, it is best to obtain this

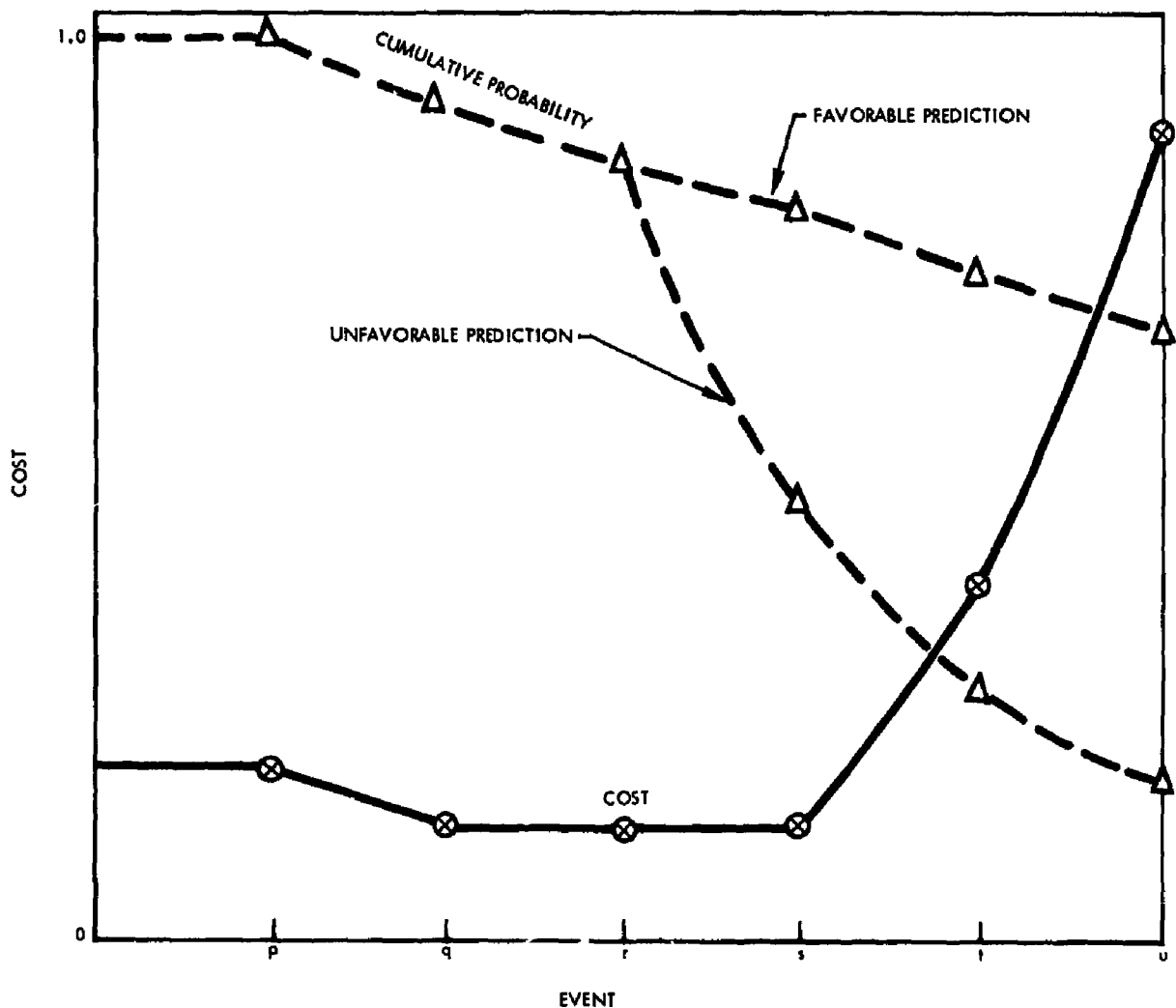


Figure 2. Cumulative Probability and Individual Costs

information at once. Later tests can be used for variation of parameters, for statistical verification of conclusions, or for test of modified design. Second, the a priori expected cost of this flight-test plan is less than for a different plan. If the questionable event is not investigated, the expected cost is that for the preceding events (first flight), plus the probability (high) of favorable result from first flight, which permitted going to the second flight, times the cost (second flight) of testing the questionable event, plus probabilities (low) of proceeding to later events, times cost of later flights. If the first test is stretched to include the questionable event, the expected cost is that of the first flight plus a low expectation of having to proceed, unless a modification of test articles or plans is made.

It is to be noted, of course, that the remarks above pertain to the original planning of the complete program of several flights. After each flight, the program must be revised, if time permits, but the same rules will hold. Since, in general, the flight test program will not be terminated even though a predicted unfavorable answer is received, but will be used for exploration, then it is desirable to start gathering information as early as possible, not only on the first expected stopping event, but also on all predicted unfavorable ones, cost and payload permitting. Tests on predicted unfavorable events may be designed to verify that answer rather than to test for a positive answer. For instance, even if the prediction is made that the fuel elements will not emerge from the reactor can, it may be desirable at the same time to instrument the range to prove that the fuel elements do not burn up even if they are exposed, and if possible, individual rods should be deployed at selected altitudes and an effort made to track them to the ground.

Not only does each event imply that the preceding one must have occurred, but that it must have occurred early enough, that is by a certain altitude, since the given heat of re-entry is the only agent and it must perform the steps in sequence. Therefore, if exploration is warranted on the basis that design provision can be made to give a higher-altitude exposure for a given step, the tests should be designed to test the phenomenon as a function of altitude - for instance, the exposure of individual fuel rods at different altitudes. For legitimate comparison, these exposures should be made on the same flight, if possible, and may involve both captive and free-falling rods.

In the situation of actual orbital decay, the condition where the fuel elements will be least likely to burn up is that for an easterly orbit. The reason for this is that the atmosphere has essentially the direction and speed of the earth's surface due to earth rotation, while the orbital velocity is a constant independent of earth rotation. Therefore, the circular orbit velocity relative to the atmosphere, the V_c used later, should be taken as the relative velocity for an eastward launch. If burnup could not be proved for this

condition, even though it might for westerly or polar orbits, the implication would be that certain orbital directions for missions would have to be "red-lined."

For evaluation of any specific mission, the orbital velocity (V_c) relative to the atmosphere for that mission inclination and direction must be used in the parametric relation of test re-entry velocity to circular orbital velocity.

Similarly, the most unfavorable realistic condition for fuel-element burnup exists when the fuel element is tumbling, as is discussed later, and flight test must prove burnup under the actual conditions expected to exist. However, as shown in the analysis later, the first and simplest case to analyze is whether a fuel element will burn up under favorable circumstances, namely, in a stable transverse position. If analysis indicates burnup is questionable in this case, it would be even less probable in the tumbling mode.

The spacecraft is assumed in the analysis herein to be oriented during re-entry so that the NAP unit is the leading element. Burnup under any other assumption appears so unlikely as not to warrant serious evaluation. A design requirement for a mission spacecraft, therefore, would be that its re-entry have such a stable orientation.

ASSURANCE OF SAFETY

The flight test safety program is a failure unless it ends in assurance that a non-hazardous condition will exist. Therefore, it must be designed to make a positive demonstration in the final analysis, although, as noted earlier, a negative test may be the first one made on an event if the prediction is unfavorable, because flight test must get to the truth as directly as possible.

Assurance of safety requires both that the data be received and that they give a definite implication. One cannot completely be separated from the other. It is important, first of all, in the design of a flight test program, to see that reliability of getting information is made as high as possible. Therefore, equipment to test either an event or to get quantitative data should be as simple and direct as possible. Furthermore, wherever a failure may mean complete loss of data, there should be a redundant piece of equipment. If the failure which might be expected is not one of reliability but of failure in the environment, then the redundant equipment would preferably be of a different type (e. g. in telemetry).

In testing for the occurrence of an event, a simple yes-no instrumentation should in general be provided, but cannot be relied on by itself because of the likelihood of error. The confidence in it rises if it can be given statistical validation, and such is highly desirable if it can be done on a single flight. Thus, a simple tether wire attached to each fuel element will give a quite definite answer if all the answers are the same. If possible, a yes-no instrumentation should always be backed up by equipment which will give a quantitative picture, related to time and environment, leading to the occurrence of the event. For instance, separation of the reflector retaining band should be backed up by thermocouples giving a time history of the heat, correlated with other data such as vehicle attitude, if questionable. Such quantitative data not only give the basis for accepting the indication that the event did in truth occur, but also, if the event fails to occur, give diagnostic information as to how far it proceeded.

Assurance that the instrumentation is adequate to give the data required, and that these data will give a definite conclusion, is susceptible to evaluation beforehand, just as reliability is. Various instrumentation concepts must be carefully studied as to their adequacy. Also, it must be noted that the assurance, both as to adequacy and meaning of results, must be evaluated after each flight, and it may be necessary to modify equipment.

In the final analysis, high assurance that burnup will occur will be based on the following considerations.

- 1 A soundly-based theoretical analysis indicating that burnup will occur under a set of conditions that are reasonable for operational use, verified as to both nature and magnitude of predicted phenomena by the flight test results
- 2 Demonstration, by flight test, of a margin in the performance of the desired results (if, for instance, one could show that each of the required events in the chain leading through fuel-element exposure and burnup can be demonstrated to occur without overlap in the conditions of re-entry, then the amount of that margin, interpreted in terms of the basic requirement and the excess measured relative to the sharpness of the requirement, can be evaluated to give the assurance.)
- 3 Statistical repetition (which is generally expensive)

In a strict sense, statistical verification requires that data regarding phenomena be taken under exactly duplicated conditions. If this is done, a number of measurements may be made, and from these a mean value, \bar{x} , and a dispersion, s , may be directly computed. These do not, of course,

necessarily represent the true mean, μ , and true standard deviation, σ , which are forever unknown, but they do represent best estimates of μ and σ . From \bar{x} and s and the number of observations, n , statistical theory permits a direct calculation (presented in existing tables) as to confidence limits on μ and σ . That is, for any assigned interval centered on \bar{x} and s , the probability (confidence) can be found that the true μ and σ lie within those limits. Naturally, the larger the tolerance is permitted to be, the greater is the confidence that the true values lie within it, and as the number of measurements increases the greater the confidence for any given interval.

Although tests may be designed to attain confidence, or assurance, in the preceding strict sense, repetition is in general expensive, particularly in flight testing. Furthermore, the interpretation often may be faulty, since either the conditions were not exactly reproduced, or there may have been factors entering into the actual test which were not considered in the analysis and design of the test.

Often it is more desirable in flight tests to choose to vary conditions (e. g. release fuel elements at various altitudes) than to try to reproduce them exactly. The correlation between results must then come from the theory of re-entry phenomena. The interpretation of the data in terms of mathematical confidence becomes more complex; but actually more meaningful results can often be obtained. An interpretation of the results may be made by seeing whether the functional relation believed to hold from physical theory gives a better least-squares fit to the data than other reasonable functions do, and from the precision with which the data-points fall on the functional curve.

REPRESENTATIVE SYSTEM FOR STUDY

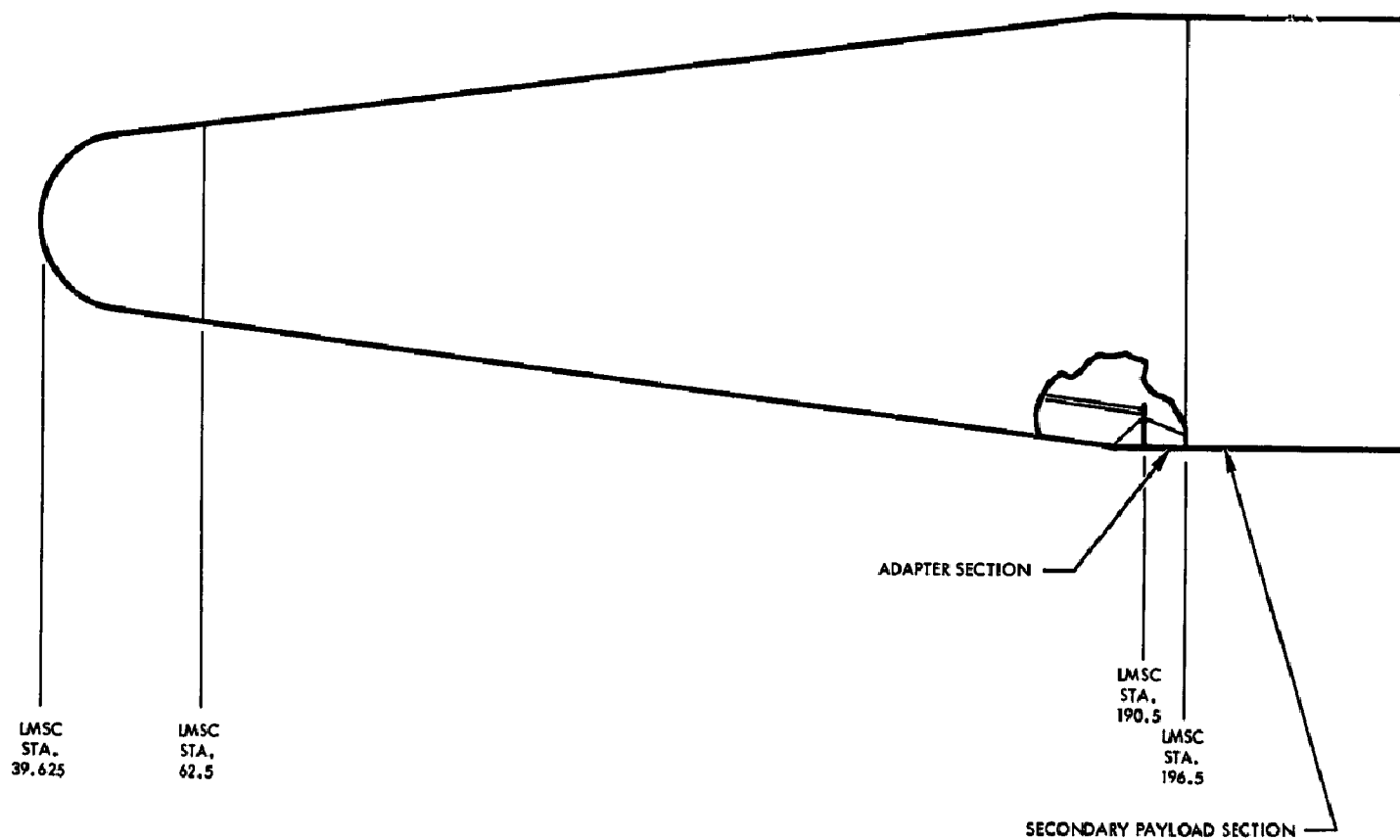
This study is intended to be universal in application to NAP re-entry phenomena. The criteria derived from the study should be independent of the design and hardware of the reactor system or the vehicle used in any mission application. A current design for a planned mission was designated to provide a system for analysis to determine potential sequences of events and predicted heat transfer data. This configuration has been designated for a study guide. The Atomics International SNAP 10A is the NAP system used, which is attached to the Agena B vehicle for the orbiting spacecraft. All trajectories, heat flux data, and heat transfer calculations were performed using the design data available for this spacecraft system.

SPACECRAFT

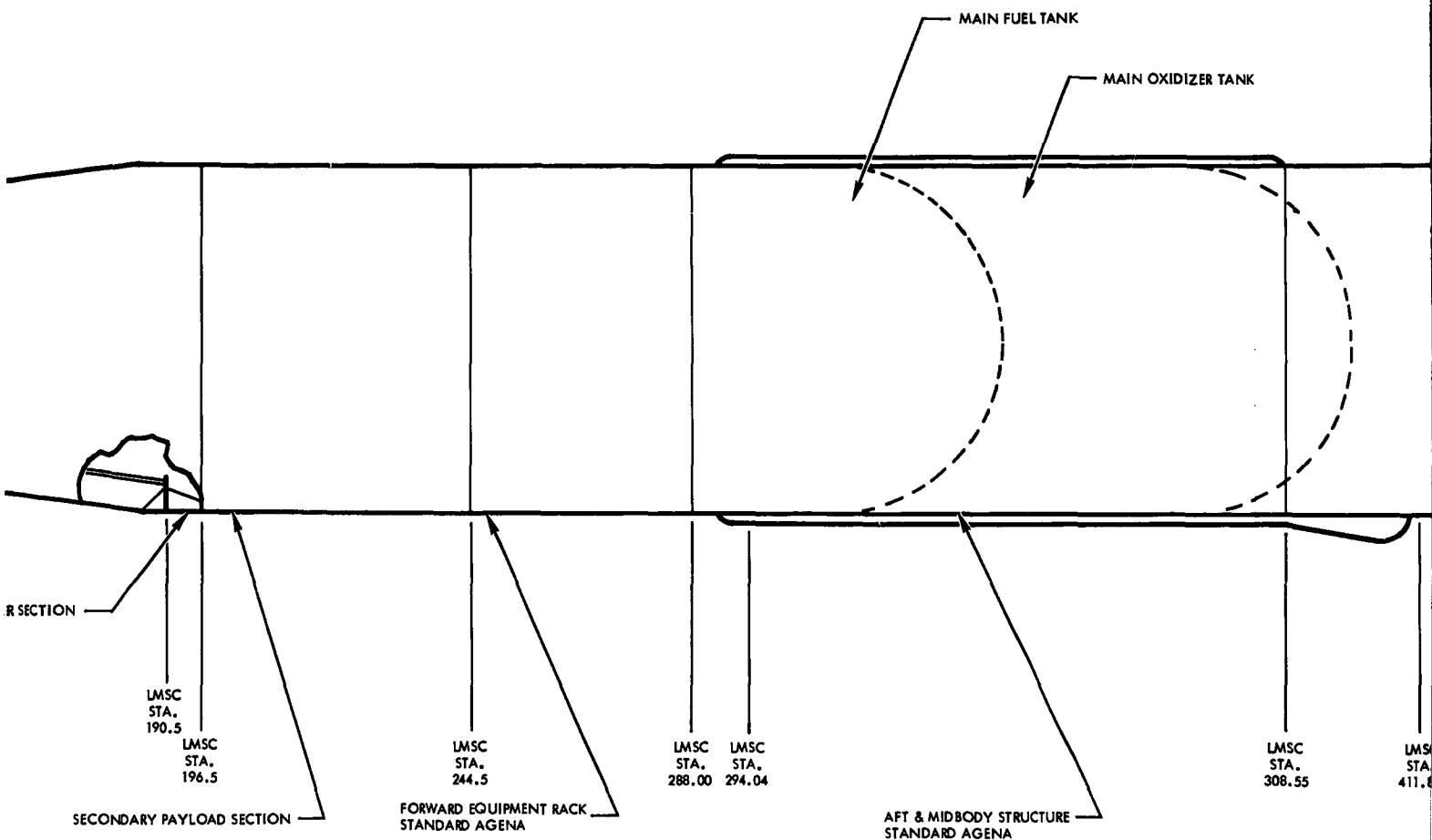
The orbiting spacecraft is shown in Figure 3. This vehicle is assumed to be in a decaying orbit which places the spacecraft at 400,000 ft with .999 x circular orbit velocity and $\gamma = 0$.

SNAP 10A SYSTEM

The SNAP 10A nuclear auxiliary power system is shown in Figure 4. Currently available design information has been obtained from Atomics International. No attempt was made to obtain later design data which may include revisions. Thus, the design information shown is not necessarily representative of the present design and cannot be assumed to be the design of hardware to be used for any mission application. The reactor vessel and the fuel elements used in this study are shown in Figure 5.



1



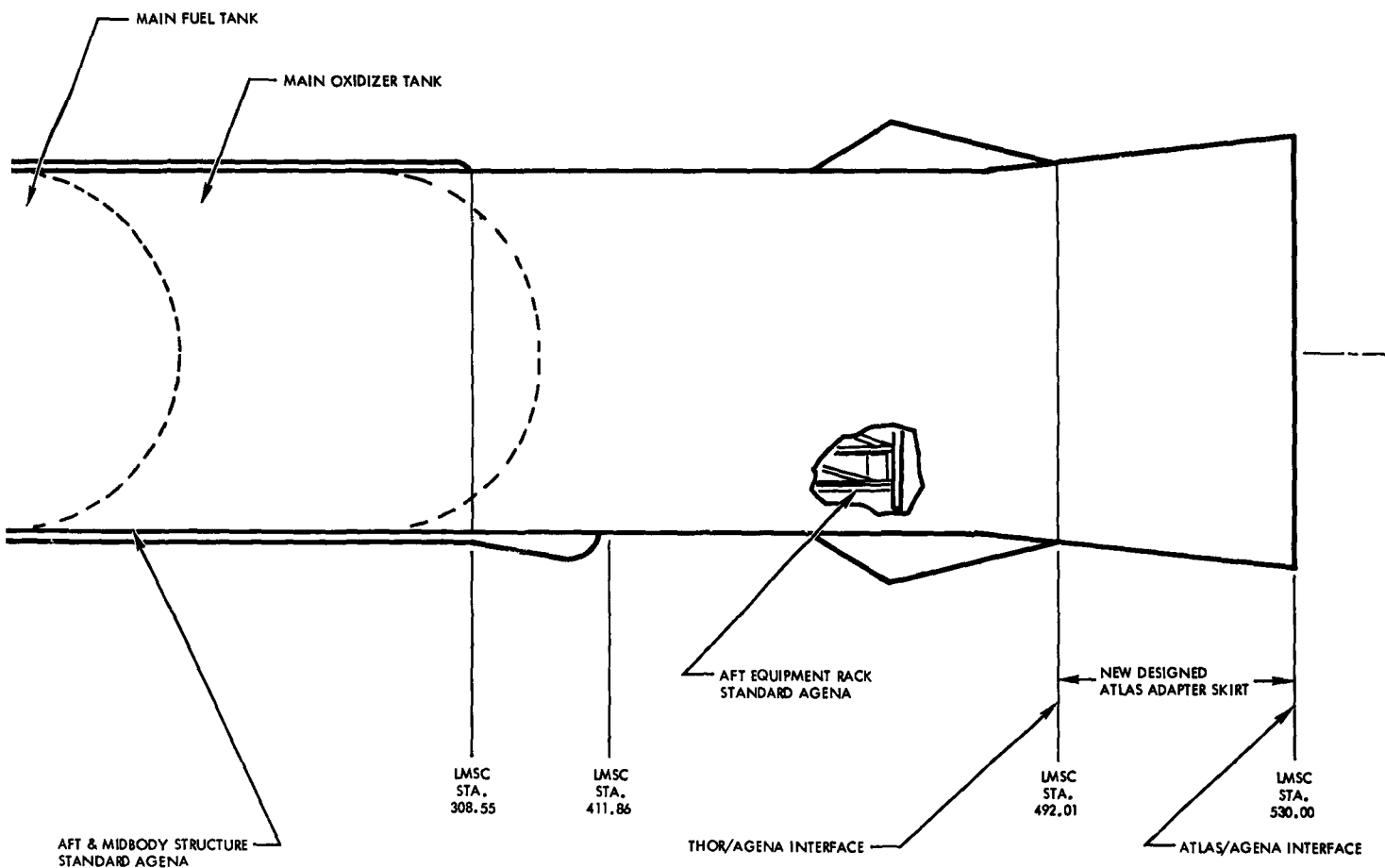
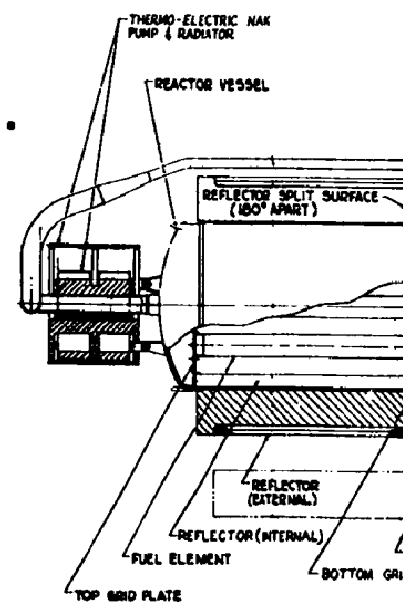
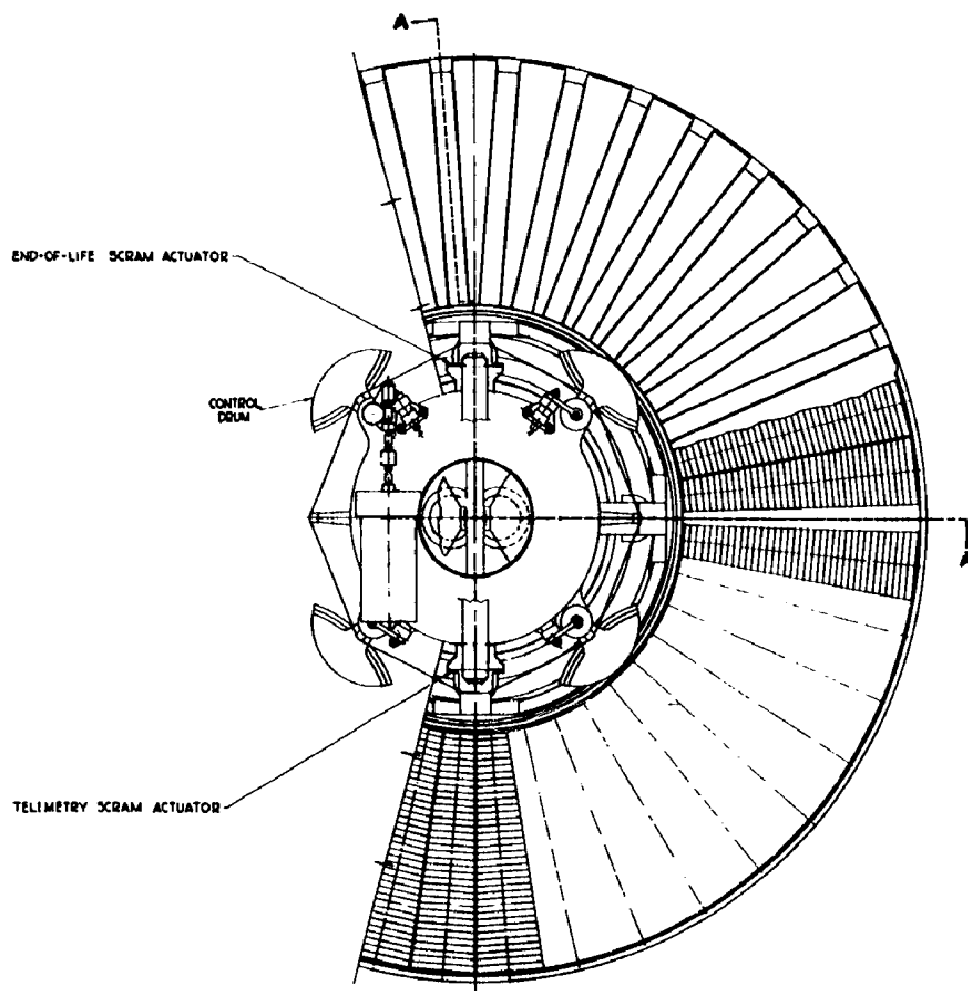
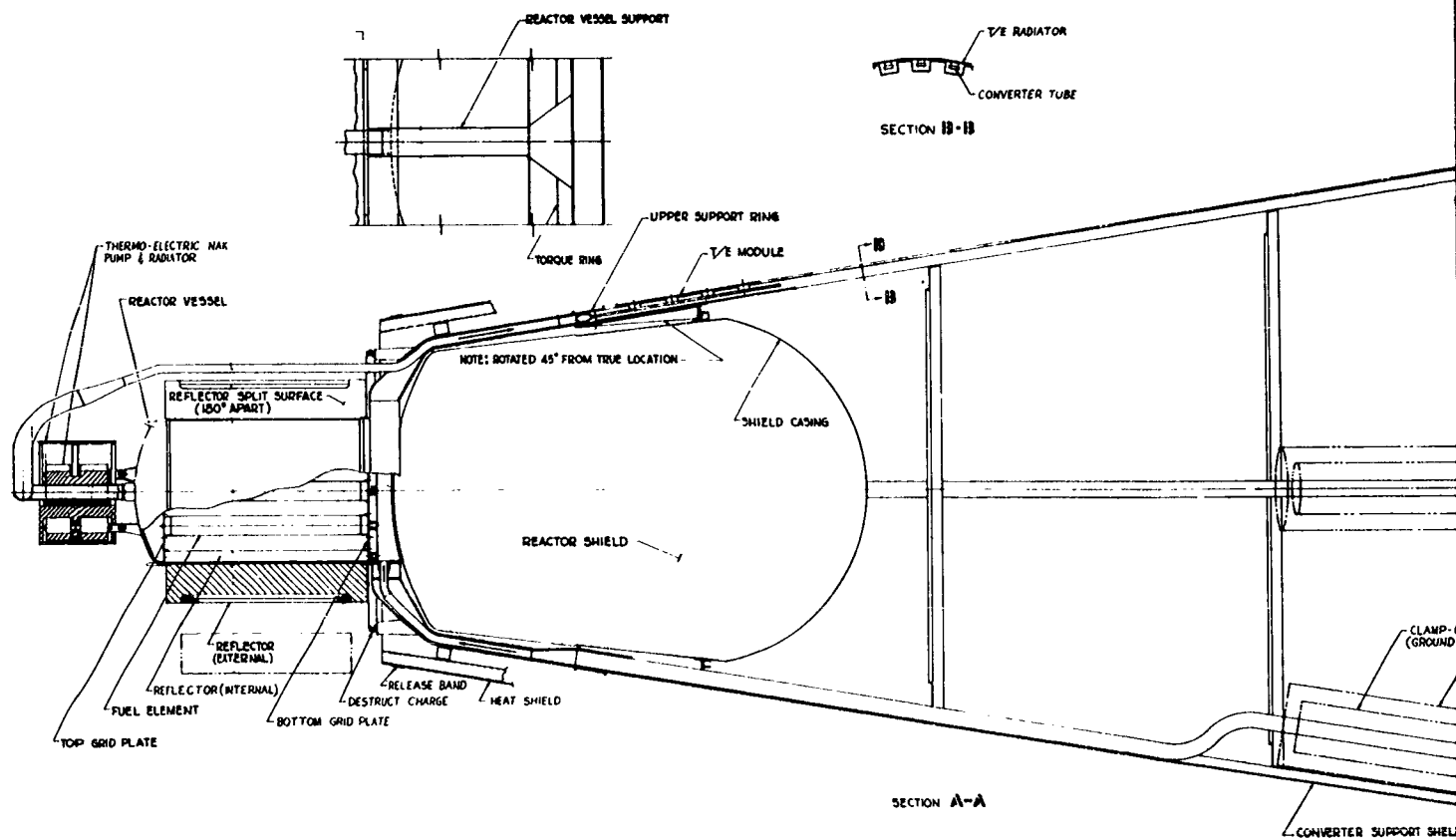


Figure 3. Orbiting Spacecraft Study Model





2

3

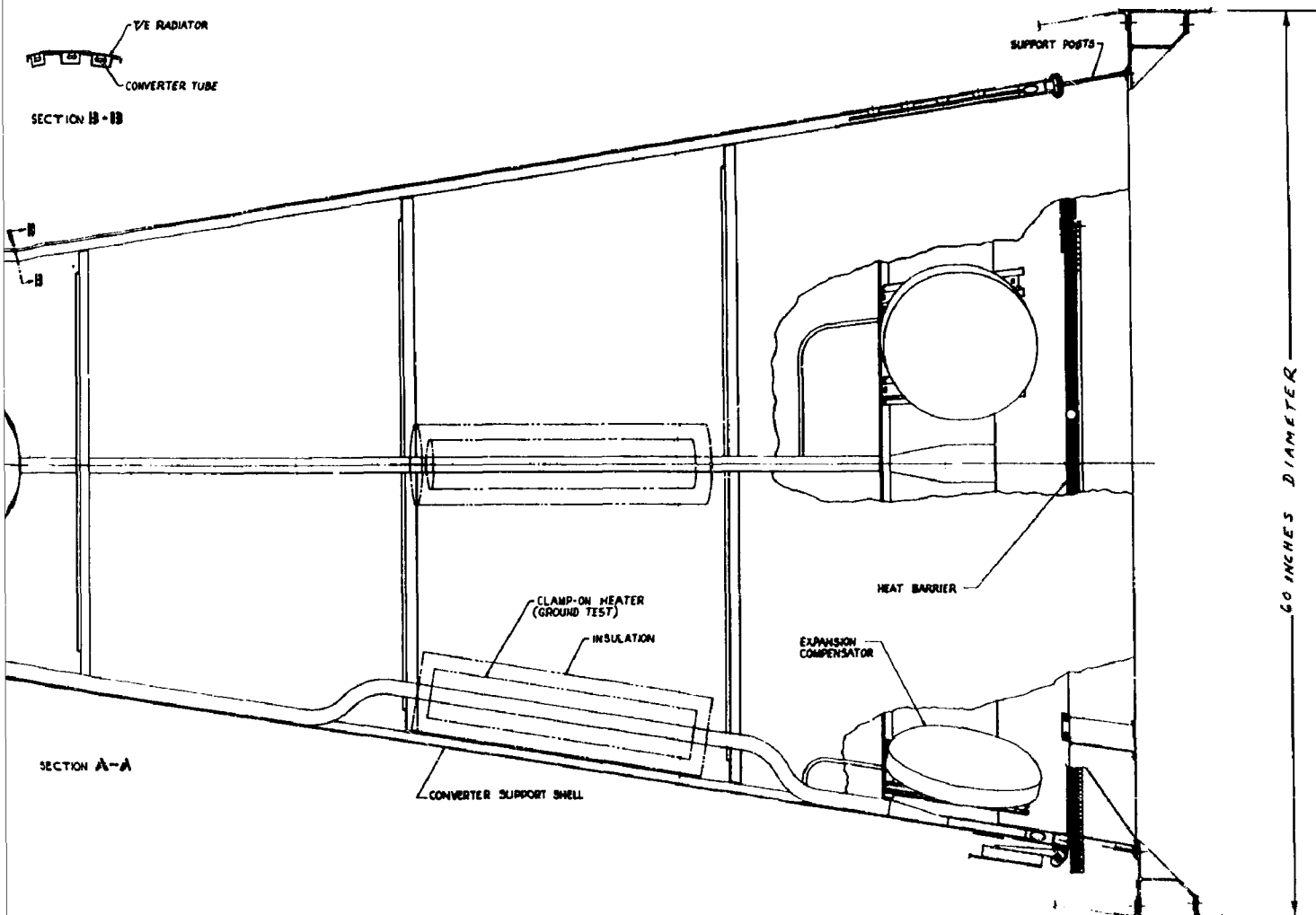
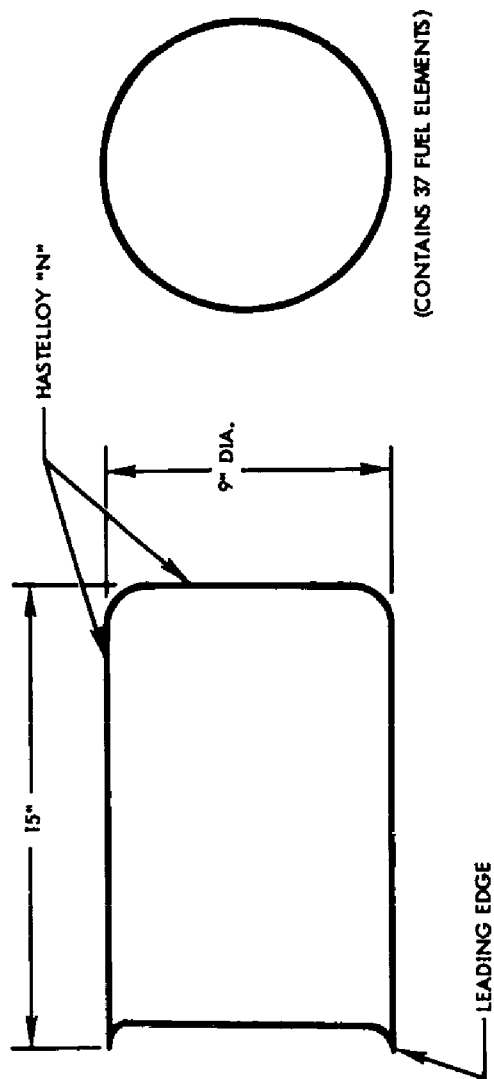


Figure 4. SNAP 10A Study Model Design



REACTOR VESSEL

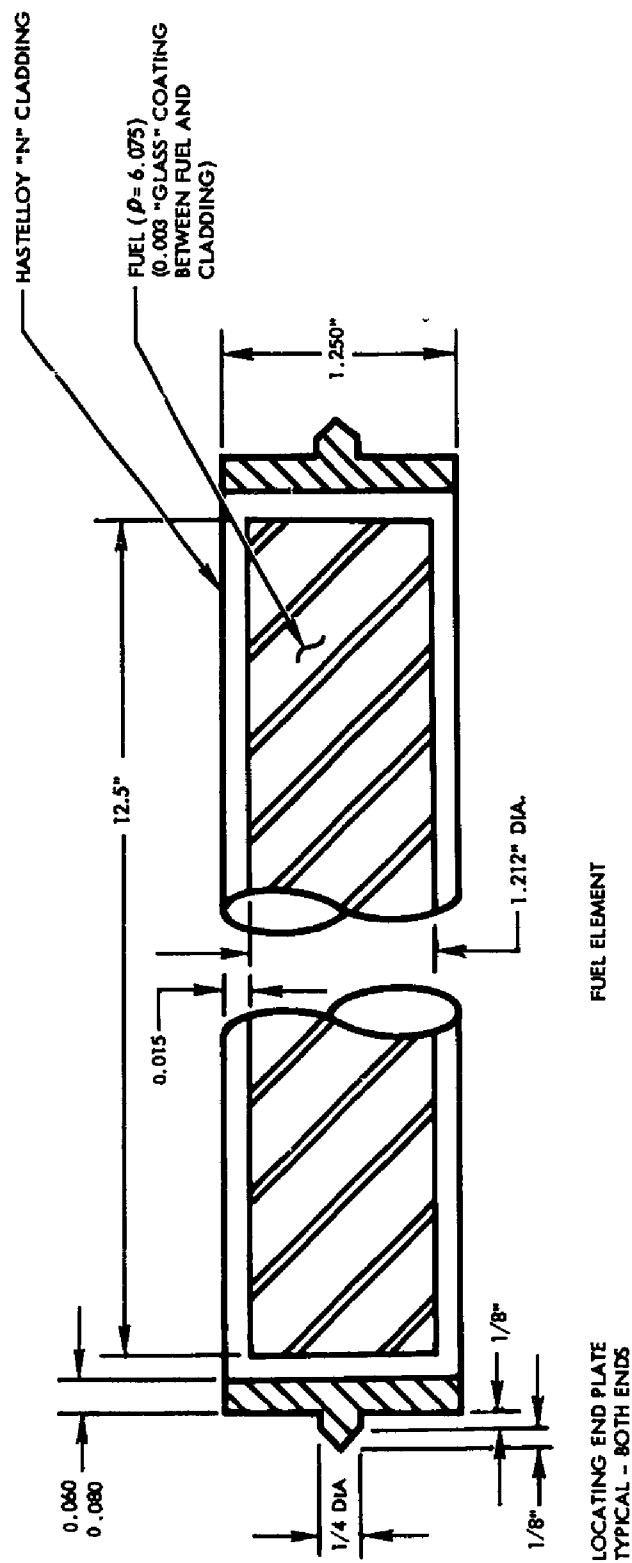


Figure 5. SNAP 10A Reactor Vessel and Fuel Element Data

ORBITAL DECAY

SIGNIFICANT PARAMETERS

Establishing flight test criteria to simulate the orbital decay trajectories of NAP units requires a knowledge of the aerodynamic and thermodynamic parameters that significantly affect the heating environment during re-entry. Aerodynamic parameters of importance are the drag-to-mass relationship (CDA/m) which, with the lift coefficient if a nonsymmetrical configuration is involved, determines the trajectory, and the static and dynamic stability characteristics which define the attitude of a component as a function of the initial re-entry conditions.

The thermodynamic parameters of importance include the physical properties of the materials (e. g. , density, thermal conductivity, latent heats of fusion and vaporization, heat of combustion), the gas characteristics affecting heat and mass transfer in the boundary layer, and the geometry, size and flight attitude of the object under consideration. These parameters are discussed in detail in Reference 1.

The problems associated with the burn-up of the components of a particular NAP system (SNAP) have received considerable attention by aerospace companies. The results of many of these studies are applicable to NAP systems in general. A study of the re-entry attitude of the entire SNAP vehicle and the type of motion that the fuel elements assume was made by AVCO and reported in Reference 2. From the results presented in this report, it may be seen that the fuel elements will either tumble, oscillate about an angle of attack corresponding to cross flow, or re-enter in a cross-flow attitude. For moderate initial tumble rates, the AVCO study showed that the fuel elements continue to tumble to the time of peak heat flux. Available aerodynamic-force and moment data for flat faced cylinders (Reference 3) indicate that the center of pressure at zero angle of attack is at approximately one caliber aft of the front face and is fairly independent of length-to-diameter ratio and Mach number for Mach numbers greater than 3. Thus, from stability considerations, flight of the fuel elements in an axial flow attitude is precluded. Since a tumbling motion of the fuel elements during re-entry will tend to inhibit their burnup, this type of motion was assumed for all trajectory computations. A lower surface temperature will result from the distribution of the aerodynamic heat over all surfaces, so that melting is less likely to occur.

The ballistic coefficients computed for the fuel element, reactor vessel, and spacecraft for axial, tumbling, and cross-flow attitudes are given in Table 1.

Table 1. Re-Entry Ballistic Coefficients, $W/C_D A$
(pounds per square foot)

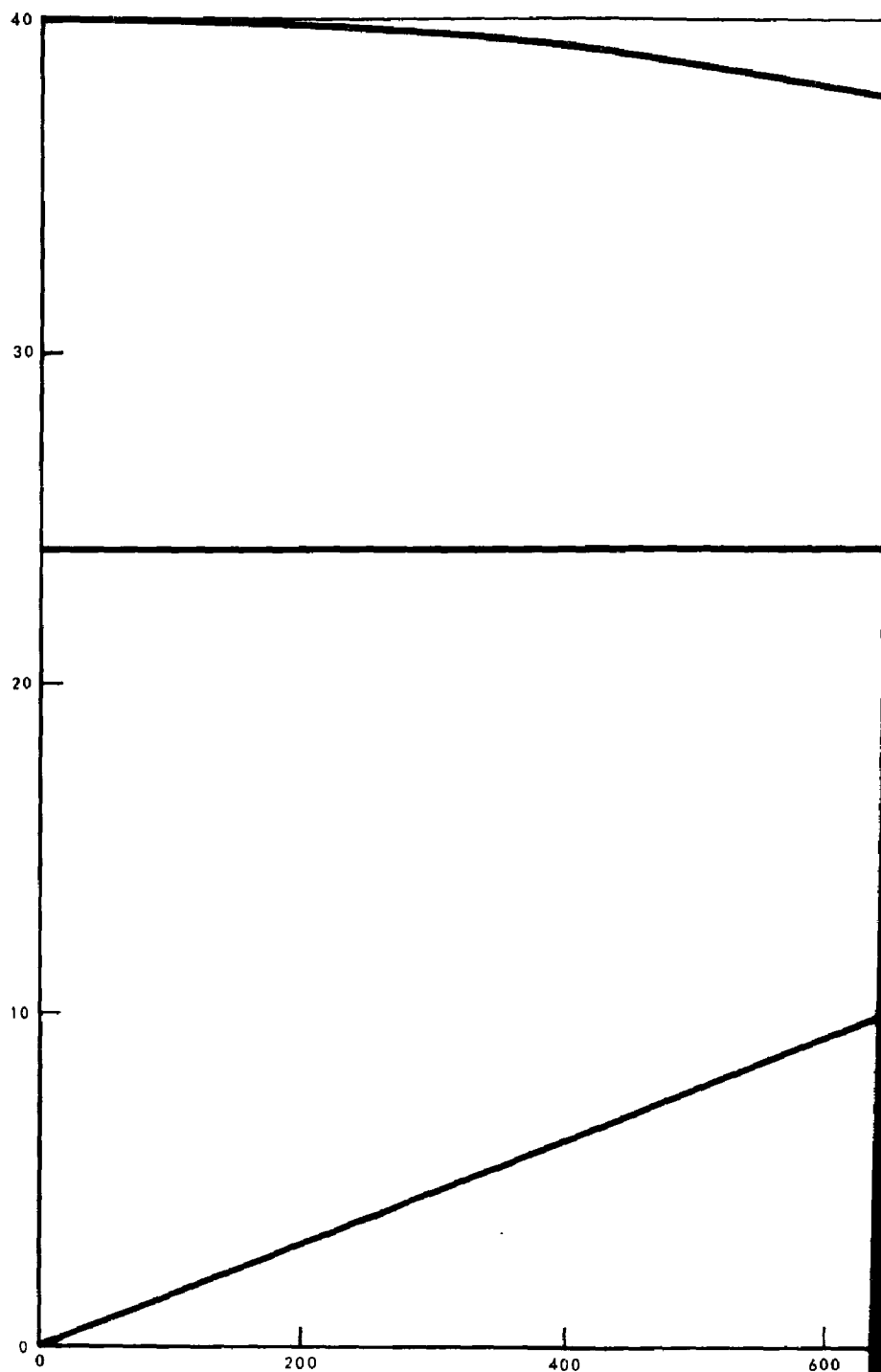
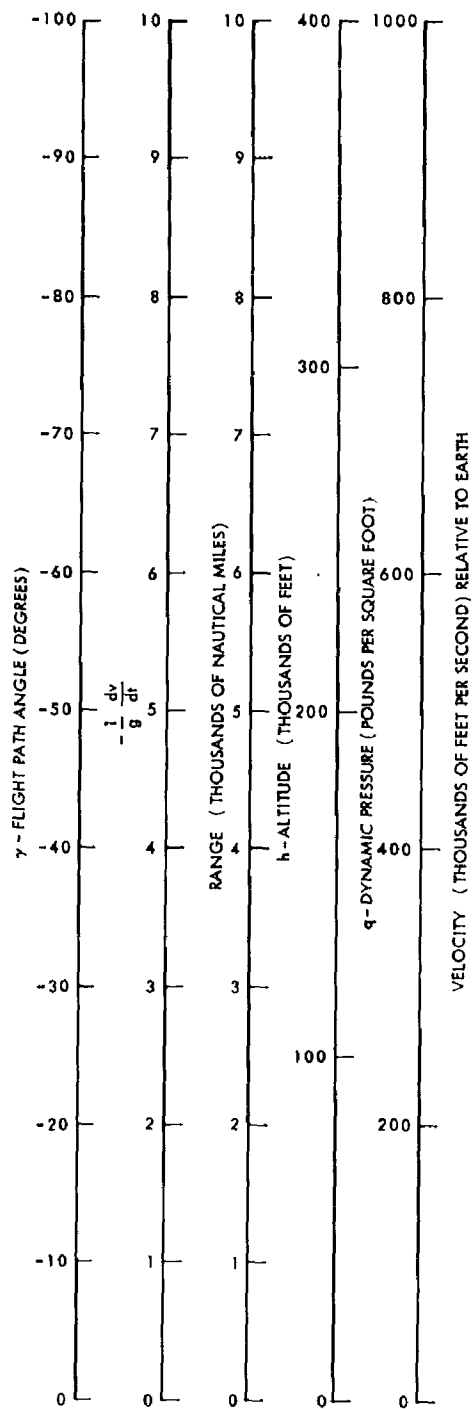
Component	Attitude		
	Axial	Tumbling	Cross-Flow
Fuel Element	211	52	25
Reactor Vessel	184	185	138
Spacecraft	300	62.3	--

DECAY TRAJECTORY AND HEAT PULSE

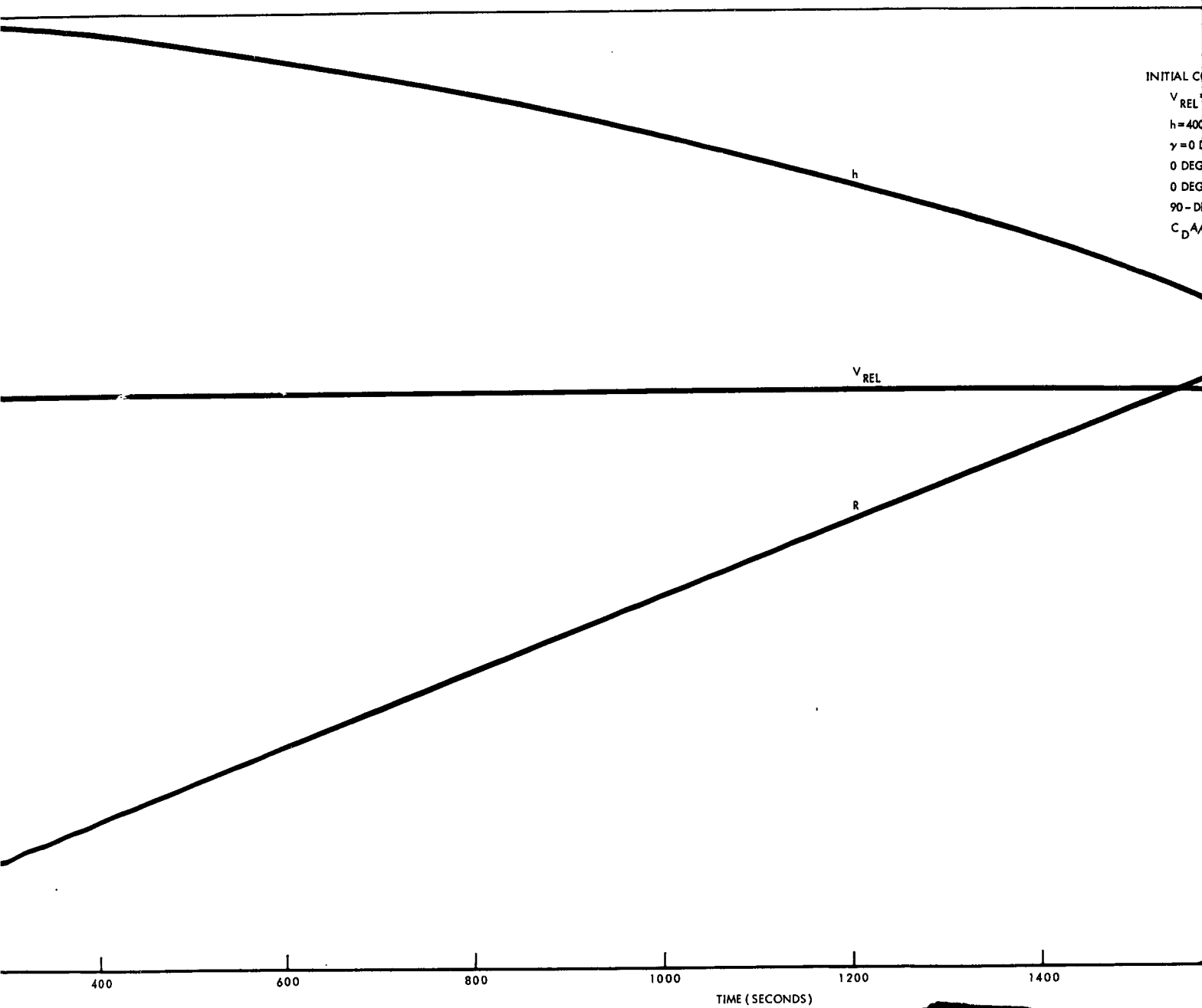
Trajectories and aerodynamic heating were determined for the complete NAP unit, the reactor vessel, and for the fuel elements alone. Figures 6 through 13 present data regarding the trajectories at various flight-path angles; Figures 14 through 19 present aerodynamic heating data. Figure 20 shows variations in re-entry range resulting from variations in flight-path angle and velocity.

Orbital decay trajectories for the complete spacecraft with NAP unit in the axial and cross-flow attitudes were obtained from GD/Astronautics. To avoid duplication of effort, computations for this case were made for tumbling motion only. The data for a tumbling vehicle is presented for comparison with the analysis and data for tumbling reactor and tumbling fuel element. It is assumed that any spacecraft employing a NAP unit for an orbital mission must be stable during re-entry and oriented with the reactor end first. Otherwise, the NAP unit would be protected during re-entry so that the NAP breakup and fuel element burnup could not occur. These re-entry trajectories for the tumbling spacecraft are given in Figures 6 through 8. Resulting heat flux at the stagnation point for angle of attack of 90° is presented in Figures 14 and 15.

The trajectory for the reactor vessel alone was computed assuming an orbital decay. The trajectory for an initial flight path angle of zero degrees is shown in Figure 9 with corresponding heating rates at the stagnation point for angle of attack of 90° included in Figure 16. As discussed previously, the



1



2

Figure 6.

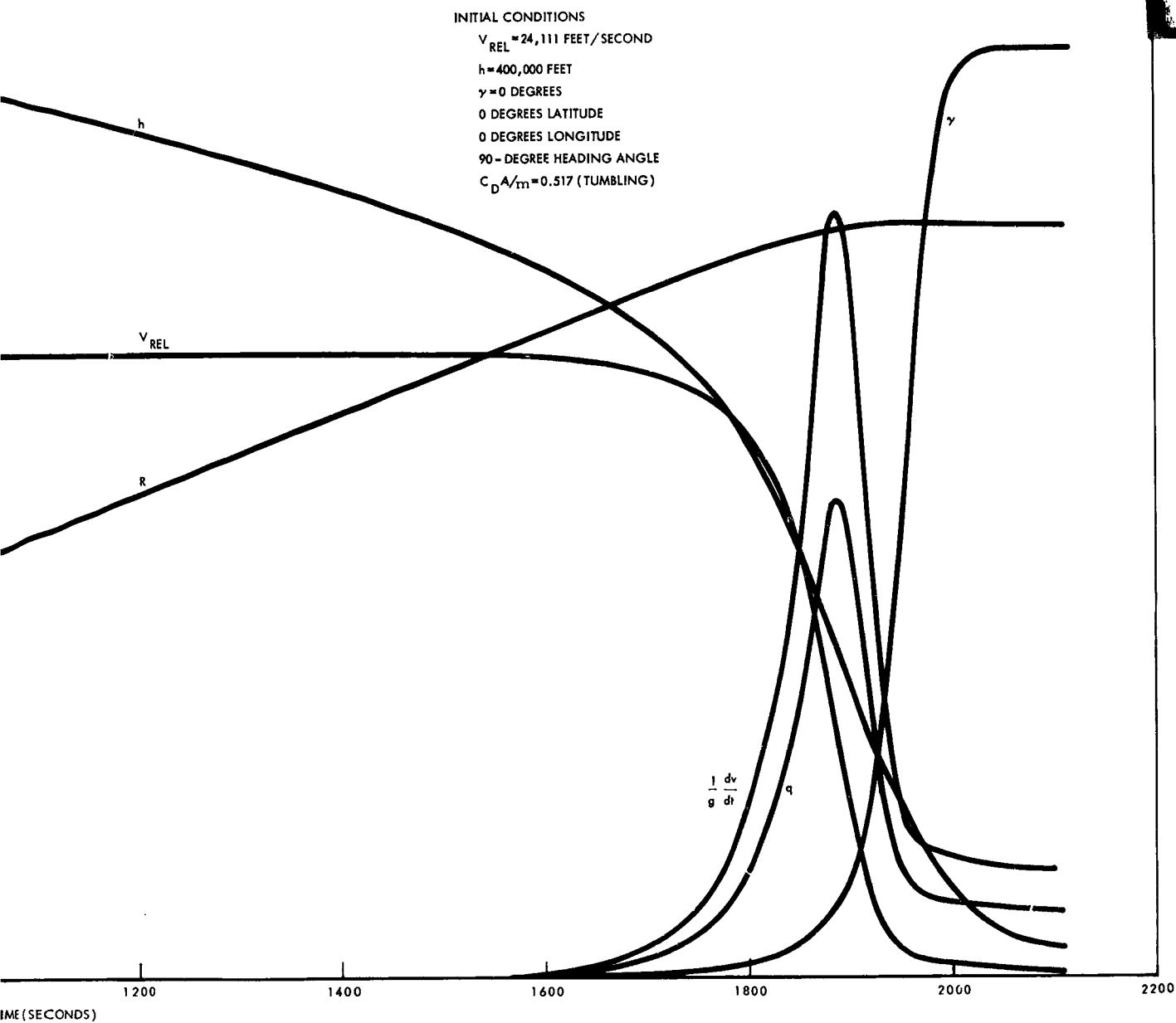
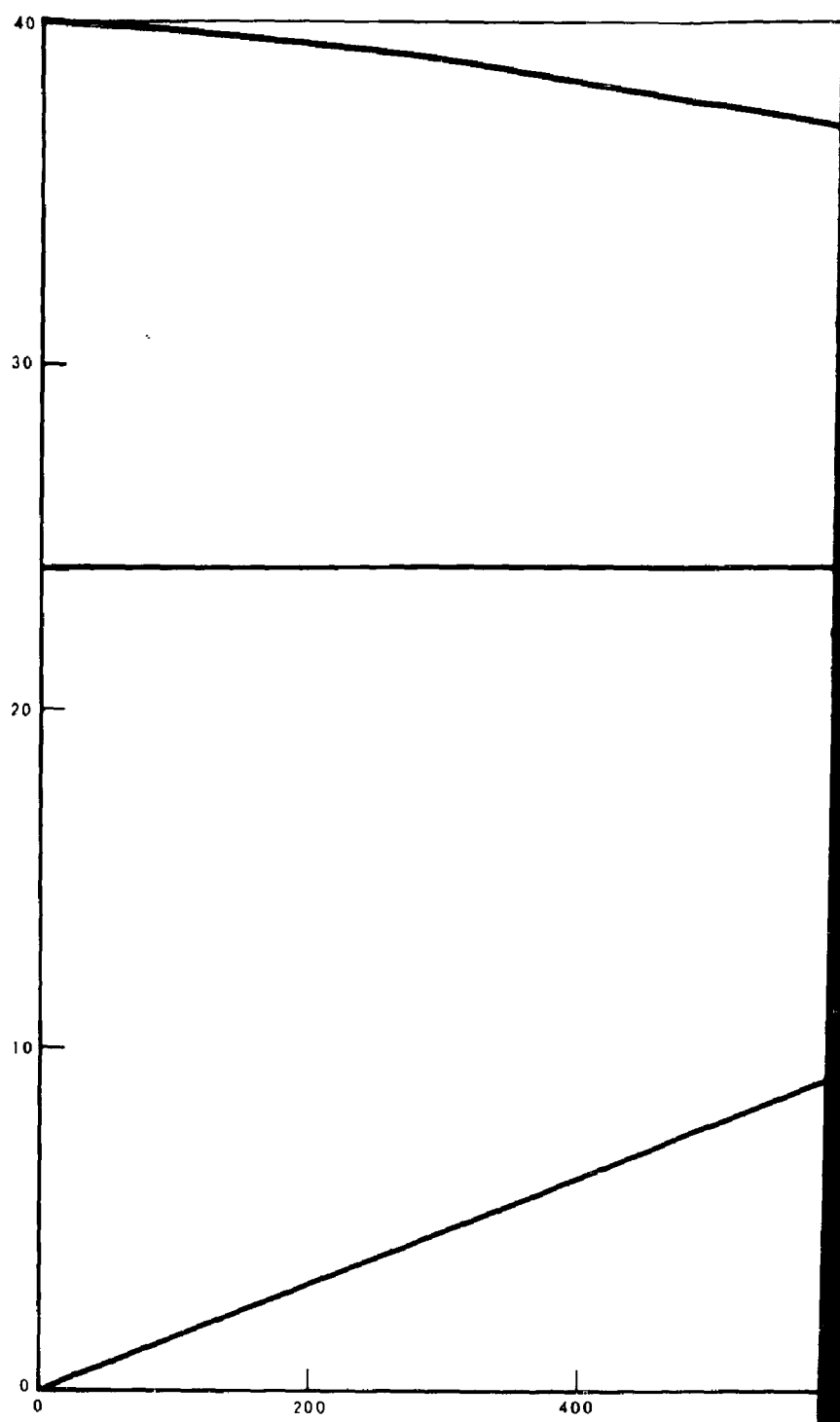
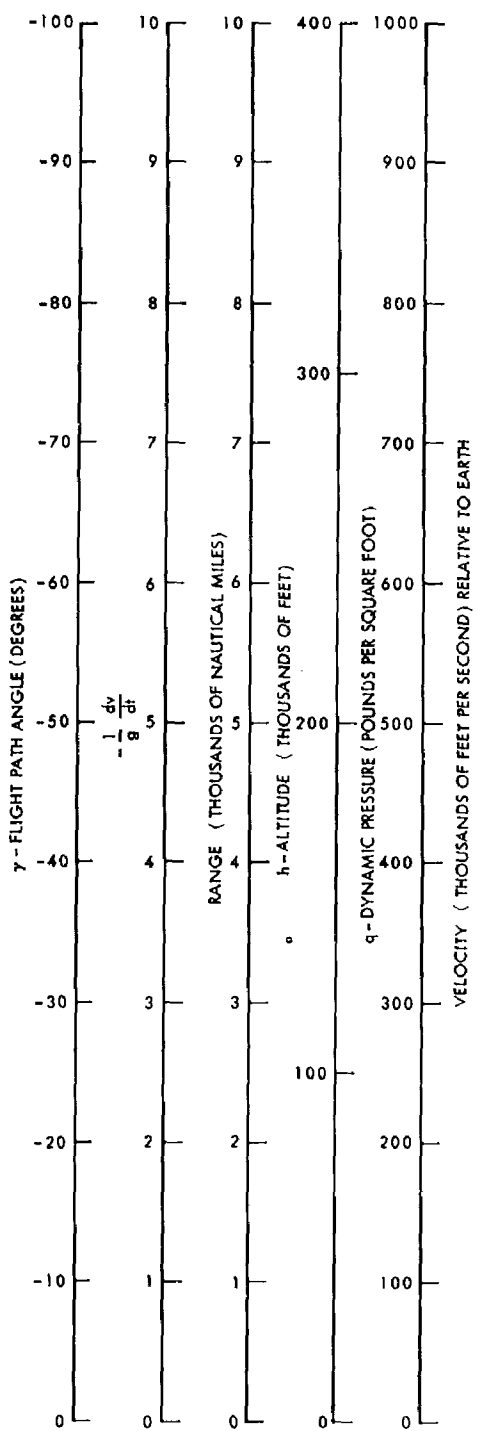
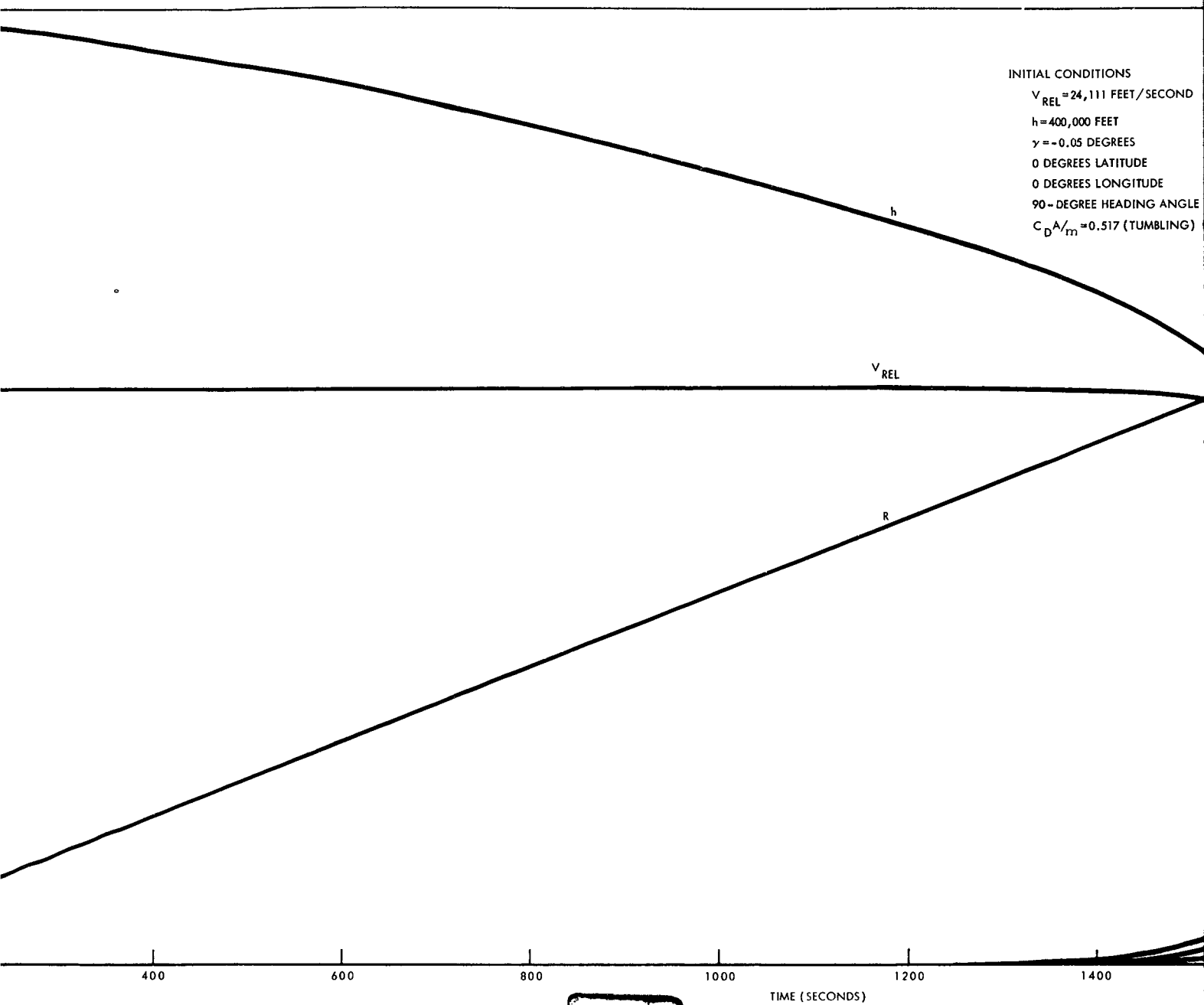


Figure 6. Orbital Decay Trajectory of Tumbling Spacecraft, Flight-Path Angle Zero Degrees





2

Figure 7. Orbital Decay
Angle Minus 0.

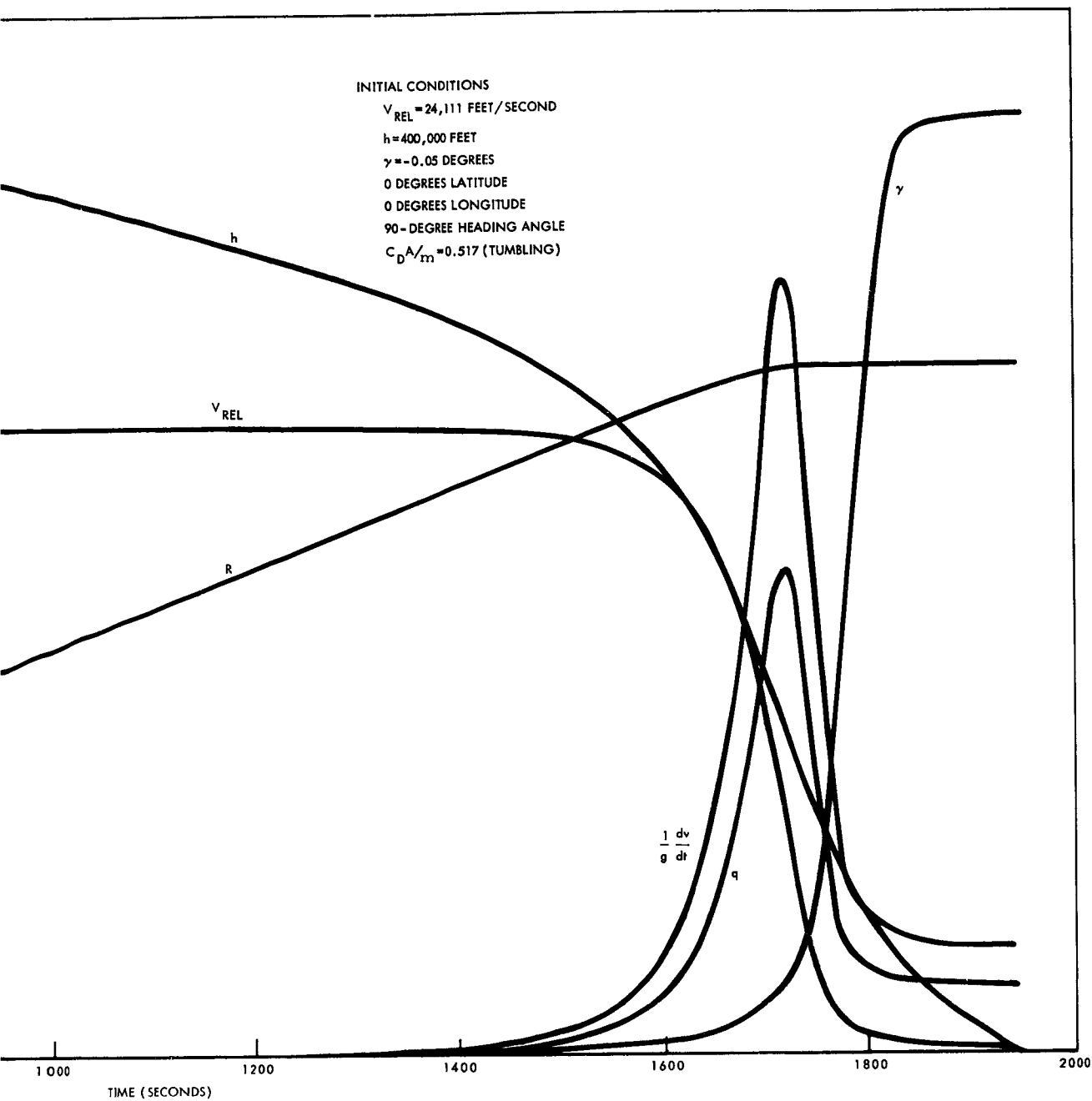
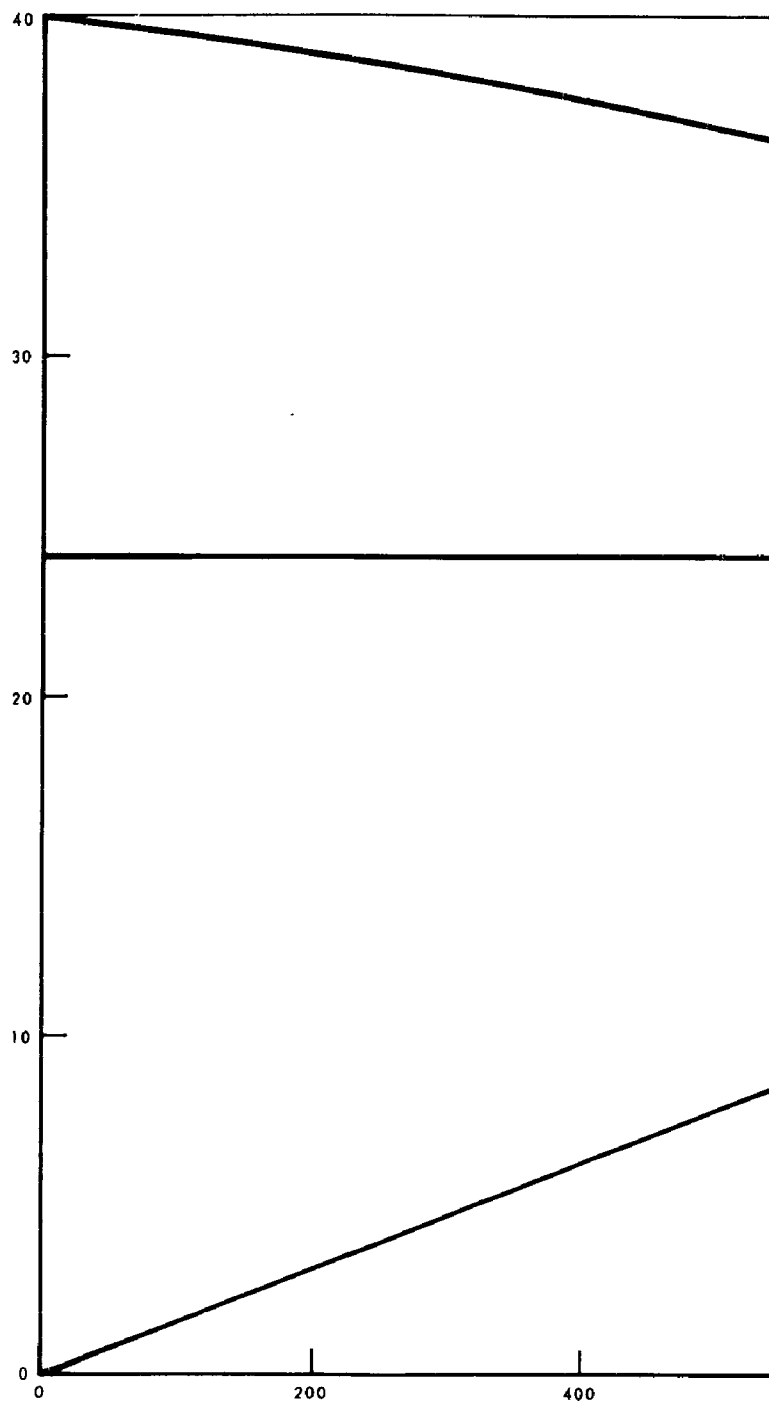
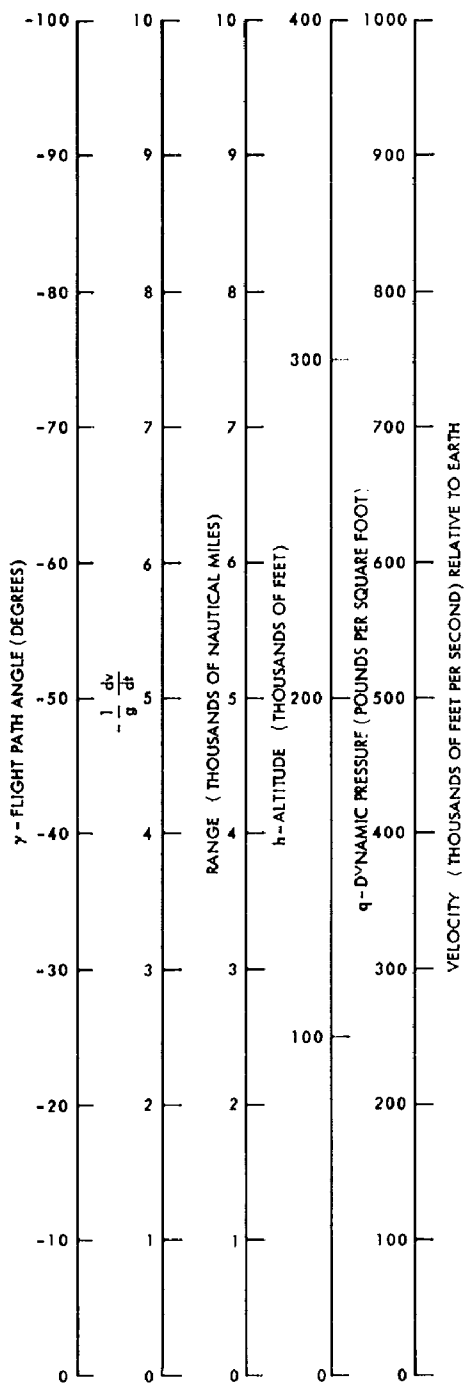


Figure 7. Orbital Decay Trajectory of Tumbling Spacecraft, Flight-Path Angle Minus 0.05 Degree



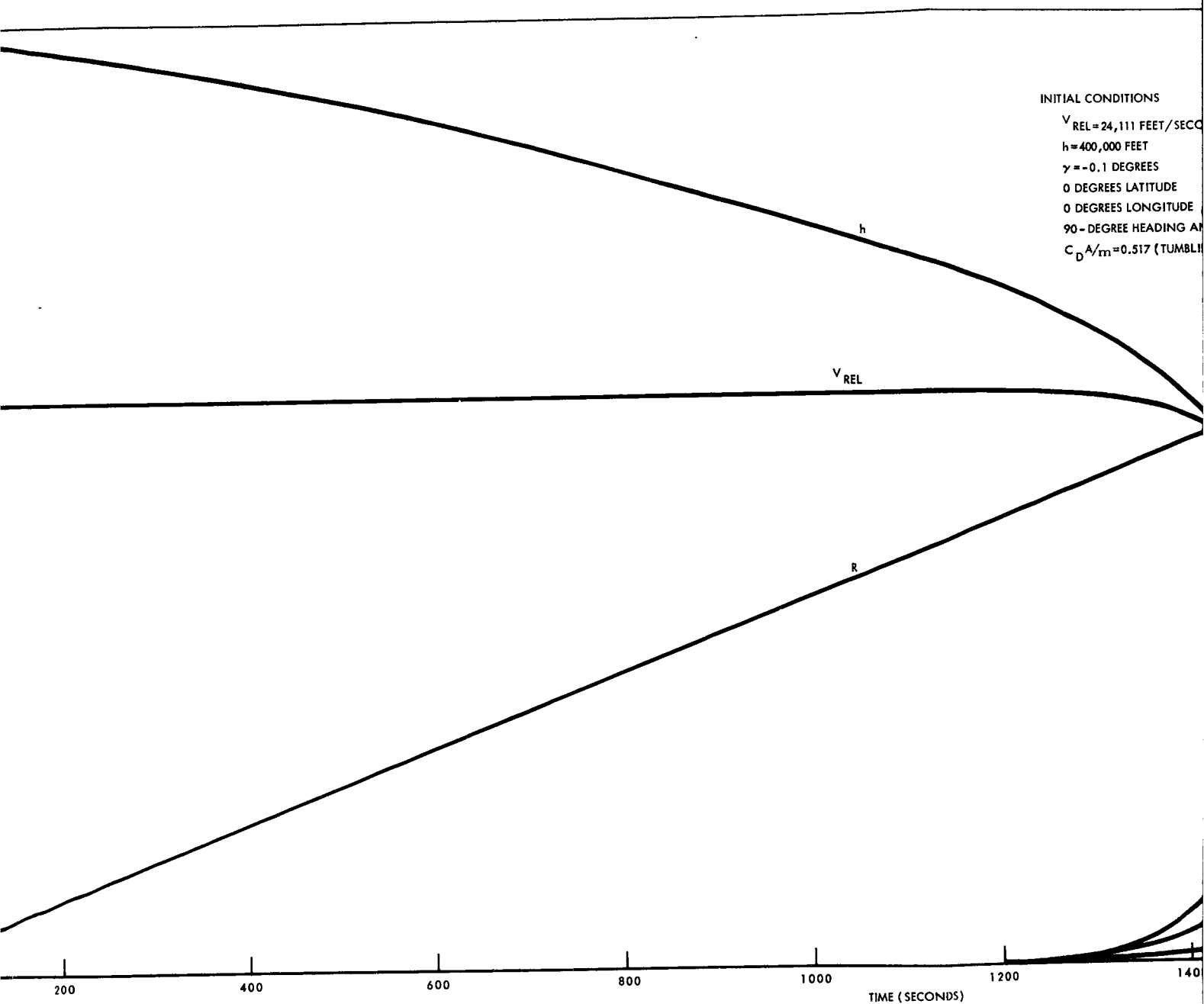


Figure 8. Orbit
Angle

2

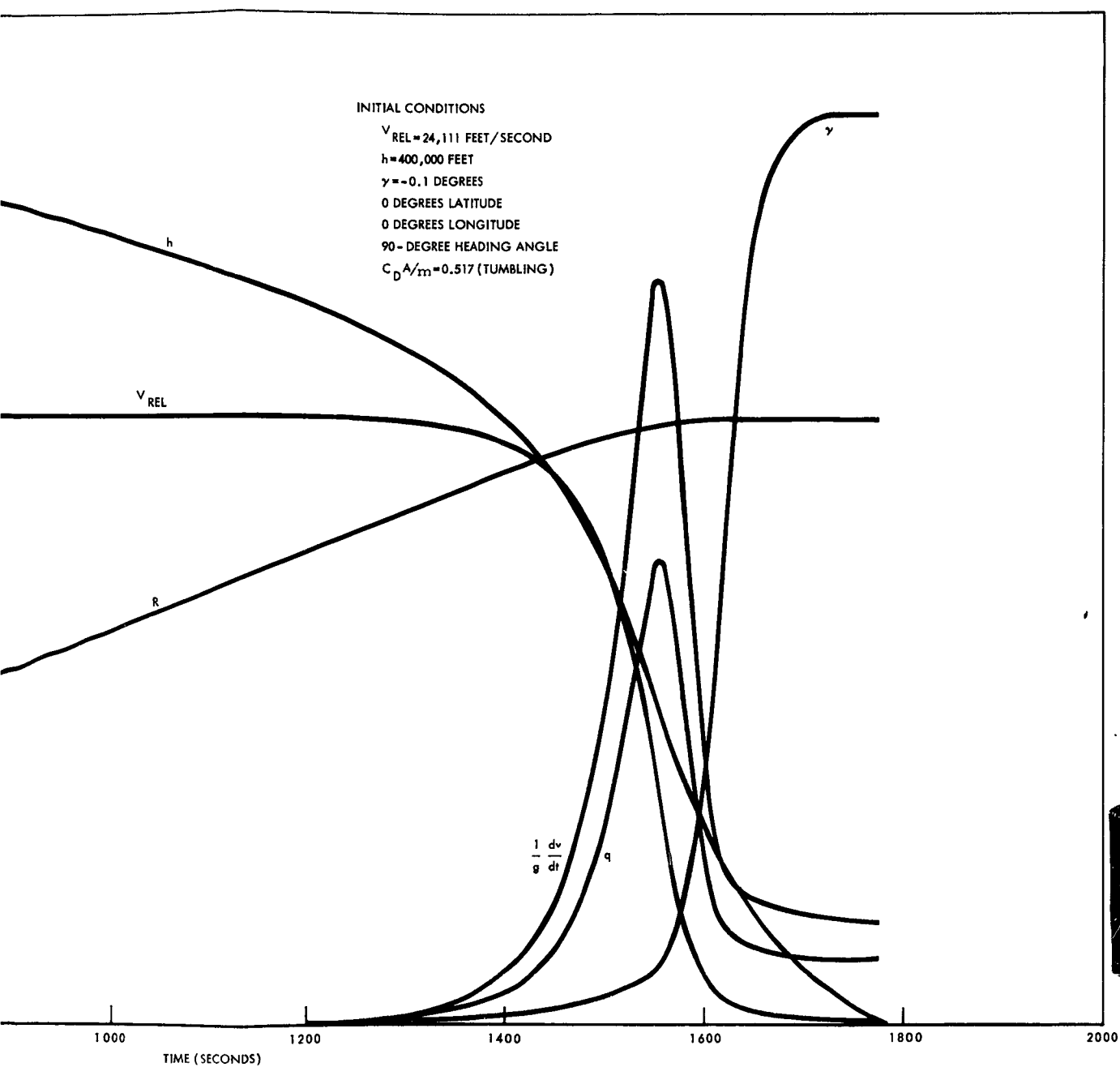
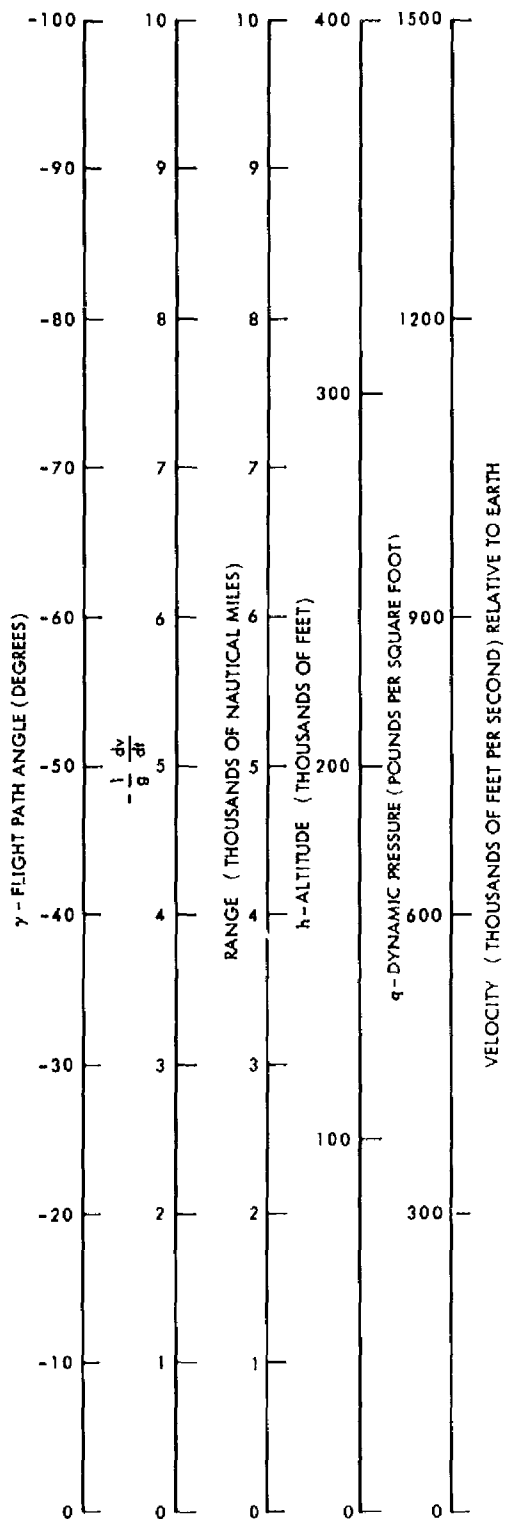
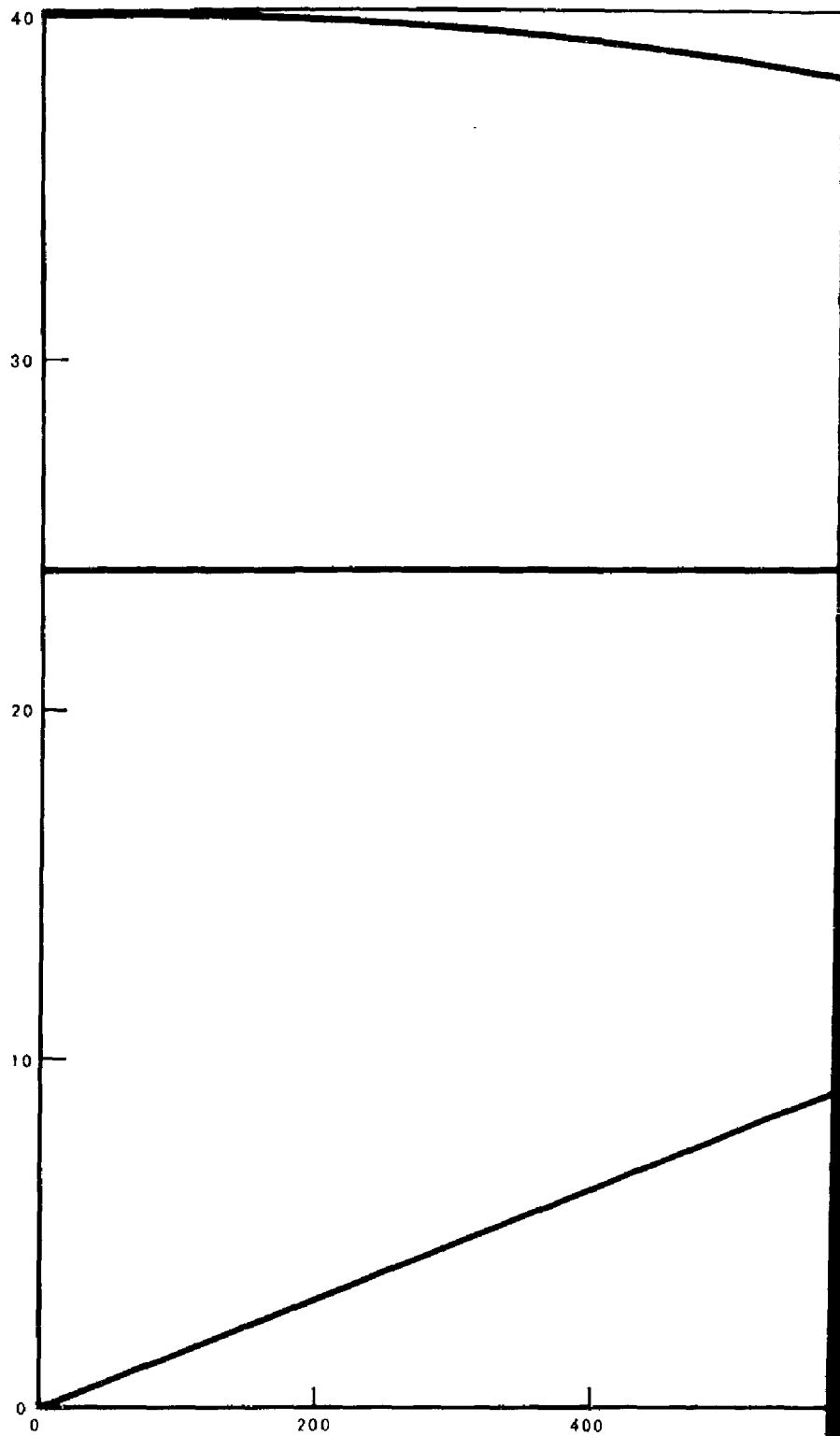
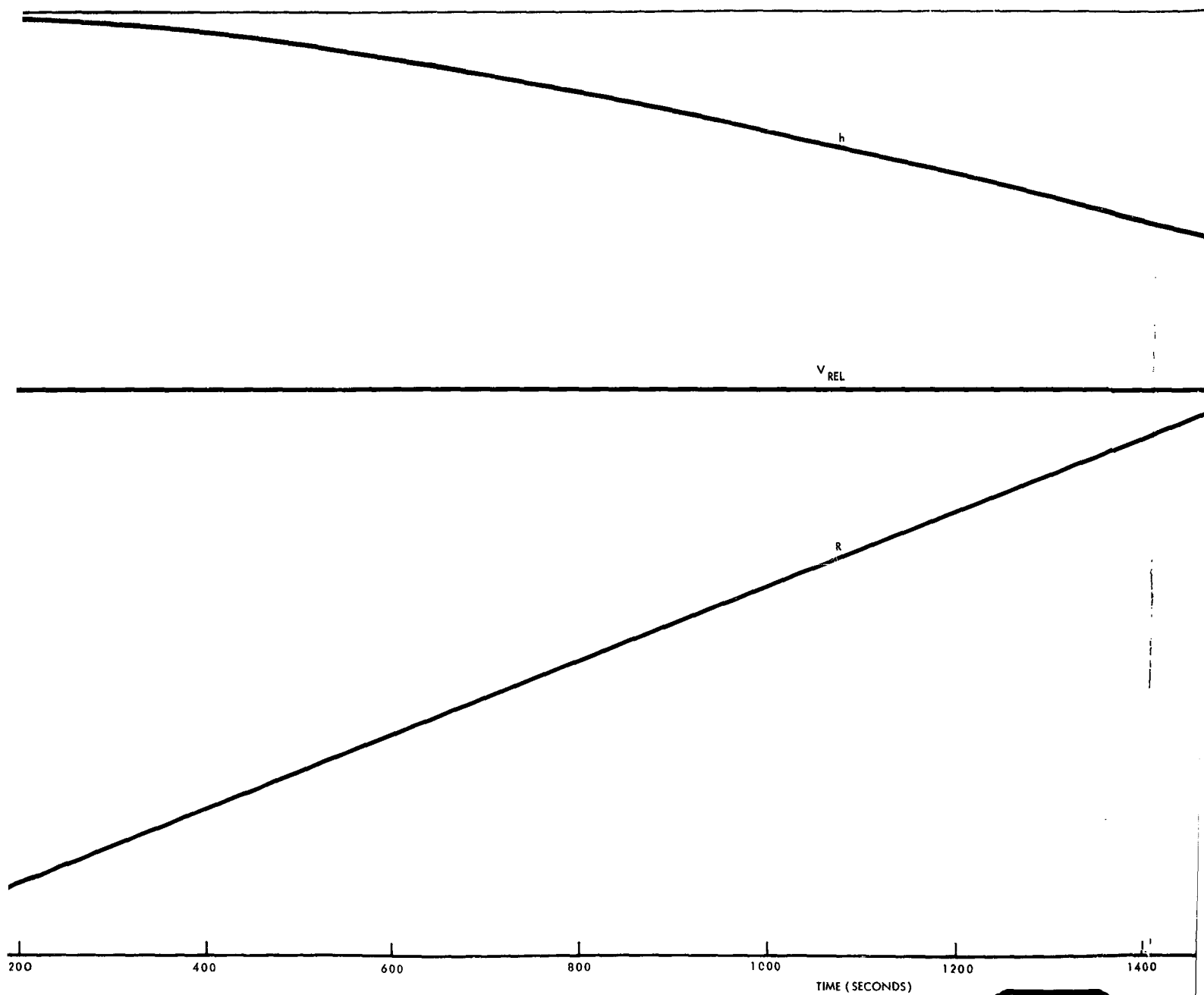


Figure 8. Orbital Decay Trajectory of Tumbling Spacecraft, Flight-Path Angle Minus 0.1 Degree



VELOCITY (THOUSANDS OF FEET PER SECOND) RELATIVE TO EARTH





2

3

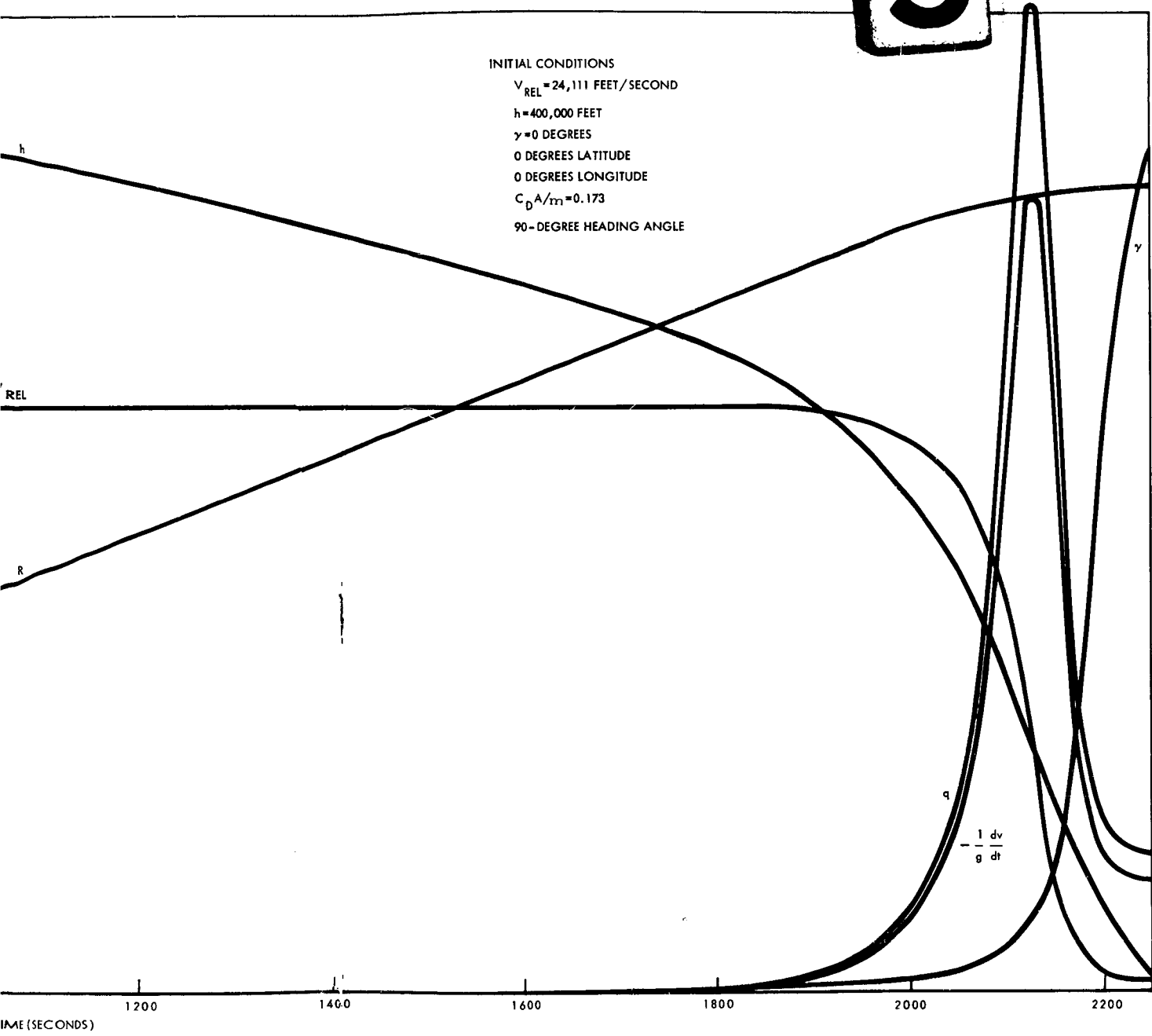
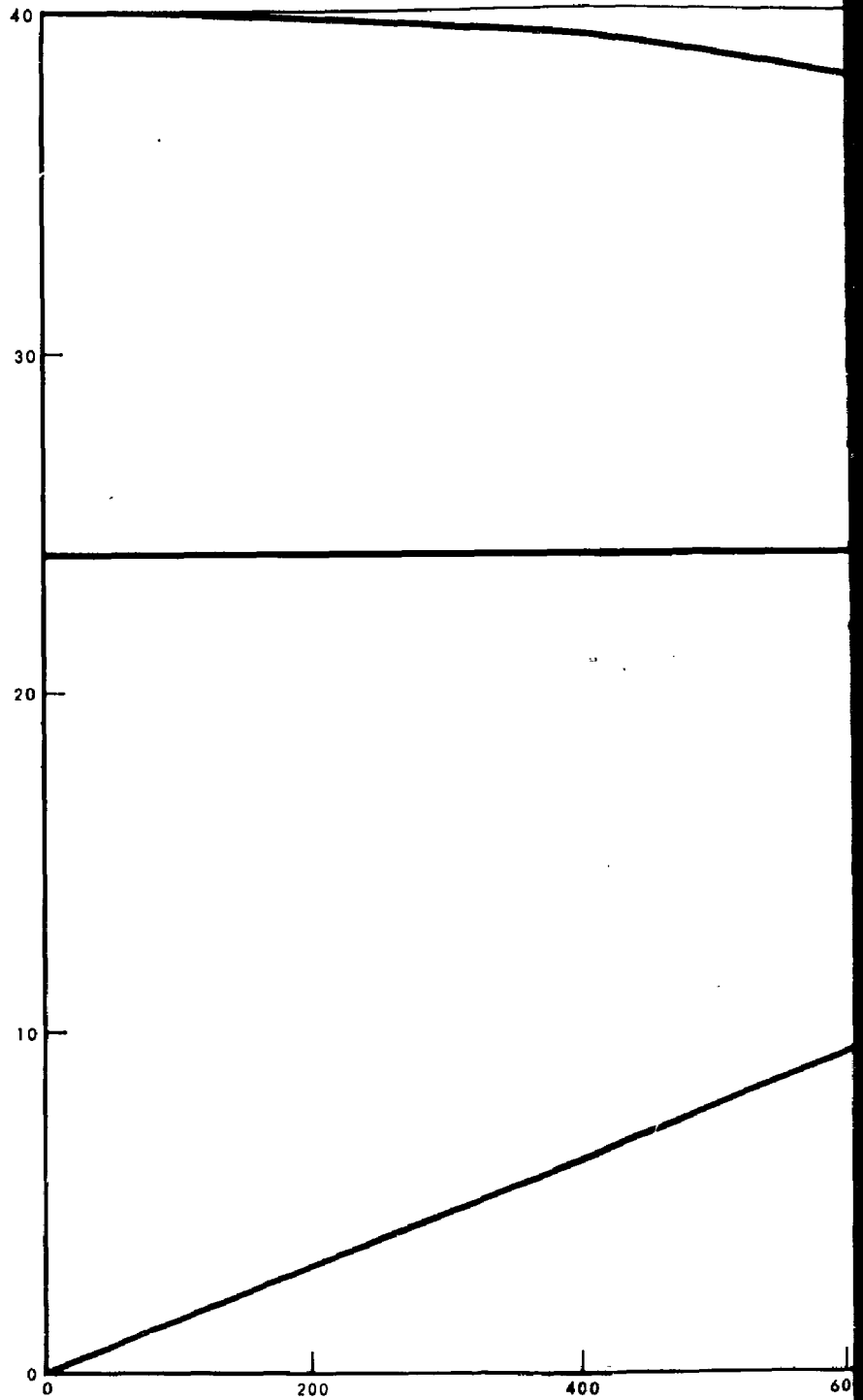
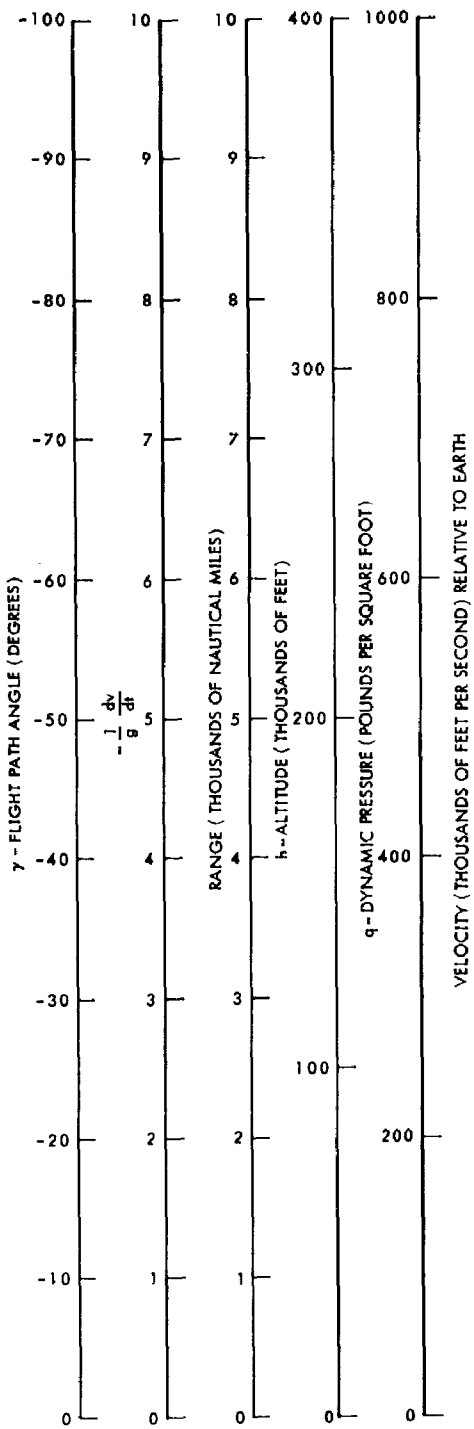
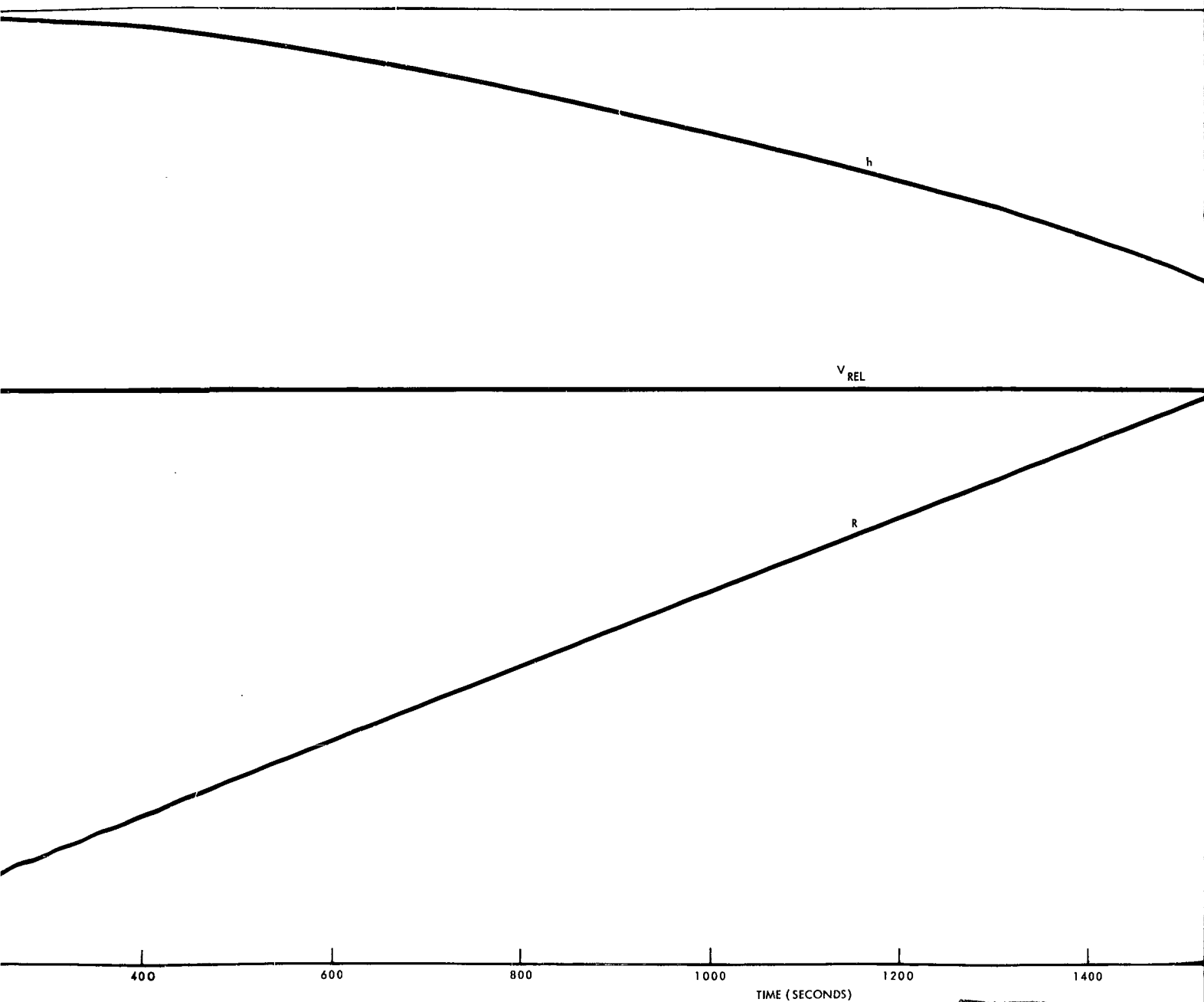


Figure 9. Orbital Decay Trajectory of Axial or Tumbling Reactor Vessel, Flight Path Angle Zero Degrees

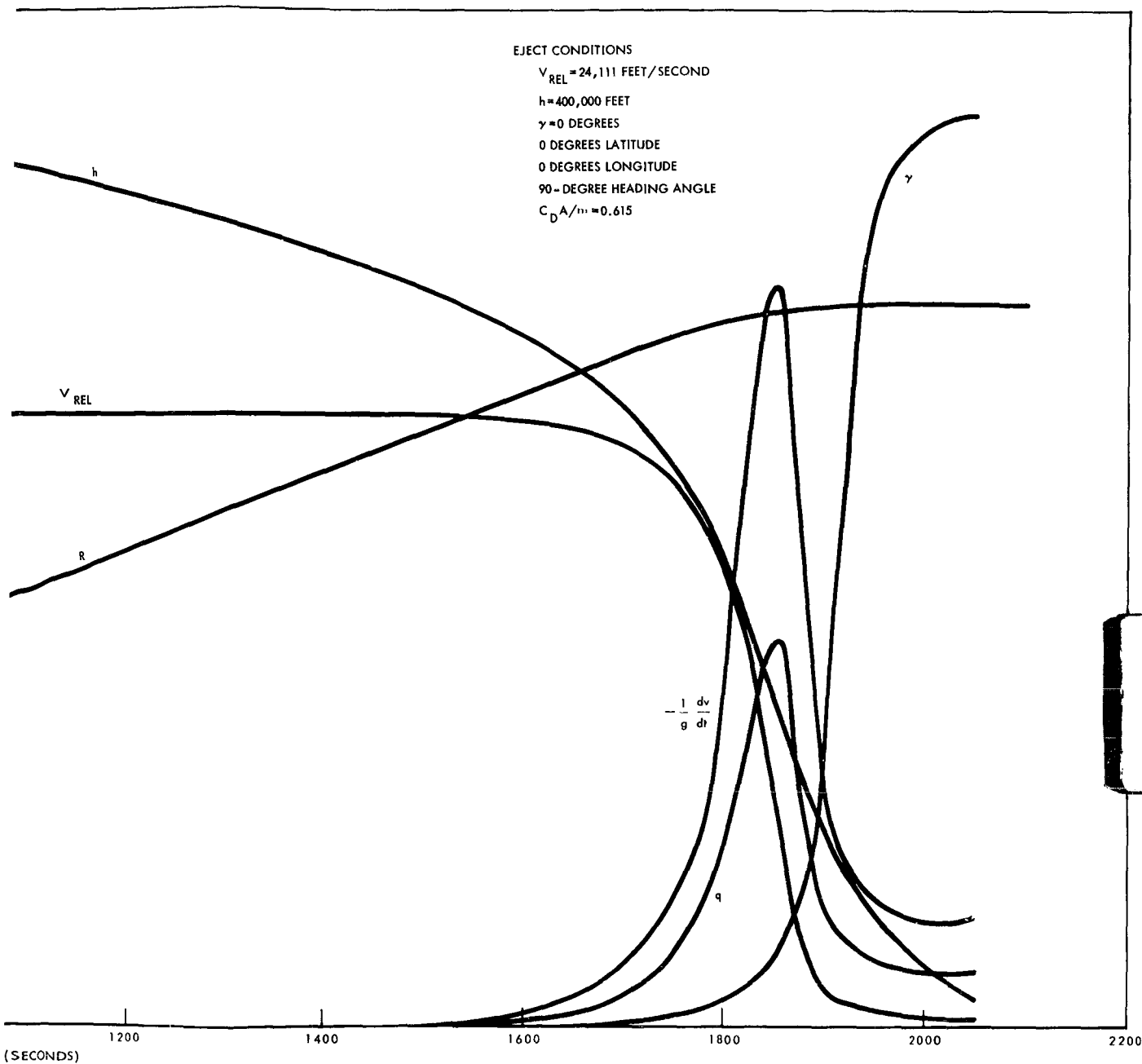


1



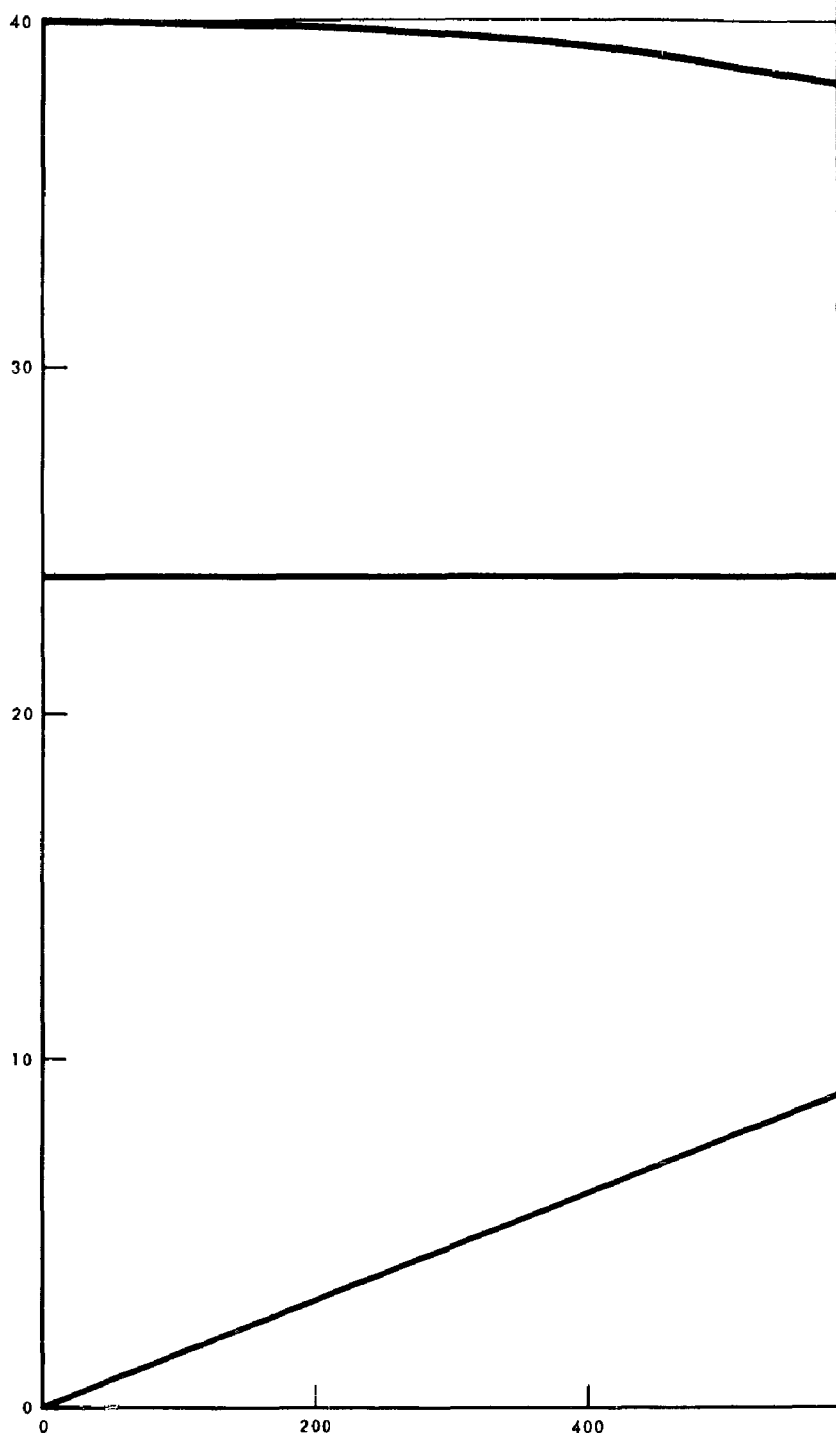
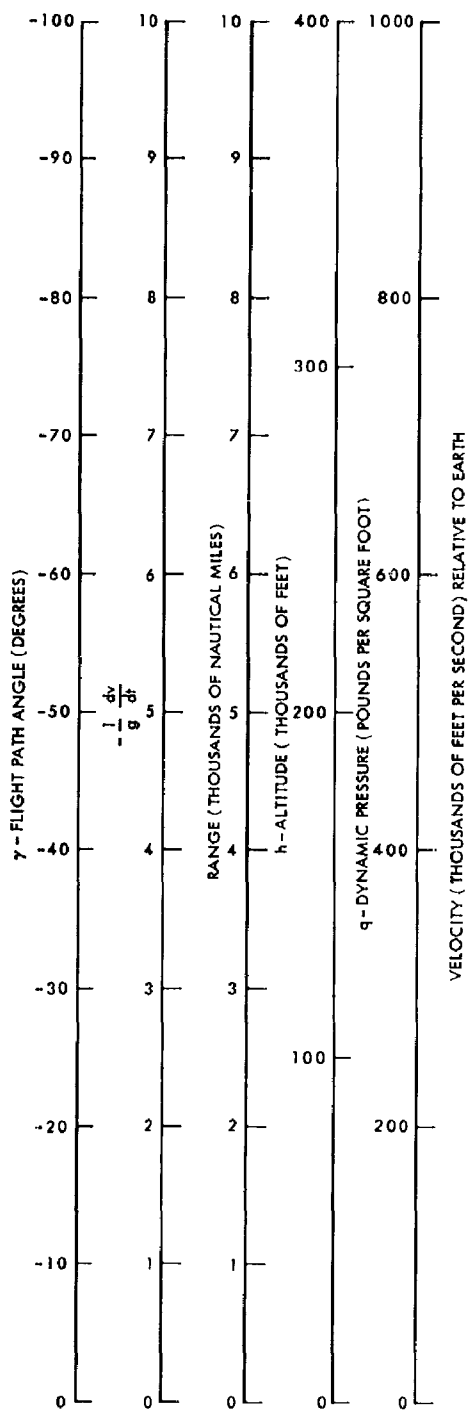
2

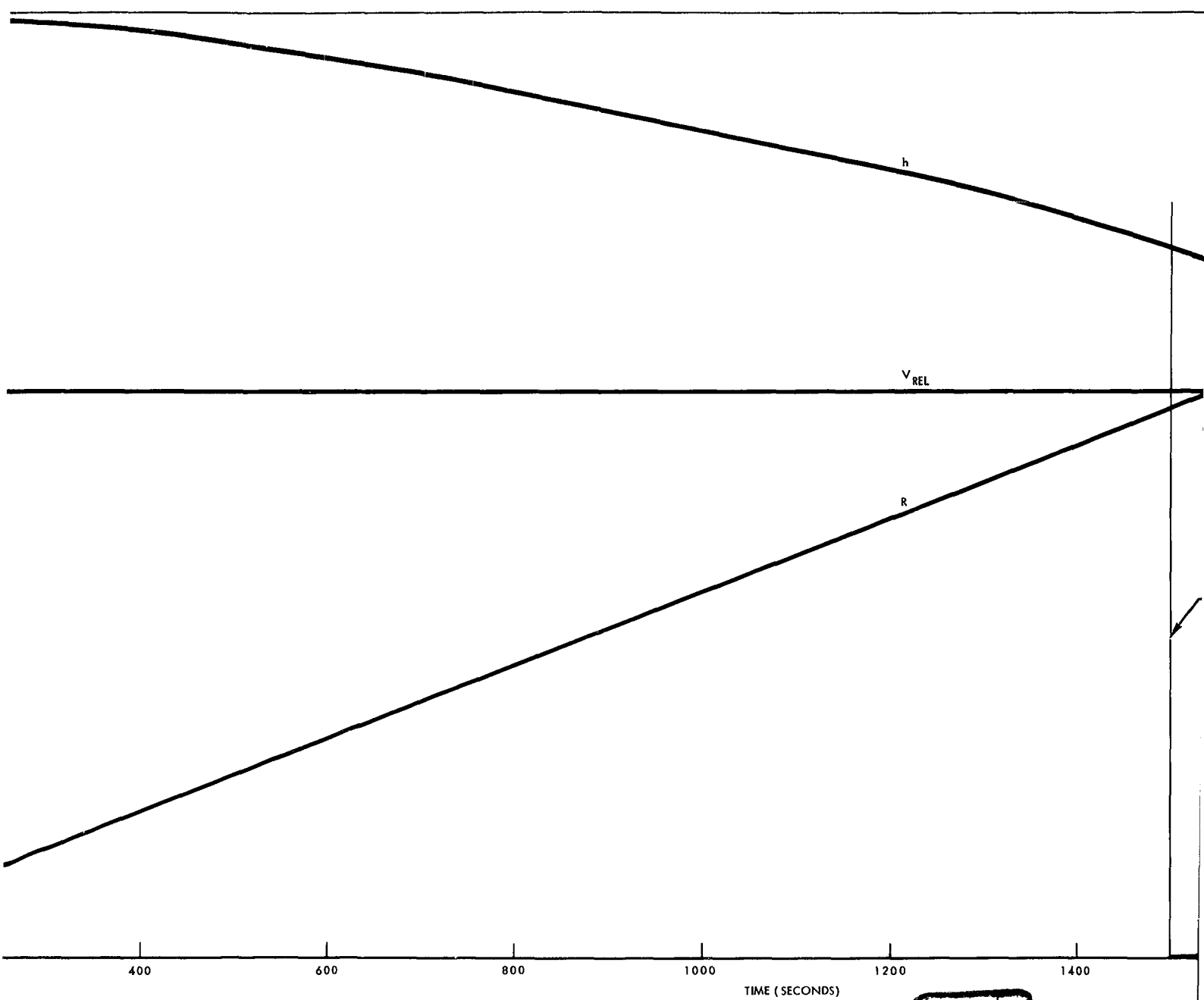
Figure 10.



3

Figure 10. Orbital Decay Trajectory of Tumbling Fuel Element Ejected from Reactor Vessel at 400,000 Feet





2

Figure

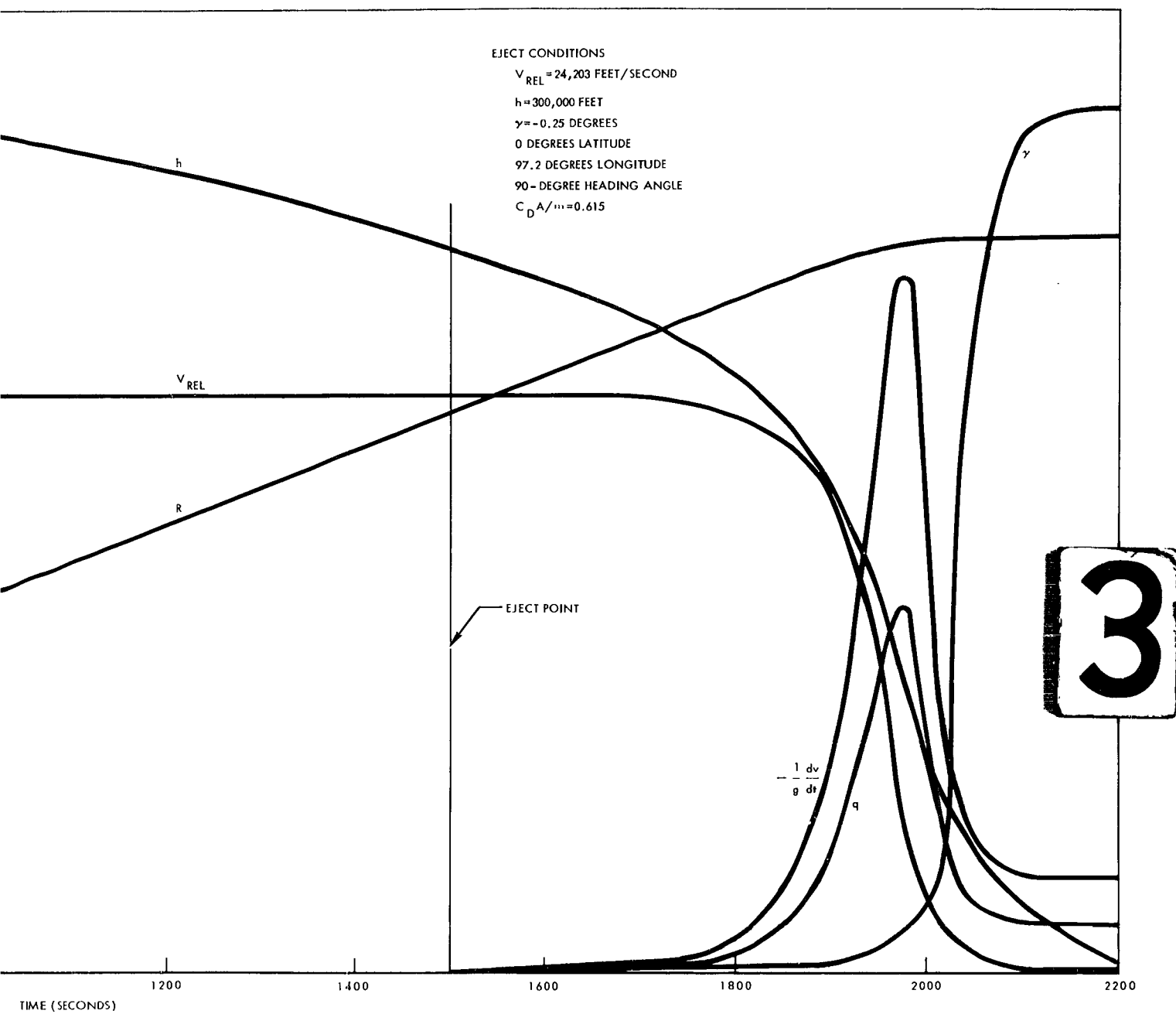
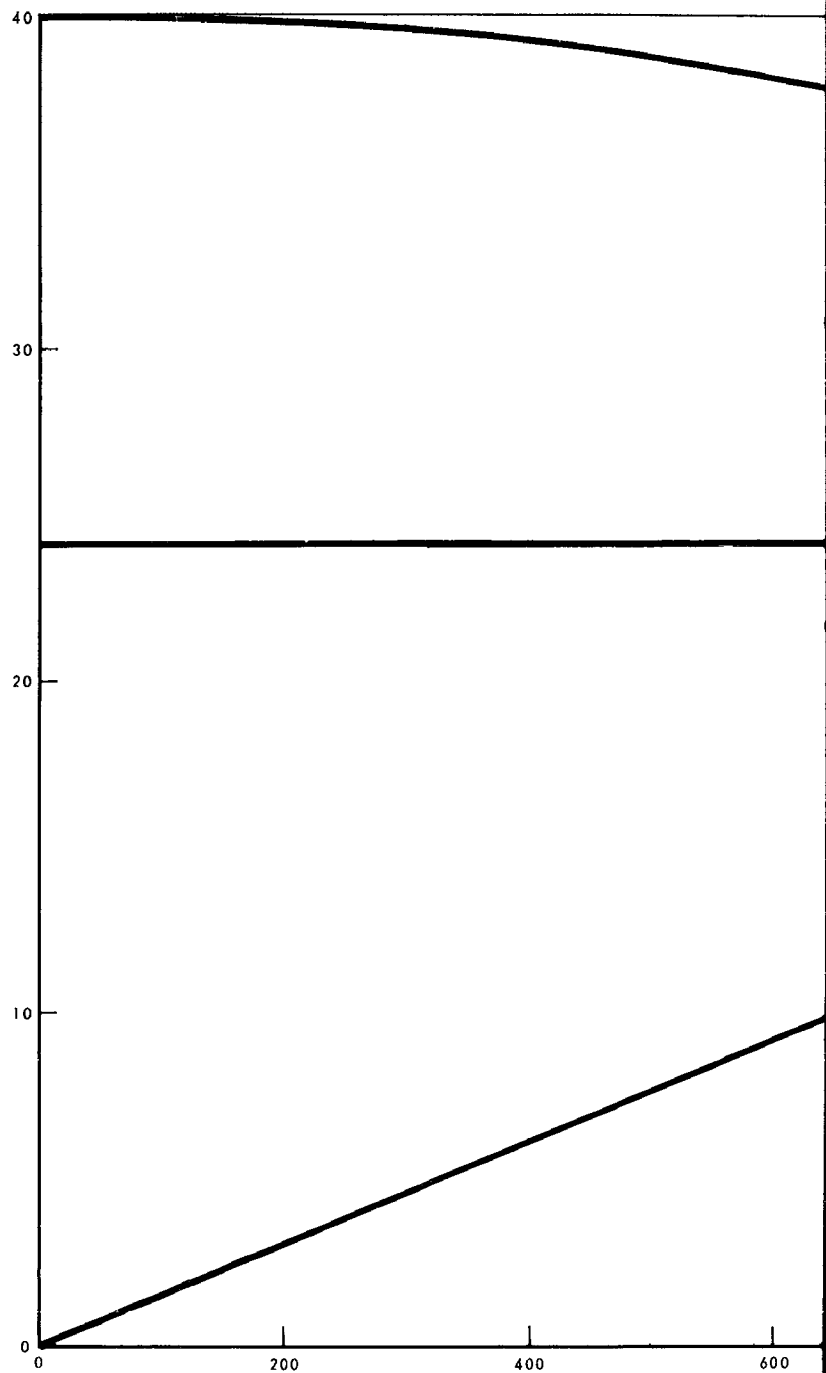
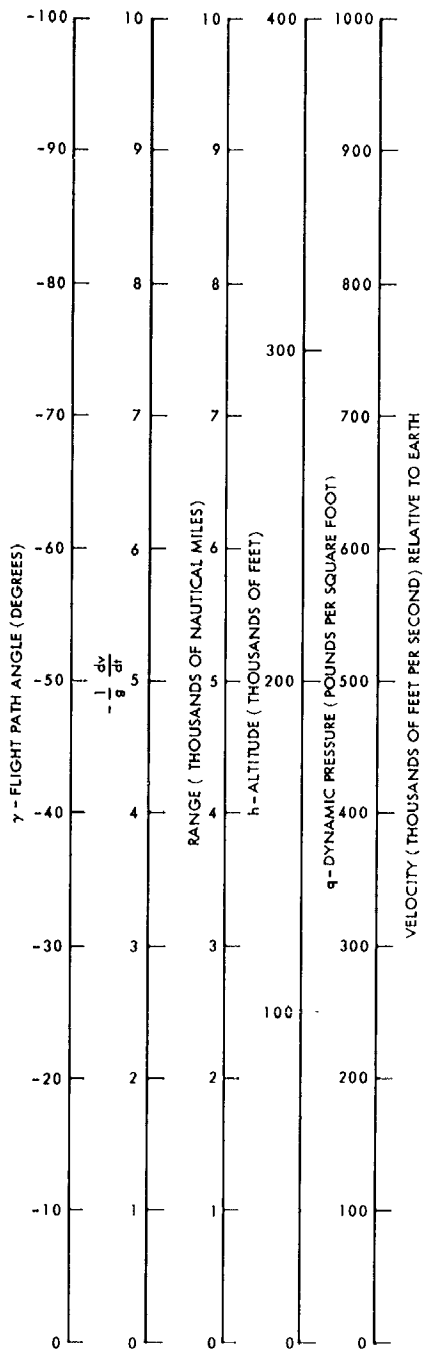
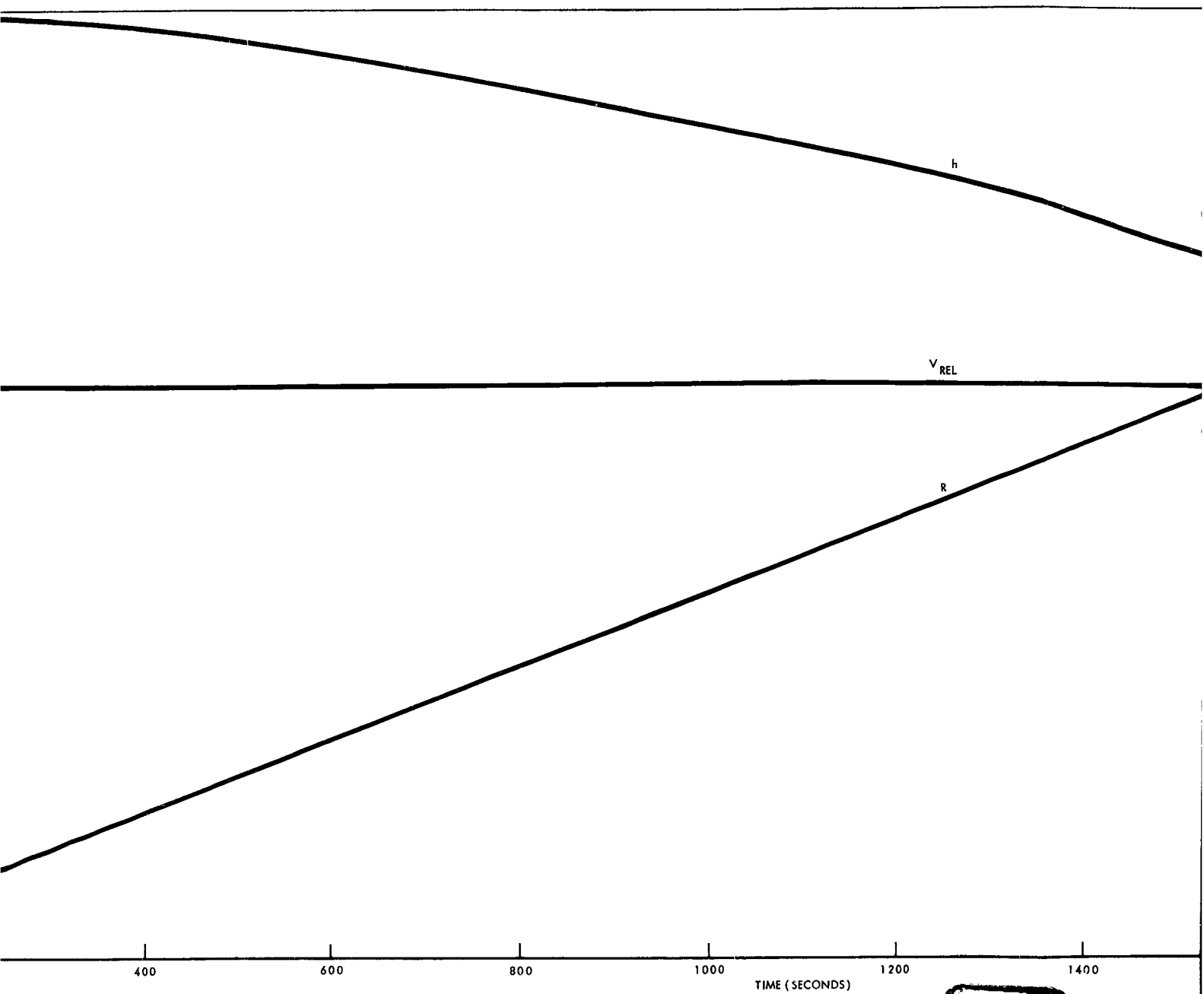


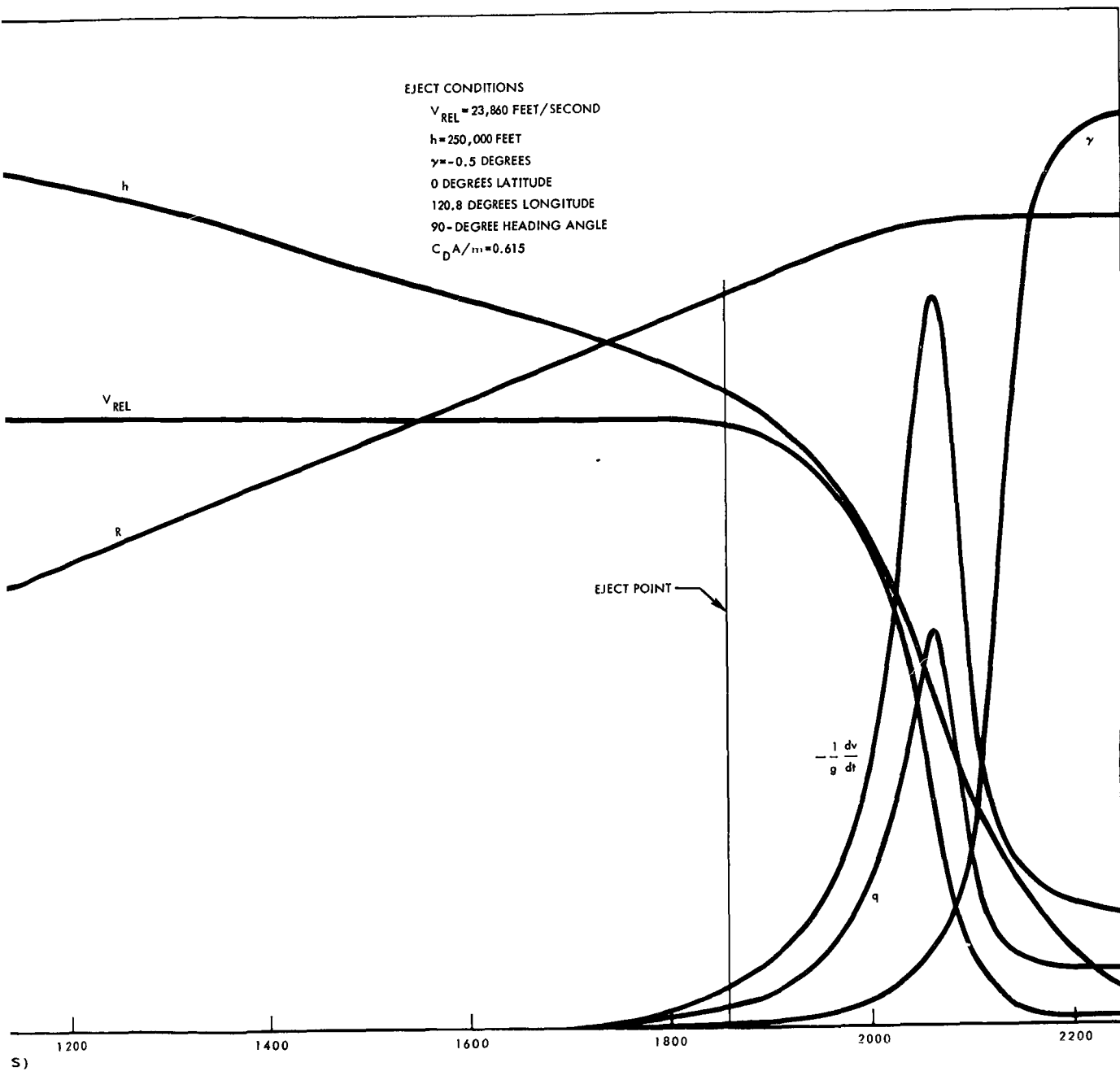
Figure 11. Orbital Decay Trajectory of Tumbling Fuel Element Ejected from Reactor Vessel at 300,000 Feet





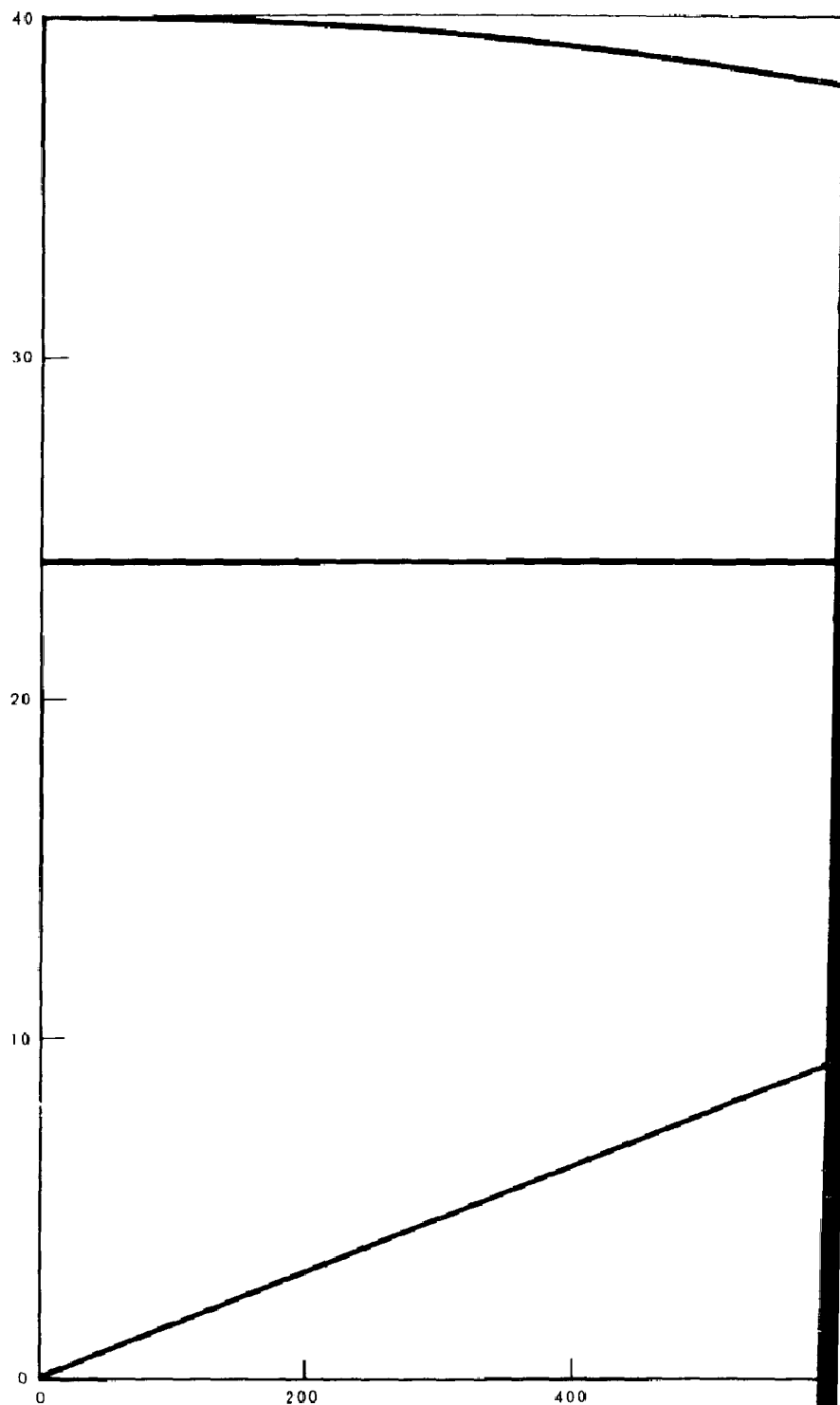
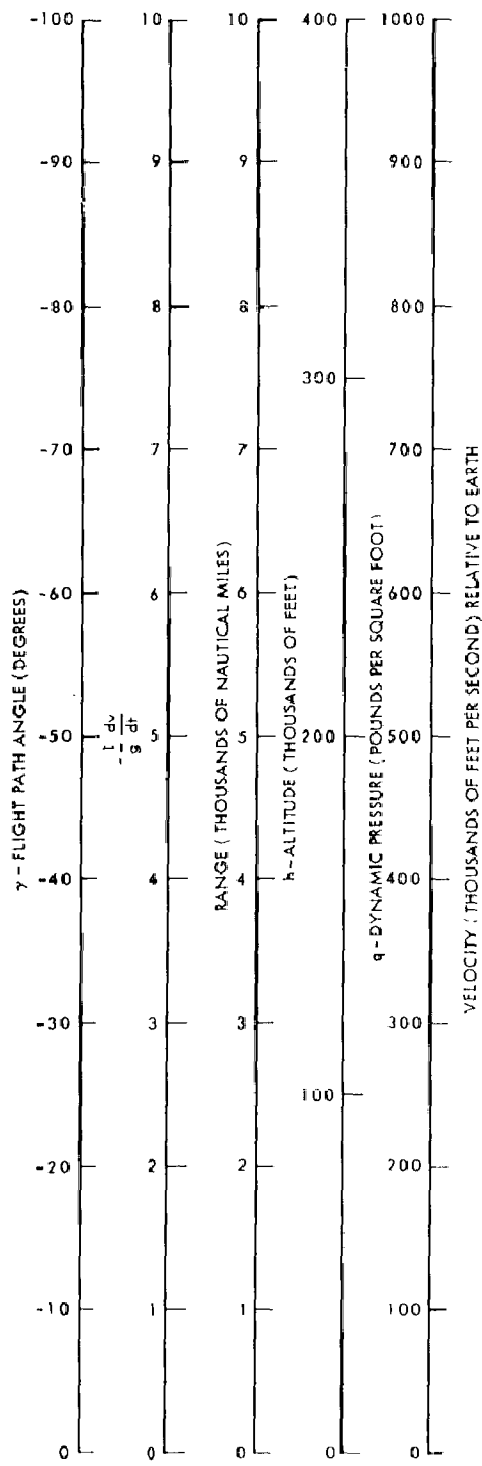
2

Figure

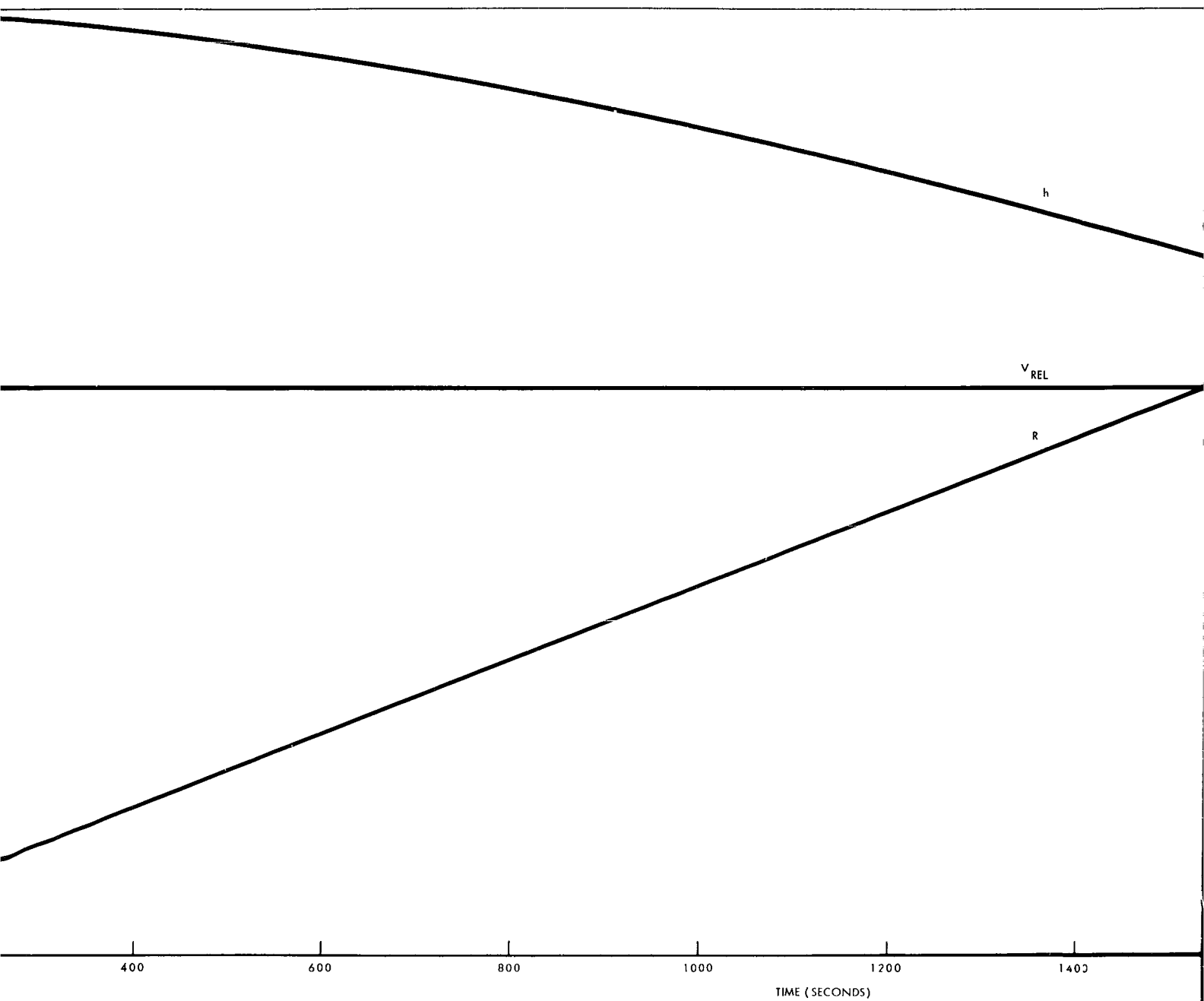


3

Figure 12. Orbital Decay Trajectory of Tumbling Fuel Element Ejected from Reactor Vessel at 250,000 Feet



1



2

Figure 13. O
R

3

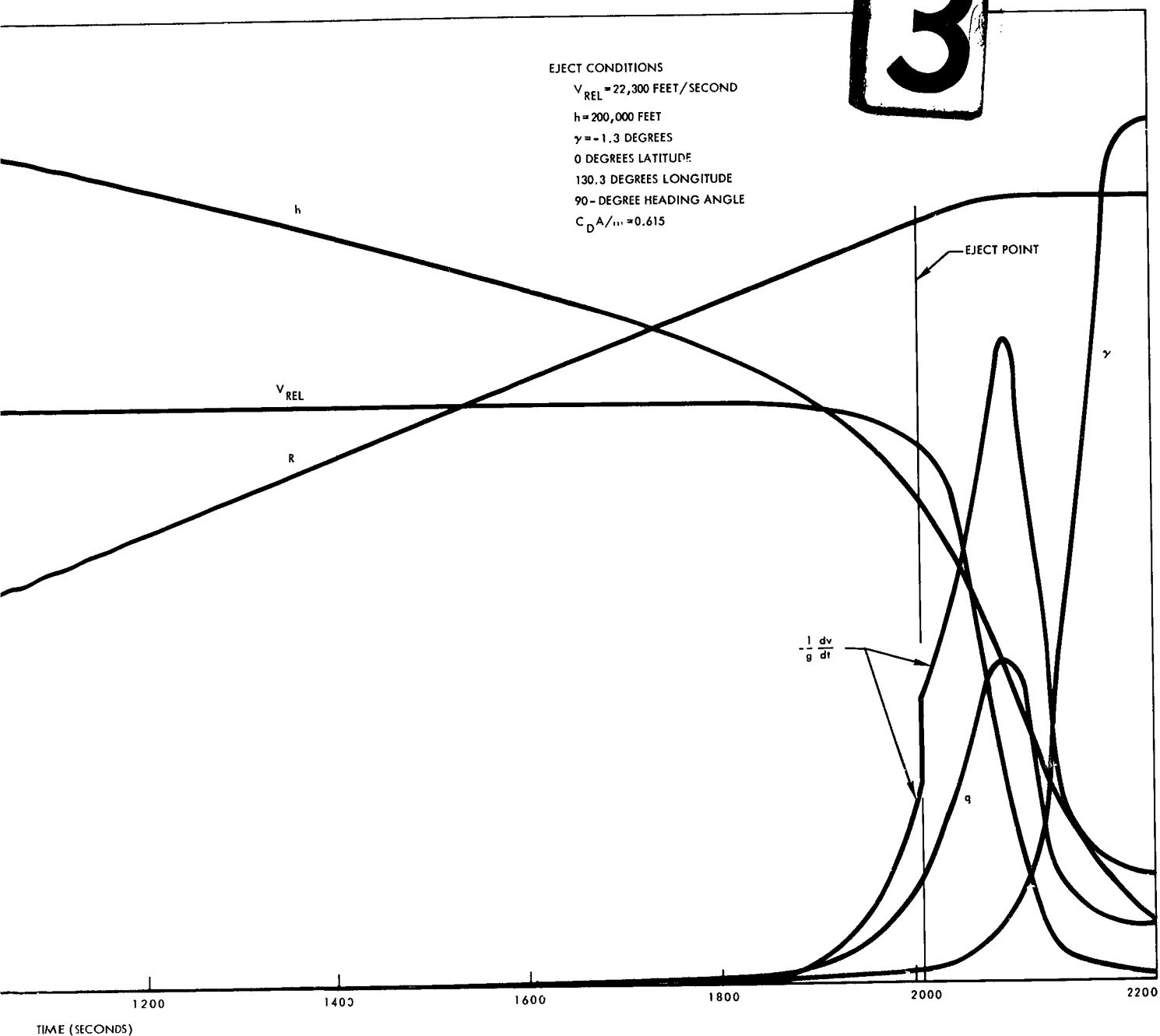


Figure 13. Orbital Decay Trajectory of Tumbling Fuel Element Ejected from Reactor Vessel at 200,000 Feet

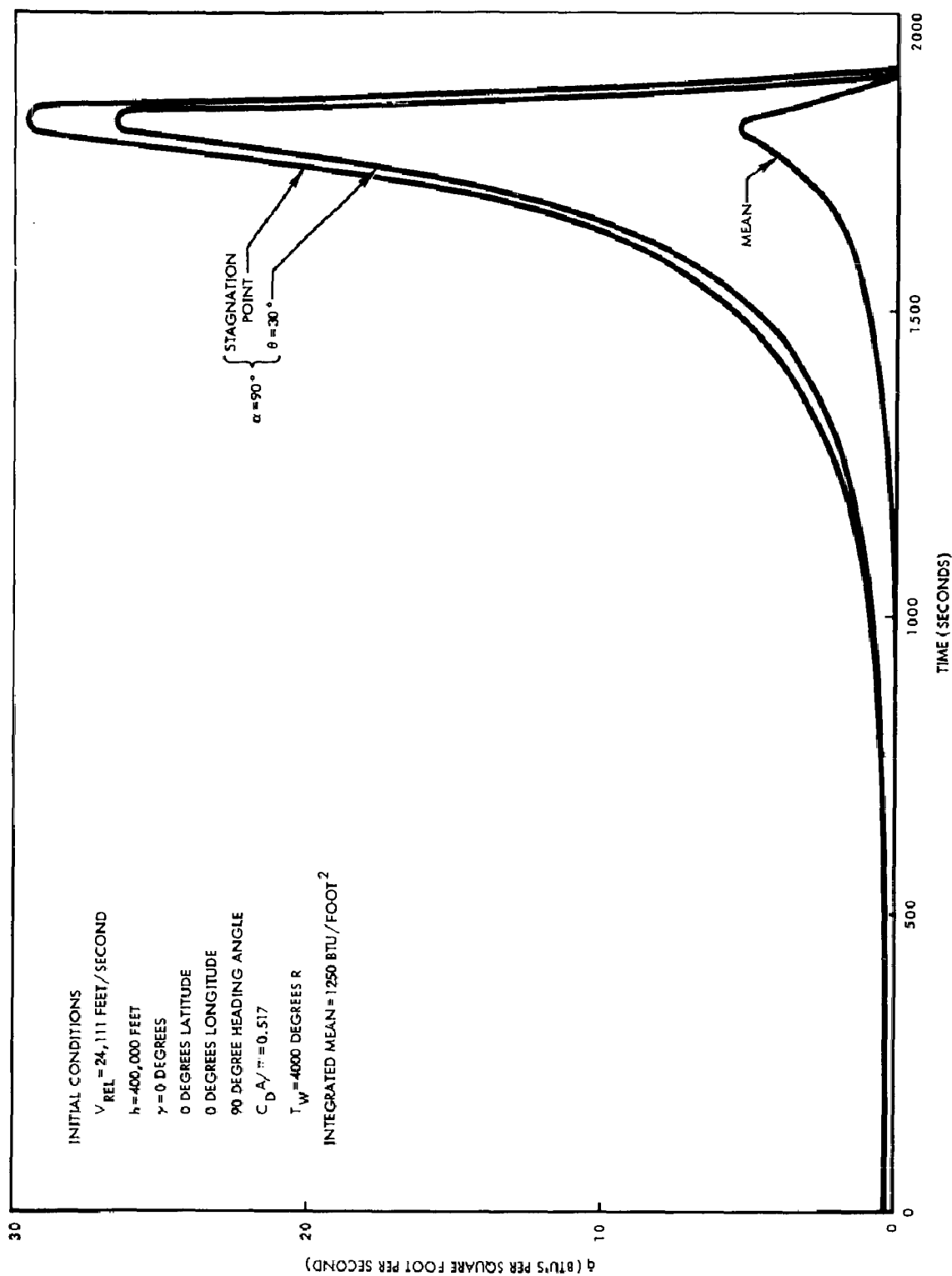


Figure 14. Heat-Transfer Rate Versus Time for Spacecraft Tumbling in Trajectory, Flight-Path Angle Zero Degrees

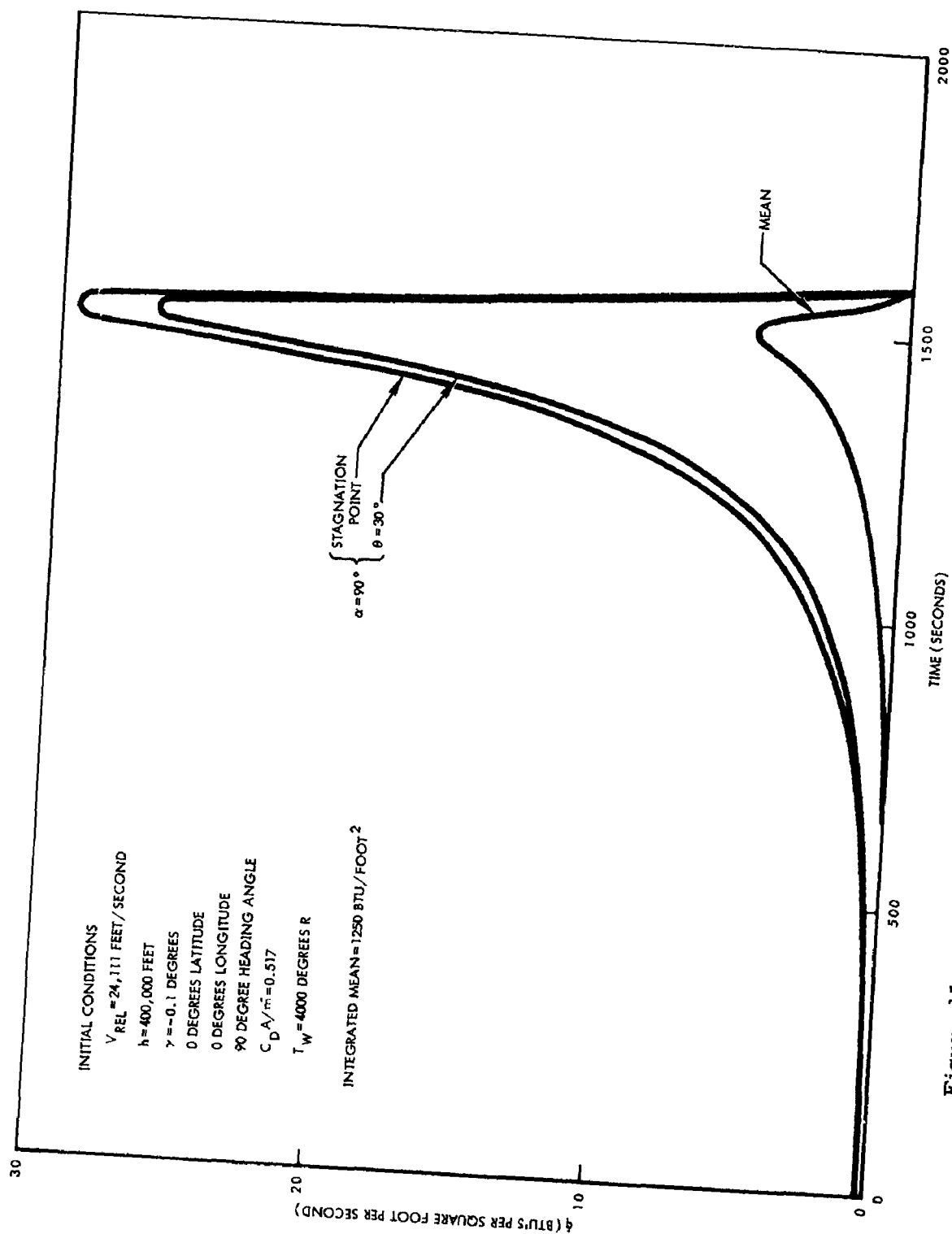


Figure 15. Heat-Transfer Rate Versus Time for Spacecraft Tumbling in Trajectory, Flight-Path Angle -0.1 Degree

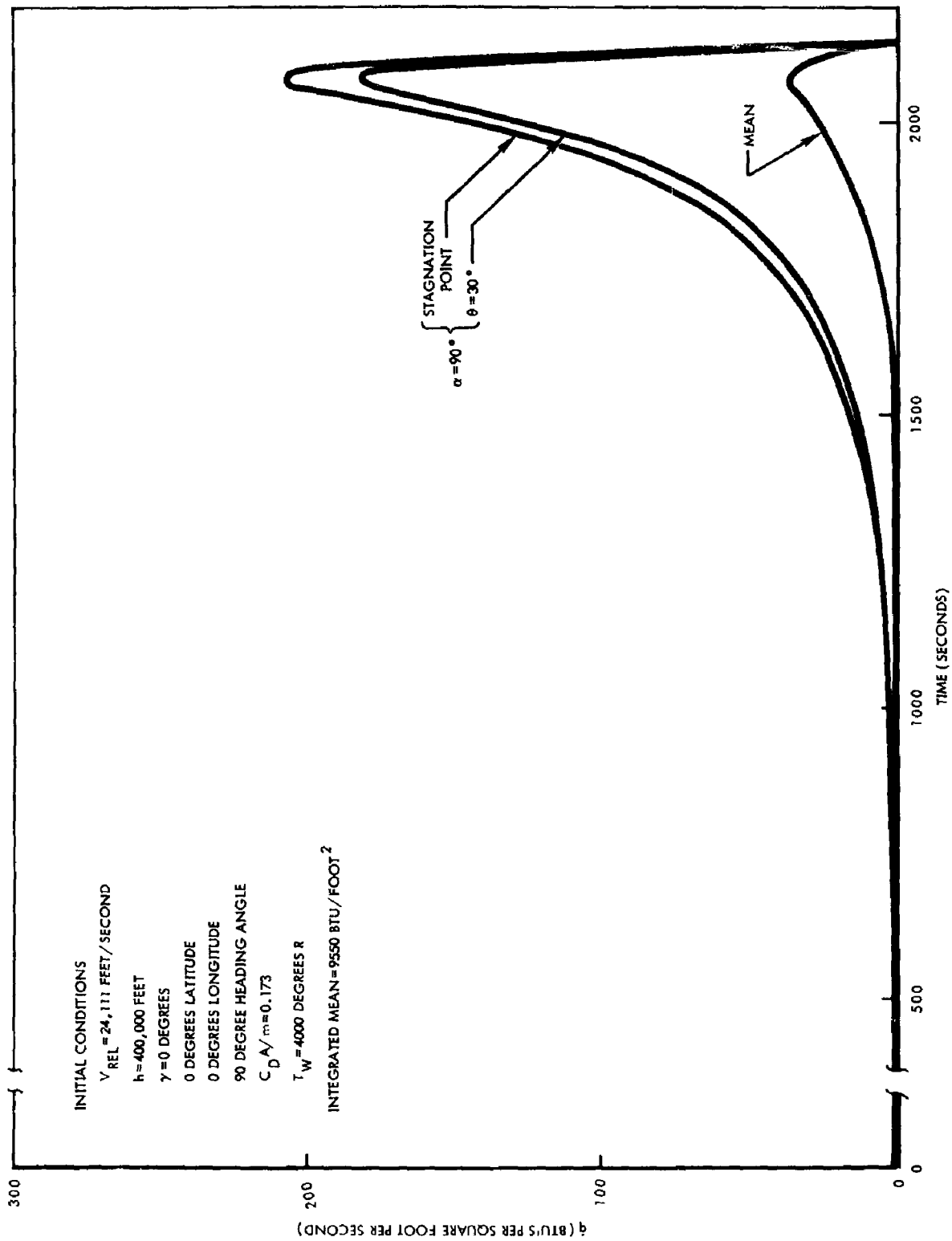


Figure 16. Heat-Transfer Rate Versus Time for Reactor Vessel Tumbling in Trajectory, Flight-Path Angle Zero Degrees

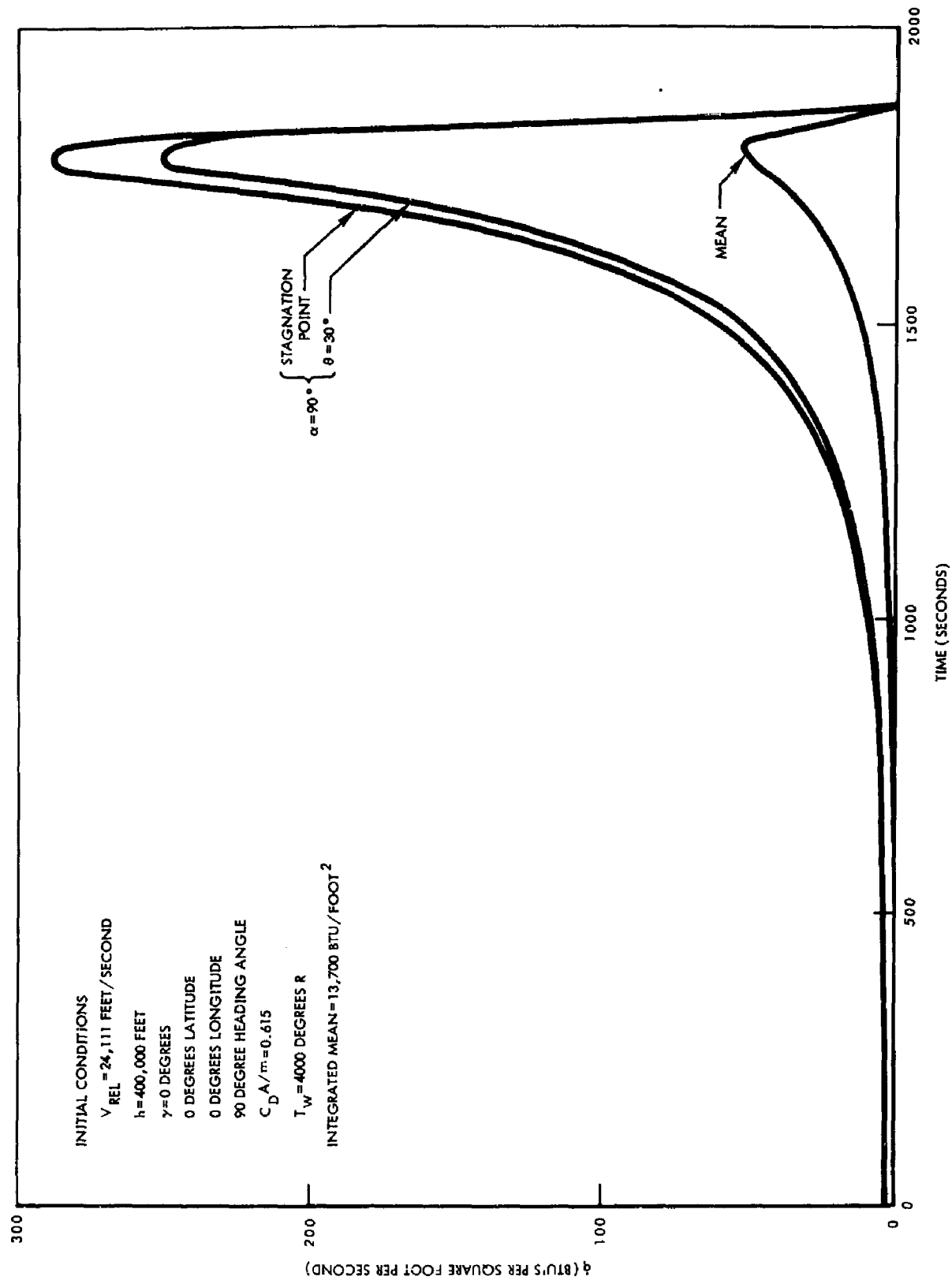


Figure 17. Heat-Transfer Rate Versus Time for Fuel Element Tumbling in Trajectory, Flight-Path Angle Zero Degrees

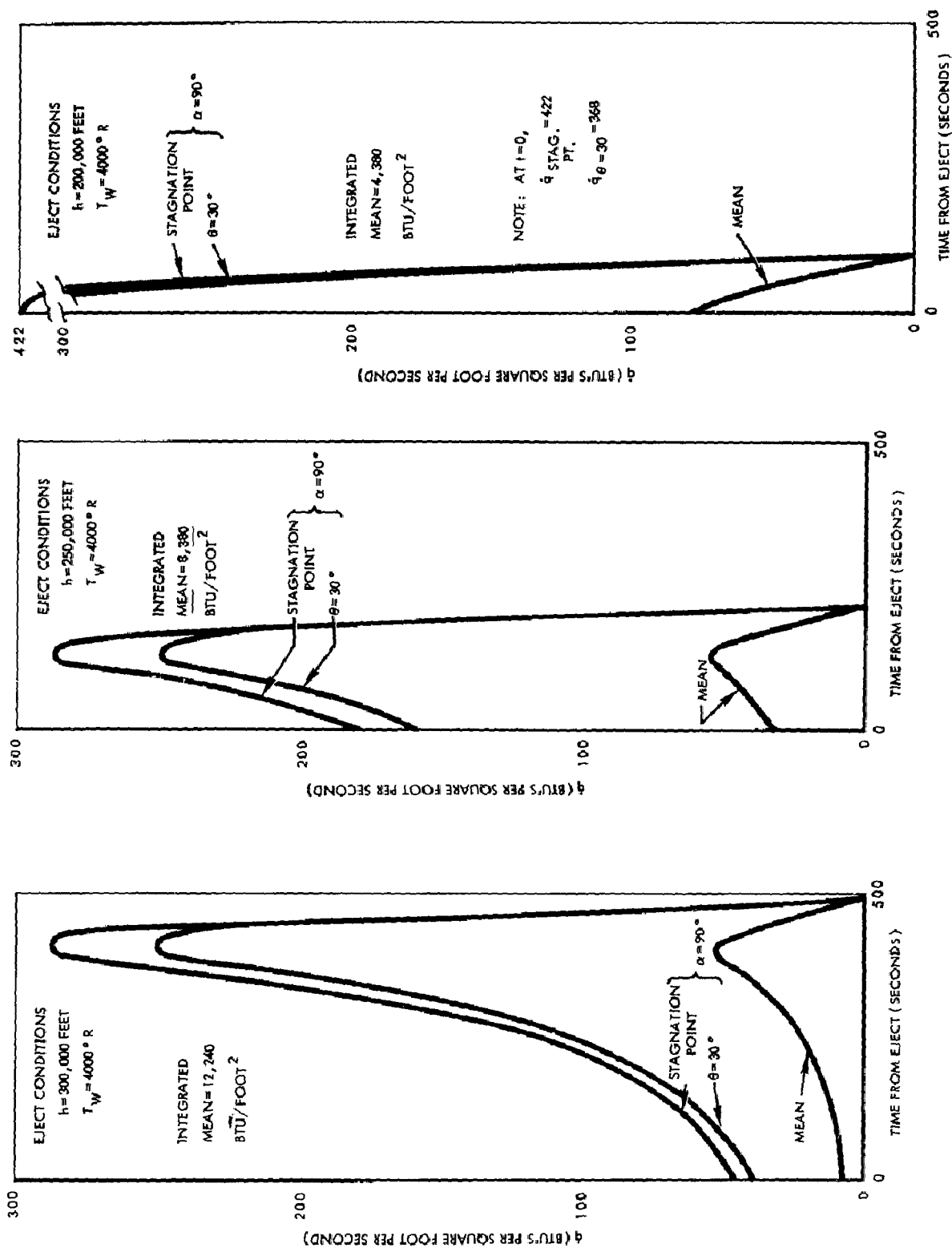
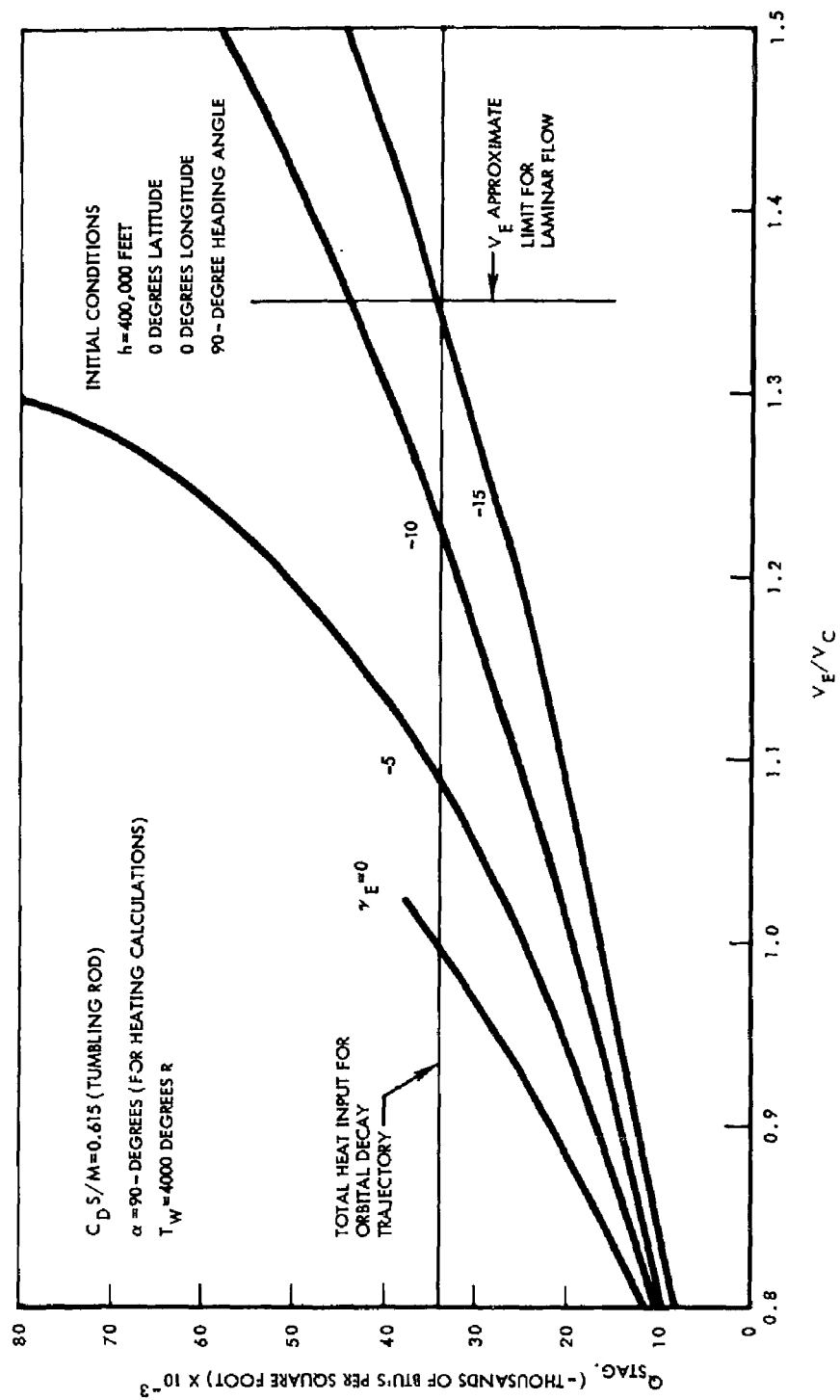


Figure 18. Heat-Transfer Rate Versus Time for Fuel Element After Ejection from Reactor Vessel



NOTE: Heat transfer rates were integrated above radiation value of 65 Btu per square foot per second

Figure 19. Total Heat Input to Fuel Element During Re-entry at Stagnation Point

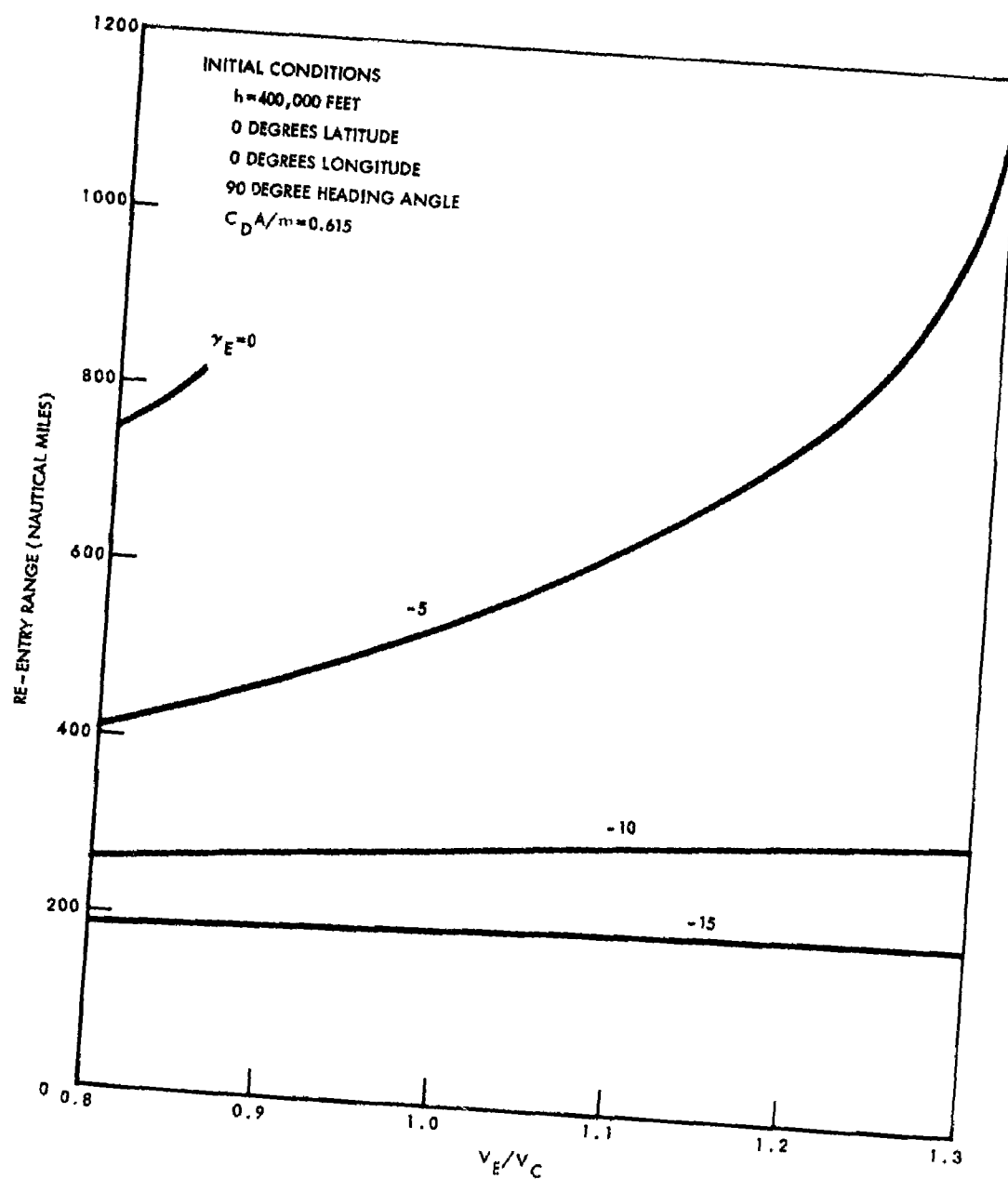


Figure 20. Variation of Fuel Element Re-Entry Range With Entry Velocity and Flight-Path Angle Variations

center of pressure of flat-faced cylinders for the velocity range of interest is at approximately one caliber aft of the front face. If the reactor vessel were "clean" (i. e. , no tubing attached), the center of gravity would be less than one caliber aft of the front face. Hence, the reactor vessel may tend to stabilize at zero angle of attack. The modified Newtonian drag coefficient for a flat-faced cylinder at zero angle of attack is 1.82, based on the cross-sectional area. Based on the same area, the mean modified Newtonian drag coefficient of a tumbling cylinder of the same overall dimensions as the reactor vessel is 1.81. Thus the reactor vessel trajectories are valid for either axial or tumbling attitudes.

The rod trajectories were computed for the orbital decay of the fuel element alone and for initial conditions occurring from the decay trajectories of the reactor vessel at assumed ejection altitudes of 400,000, 300,000, 250,000, and 200,000 feet. The trajectories for ejection from the reactor vessel are presented in Figures 10 through 13. Corresponding heat-transfer rates are given in Figures 17 and 18.

The heat flux on the front face of the reactor vessel (Figure 21) was computed using the trajectory data obtained from GD/Astronautics, assuming the reactor vessel to be attached to the complete NAP unit mounted on an Agena B, and complete unit to be in the axial flow attitude.

This is considered the most likely attitude of re-entry for the reactor vessel, since the vessel will probably remain attached to the nose of the vehicle during re-entry. However, the NAP unit accessories (pump and plumbing) must be removed to expose the reactor vessel to the heating environment.

All trajectories were equatorial-east heading and were calculated utilizing the AFSWC earth coordinate trajectory program described in Reference 4. Circular orbital velocity at 400,000 feet altitudes is 24,111 feet per second relative to the earth.

Heat-transfer rates were determined utilizing an IBM 7090 program which incorporated the assumptions of Laminar flow and Newtonian pressure distribution.

The mean value of heat-transfer rate accounting for circumferential distribution and tumble by an approximation of Lee's distribution was found to be 0.185 of the stagnation value for the fuel element in cross flow.

Some of the important results of these studies are summarized below.

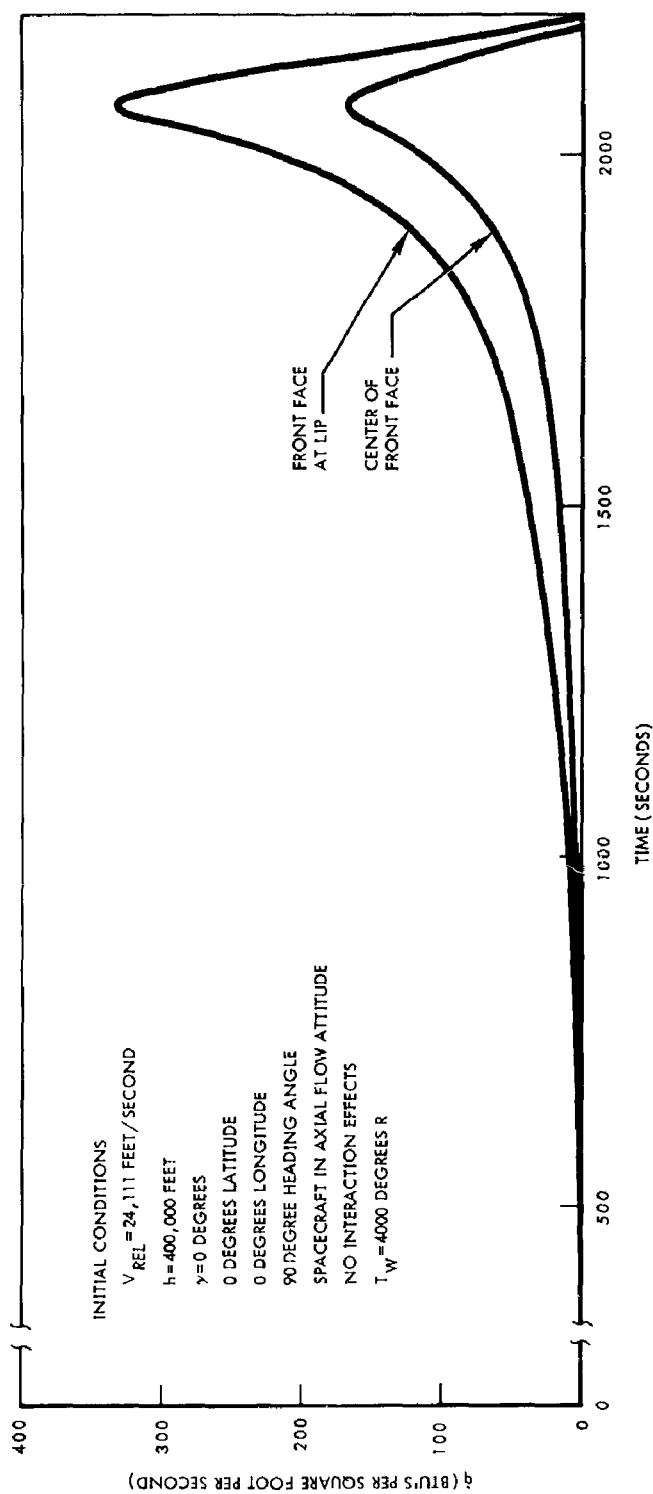


Figure 21. Heat-Transfer Rate Versus Time for Exposed Reactor Vessel Attached to Spacecraft in Axial Re-Entry

Effect of Initial Flight-Path Angle for Decay Trajectories

Decay trajectories were computed assuming that the flight path angle at 400,000 feet was 0, -0.05, and -0.1 degrees with an initial velocity relative to the rotating earth of 24,111 feet per second. The effect of changing flight-path angle was to shift the time scale of significant occurrences such as peak g's and peak heating; e. g., for the complete NAP unit (Figures 1 through 3, when $\gamma_E = 0$ degrees, $t_{gmax} = 1887$ seconds; when $\gamma_E = -0.05$ degrees, $t_{gmax} = 1718$ seconds; and when $\gamma_E = -0.1$ degrees, $t_{gmax} = 1555$ seconds. The peak value of g in all cases is virtually identical, $g_{max} = 7.35$, and the variations with time when the value is significant are virtually identical. Therefore, within the limits of initial flight-path angles, an angle of -0.1 degrees $\leq \gamma_E \leq$ an angle of 0 degree for the decay trajectories,

$$f_1(t_1) = f_2(t_2 + \tau) \quad (1)$$

where f_1 is the value of some independent variable such as deceleration for a given decay trajectory, f_2 is the same independent variable with a different assumed initial flight path angle, and τ is the incremental time difference for, say, peak deceleration of trajectories 1 and 2. Such a relationship would apply during the time that the variables have significant values.

In the case of aerodynamic heating, this would mean that the heating rate history for a decay trajectory with $\gamma_E = 0$ degrees and $\gamma_E = -0.1$ degrees would be similar except that the peak heat flux for $\gamma_E = 0$ degrees would occur later than the peak for $\gamma_E = -0.1$ degrees. The major difference would be a very low heating rate of long duration for $\gamma_E = 0$ degrees as compared to $\gamma_E = -0.1$ degrees. This may be seen in Figures 14 and 15 for the complete NAP system spacecraft.

Effect of Fuel Element Ejection at Different Altitudes

Decay re-entry trajectories were run for the reactor vessel containing the fuel elements to determine initial conditions for the fuel elements when they are ejected at 400,000, 300,000, 250,000 and 200,000 feet. The aerodynamic heating rate to the fuel element stagnation line and the mean heating rate after ejection from the reactor vessel at 400,000, 300,000, 250,000 and 200,000 feet is summarized in Figures 17 and 18. This figure shows that at 300,000 and 250,000 feet ejection altitudes, the peak heat flux is virtually identical but that the integrated heating under the curve is less for the 250,000 feet ejection case. The 200,000 feet altitude ejection case has a much higher heat transfer rate peak, the peak occurring immediately upon ejection. The curve of \dot{q} versus time for ejection at 400,000 feet (Figure 17) is similar to the 300,000 feet ejection curve except that it has an appreciable period of time at a very low heat flux. The area under the curve

of \dot{q} versus time is nearly the same for the 400,000 and 300,000 feet altitude fuel-element-ejection cases.

An examination of the time histories of fuel element heat flux (Figures 17 and 18) and the re-entry trajectories (Figures 10 through 13) indicates that peak heat flux occurs at an altitude of approximately 200,000 feet for all fuel element ejection cases.

THERMODYNAMIC DATA

Thermodynamic analysis of NAP reactor component heating is based on the stagnation-point temperature history and heat-flux distribution determined through aerodynamic analysis of credible re-entry trajectories. Thermodynamic consideration of component heating, therefore, originates at the surface, using the results of aerodynamic analysis as input data. Primary interest is focused on the temperature and input heat flux associated with melting, ablation, or combustion of the component.

In order to coordinate the studies in different discipline areas and efficiently evolve applicable data, certain basic assumptions have been made for this study. Primary attention was centered on the fuel elements, as the most important component under consideration. Fuel element wall temperature for stagnation-point temperature and heat-flux computations was taken as 4000 R. Heat-flux distribution over a fuel element follows the cosine law: $\dot{q}_\theta = \dot{q} \cos^n \theta$ (An acceptable value of n was considered to be 3/2.) Heat transfer computations are based on fuel element angle of attack of 90 degrees, vehicle and reactor angle of attack of zero degrees. Heat loss by radiation is computed on the basis of radiation to space at zero degrees R.

REQUIREMENTS

In actual re-entry, the reactor assembly would be attached to a space vehicle. A combination of aerodynamic heating and aerodynamic pressure would furnish the means for breakup and fuel element exposure. These effects must be great enough and must occur at sufficient altitude to permit separation of the reactor from the vehicle, failure of the reflector retaining strap, failure of the reactor vessel lip (lid attachment), exposure of the fuel elements, and dispersal of the fuel element material.

Computations of aerodynamic heating and pressure forces were made for the complete vehicle, the reactor vessel, and the fuel elements for various conditions of re-entry. Computed results which indicate that aerodynamic heating or pressure effects are not sufficient to cause failure are interpreted to show that failure will not occur. It is of value to determine whether the above events can occur in sequence in order to determine the extent of the assembly which may validly be tested. The establishment of the altitudes at which appreciable heating or pressure may be present establishes the limits of altitude which may yield interpretable test results.

PREDICTED FAILURE OF COMPONENTS

In order to determine the behavior of components under the conditions most likely to cause failure, attitudes in the trajectory as indicated above, were assumed. Reference to Figures 6 and 14 indicates that at an altitude of 260,000 feet the stagnation-point heat flux on the complete vehicle is only 10 BTU's per square foot per second and the dynamic pressure 20 pounds per square foot. This dynamic pressure is very small, and the stagnation-point heat flux corresponds to a mean heat flux over the vehicle circumference of about 2 BTU's per square foot per second, which would be balanced by heat radiation at less than 1000 F, so that the structure could not start to fail above this altitude. Similar comparison (Figure 22) indicates that the reactor-vessel lip (if the reactor entered alone) could not start to fail above 250,000 feet.

On the basis of the above indications, it appears that sequential separation of the reactor from the vehicle exposure of the fuel elements, and fuel element dispersal through aerodynamic effects is not to be expected. These events can conceivably be effected, however, by other means; therefore, further effort was concentrated on the possible dispersal of the fuel elements alone. Figures 10, 17, and 18 indicate that if the fuel elements are ejected at 400,000 or 300,000 feet, the stagnation-point heat flux is almost the same (40 versus 43 BTU's per square foot second) and the mean heat flux is identical (8 BTU's per square foot-second). This would indicate that there is no advantage in fuel-element exposure above 300,000 feet. In fact, as in the case of the complete vehicle, the rod would tend to cool rather than heat during the interval from 400,000 to 300,000 feet if the temperature at exposure were in the order of 1300 F. The integrated stagnation-point heat flux is almost identical for the two altitudes of exposure, and integrated mean heat flux values are within 10 percent of each other. This means that whether or not the fuel element is heated in the interval from 400,000 to 300,000 feet, the total heat input is closely identical for exposure at either altitude.

Expected extent of fuel element heating may be clearly shown by study of the heating requirements for fuel element ablation and comparison with the heat input available after exposure at 300,000, 250,000, and 200,000 feet. The latter values are presented in Figure 23. The following simple computations indicate the relation between required and available heat inputs.

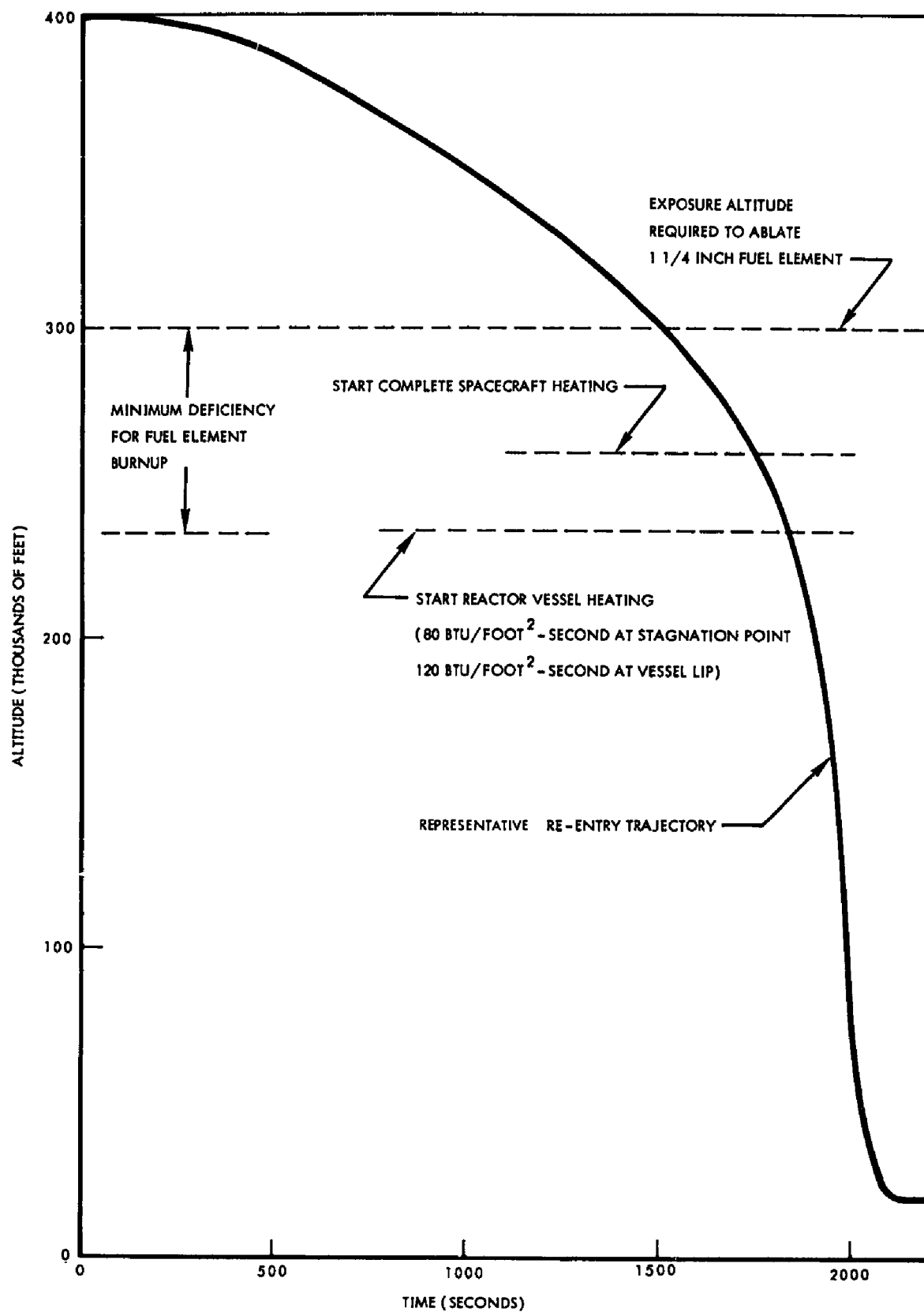


Figure 22. Altitude Deficiency for Fuel Element Burnup

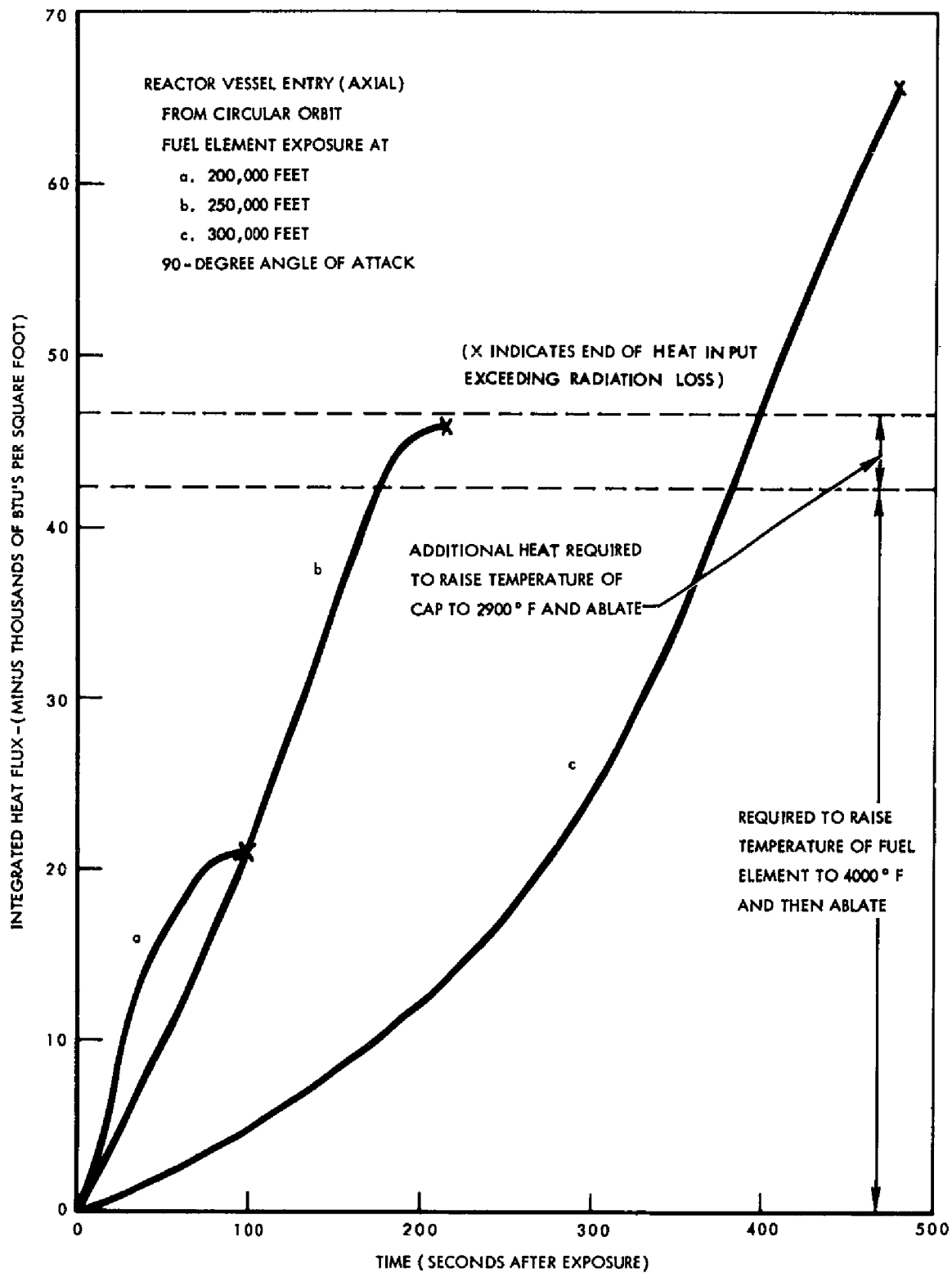


Figure 23. Fuel Element Aerodynamic Heating at Stagnation Point Versus Time

HEAT REQUIRED TO ABLATE FUEL ROD AND CLADDING

Heat capacity per inch of fuel element (1 1/4-inch nominal diameter) equals $\rho C \pi R^2$

$$= 0.2168 \text{ lbs/in}^3 \times 0.18 \frac{\text{BTU}}{\text{Lb}^\circ \text{F}} \times 3.1416 \times 0.606^2 \text{ in}^2$$

$$= 0.04502 \text{ BTU/in/}^\circ \text{F}$$

Heat required to raise temperature of an inch of fuel element from 200° F to 4000° F (3800 degrees)

$$0.04502 \times 3800 = 171.07 \text{ BTU per inch of fuel element length}$$

Heat capacity per inch of cladding

$$= \rho C \pi (R_1^2 - R_2^2)$$

$$= 0.317 \frac{\text{lbs}}{\text{in}^3} \times 0.095 \frac{\text{BTU}}{\text{lb}^\circ \text{F}} \times 3.1416 \times (0.621^2 - 0.606^2) \text{ in}^2$$

$$= 0.00174 \text{ BTU/}^\circ \text{F}$$

Heat required to raise temperature of cladding from 200° F to 2900° F (2700 degrees)

$$= 0.00174 \times 2700 = 4.698 \text{ BTU/inch of fuel element length}$$

Heat required to ablate fuel element (per inch) equals $\rho Q_a \pi R^2$

$$= 0.2168 \times 540 \times 3.1416 \times 0.606^2$$

$$= 540 \times 0.255 = 137.7 \text{ BTU/inch of fuel element length}$$

Heat required to ablate cladding (per inch)

$$= \rho Q_a \pi (R_1^2 - R_2^2)$$

$$= 0.317 \times 1500 \times 0.0578 = 27.5 \text{ BTU/inch}$$

Total heat required is then 341 BTU/inch of fuel element length:

$$\begin{array}{r}
 171.1 \\
 4.7 \\
 137.7 \\
 \hline
 27.5 \\
 341.0 \text{ BTU}
 \end{array}$$

REQUIRED HEAT FLUX TO SUPPLY HEAT NECESSARY FOR FUEL ELEMENT ABLATION

Effective heating area, assuming distribution of $\cos^{3/2} \theta$

$$A = \int_A \frac{q\theta}{q} dA = \int_L \int_{-\pi/2}^{+\pi/2} R \cos^{3/2} \theta d\theta dL$$

where $dA = R d\theta dL$ or, per inch of length,

$$\begin{aligned}
 A_e &= R \int_{-\pi/2}^{+\pi/2} \cos^{3/2} \theta d\theta = 2R \int_0^{\pi/2} \cos^{1.5} \theta d\theta \\
 &= 2R \left[\frac{\sqrt{\pi}}{2} \frac{\Gamma(1.25)}{\Gamma(1.75)} \right] \quad (\text{Reference 5}) \\
 &= 1.7482R \text{ square inches} \\
 &= \frac{1.7482 \times 0.621}{144} = 0.007534 \text{ square feet per inch of fuel element length}
 \end{aligned}$$

Required heat input (BTU/ft²) is then $341/0.007534 = 45,460$ BTU/ft² greater than the heat lost by radiation about 70 BTU per square foot per second at ablation temperature.

Heat loss by radiation is $\sigma A \epsilon T^4 = Q_R$

$$\sigma = 0.173 \times 10^{-8} \frac{\text{BTU}}{\text{ft}^2/\text{hr}/^\circ\text{R}^4}$$

$$\sigma = 0.48 \times 10^{-12} \frac{\text{BTU}}{\text{ft}^2/\text{sec}/\text{R}^4}$$

or

$$Q_R = 0.481 \epsilon \frac{T^4}{1000} \frac{\text{BTU}}{\text{ft}^2/\text{sec}}$$

Table 2 shows the variation in radiant heat loss as a function of fuel-element temperature and emissivity.

Table 2. Variations in Radiant Heat Loss

Fuel Element Temperature	Emissivity	
	$\epsilon = 0.3$	$\epsilon = 0.6$
1000 R	0.144	0.288
2000 R	2.3	4.6
3000 R	11.7	22.3
4000 R	36.9	73.7

This value of integrated heat flux corresponds to entry from circular orbit with fuel element exposure above 250,000 feet. However, this heat input is for a 90-degree angle of attack without tumbling or spinning, and is based on physical constants of the rod material which are extrapolated from data obtained at temperatures below 1200 F. It therefore appears reasonable to assume an arbitrary factor of safety of at least 1.5 in determining required heat input. This corresponds to rod exposure at 300,000 feet as the minimum altitude for conceivable ablation of an 1 1/4-inch fuel element.

Continuing this analysis, a relationship can be obtained between altitude of exposure and the diameter of fuel element which can theoretically be ablated. If the diameter is varied, the mass to be heated and ablated varies as the square of the diameter per unit length of fuel element. The area available to accept this heat input varies as the first power of fuel element diameter. This assumes an isotropic fuel element, but on this basis, the ratio of heat input required to heat available is equal to $D^2/D = D$ (fuel element diameter). Therefore, as heat input varies with altitude of exposure, so fuel element diameter must vary directly with available heat input, if the

fuel element is to be heated and ablated. This would not be true if input heat varied with fuel element diameter; however, analysis indicates that when change in trajectory with fuel element diameter is considered, the integrated heating rate is independent of fuel element diameter. The relationship between the altitude of exposure and the diameter of fuel element which can theoretically be heated and ablated is shown in Figure 24.

These data may also be interpreted from the standpoint that if a fuel element smaller in diameter than that which can be dispersed from a given altitude of exposure be included in a test package, then the heat available exceeds the requirement by the ratio of fuel element diameters. On this basis, it is suggested that tests include fuel elements of a range diameters ranging from full-scale down to quarter-scale. Such procedure should also yield some data on the probability of rods tumbling or spinning, or both. The data concerning available heat input used herein apply to a stable fuel element in crossflow. Investigations show that if the fuel element is actually both tumbling and spinning at an appreciable rate (more than one radian per second), the heat input will decrease to a value in the order of 20 percent of that for the stable fuel element. Extent of damage to varying fuel element diameters entering from the same altitude of exposure may indicate the extent of tumble and spin which the sample undergoes.

Justification for assuming a 4000 F wall temperature for fuel element melting and ablation requirements is presented as follows. Temperature distribution through the fuel element results in a temperature differential of about 1200 F between front face and rear face. This results in an arithmetic mean temperature of 3400 F; a little above the melting point of the rod material. The actual temperature of the rod leading edge is unknown, but this appears to be a reasonable estimate. Actually, heat flux over the leading edge is sufficiently high that a difference of 1000 F or more does not affect computed stagnation-point heat flux.

HEAT TRANSFER WITHIN THE FUEL ELEMENT

Heat transfer within the fuel element apparently does not vary with fuel element diameter, due to the lack of dependence on diameter of stagnation-point heat flux and of heat-flux distribution around the circumference. Temperature distribution depends on conductivity and on the ratio k/C . It is recommended that the actual fuel element material be fabricated for these tests so that the values of conductivity and of thermal diffusivity will be identical.

Heat transfer within the fuel element also depends on stagnation-point heat flux and stagnation-point recovery temperature. Test trajectories should, therefore, duplicate integrated stagnation-point heat flux and maximum heat-flux rate of the actual trajectory for the test flight period.

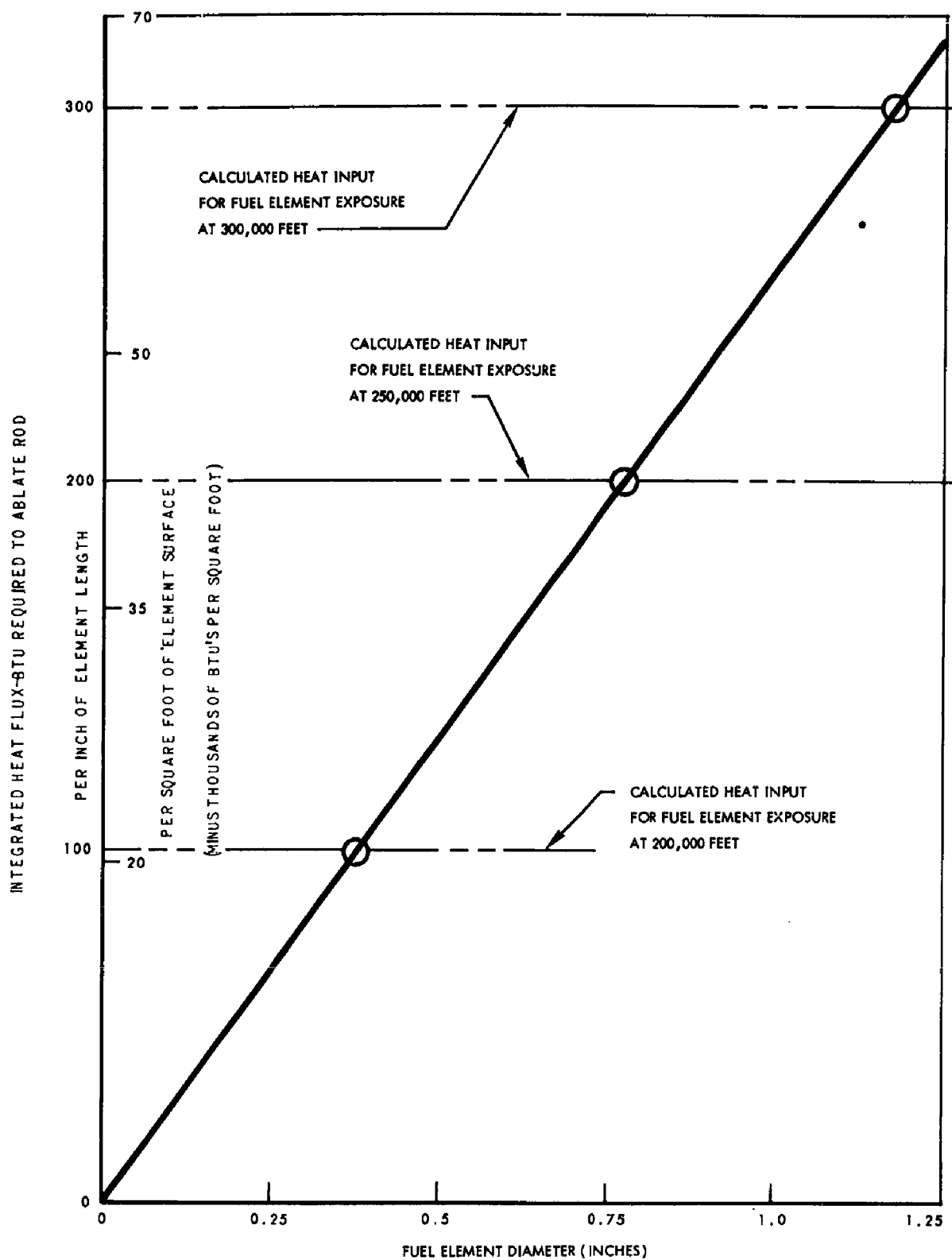


Figure 24. Heat Input Required for Fuel Element Heating and Ablation Versus Diameter

Expected fuel element ablation will then vary with diameter. Fuel element length should be great enough so that temperature gradient along the length may be disregarded. A length of 5 diameters should be sufficient to accomplish this. Stagnation point temperature-time history of the fuel element is shown in Figure 25.

CONCLUSIONS

The following conclusions affect the formulation of test criteria.

Separation from the space vehicle, release of reflectors, failure of the reactor vessel lid attachment, and exposure of the fuel elements in sequence through the action of aerodynamic forces and aerodynamic heating effects alone cannot result in dispersal of the fuel element material, with the present design of components.

There is no value in exposing any components for test above 300,000 feet, provided the requirements for angle and velocity of injection are met.

The major uncertainties affecting this study are the probability of tumbling and spinning during re-entry, and the determination of flow regime during the period of high heat flux. Tumbling and spinning greatly decrease heat input, and appreciable exposure to the turbulent flow regime would greatly increase heat input.

It is very unlikely that the present 1 1/4-inch fuel elements will be dispersed, or even seriously deformed due primarily to a high probability that they will tumble and may spin during re-entry. The effects of tumble and spin are much greater than the probable errors in the physical constants used.

THERMODYNAMIC TEST CRITERIA

It is recommended that the following criteria be applied as a result of this study.

Integrated aerodynamic heat input should be equal to that for the same component re-entering from orbit.

Maximum stagnation-point heat flux should be not less than that corresponding to orbital re-entry. There is no practical upper limit of heat flux from the standpoint of heat transfer; however, a question has been raised concerning a maximum in relation to chemical reaction in the boundary layer, primarily with possible evolved hydrogen. There is insufficient information as to the sequence and mechanism of hydrogen evolution and on the process of zirconium combustion to analyze these possible chemical effects.

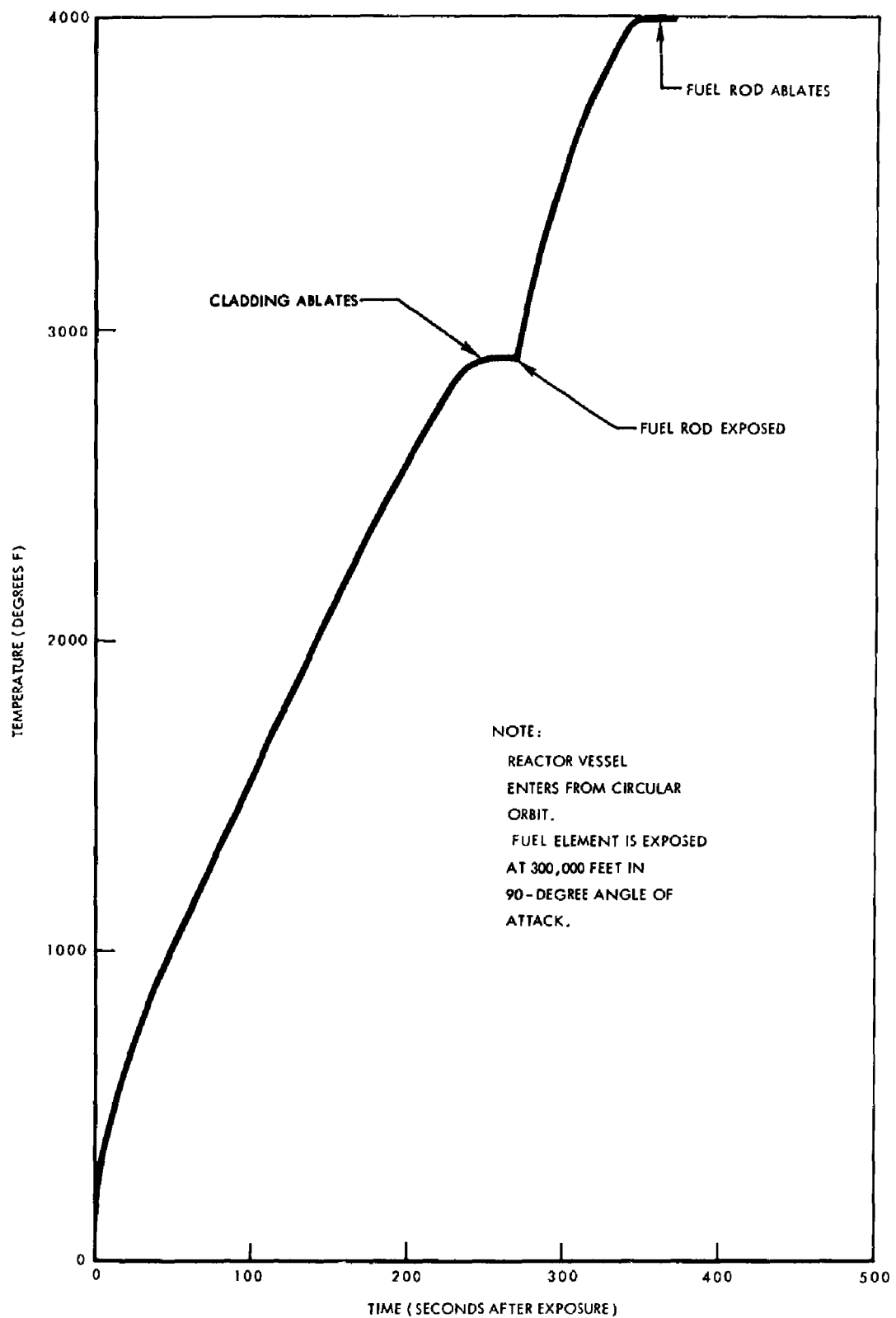


Figure 25. Fuel Element Stagnation Point Temperature Versus Time

Fuel element material and structure should be identical with the actual reactor fuel elements, primarily because uncertainty exists regarding physical properties and chemical behavior at high temperatures.

Fuel element length may be any value, provided it is great enough so that axial temperature differential is negligible. A minimum length of five diameters is recommended.

Required heat input for heating and ablating varies directly with fuel element diameter. Test trajectories may originate at a range of altitudes, but the diameter of fuel element test specimens should be correspondingly varied.

The fuel element must be isotropic. If the material changes across the cross section, the path of heat flow across the fuel element will be seriously altered. This would preclude the possibility of testing a hollow fuel element with instrumentation contained in the cavity, because heat flow through an annulus follows a greatly different pattern from that through a solid rod. Conversely, addition of a heavier material to increase apparent density would also distort the heat flow pattern.

SCALING

To maintain a reasonable cost level for the flight test program and verification of the destruction of re-entering NAP systems, scaling of the test configurations and trajectory variables will be necessary.

An excellent insight into the effect of body geometry and trajectory parameters upon the heating to the body during re-entry may be obtained from the following analytical study.

APPROXIMATE SCALING EFFECTS

The equations of motion for a drag re-entry into the atmosphere are

$$\cos \gamma = \frac{1}{g} \frac{V^2}{r_c} \quad (2)$$

normal to the flight path and

$$\frac{C_D A}{W} \frac{\rho V^2}{2} + \frac{g}{g_o} \sin \gamma = - \frac{1}{g_o} \frac{dV}{dt} \quad (3)$$

along the flight path.

Some Aspects of Trajectory Similarity

If it is assumed that the altitudes of interest are small compared to the radius of the earth, g in equations 2 and 3 may be considered as constant. Furthermore, if we assume an isothermal atmosphere, then

$$\rho = \rho_o e^{-\beta h} \quad (4)$$

An investigation of the term $(C_D A/W) \rho$ shows that

$$\frac{C_D A}{W} \rho = \frac{C_D A}{W} \rho_o e^{-\beta h} \quad (5)$$

Consequently, if we consider vehicles with two different values of $C_D A/W$, whose flight-path angles and velocities are the same, the same forces will be acting on the vehicles if

$$\left(\frac{C_D A}{W}\right)_1 \rho_1 = \left(\frac{C_D A}{W}\right)_2 \rho_2 \quad (6)$$

or

$$\frac{\rho_1}{\rho_2} = \frac{e^{-\beta h_1}}{e^{-\beta h_2}} \quad (7)$$

This shows that

$$h_1 - h_2 = \frac{1}{\beta} \ln \left[\frac{(C_D A/W)_1}{(C_D A/W)_2} \right] \quad (8)$$

which means that vehicle 1 and vehicle 2 will have the same velocity history and flight-path history at altitudes differing by equation 8, a constant difference for constant values of $C_D A/W$.

Aerodynamic heating rate to a body is approximately given by relations of the form

$$\dot{q} = \frac{k \rho^m V^n}{1^p} \quad (9)$$

if the wall enthalpy is small compared to recovery enthalpy. The constants m , n , and p , have specific values depending upon whether the heating is laminar or turbulent and the constant k depends upon body geometry and whether the flow is laminar or turbulent.

Since in equation 7 the velocity is always the same, for vehicle 1 and 2 we have

$$\frac{\dot{q}_1}{\dot{q}_2} = \left(\frac{\rho_1}{\rho_2}\right)^m \left(\frac{1_2}{1_1}\right)^p = \left[\frac{(A/W)_1}{(A/W)_2}\right]^{-m} \left(\frac{1_2}{1_1}\right)^p \quad (10)$$

as long as the bodies are geometrically similar. If the bodies are not geometrically similar, k would be different and C_D would be different. If homogeneous similar bodies are considered, $W a l^3$, $A a l^2$, and

$$\frac{\dot{q}_1}{\dot{q}_2} = \left(\frac{l_2}{l_1}\right)^{-m} \left(\frac{l_2}{l_1}\right)^p = \left(\frac{l_2}{l_1}\right)^{p-m} \quad (11)$$

The heating integrated over time is given by

$$Q = \int_0^t \dot{q} dt = \int_{V_i}^V \dot{q} \frac{dt}{dV} dV \quad (12)$$

The period of high heating rates and the period of high deceleration rates are very nearly concomitant conditions, and in equation 3 during these times, it is sufficient to approximate

$$\frac{dV}{dt} \approx - \frac{C_D A}{W} g_o \frac{\rho V^2}{2} \quad (13)$$

Therefore,

$$Q = - \int_{V_i}^{V_f} \frac{2k \rho^m V^n dV}{g_o l^p \frac{C_D A}{W} \rho V^2} = \frac{2k V_i^{n-1}}{g_o \frac{C_D A}{W} l^p} \int_1^\lambda \rho^{m-1} \left(\frac{V}{V_i}\right)^{n-2} d(V/V_i) \quad (14)$$

From equations 7 and 14

$$\frac{Q_1}{Q_2} = \frac{(C_D A/W)_2 l_2^p}{(C_D A/W)_1 l_1^p} \frac{\int_1^\lambda \rho_1^{m-1} \left(\frac{V}{V_i}\right)^{n-2} d\left(\frac{V}{V_i}\right)}{\int_1^\lambda \rho_1^{m-1} \left[(C_D A/W)_1 / (C_D A/W)_2 \right]^{m-1} \left(\frac{V}{V_i}\right)^{n-2} d\left(\frac{V}{V_i}\right)} \quad (15)$$

$$= \frac{(C_D A/W)_2^m l_2^p}{(C_D A/W)_1^m l_1^p} \quad (16)$$

Once again considering homogeneous similar bodies with $W a l^3$ and $A a l^2$, equation 16 shows that

$$\frac{Q_1}{Q_2} = \left(\frac{l_2}{l_1} \right)^{p-m} \quad (17)$$

It is interesting to note that for laminar flow $p = m = 1/2$ and $Q_1 = Q_2$, so that the total heating per unit area is independent of body size. For turbulent flow $p = 0.2$ and $m = 0.8$ so that the larger the body the greater the total heating per unit area. Furthermore, an inspection of equation 14 shows that the total heating to the body varies with V^{n-1} . For laminar flow $\dot{q} \propto V^{3.15}$ and, consequently, $Q \propto V_i^{2.15}$ or very nearly, Q varies with the square of the re-entry velocity. For turbulent flow $\dot{q} \propto V^{3.5}$ and Q varies with $V^{2.5}$. The effect of initial flight path angle is not obvious from the above analysis. This effect is obtained by integration of the motion equation with appropriate boundary conditions.

Approximate Solution of the Equations of Motion

An approximate solution of the equations of motion can be obtained for an important range of initial conditions. If the flight path angle is large enough (for example, $\gamma < -10$ degrees), it is found that the flight path angle does not vary significantly during the high heating and deceleration portion of re-entry.

Since during this same period

$$-\frac{C_D A}{W} \frac{\rho V^2}{2} \gg \sin \gamma \quad (18)$$

only the aerodynamic term in equation 3 need be retained. With $\gamma = \text{constant} = \gamma_i$ equation 3 becomes

$$\frac{C_D A}{W} \frac{\rho V^2}{2} \approx -\frac{1}{g_0} \frac{dV}{dt} = -\frac{\sin \gamma_i}{g_0} \frac{d(V^2/2)}{dh} \quad (19)$$

or

$$-\frac{C_D A}{W \sin \gamma_i} \rho g_0 dh = \frac{C_D A}{W \sin \gamma_i} dp = \frac{d(V^2/2)}{V^2/2} \quad (20)$$

Integration yields

$$\frac{C_D A}{W \sin \gamma_i} (p - p_i) = \ln \frac{V^2}{V_i^2} \quad (21)$$

If the initial altitude chosen is very high, $p \gg p_i$ and

$$\frac{C_D A}{W \sin \gamma_i} p \approx \ln \frac{V^2}{V_i^2} \quad (22)$$

If an isothermal atmosphere is assumed

$$p = \int_{\infty}^h -\rho g dh = - \int_{\infty}^h \rho_o g e^{-\beta h} dh = \frac{\rho_o g e^{-\beta h}}{\beta} = \frac{\rho g}{\beta} \quad (23)$$

and equation 22 becomes

$$\frac{C_D A g}{\beta W \sin \gamma_i} p \approx \ln \frac{V^2}{V_i^2} \quad (24)$$

From equation 14

$$\begin{aligned} Q &= - \frac{2k V_i^{n-1}}{g_o \frac{C_D A}{W} l^p} \int_1^{\lambda} \left(- \frac{\beta W \sin \gamma_i}{C_D A g_o} \right)^{m-1} \left(\frac{V}{V_i} \right)^{n-2} \left(- \ln \frac{V^2}{V_i^2} \right)^{m-1} d \left(\frac{V}{V_i} \right) \\ &= - \frac{2k V_i^{n-1} (-\beta \sin \gamma_i)^{m-1}}{\left(\frac{C_D A g_o}{W} \right)^m l^p} \int_1^{\lambda} \left(\frac{V}{V_i} \right)^{n-2} \left(- \ln \frac{V^2}{V_i^2} \right)^{m-1} d \left(\frac{V}{V_i} \right) \quad (25) \end{aligned}$$

Defining

$$\left[- \left(\frac{n-1}{2} \right) \ln \frac{V^2}{V_i^2} \right]^{1/2} = \eta \quad (26)$$

$$\frac{d\eta}{d(V/V_i)} = - \frac{\frac{n-1}{2} \left[- \frac{n-1}{2} \ln \frac{V^2}{V_i^2} \right]^{-1/2}}{V/V_i} \quad (27)$$

and the integral in equation 23 becomes

$$\begin{aligned} & \int_1^\lambda \left(\frac{V}{V_i} \right)^{n-2} \left(\frac{2}{n-1} \right)^{m-1} \left[- \left(\frac{n-1}{2} \right) \ln \frac{V^2}{V_i^2} \right]^{m-1} d \left(\frac{V}{V_i} \right) \\ &= - \int_0^\phi \left(\frac{2}{n-1} \right)^m \left(\frac{V^2}{V_i^2} \right)^{\frac{n-1}{2}} \left[- \left(\frac{n-1}{2} \right) \ln \frac{V^2}{V_i^2} \right]^{\frac{2m-1}{2}} d\eta \\ &= - \int_0^\phi \left(\frac{2}{n-1} \right)^m \eta^{2m-1} e^{-\eta^2} d\eta \end{aligned} \quad (28)$$

For laminar flow $m = 1/2$, $n = 3.15$ and the integral becomes

$$= 0.964 \int_0^\phi e^{-\eta^2} d\eta \quad (29)$$

which is the integral of the error function. For turbulent flow $m = 0.8$, $n = 3.5$ and the integral becomes

$$= 0.836 \int_0^\phi \eta^{0.6} e^{-\eta^2} d\eta \quad (30)$$

From equations 25, 29, and 30, the result is

$$Q_L = 1.93 K_L V_i^{3.15} \sqrt{\frac{-\frac{W}{C_D A}}{g_o l \beta \sin \gamma_i}} \int_0^\phi e^{-\eta^2} d\eta \quad (31)$$

for laminar flow and

$$Q_T = 1.67 K_T V_i^{2.5} \frac{\left(\frac{W}{C_D A g_o}\right)^{0.8}}{(-\beta l \sin \gamma_i)^{0.2}} \int_0^\phi \eta^{0.6} e^{-\eta^2} d\eta \quad (32)$$

for turbulent flow. The effect of body dimension is the same as for laminar flow. If in the above integrals the upper limit is for a velocity $V = 0$, the integral limits are between 0 and ∞ .

The heating rate can be obtained from equations 9 and 22, and the result is

$$\dot{q} = \frac{k \rho^m V^n}{l^p} = \frac{K V_i^n}{l^p} \left(\frac{V}{V_i}\right)^n \left(-\frac{\beta W \sin \gamma_i}{C_D A g_o}\right)^m \left(-\ln \frac{V^2}{V_i^2}\right)^m \quad (33)$$

Differentiating this expression to determine the velocity of maximum heating, it is found that

$$\left(\frac{V}{V_i}\right)_{\dot{q}_{\max}} = e^{-m/n} \quad (34)$$

For laminar flow,

$$\left(\frac{V}{V_i}\right)_{\dot{q}_{\max L}} = 0.853 \quad (35)$$

and for turbulent flow,

$$\left(\frac{V}{V_i}\right)_{\dot{q}_{\max T}} = 0.796 \quad (36)$$

From equations 33 and 34

$$\dot{q}_{\max} = \frac{K}{l^P} \left(\frac{\beta W \sin \gamma_i}{C_D A g_o} \right)^m V_i^n e^{-m \left(\frac{2m}{n} \right)^m} \quad (37)$$

For Laminar flow

$$\dot{q}_{\max L} = 0.342 K_L V_i^{3.15} \sqrt{\frac{\beta W \sin \gamma_i}{C_D A g_o l}} \quad (38)$$

and for turbulent flow

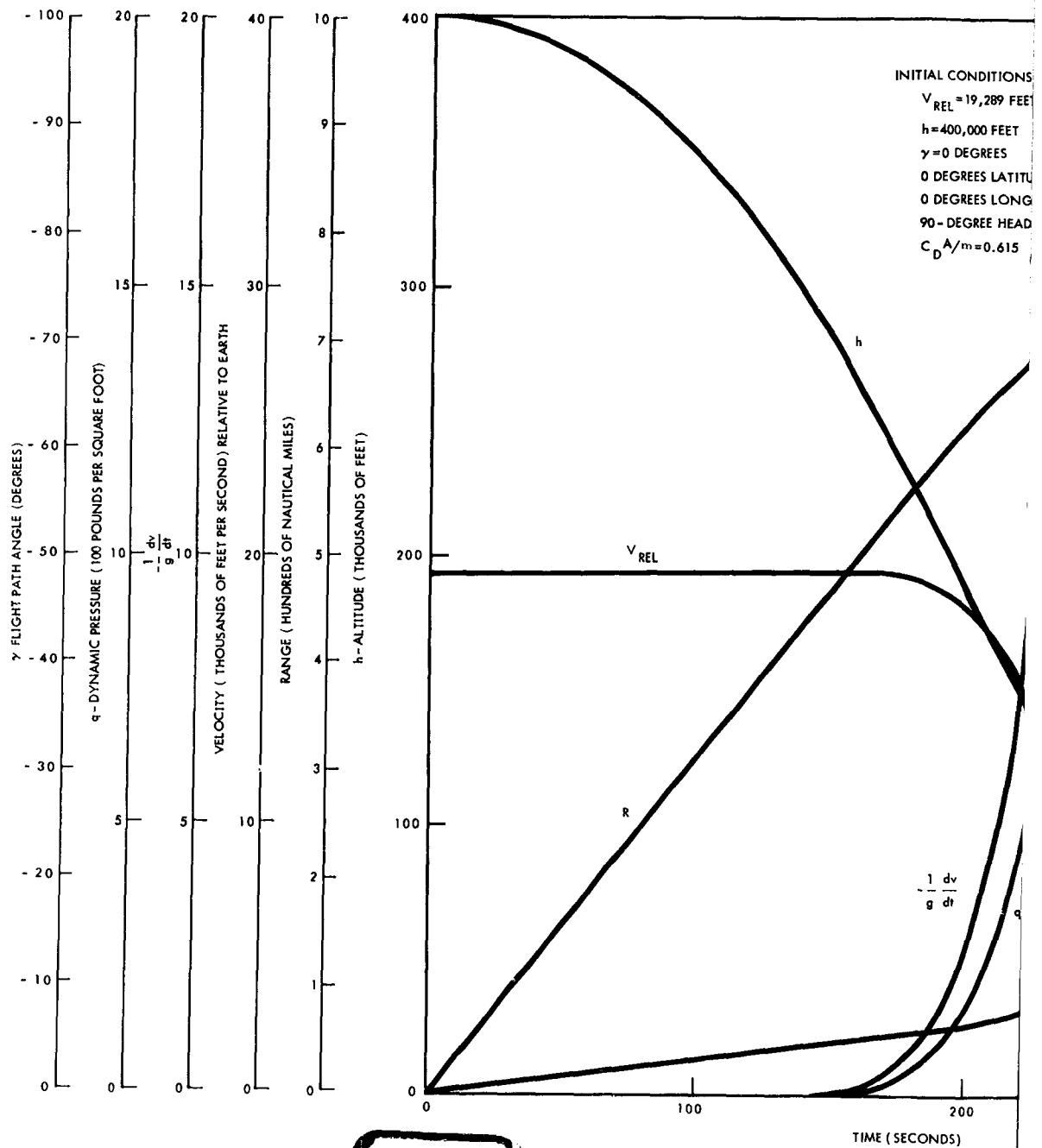
$$\dot{q}_{\max T} = 0.240 K_T \frac{\left(\frac{\beta W \sin \gamma_i}{C_D A g_o} \right)^{0.8} V_i^{3.5}}{l^{0.2}} \quad (39)$$

The approximate relations presented above indicate that the total heating per unit area is independent of body size for homogeneous similar shapes. This means that the amount of body destroyed would be independent of body length. If a given body would just be destroyed by the heating, a larger body would not be destroyed because of the mass varying with l^3 and the area with l^2 .

The total heating per unit area increases with increasing (positive upwards) flight path angle and increases with increasing velocity. Consequently, to simulate the NAP decay heating effect with a ballistic sub-circular trajectory would require a smaller than actual fuel element.

SCALING INVESTIGATION UTILIZING THE IBM 7090 COMPUTER

Trajectories of fuel elements alone were computed for $0.8 \leq V_i/V_c \leq 1.5$, $-15 \text{ degrees} \leq \gamma_i \leq 0 \text{ degrees}$ at an initial altitude of 400,000 feet using the IBM 7090 computer to determine the effect of flight-path angle and velocity on the trajectories and heating of the fuel element during re-entry. In all cases, it was assumed that the fuel element was tumbling and a constant mean value of $C_D A/m = 0.615 \text{ ft}^2/\text{slug}$ ($W/C_D A = 52.2 \text{ pounds per square foot}$) was used. The trajectories for $V/V_c \leq 1.2$ are shown in Figures 26 through 35, and resulting heat transfer rates in Figures 36 through 45. Figure 19 gives the integrated heating at the stagnation line of a tumbling fuel element above the estimated radiation value of $\dot{q} = 65$ for $T_W = 4000 \text{ degrees R}$, and assumes that the fuel element



1

Figure 26. Re-Entry Trajectory of Tun
Angle Zero Degrees, V_E / V

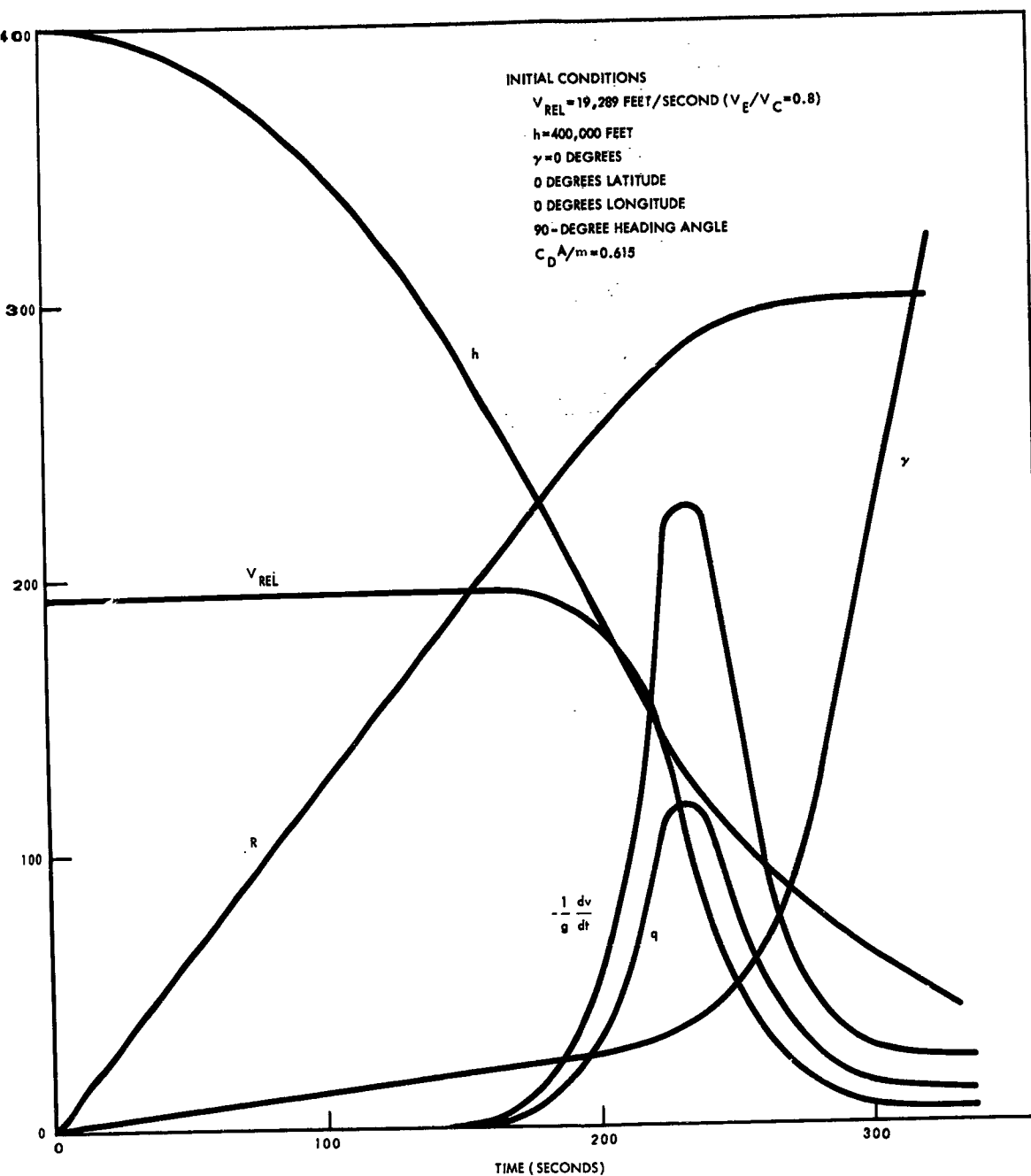
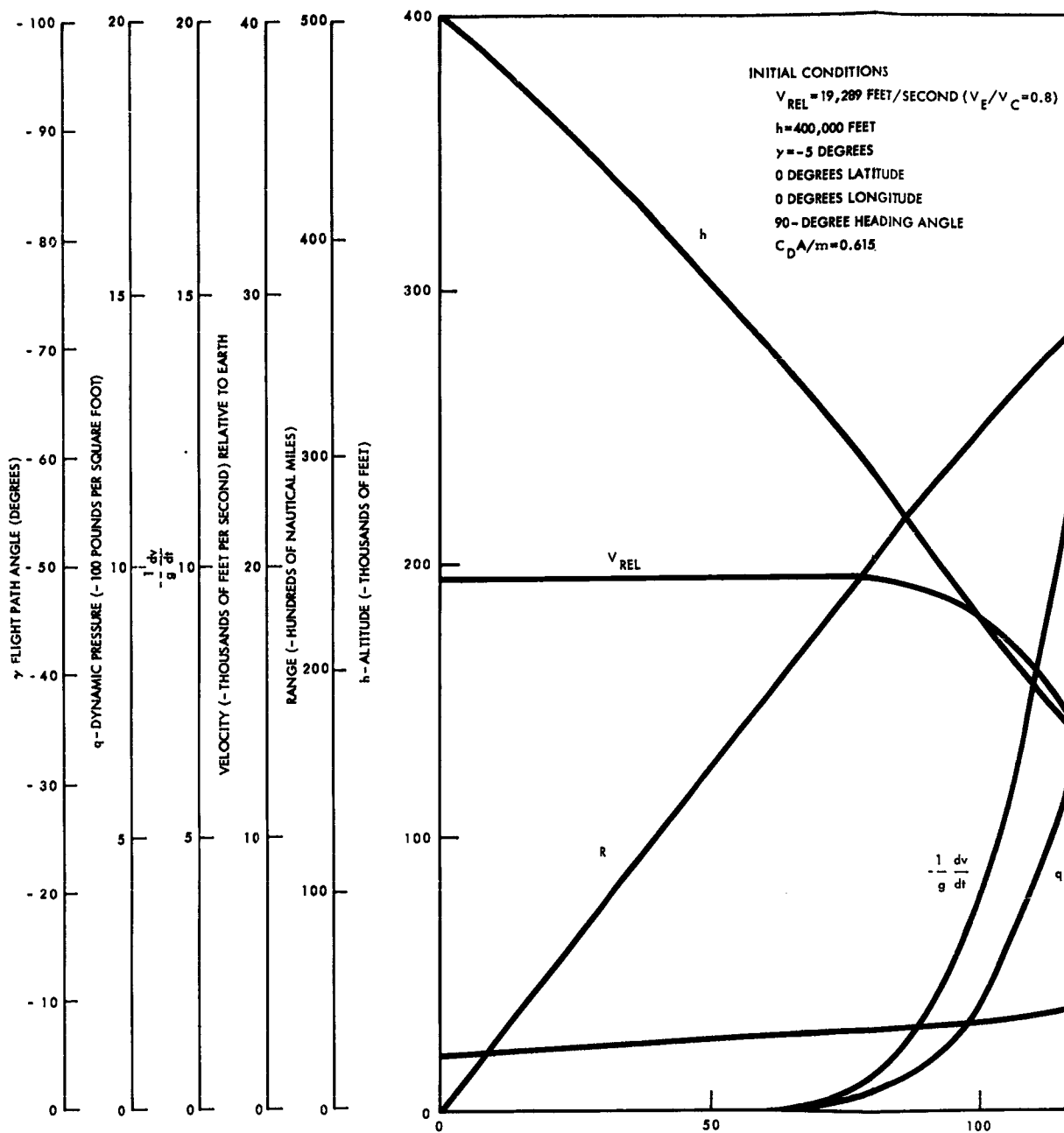


Figure 26. Re-Entry Trajectory of Tumbling Fuel Element, Flight-Path Angle Zero Degrees, V_E/V_C Equals 0.8





1

Fi

INITIAL CONDITIONS

$V_{REL} = 19,289$ FEET/SECOND ($V_E/V_C = 0.8$)

$h = 400,000$ FEET

$\gamma = -5$ DEGREES

0 DEGREES LATITUDE

0 DEGREES LONGITUDE

90-DEGREE HEADING ANGLE

$C_D A/m = 0.615$

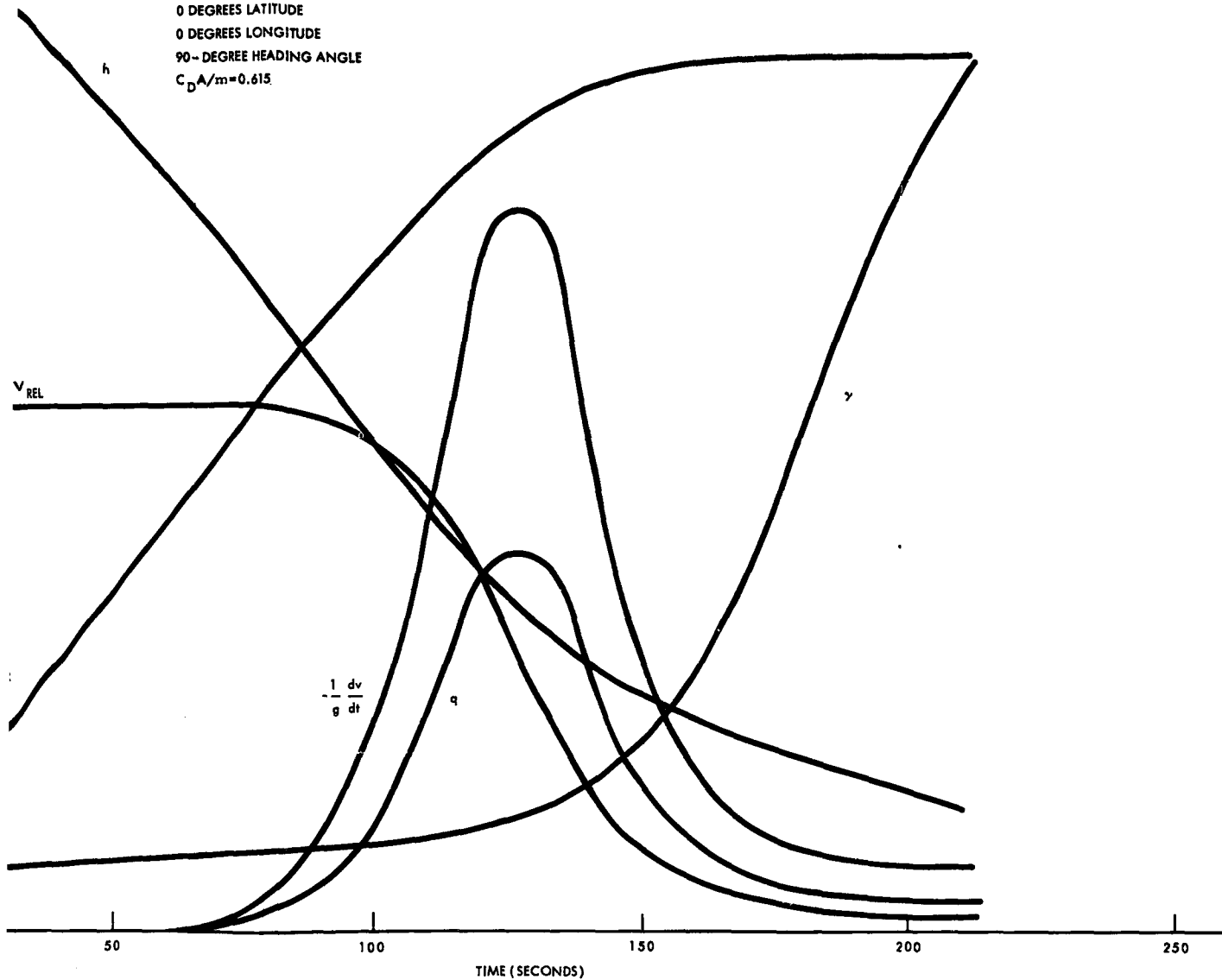
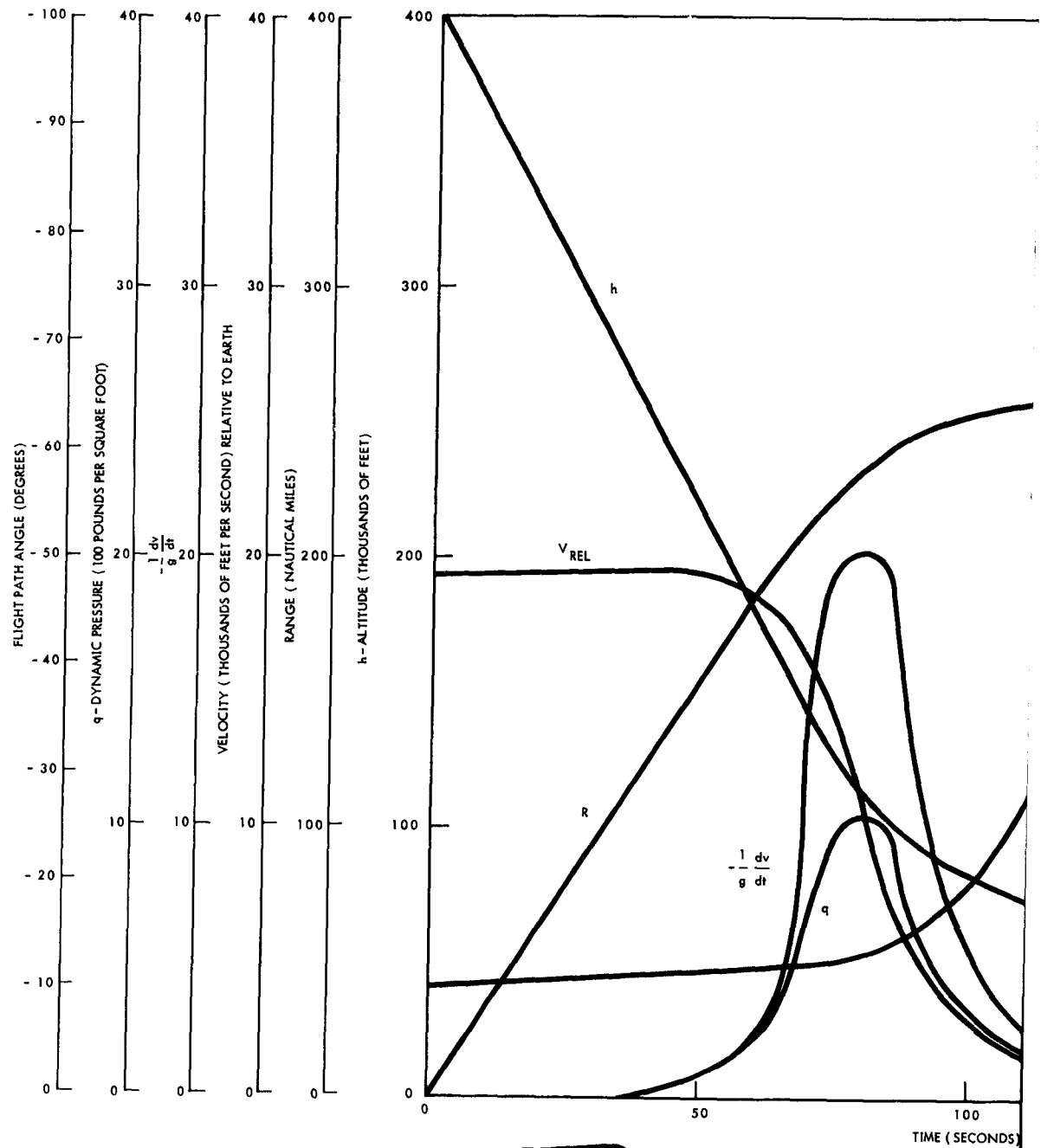


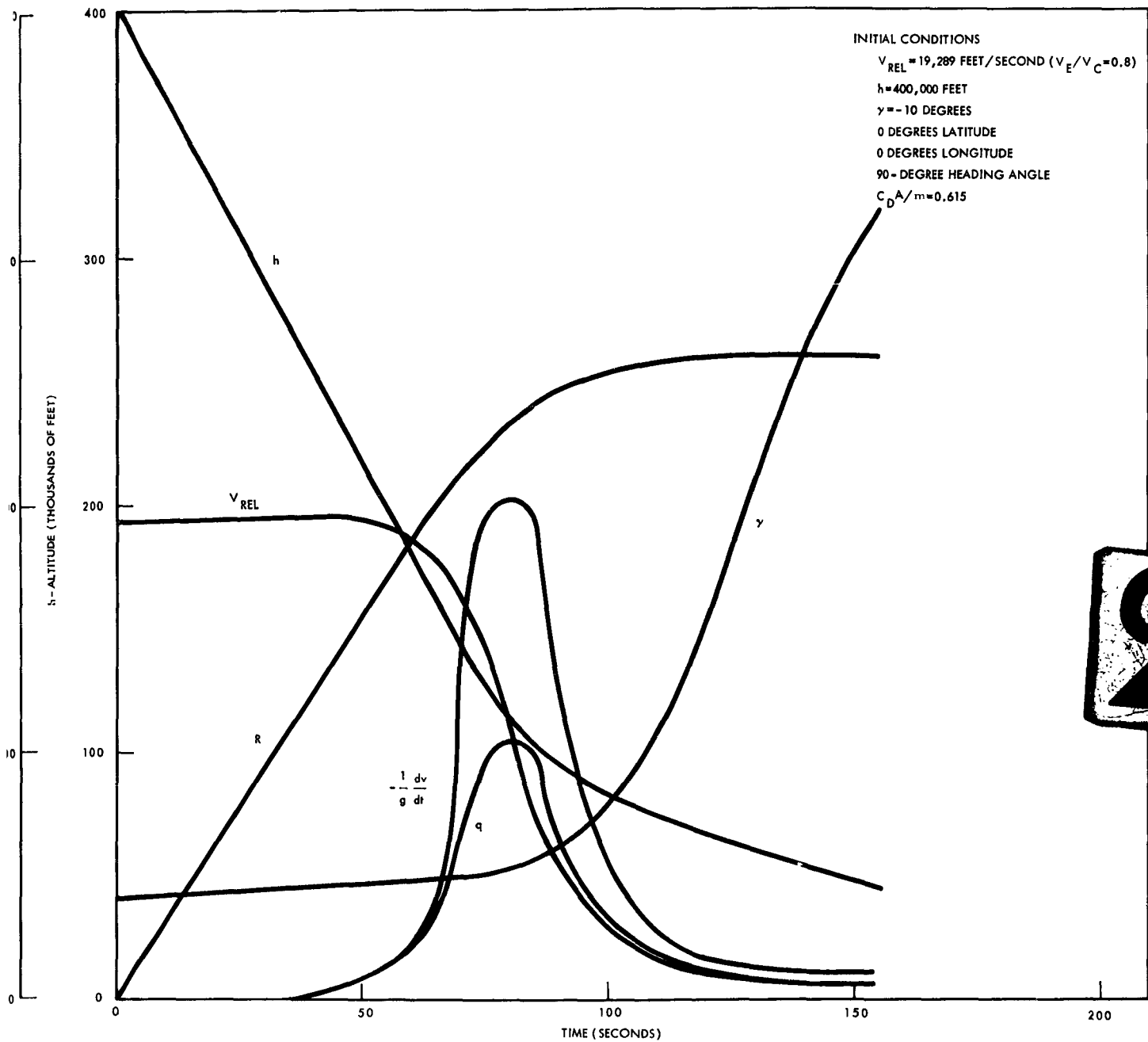
Figure 27. Re-Entry Trajectory of Tumbling Fuel Element, Flight-Path Angle Minus 5 Degrees, V_E/V_C Equals 0.8





1

Figure 28. Re-Entry Trajectory
Angle Minus 1



2

Figure 28. Re-Entry Trajectory of Tumbling Fuel Element, Flight-Path Angle Minus 10 Degrees, V_E/V_C Equals 0.8

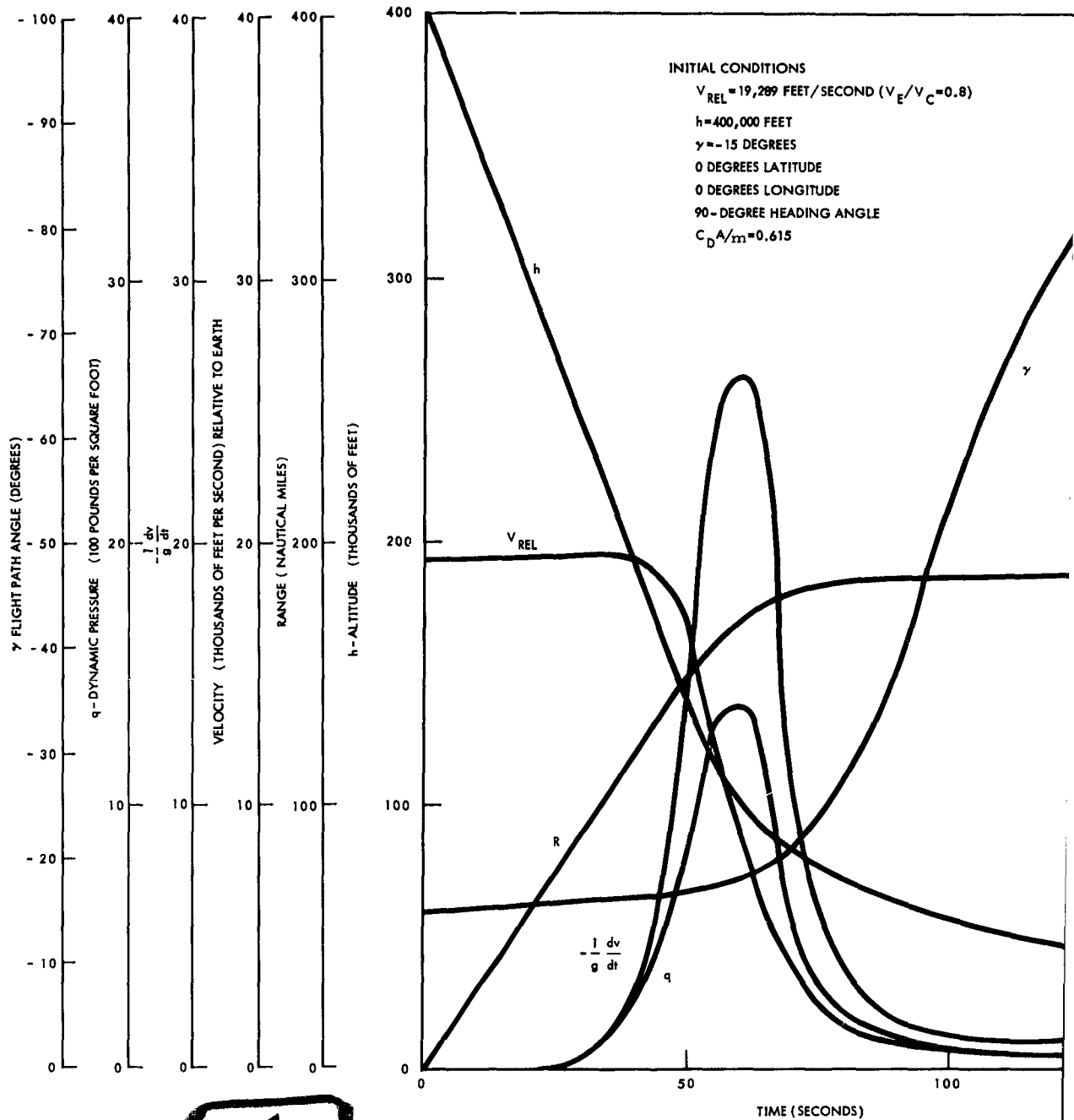
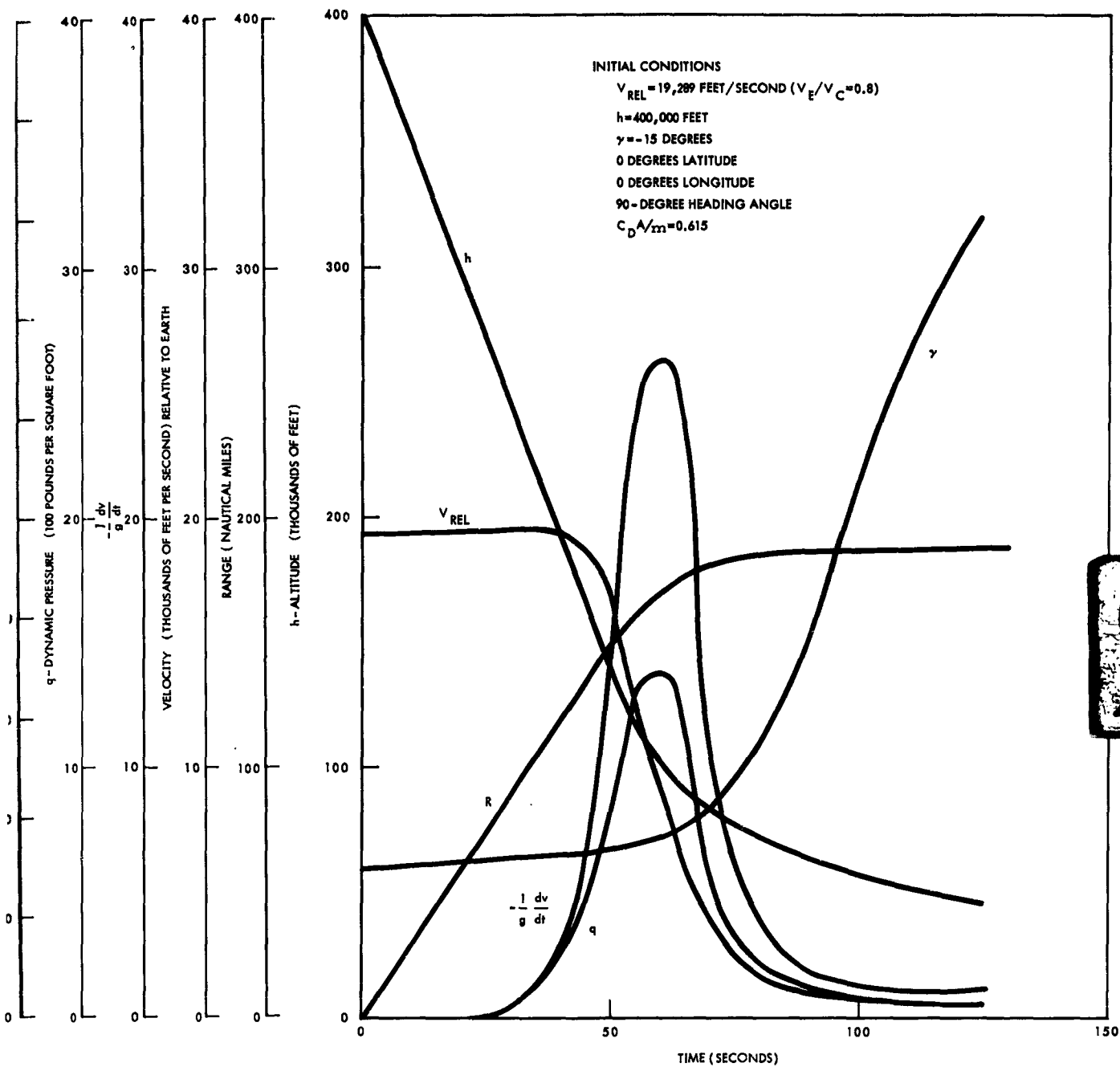


Figure 29. Re-Entry Trajectory of Tumbling Fuel Element Minus 15 Degrees, V_E/V_C Equals 0.8

60

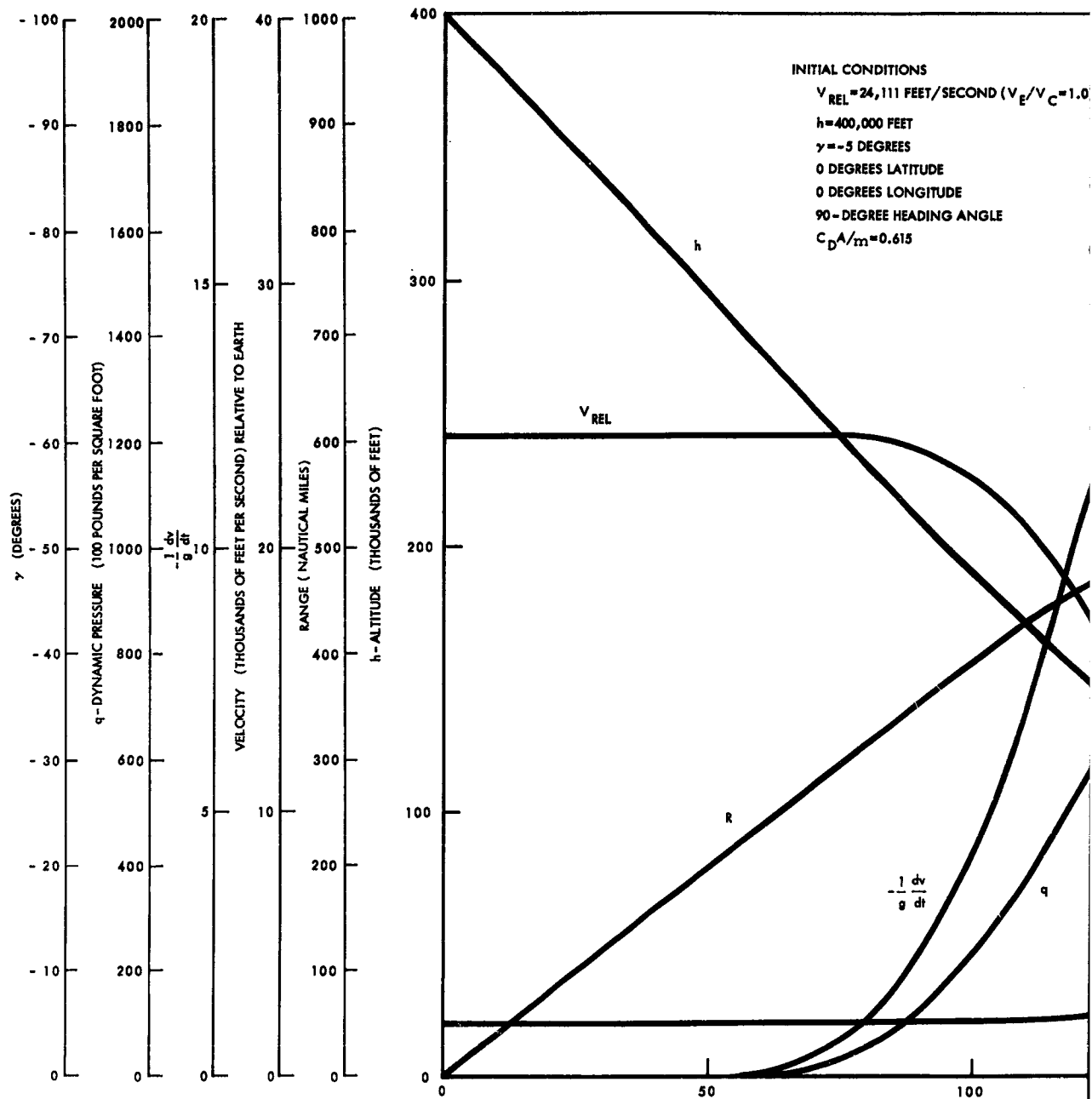
SID 62-1093





2

Figure 29. Re-Entry Trajectory of Tumbling Fuel Element, Flight-Path Minus 15 Degrees, V_E/V_C Equals 0.8



TIME (

Figure 30.



INITIAL CONDITIONS

$V_{REL} = 24,111$ FEET/SECOND ($V_E/V_C = 1.0$)

$h = 400,000$ FEET

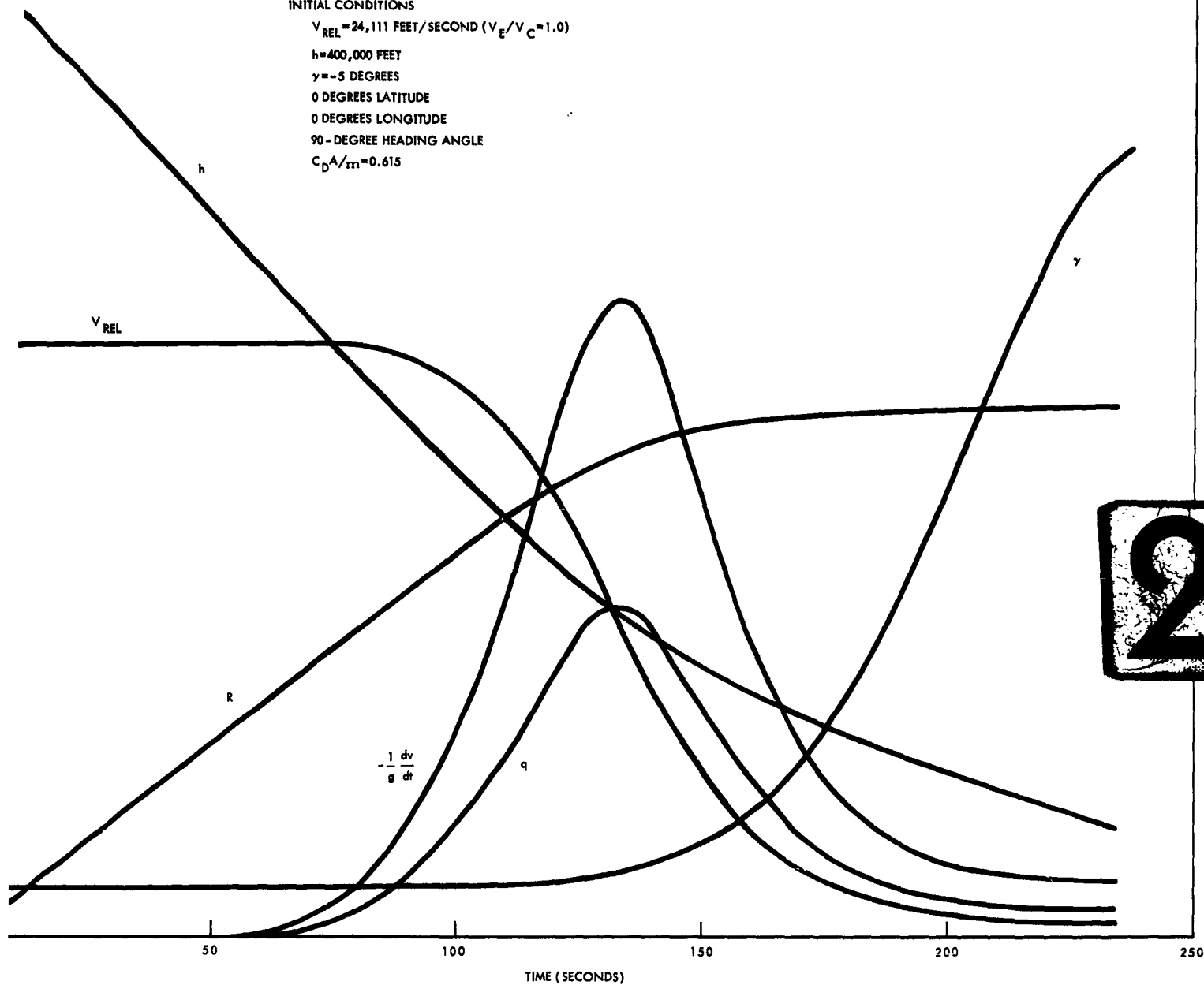
$\gamma = -5$ DEGREES

0 DEGREES LATITUDE

0 DEGREES LONGITUDE

90 - DEGREE HEADING ANGLE

$C_D A / m = 0.615$



2

Figure 30. Re-Entry Trajectory of Tumbling Fuel Element, Flight-Path Angle Minus 5 Degrees, V_E/V_C Equals 1

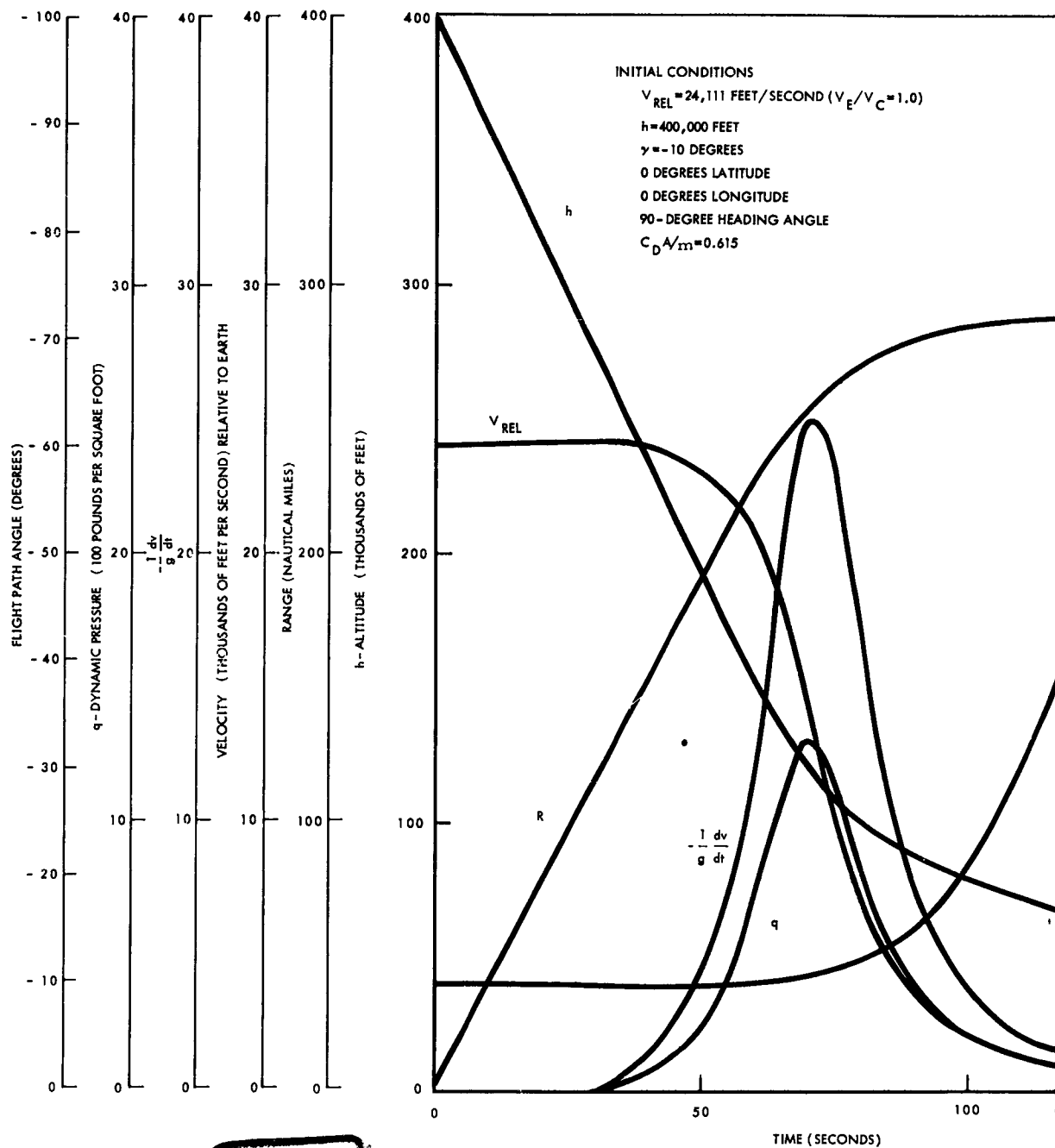


Figure 31. Re-Entry Trajectory of Tumbling Fuel Element
 Angle Minus 10 Degrees, V_E/V_C Equals



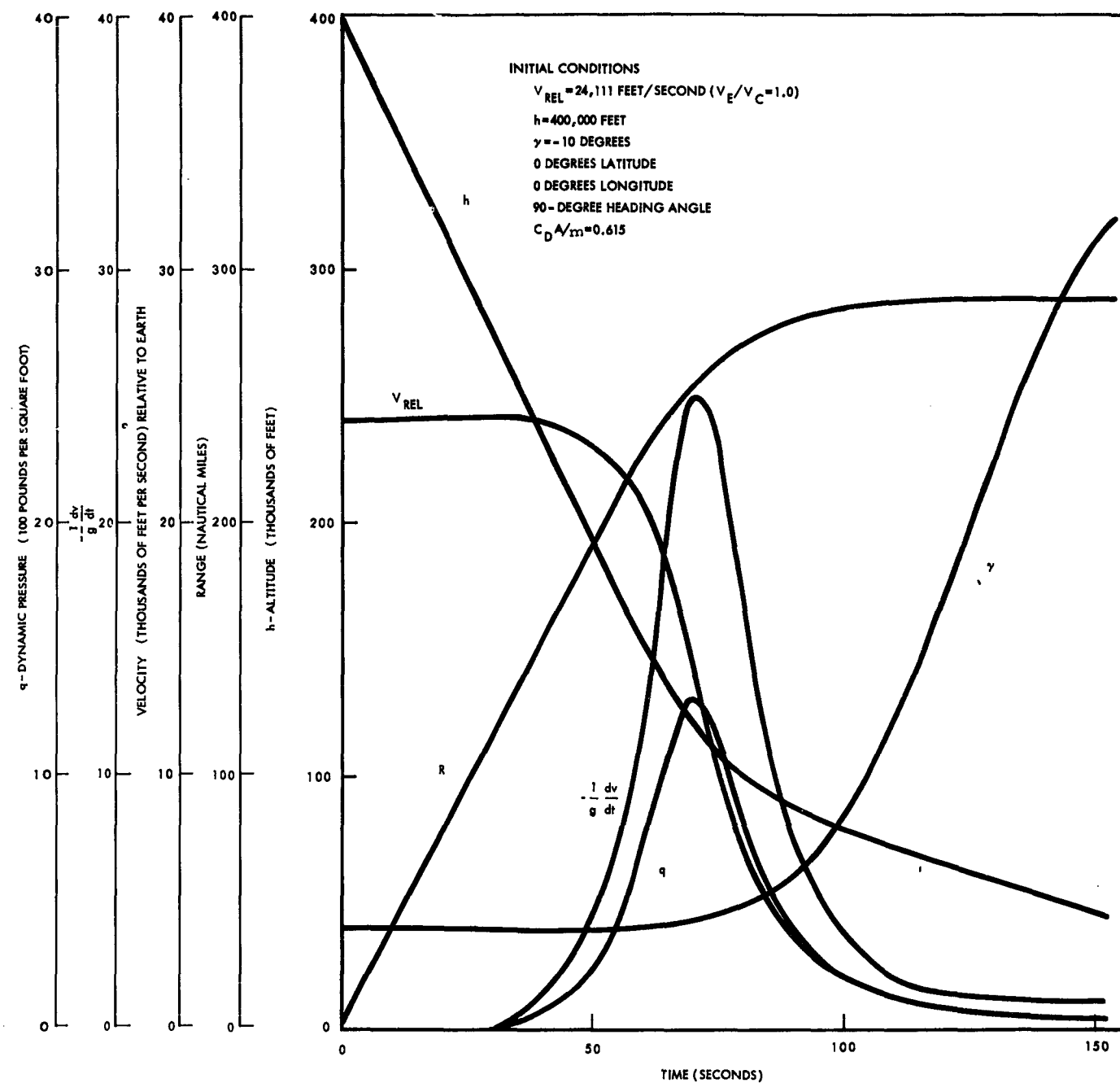


Figure 31. Re-Entry Trajectory of Tumbling Fuel Element, Flight-Path Angle Minus 10 Degrees, V_E/V_C Equals 1



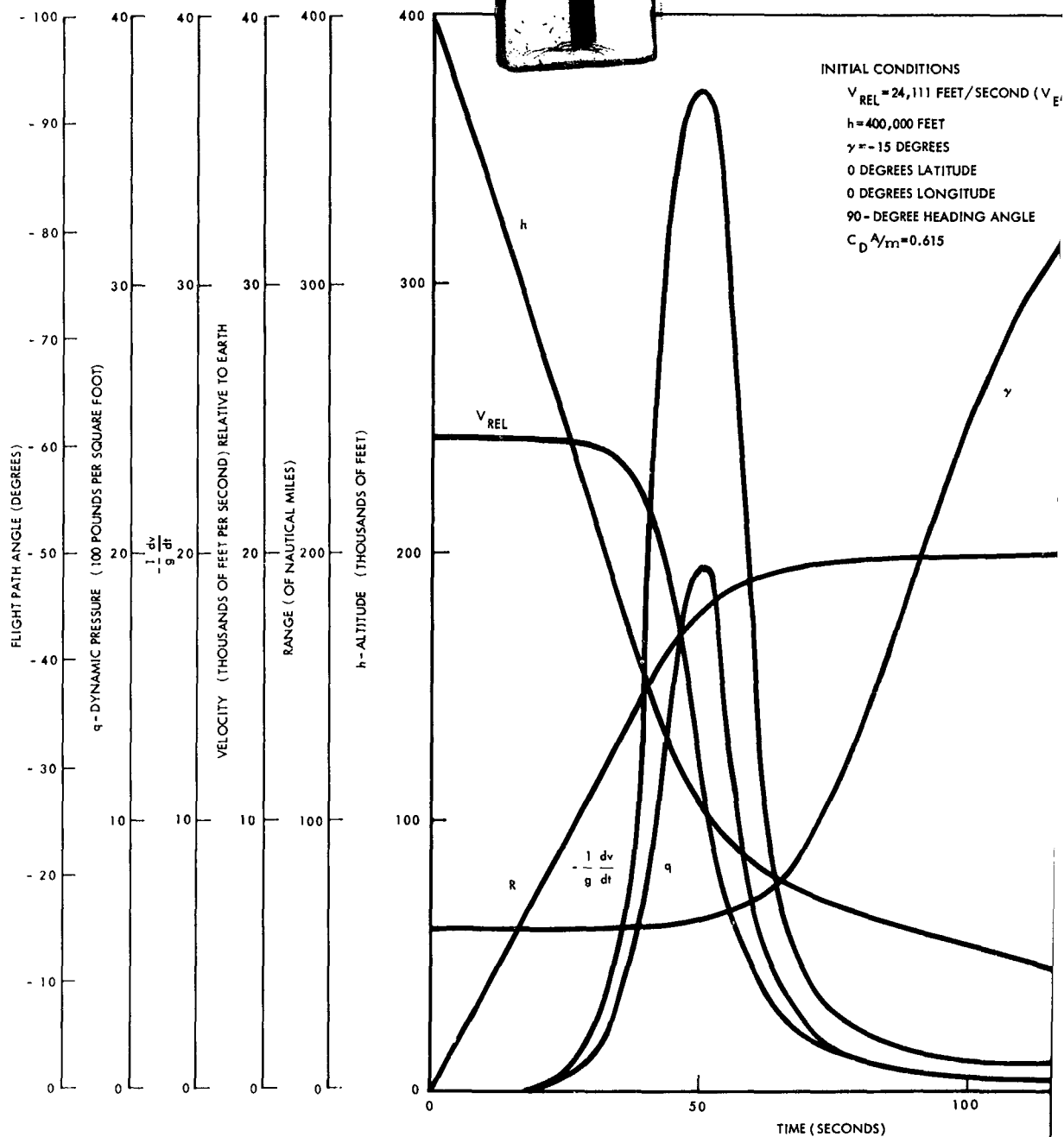


Figure 32. Re-Entry Trajectory of Tumbling Fuel Element
Angle Minus 15 Degrees, V_E / V_C Equals 1

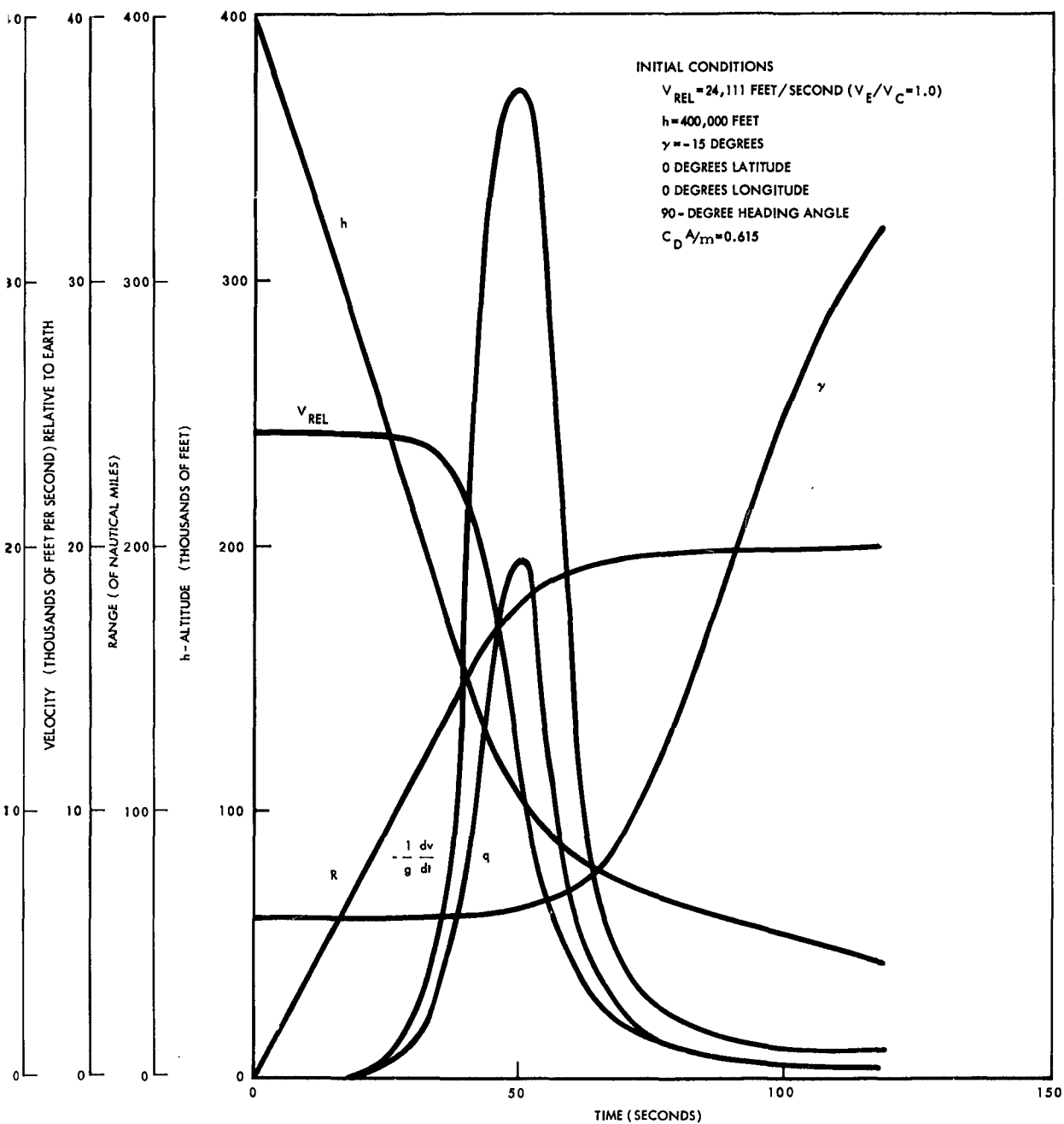
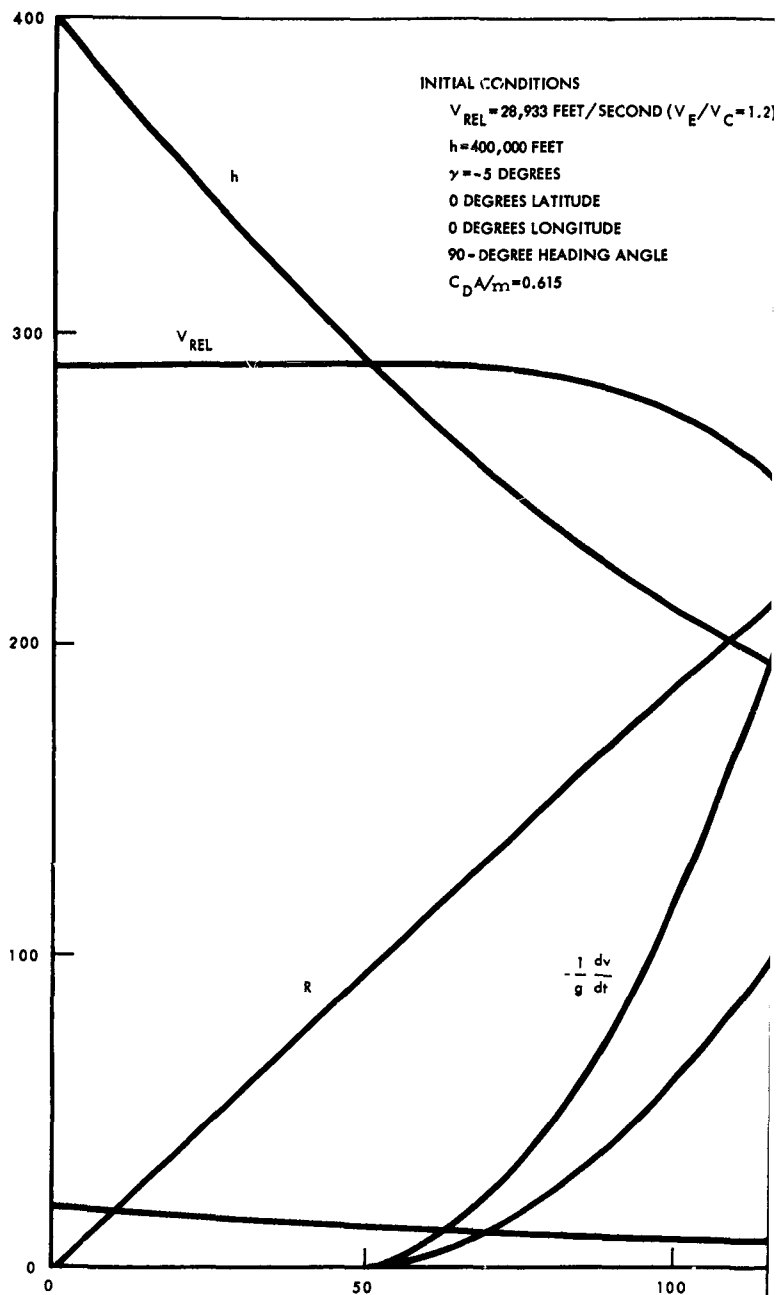
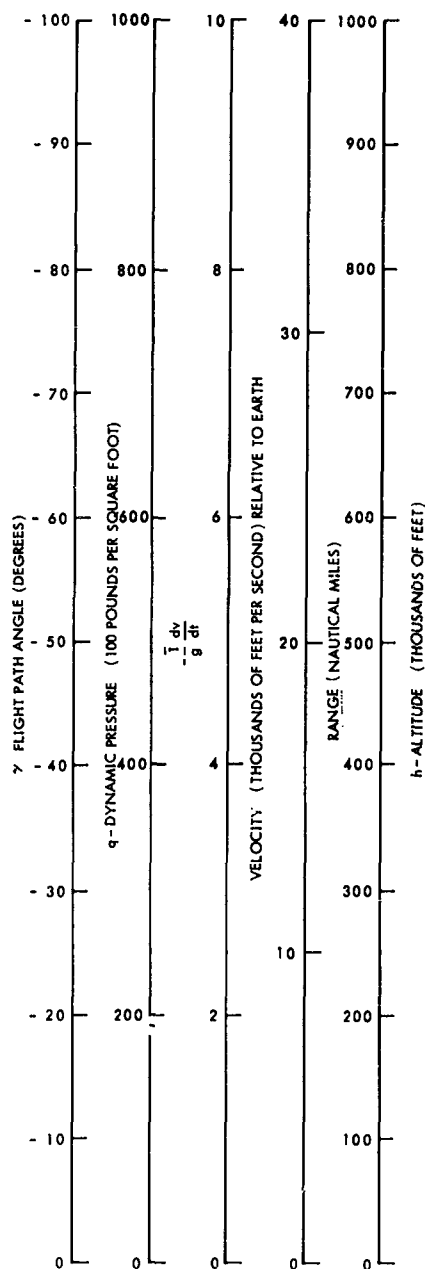


Figure 32. Re-Entry Trajectory of Tumbling Fuel Element, Flight-Path Angle Minus 15 Degrees, V_E/V_C Equals 1





1

2

INITIAL CONDITIONS

$V_{REL} = 28,933$ FEET/SECOND ($V_E/V_C = 1.2$)

$h = 400,000$ FEET

$\gamma = -5$ DEGREES

0 DEGREES LATITUDE

0 DEGREES LONGITUDE

90-DEGREE HEADING ANGLE

$C_D A/m = 0.615$

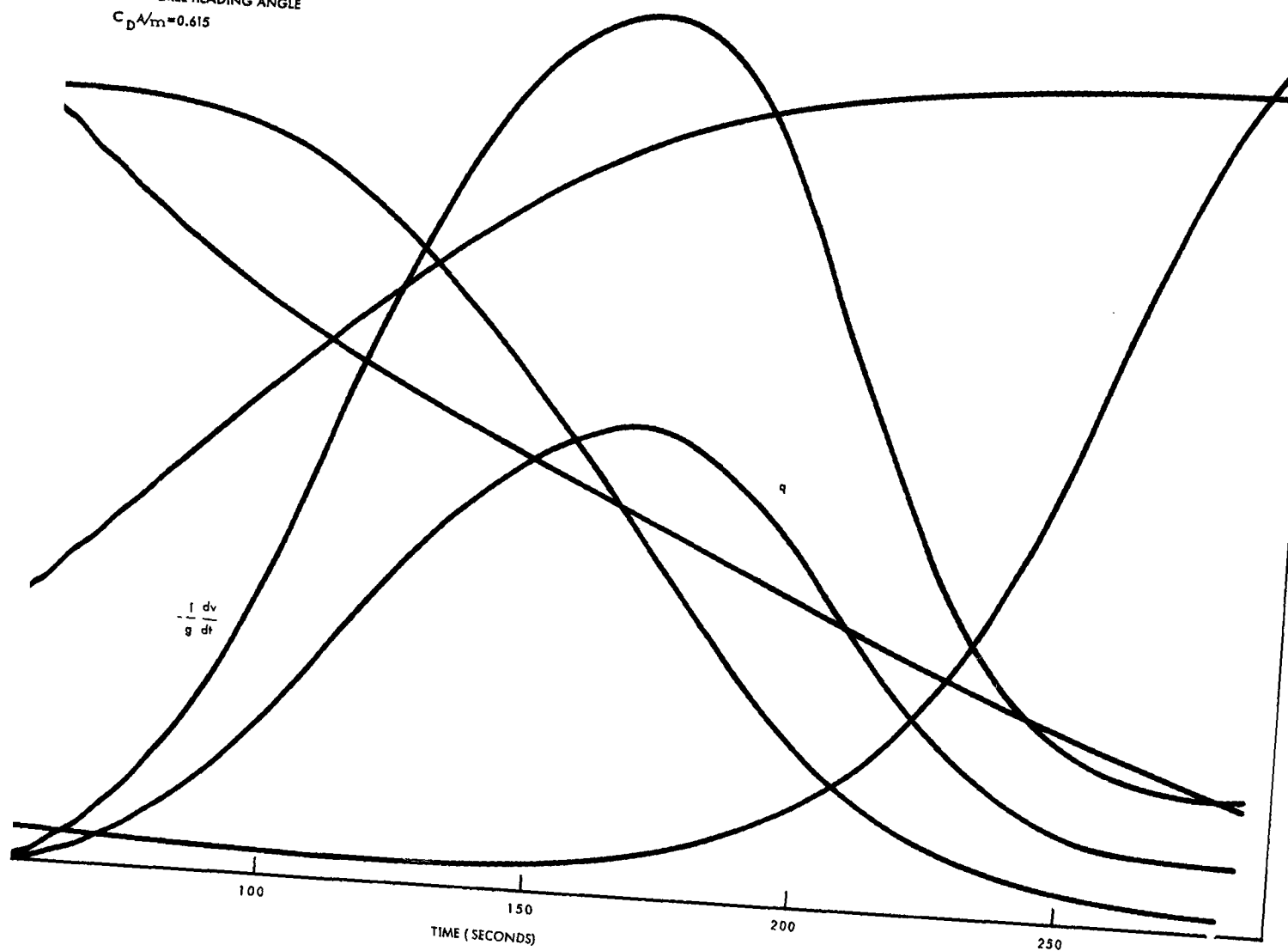
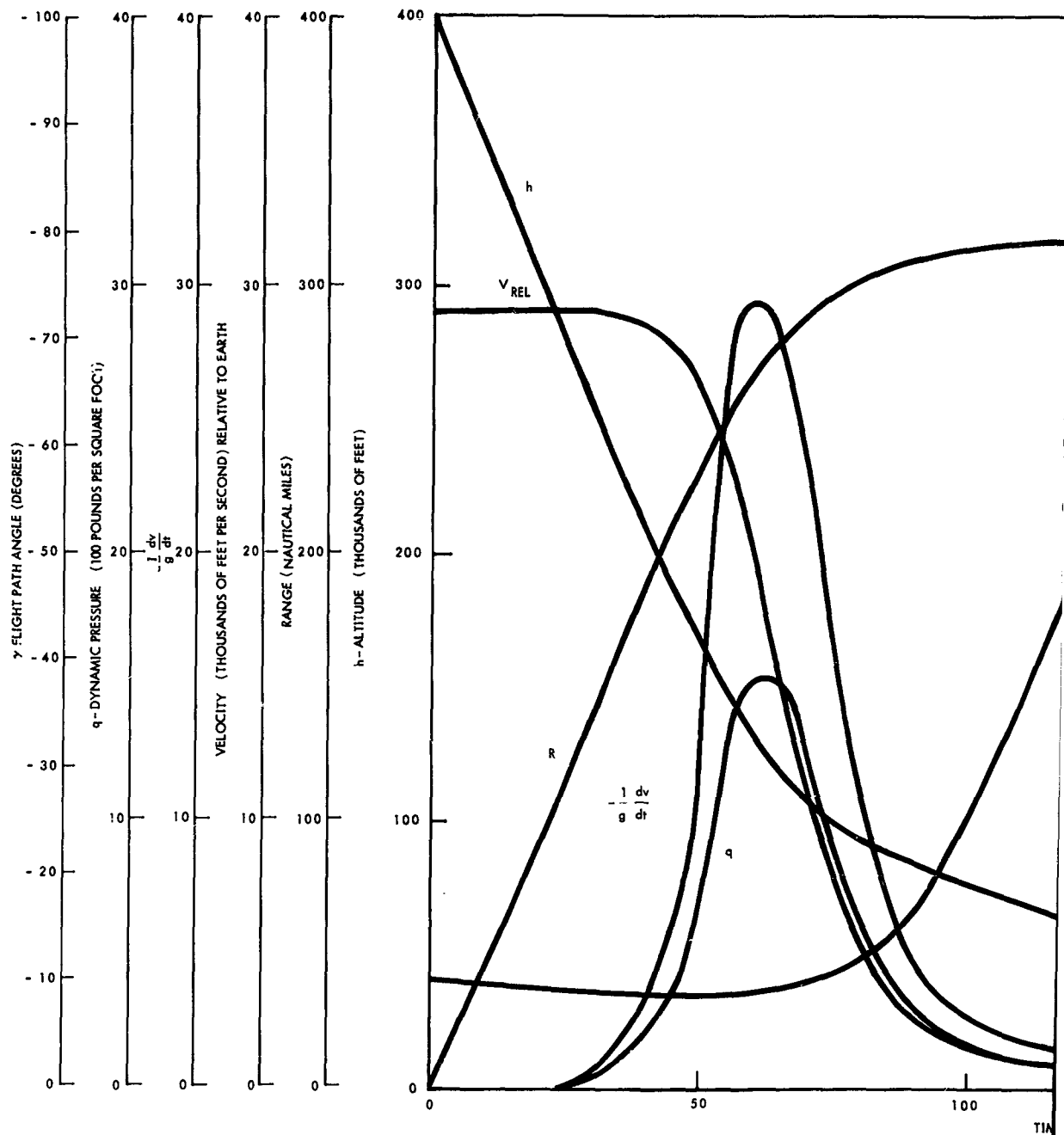


Figure 33. Re-Entry Trajectory of Tumbling Fuel Element, Flight-Path Angle Minus 5 Degrees, V_E/V_C Equals 1.2



1

Figure 34

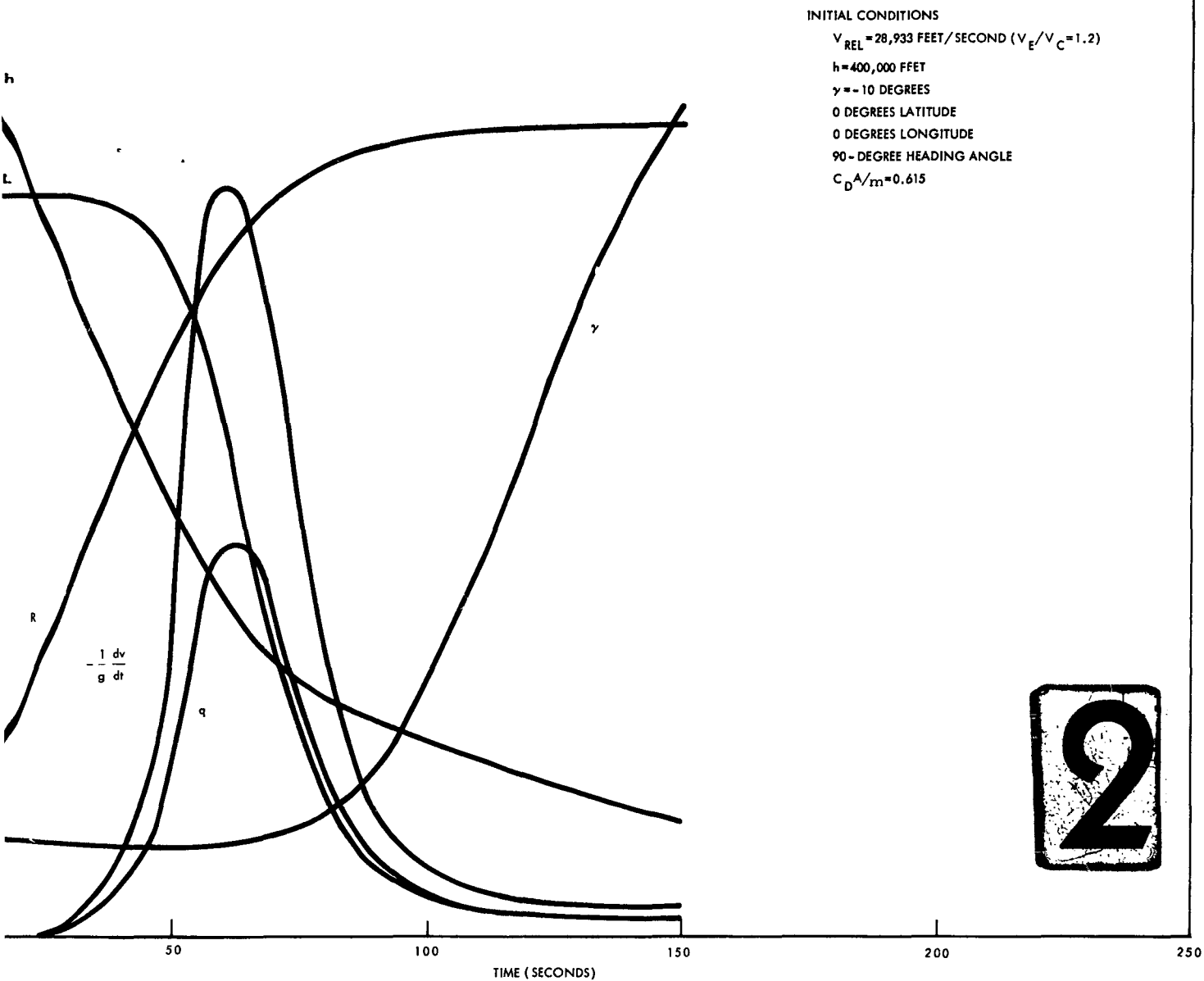
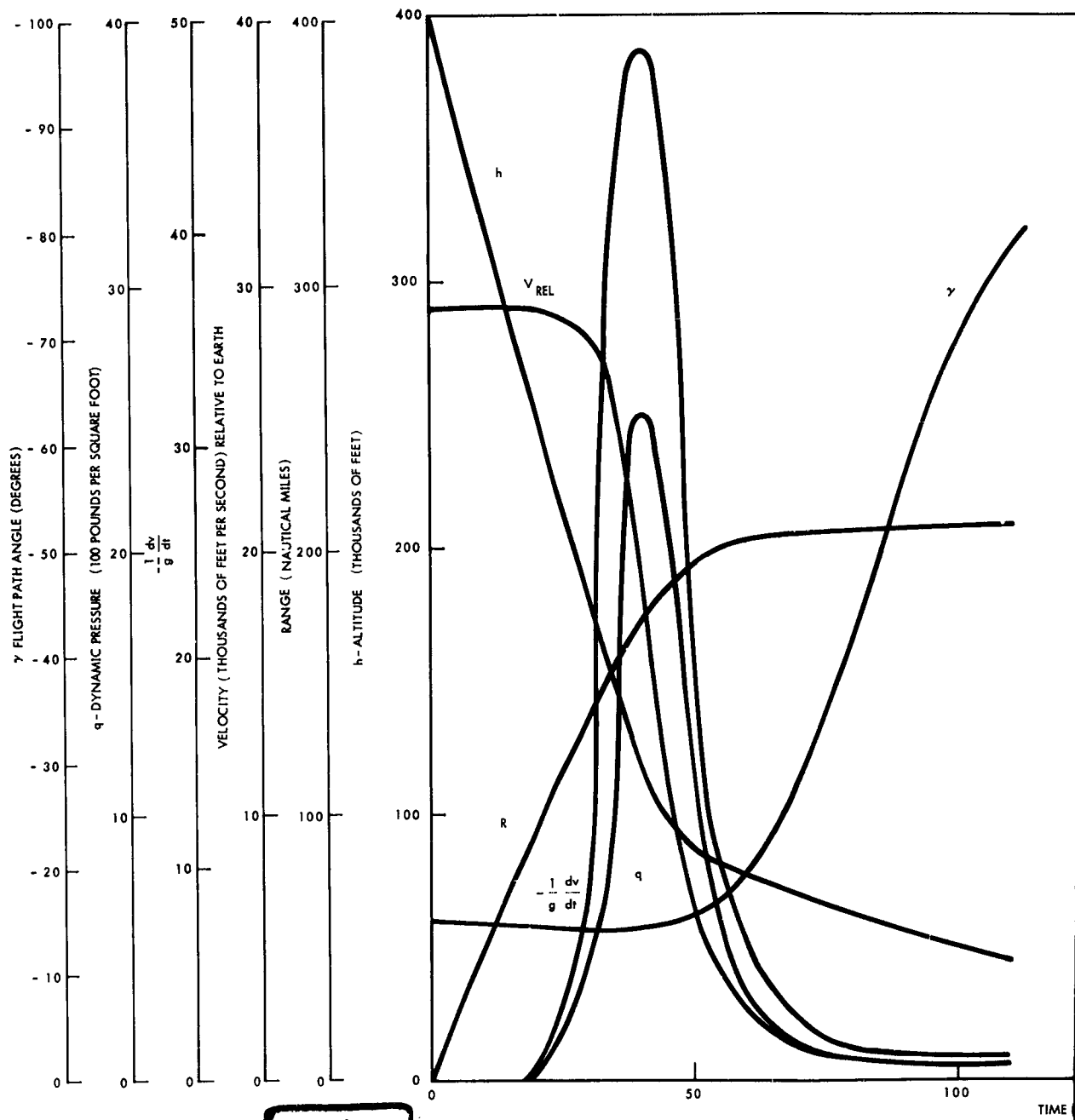


Figure 34. Re-Entry Trajectory of Tumbling Fuel Element, Flight-Path Angle Minus 10 Degrees, V_E/V_C Equals 1.2



1

Figure 35.

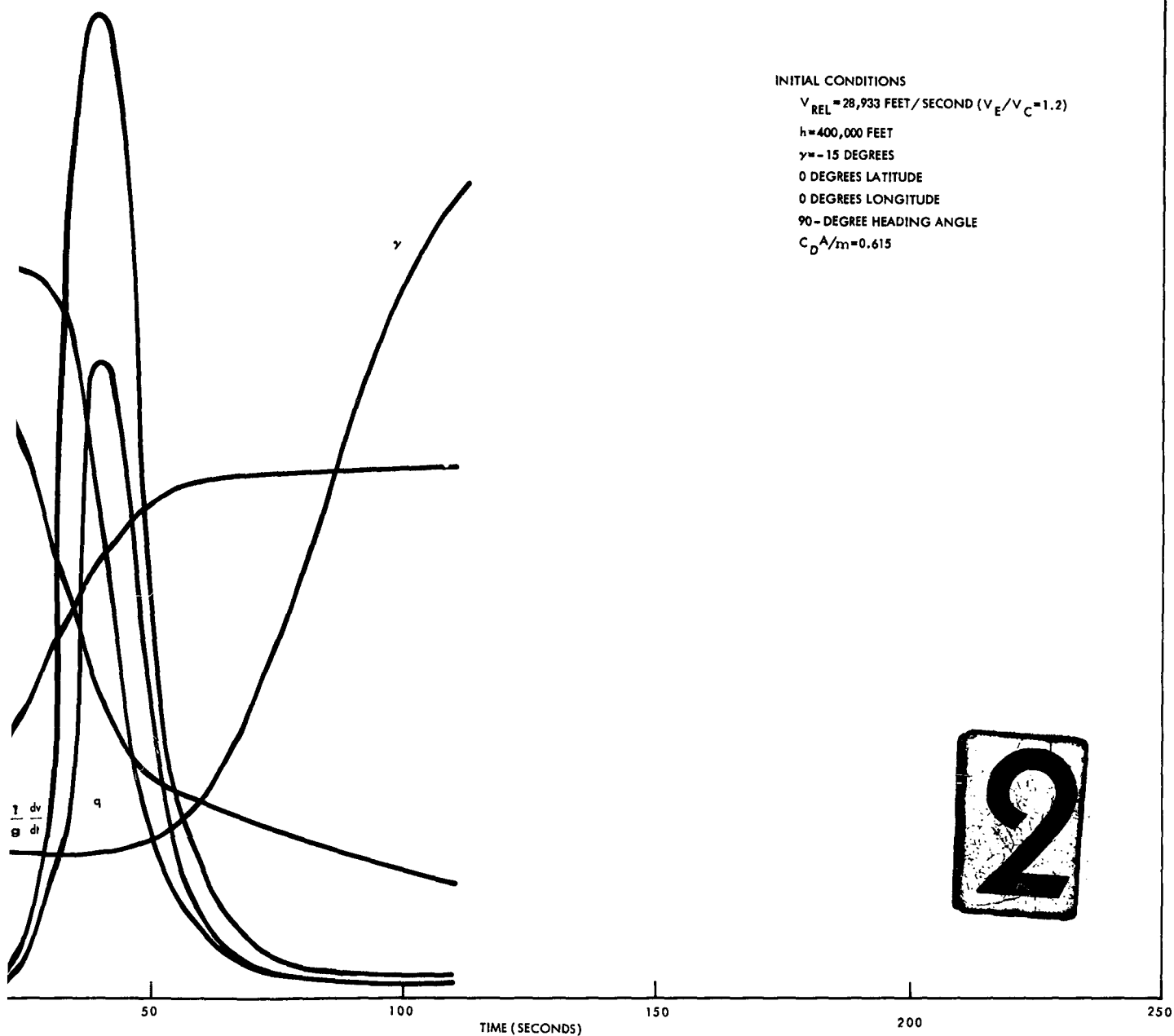


Figure 35. Re-Entry Trajectory of Tumbling Fuel Element, Flight-Path Angle Minus 15 Degrees, V_E/V_C Equals 1.2

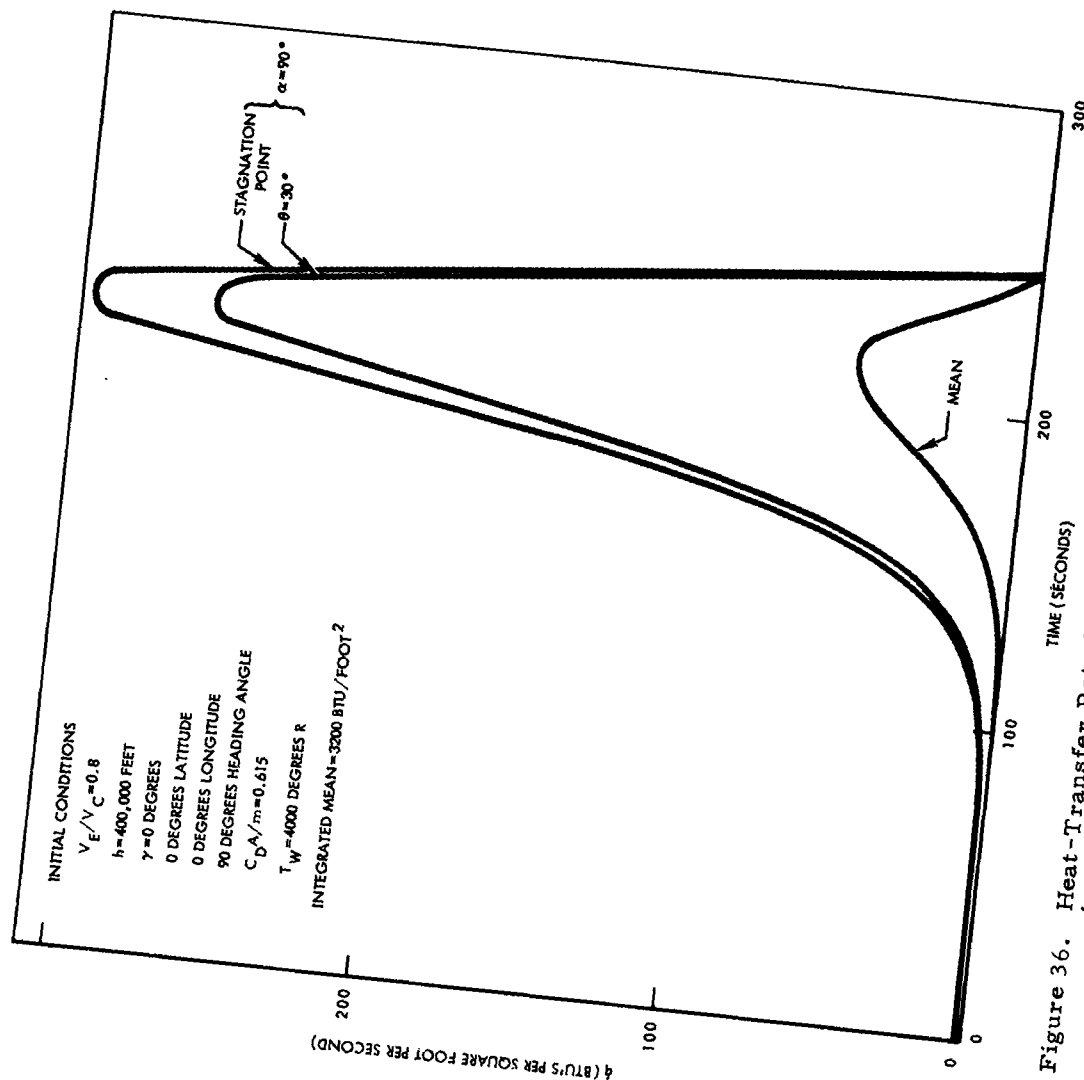


Figure 36. Heat-Transfer Rate Versus Time for Tumbling Fuel Element in Trajectory Flight-Path Angle Zero Degrees, V_E/V_C Equals 0.8

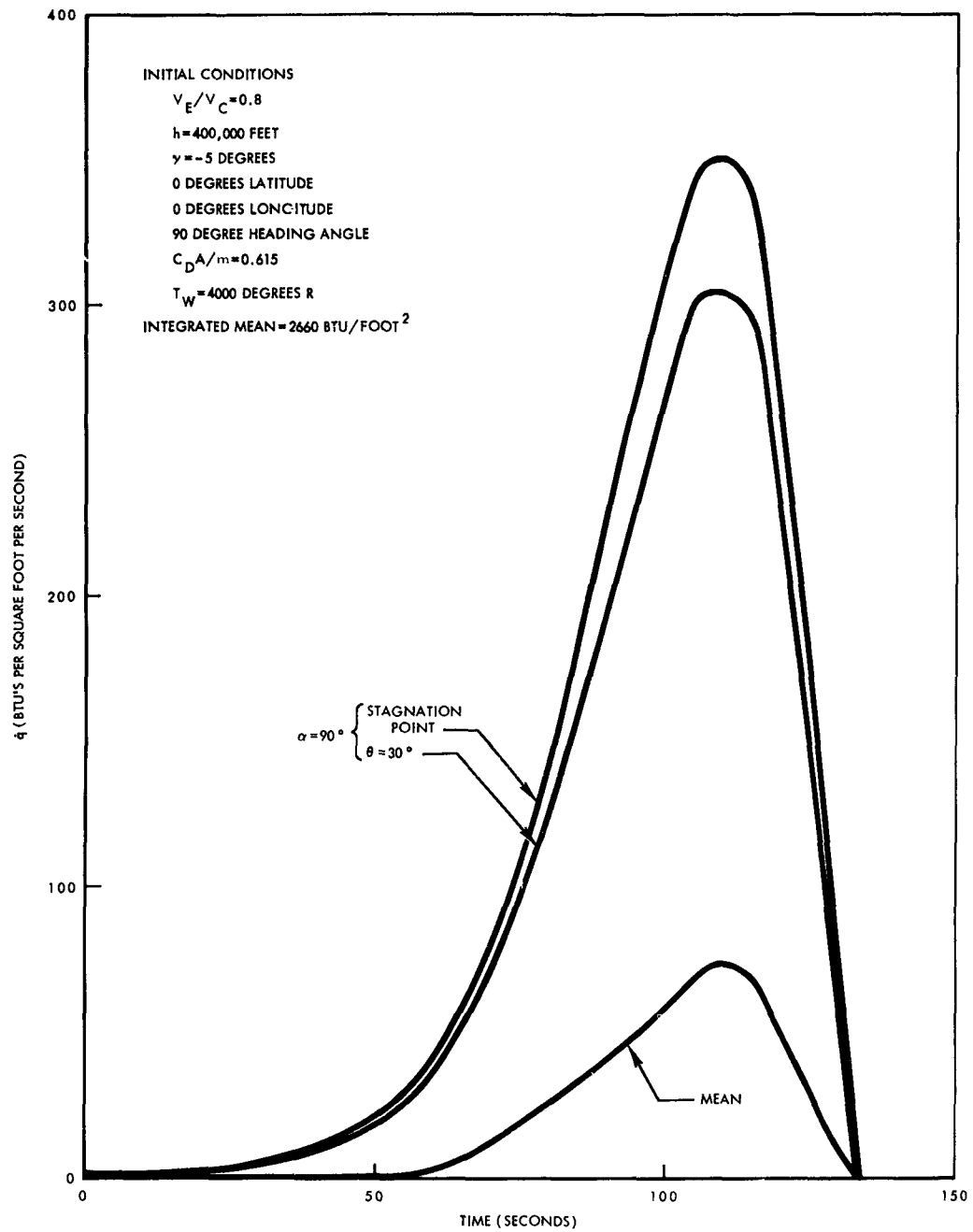


Figure 37. Heat-Transfer Rate Versus Time for Tumbling Fuel Element in Trajectory Flight-Path Angle Minus 5 Degrees, V_E/V_C Equals 0.8

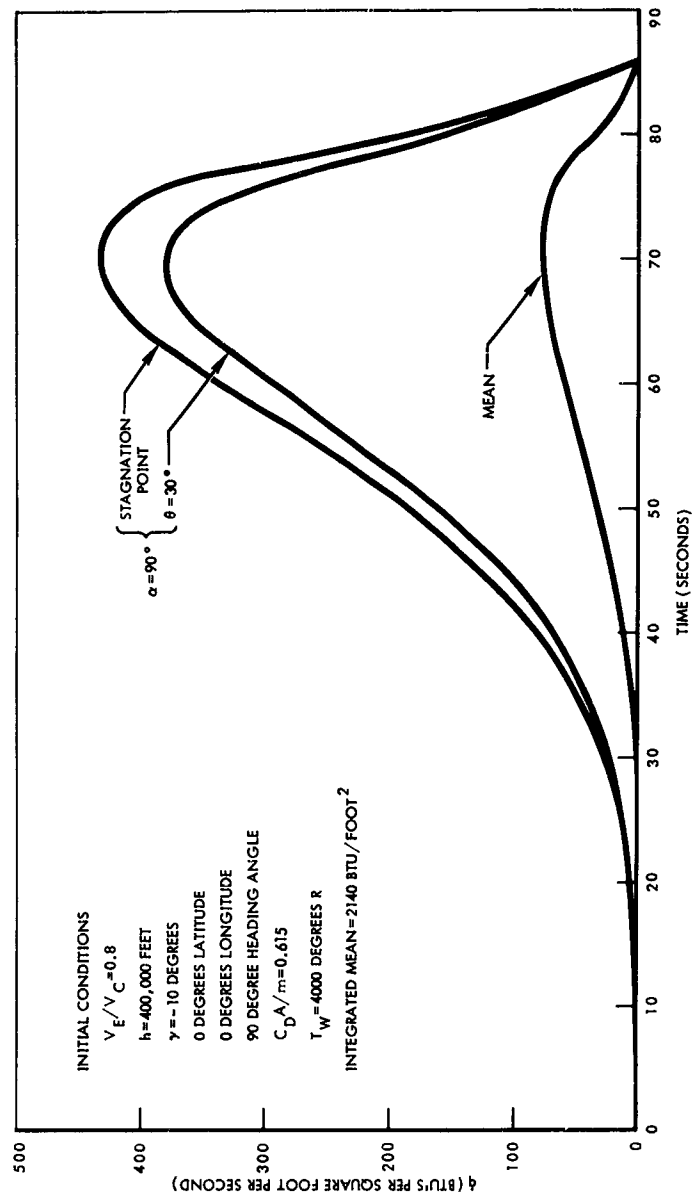


Figure 38. Heat-Transfer Rate Versus Time for Tumbling Fuel Element in Trajectory Flight-Path Angle Minus 10 Degrees, V_E/V_C Equals 0.8

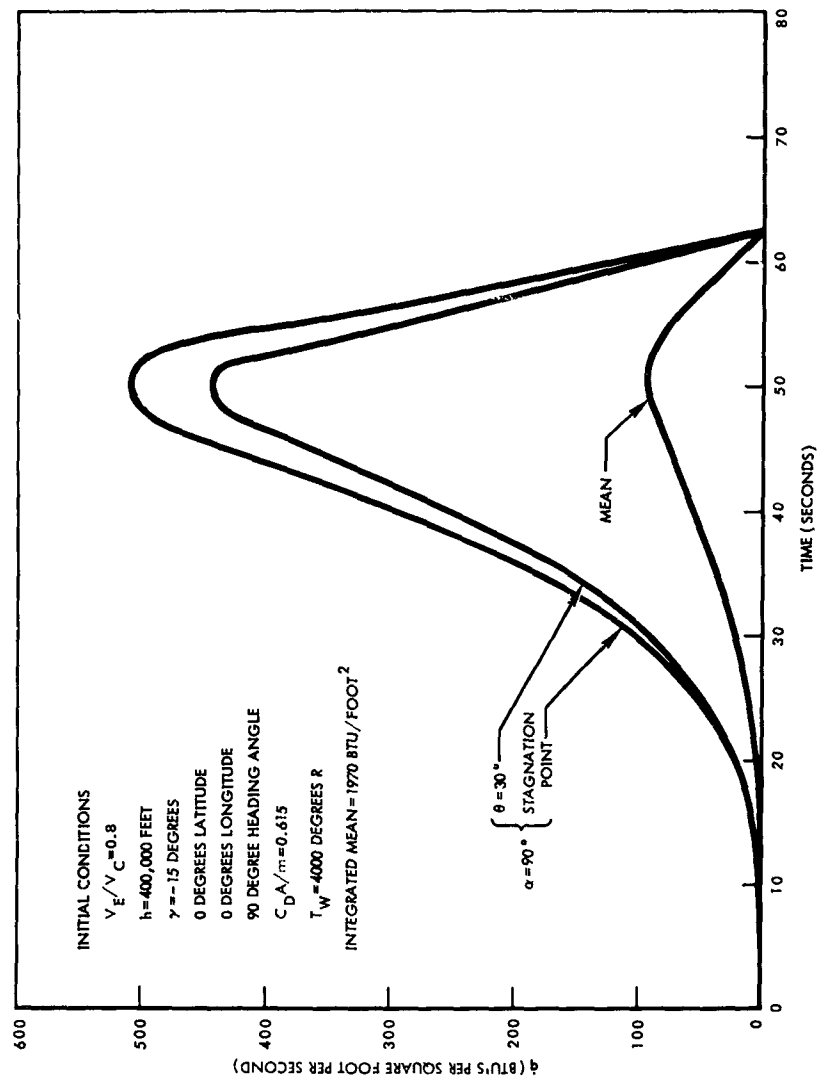


Figure 39. Heat-Transfer Rate Versus Time for Tumbling Fuel Element in Trajectory Flight-Path Angle Minus 15 Degrees, V_E/V_C Equals 0.8

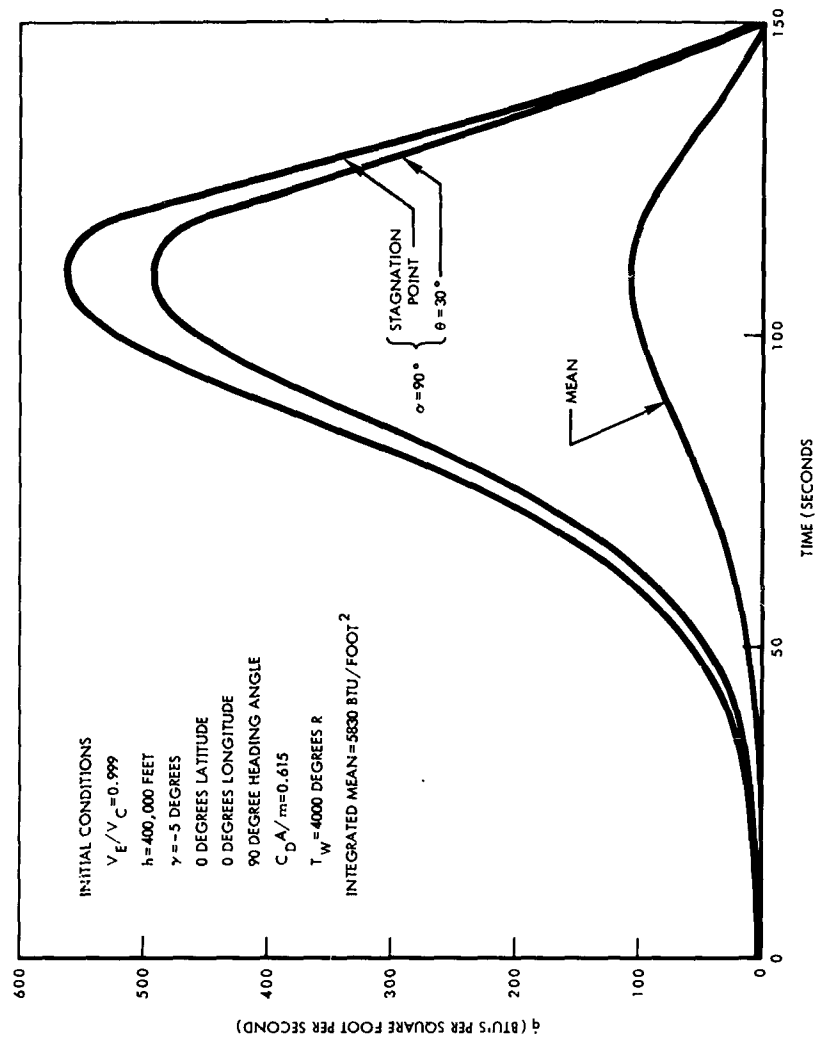


Figure 40. Heat-Transfer Rate Versus Time for Tumbling Fuel Element in Trajectory Flight-Path Angle Minus 5 Degrees, V_E/V_C Equals 0.999

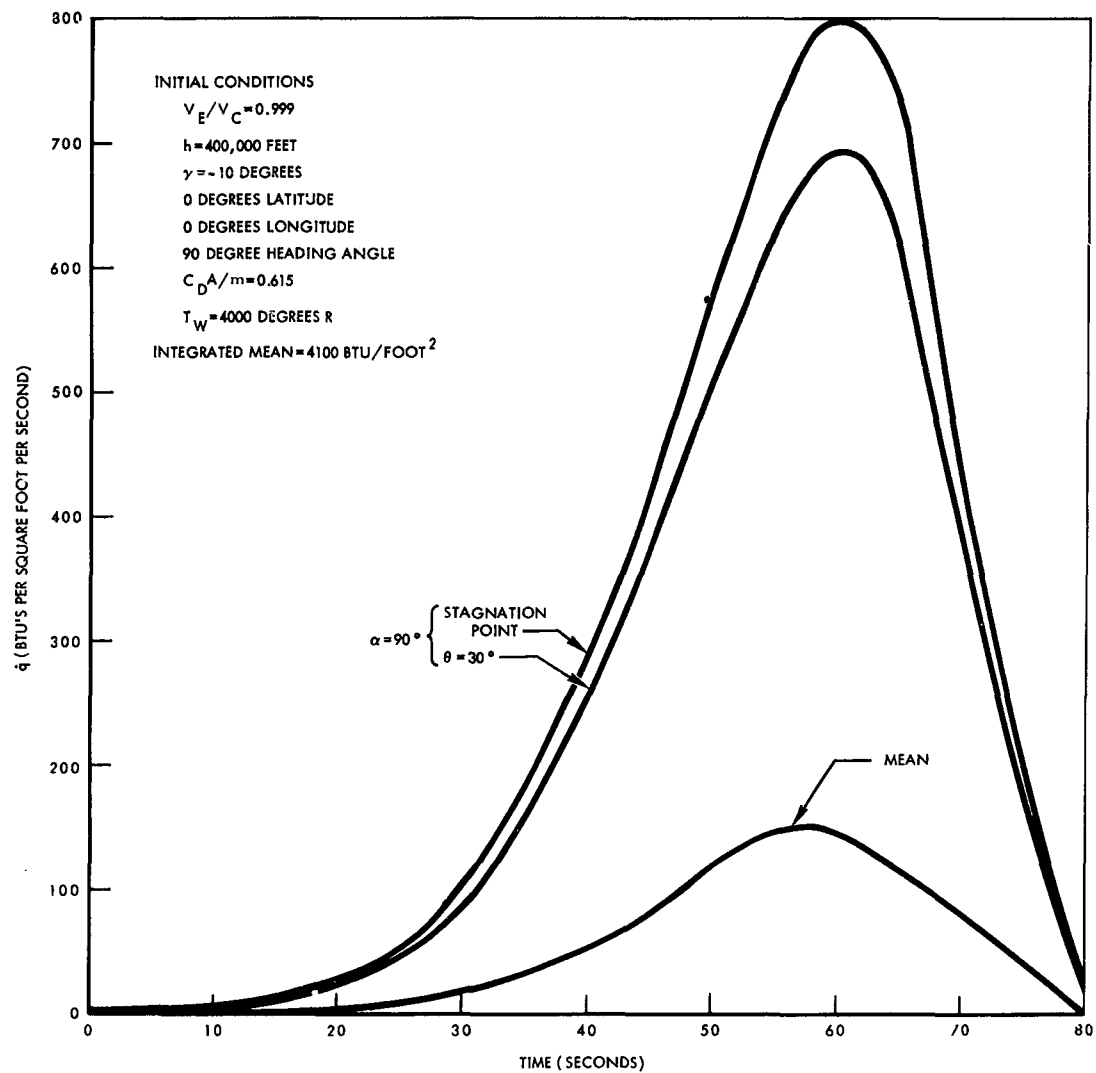


Figure 41. Heat-Transfer Rate Versus Time for Tumbling Fuel Element in Trajectory Flight-Path Angle Minus 10 Degrees, V_E/V_C Equals 0.999

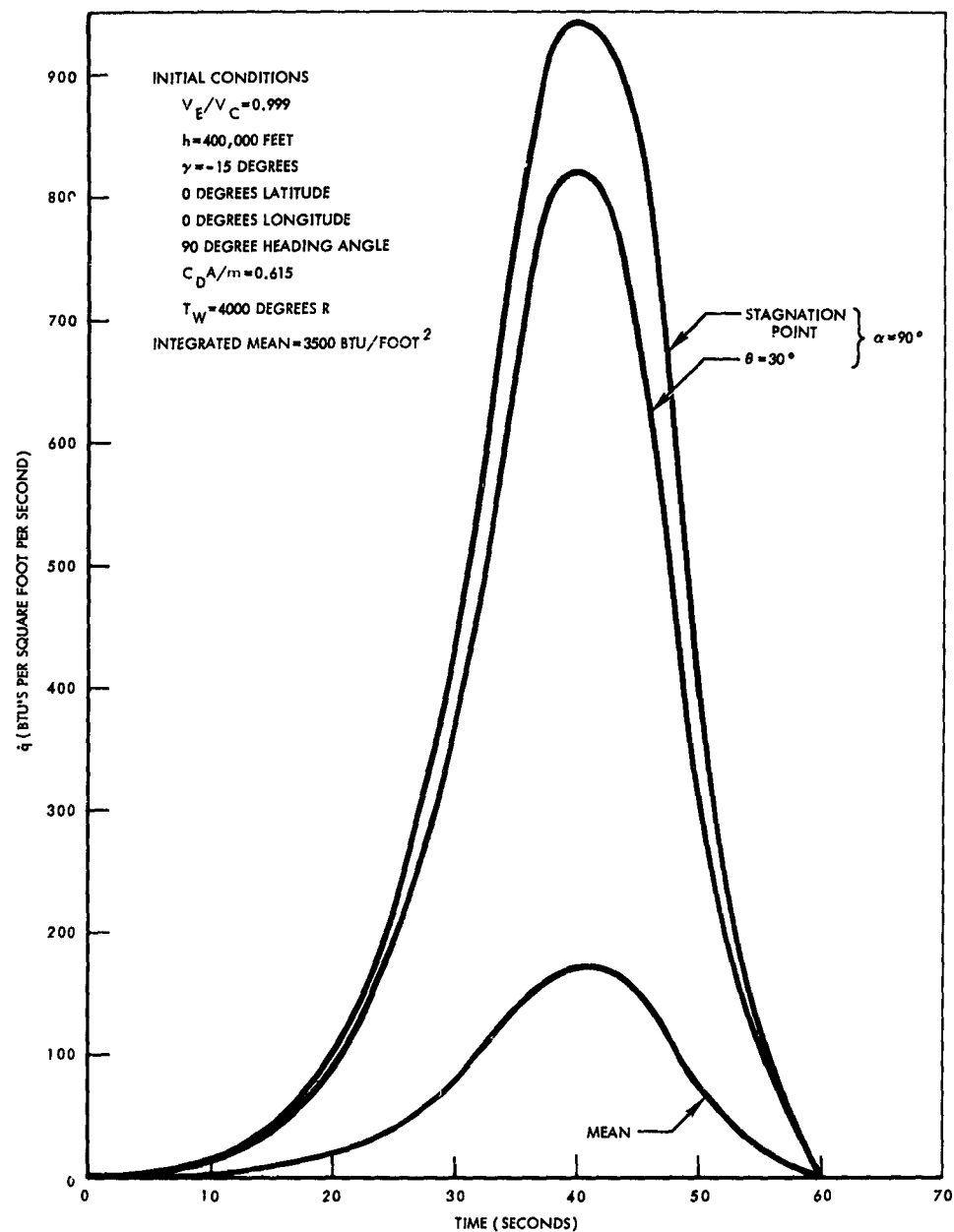


Figure 42. Heat-Transfer Rate Versus Time for Tumbling Fuel Element in Trajectory Flight-Path Angle Minus 15 Degrees, V_E/V_C Equals 0.999

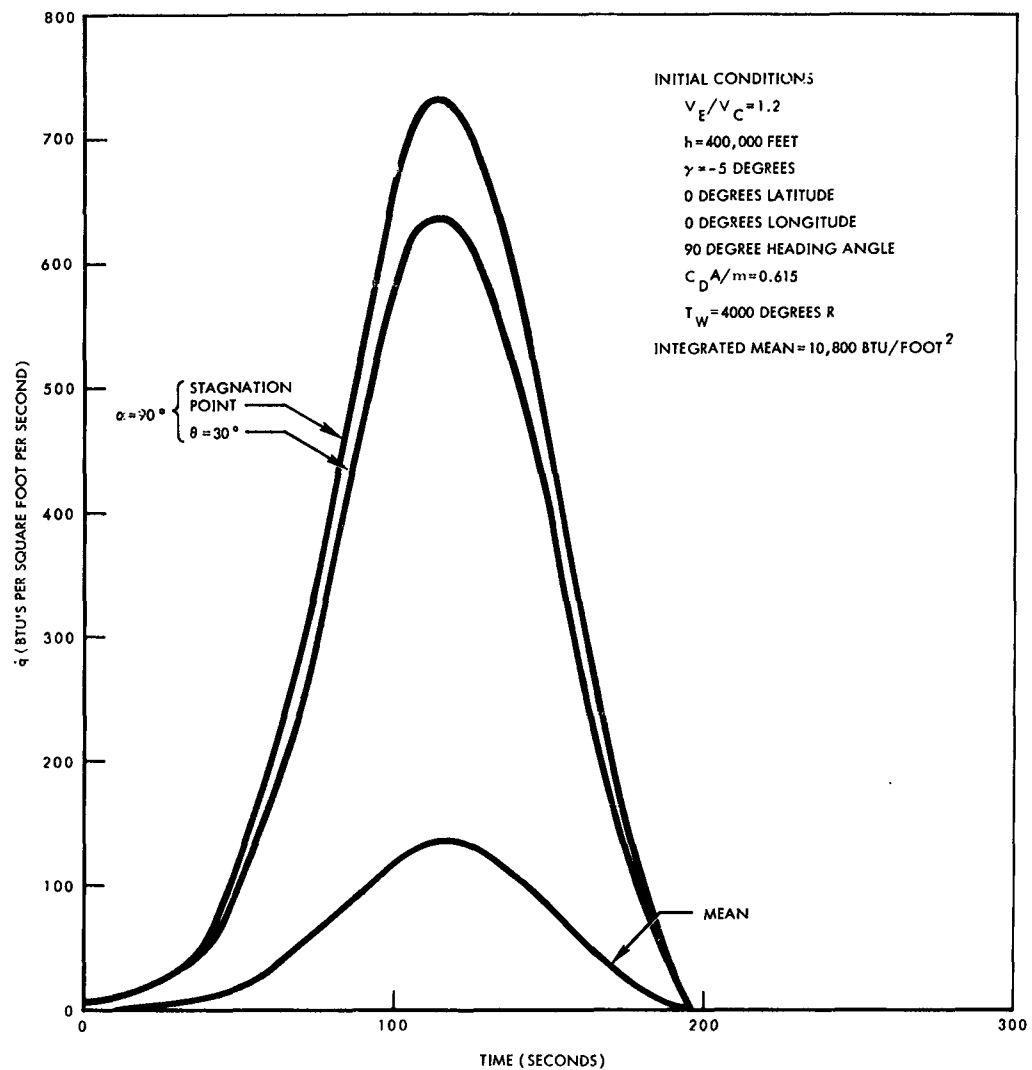


Figure 43. Heat-Transfer Rate Versus Time for Tumbling Fuel Element in Trajectory Flight-Path Angle Minus 5 Degrees, V_E/V_C Equals 1.2

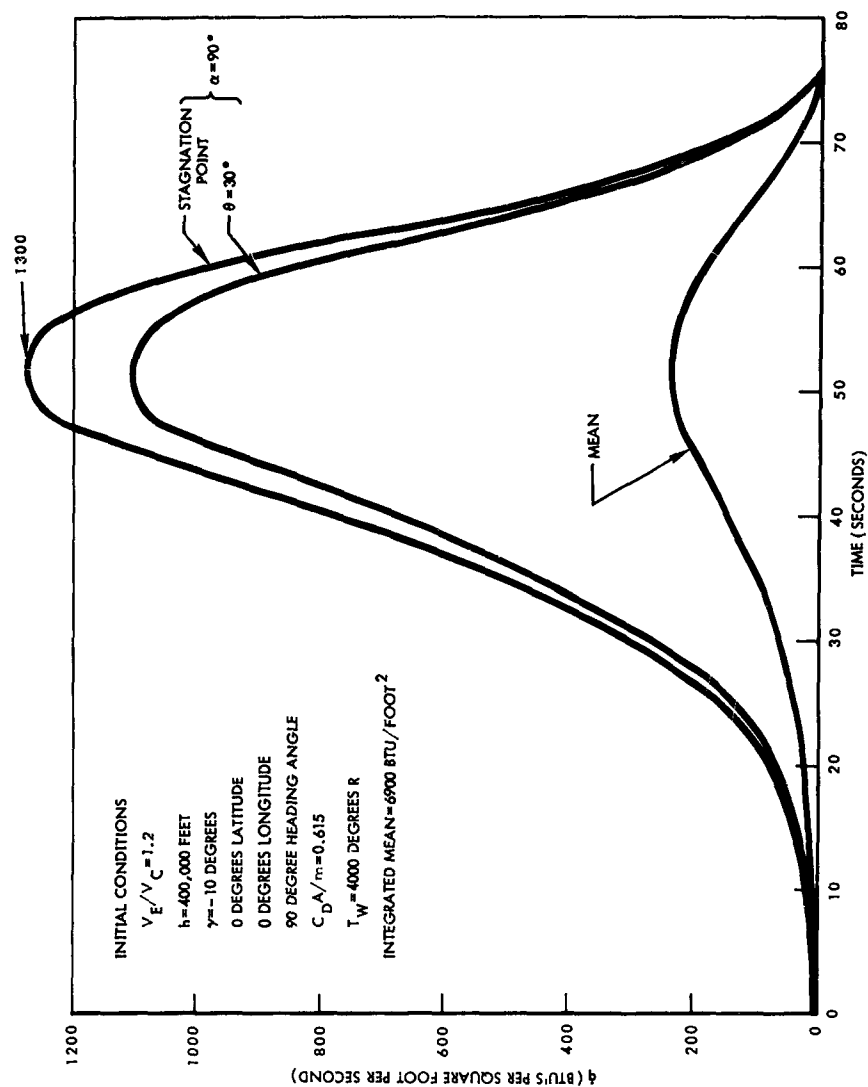


Figure 44. Heat-Transfer Rate Versus Time for Tumbling Fuel Element in Trajectory Flight-Path Angle Minus 10 Degrees, V_E/V_C Equals 1.2

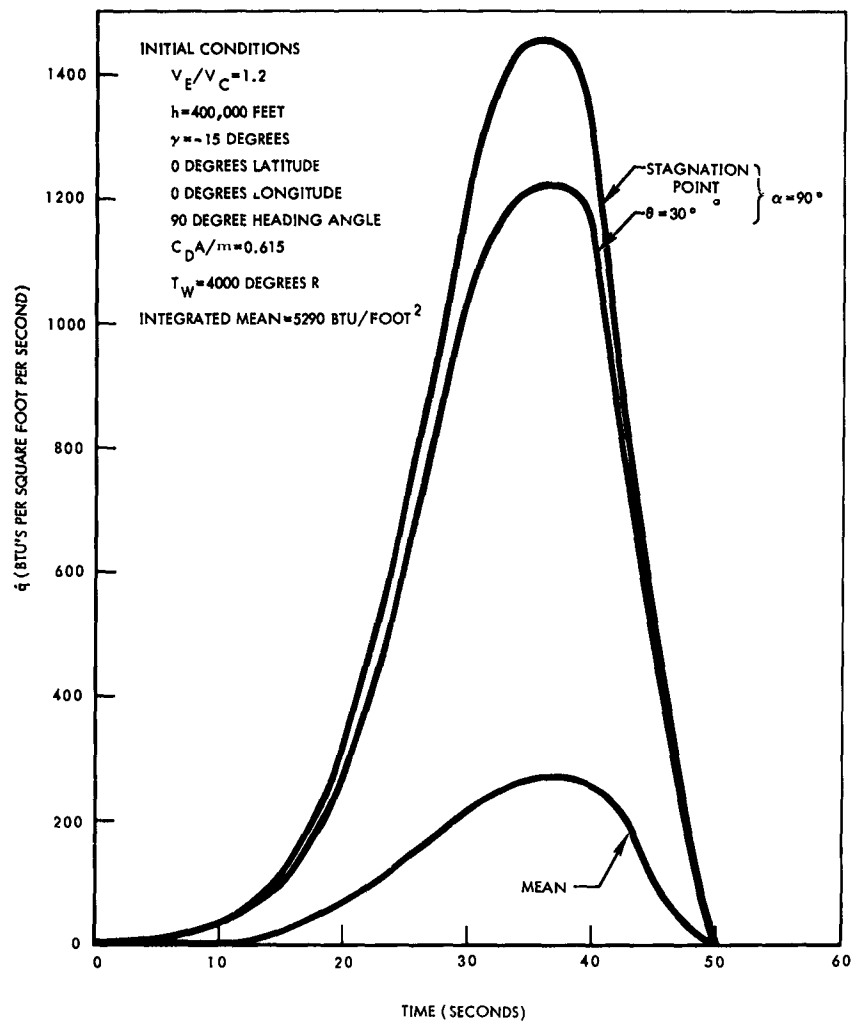


Figure 45. Heat-Transfer Rate Versus Time for Tumbling Fuel Element in Trajectory, Flight-Path Angle Minus 15 Degrees, V_E/V_C Equals 1.2

axis is normal to the flow for the heating computation. The re-entry ranges are given in Figure 20.

Re-entry Velocity and Flight Path Angle

The combinations of re-entry flight path angle and velocity at an altitude of 400,000 feet which simulate the fuel element orbital decay total heat input are shown in Figure 19. This figure also shows that the integrated heating is increased with increasing re-entry velocity and increasing flight path angle, thus substantiating the results of the preceding approximate analysis.

Re-entry Altitude

Examination of the heat-transfer rate time histories for the fuel element and the associated trajectories for re-entry conditions of $-15 \text{ degrees} \leq \gamma_E \leq 0 \text{ degrees}$, $0.8 \leq V_E/V_C \leq 1.2$ at an altitude of 400,000 feet shows that at 300,000 feet altitude the heating pulse ranges from 3.5 percent of maximum for the case of $\gamma_E = -15 \text{ degrees}$, $V_E/V_C = 1.2$ to 15 percent of maximum for $\gamma_E = 0 \text{ degrees}$, $V_E/V_C = 1.0$, indicating the time of travel from 400,000 feet altitude to 300,000 feet altitude is primarily a period of heat soaking. Thus, it is felt that acceptable heating characteristics may be attained if the flight tests are conducted at initial re-entry altitudes as low as 300,000 feet.

Fuel Element Geometric Scale

Re-entry trajectories and heat-transfer rates were also computed for half-scale and quarter-scale homogeneous tumbling fuel elements for $0.8 \leq V_E/V_C \leq 1.2$, $-15 \text{ degrees} \leq \gamma_E \leq 0 \text{ degrees}$. For the same re-entry conditions, minor differences in heat flux variation with time occurred due to geometric scaling. However, these variations were insignificant and the time histories of heat transfer rates were essentially the same, thus further confirming the results presented in Section A. A balance exists between varying $C_D A/m$ for the different diameter fuel elements and the different heat rates for the varying rod diameter.

Reynolds Number

The variation of free-stream Reynolds number of the full scale fuel element, based on fuel element length and computed at the peak heating point, was computed for the variation in re-entry flight-path angle and velocity of $-15 \text{ degrees} \leq \gamma_E \leq 0 \text{ degrees}$, $0.8 \leq V_E/V_C \leq 1.5$. Laminar flow was found to exist for all re-entry conditions of interest except at the very high velocities such as $V_E/V_C > 1.4$ where local regions of turbulent flow may

exist. Since analysis shows that laminar flow exists in the orbital decay heating conditions, it is essential that flight tests duplicate this condition.

POSSIBLE LIMITS TO SIMULATE ACTUAL RE-ENTRY ENVIRONMENT

From the results of the scaling studies conducted, the following limits on the parameters of interest appear reasonable to assure simulation of the orbital decay heating environment:

Re-entry Velocity and Flight Path Angle

The combinations of re-entry velocity and flight path angle at an altitude of 400,000 feet for simulation of fuel element orbital decay heating environment may be obtained from Figure 19. The limits of the combination of these parameters for a test using a full scale fuel element, as indicated in the figure, are $\gamma_E = 0$ degrees, $V_E/V_C = 1.0$ to $\gamma_E = -15$ degrees, $V_E/V_C = 1.35$. Greater velocities may result in transitional flow at some point on the trajectory down to the maximum heating point. For the full scale fuel element, velocities less than circular will not simulate the required heating environment, to achieve the total heat input of orbital decay conditions. Consideration of range requirements would decrease the upper limit on flight-path angle and increase the lower limit on velocity to approximately -2.5 degrees and $1.05V_C$, respectively.

Altitude

For simulation of the orbital decay heating environment, the re-entry altitude should be at least 300,000 feet, as discussed in the preceding paragraphs.

Geometric Scale

It is not known precisely to what extent the cladding of the fuel element may be scaled down. Minimum allowable cladding thickness would be an important parameter in establishing a minimum scale of the fuel element. Until better data become available, it is felt that a quarter-scale fuel element is a reasonable lower limit.

Interaction-flow regimes will have a major influence on the heating characteristics of the retaining bands on the reactor vessel and complete NAP unit. Interference effects are difficult to scale; hence, it is difficult to establish scaling limits on these items. If geometric scaling is to be applied to the spacecraft and reactor vessel, reliability of the test results is a direct function of the scaling.

Since it is known that the complete spacecraft will re-enter in the axial attitude, and since the regions of interest are on the forward portion of the spacecraft, the uncertainty in the test results inherent in geometric scaling of these items could be eliminated by flight testing only the forward portion of the full-scale spacecraft containing the components to be evaluated and assuring that this portion re-enters in the axial attitude with ballast as required to provide the same $C_D A/m$ as for the complete spacecraft.

INSTRUMENTATION

Measurements and instrumentation devices required to evaluate validity of disintegration, burnup, and dispersion theories in flight operations are discussed in this section. The instrumentation system will require equipment within the airborne instrumentation package and also ground-based equipment.

INSTRUMENTATION DATA REQUIRED

In any test operations to determine whether or not a nuclear reactor re-entering the atmosphere disintegrates into a safe state, data of chronological nature are required. Events must take place in a definite sequence culminating in the eventual disintegration of the fuel elements and the dispersion of the particles from the ablating fuel elements. The first step in the instrumentation operation is to determine whether the instrumentation capsule has separated safely from the booster that placed the capsule in position, for the re-entry test. The test instrumentation capsule is defined to include the instrumentation compartment (with installed telemetry systems, including antenna); recorders; tracking beacons (and antennas); required power supplies and associated interconnections; and the test specimen reactor (full-scale or scaled-down) with its associated accessories, vessel, fuel elements, or the complete vehicle and system. The test specimen is mounted in front of the instrumentation compartment so that it will constitute the nose of the re-entrant test capsule, exposing the parts under test to the re-entrant environment.

During boost this capsule will be appropriately shrouded for protection. Shroud separation is a well-established art, and most booster systems have shroud designs which can be utilized. No problems are expected.

After the instrument capsule separates from the last stage of the boost vehicle, the re-entry trajectory begins. The first events in the re-entry trajectory requiring instrumentation are the failure of the reactor plumbing and failure of the reflector retaining band. Because the plumbing extends from the forward side of the pump back over the pump to the reactor can, it must fail first to provide clearance for the egress of internal reactor components. The reflector retaining band is used to hold the reactor reflectors in their proper positions. When it fails, the beryllium reflector plates fall away to permit exposure of reactor can to the re-entry heat pulse. With the reactor vessel exposed to re-entry conditions, the forward lip of the vessel should melt to allow the reactor vessel lid to fall away. The opening of the

reactor vessel is an important step in the overall re-entry. Instrumentation will be required to measure the extent of opening as well as the conditions existing at the time the event occurred.

After the reactor vessel opens, the fuel elements may be exposed for release from the vessel. Each fuel element contained within the can should be instrumented to determine whether it successfully exits and clears the can. Since the fuel elements contain the nuclear fission products, they must be ejected so that they will be burned and the resultant particles distributed through the atmosphere in a safe manner. If for some reason a fuel element (or elements) should not be ejected, it may be wise to instrument sample fuel rods with temperature transducers to measure the time-temperature history of the fuel element remaining within the can. Such temperature measurements may not provide any useful information concerning nuclear fuel safety, but the data might be useful for other investigators interested in the results of the reactions of various materials during re-entry.

Instrumentation must next be used to determine the amount of fuel element disintegration due to burning. This instrumentation should be capable of determining that re-entry heating can reduce the fuel elements to a non-hazardous residue. If a safe residue results from complete burning of the fuel elements, the temperature and ablation histories are required. If residue particle size is determined to be the criteria for a safe residue, instrumentation will be required to furnish particle size information.

Captive fuel elements could be installed on the instrument capsule to provide back-up information for that obtained from free-falling rods. Information on the ablation (burning) rate of the fuel elements (each element mounted at a different angle of attack and possibly rotating) would be quite helpful. Particle size and the distribution of particle size are also highly desirable items of information in the determination of reactor dispersal safety.

REFERENCE DATA REQUIRED

Certain reference data are required to ensure the validity of test results. These reference data would be the basis on which the reduction of test data would be judged. There should be no question on the validity of the reference data as such.

Basic Reference-Data Item

The basic item of reference data for all tests is time. In any tests made of re-entry bodies over a range of considerable distance, a basic time base must be established and supplied to all range stations operating during the tests. With such a time base, the series of events which occur during launch, mid-range, and re-entry portions of the flight can be readily related

to each other, and data reduction can be simplified. This time base is usually generated at the launch site and transmitted by wire, submarine cable, or microwave to the outlying stations. The Atlantic Missile Range has an excellent timing system. For any test at Wallops Island, timing signals would have to be transmitted by radio to the outlying range ships or aircraft; if splash area is in AMR area, Wallops timing signals could be tied into the AMR timing system. At PMR, timing signals are generated at the launch site and transmitted by radio to be utilized at downrange land stations. However, not all PMR ships are tied into this timing network. Some ships use WWVH signals or the WS 117L timing signals. It is therefore recommended that PMR ships used in any NAP re-entry tests be capable of utilizing the range-timing signals. All range-time signals must be superimposed on the range recording systems used during the tests in order to correlate the events.

Other Reference Data

The altitude of the instrumentation capsule and the free-falling rods are also required as reference data for the tests. The altitude information must be correlated with the time-base noted above so that a time-altitude history may be obtained for data reduction purposes. Obtaining the time-altitude history for the capsule will not be a major problem; however, time-altitude history of the free-falling rods after ejection from the instrument capsule will be a problem. It may not be possible to obtain this information as reference data.

Attitude Information

It is anticipated that the instrumentation capsule will be stabilized during re-entry. However, some pendulum action may take place, slow spinning may occur and tumbling may be present during any experiment. Therefore, attitude information is considered necessary. The attitude data could be added to the time-altitude data noted above. This would provide a time-altitude-attitude history. This information is within the state-of-the-art for the instrument capsule but is beyond it for free-falling rods.

Weather Data

Weather data must be available for the re-entry area. Infrared and optical energy is absorbed and scattered by moisture. Thick clouds can cause extraneous radar signals in the C-band region which will affect possible radar reflection measurements of the particle residue clouds. Temperature, humidity, wind direction and velocity information should be available. Optical and infrared measurements are best made at night; radar measurements may be made at any time.

TELEMETRY SYSTEMS NAP RE-ENTRY FLIGHT TESTS

The telemetry system used for the NAP re-entry flight tests will be required to provide essentially the same services supplied by telemetry systems on the many re-entry tests already conducted. This section defines the parameters of the blackout problem for the tests studies and describes a typical telemetry system employing currently available components.

RF Blackout

A familiar phenomenon encountered during re-entry testing is the interruption of radio frequency communications due to the enshrouding of the re-entering vehicle by a plasma sheath. This sheath, consisting of a layer of hot ionized air, affects the transmission of radio signals in certain undesirable ways. The effects of primary interest in re-entry testing are the attenuation of the rf signal and the antenna detuning and breakdown. The parameters that determine the effect of the plasma as well as some of the techniques employed to reduce this effect are discussed in the following paragraphs.

Plasma Attenuation

Attenuation of an rf signal transmitted through a plasma is determined by the signal frequency, the collision frequency, the plasma frequency, and the thickness of the plasma. The plasma frequency is a function of electron density (which is, in turn, a function of temperature and density), while the collision frequency depends upon the density of the air. The temperature and density of the plasma shroud, as well as its thickness, are functions of the velocity, altitude, vehicle geometry, and aspect and attack angles.

The general formulation of the functional relation between these parameters to predict exact attenuation characteristics is a difficult, if not impossible, task. The probable duration of the blackout can be estimated, however, because for bodies with the frontal cross section considered, (roughly 3.5 square feet) the plasma sheath will form in the vicinity of 325,000 to 300,000 feet. Assuming that the re-entry velocities are between 19 and 29 thousand feet per second, decay will occur by the time the package has reached the 100,000 foot altitude. Thus, the duration of maximum possible blackout is the time interval required for the vehicle to travel between altitudes of 325,000 feet and 100,000 feet. This time interval is plotted in Figure 46 for various values of re-entry velocity and angle.

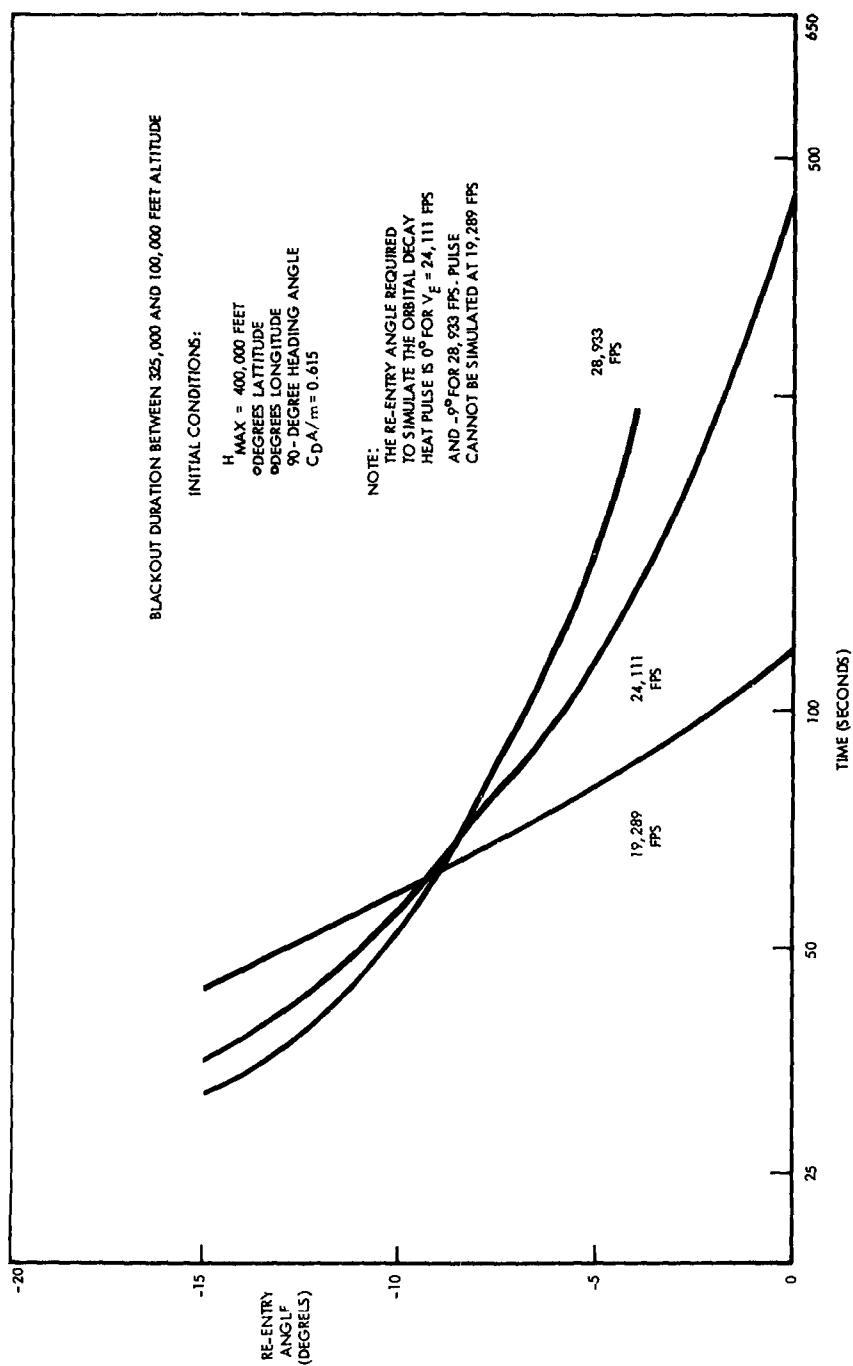


Figure 46. Maximum Duration of VHF Radio Frequency Blackout,
 Time as a Function of Re-Entry Angle

Techniques for Obtaining Data During Re-entry

There are three common methods of obtaining data during the interval of plasma generation. One method employs special vehicle geometries to produce a thinned, cooled plasma layer in the vicinity of the antennas. This method is not considered applicable to these tests, because it requires geometries and orientations that would restrict the re-entry attitudes and inhibit the reactor burnup.

A second method employs frequencies above the penetration frequency of the plasma. For the vehicle configurations considered, the frequency required will be in the SHF or EHF bands. This method is quite effective and will probably come into common use in the future. At present, although some re-entry testing has been performed using K-band telemetry systems, the availability of ground equipment is limited, and the flight hardware does not have an adequate reliability history.

The third method has been employed on the vast majority of tests to date, and while it has drawbacks, appears to be the most satisfactory method for current tests. This method simply involves the recording of the data during blackout and subsequent delayed transmission. The recorder is a source of possible failure and an added weight and power load; however, the recorders have a long history of successful flights and have been packaged to limit the physical penalties. Therefore, the system described in the following section employs a recorder as the means of procuring data during the blackout interval.

System Description

A simplified block diagram of a typical re-entry telemetry system is shown in Figure 47. The exact configuration of the commutator and channel allocations will vary with the particular mission; however, typical characteristics applicable to all test missions are discussed below.

Data Channels

Thermodynamic studies performed to date revealed that temperature sampling at intervals of five seconds provides sufficient data to determine the temperature profile accurately. More rapid sampling will yield redundant data that may be used for smoothing but is not actually required. Since there will be a large number of temperature measurements made in all cases, the low sampling-rate requirements make these measurements amenable to commutation; however, low-level signal capability is required of the commutator.

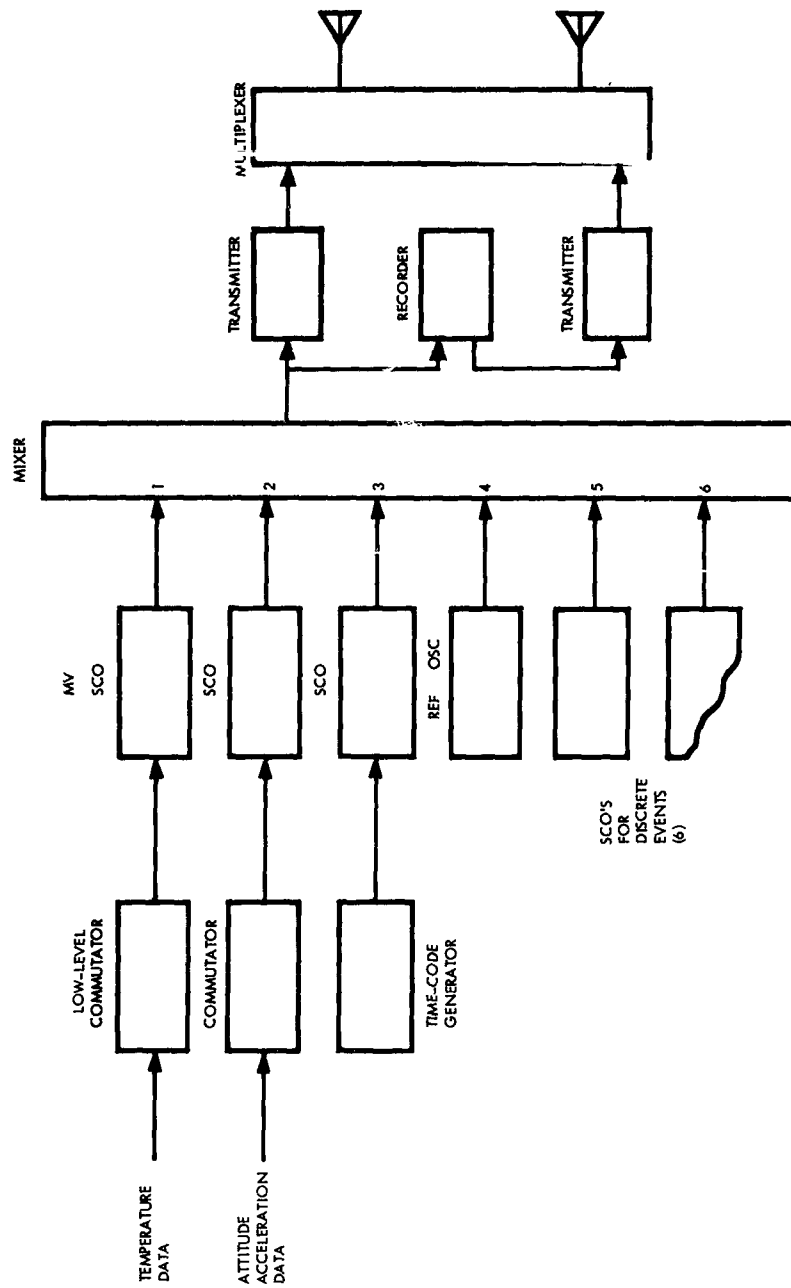


Figure 47. Typical Telemetry System for NAP Re-Entry Flight Test

Similar conditions are expected for the acceleration and attitude measurements. These values are expected to be slowly varying, so a commutated channel again seems appropriate. These quantities can usually be obtained at voltage levels such that low-level commutation is unnecessary.

The data appearing to require continuous monitoring are the occurrences of discrete events. Such events as reactor separation and fuel element ejection will have to be monitored to determine the precise time of occurrence. The characteristics of these data, as well as those typical of the commutated channels, are shown in Table 3.

Transmitters

Most ground stations have receiving equipment in the 225 to 260 Mc telemetry band. In addition, transmitters having roughly ten watts of output power and good reliability histories are available in this region. Transmissions in this band will suffer from rf blackout and will require the use of recording techniques; however, the availability of ground equipment makes this the logical choice.

Antennas

The final antenna configuration will depend upon its orientation during re-entry and upon package design. A characteristic system would employ two antennas mounted diametrically opposite each other on the surface of a cylindrical canister having a diameter of approximately eighteen inches. A good VHF antenna for such an application is the cavity-backed crossed slot. This can be packaged flush to the surface in a cylinder six inches in diameter, and two inches deep and weighing two pounds.

Recorders

This unit will be the least reliable of all of the equipment in the telemetry package. The recorder selected will ultimately be determined by the characteristics of the particular tests. Storage-capability requirements will depend upon blackout duration, record speed will depend on the recording frequency requirements, and command capability will depend upon the delayed transmission scheme selected. The storage time may vary over the ranges shown in Figure 47, this variation will require that recorders having large storage capacity be used for the low re-entry angle tests rather than more simple loops with small capacity. Frequency response requirements will vary from a possible low of 4 to 5 Kc to 70 Kc; the higher frequency response will require the use of higher recording speeds of 45 inches per second with an associated decrease in reliability. The command capability may vary from a simple on-pad turn-on to start, stop, record, and erase commands.

**Table 3. Characteristic Data Sources for NAP Re-Entry
Flight Tests**

Measurement	Voltage Level	Required Sampling Rate	Number of Measurements
Temperature	Millivolts	1 Sample 5 sec	30-70
Attitude	2-5 volts	5 sample/sec	3-5
Acceleration	2-5 volts	5 sample/sec	3-5
High Level Experimental Data	2-5 volts	5 sample/sec	3-5
Discrete Events*	2-5 volts	Continuous monitor	6-10
Reference Information Required			
Time Code Generator	2-5 volts	Continuous monitor	1
Reference Generator	2-5 volts	Continuous monitor	1
Calibrate Points	Millivolts	1 Sample 5 sec	10-25
* See Table 4 .			

Each mechanical function required deteriorates the recorder reliability. In view of the reliability consideration, it is suggested that well-proven flight equipment having a well-established record of reliable flight performance be used.

System Operation

The recorder should be started on the launch pad to prevent the freezing of the mechanical parts during boost accelerations. A recommended recording technique would involve the continuous cycle of recording and subsequent delayed readout during the entire flight. Continuous transmission of both the real time and delayed data would provide redundant data during the entire flight except during the blackout. This redundancy can be used to fill in gaps that may occur in received data at a particular station or to provide correlation between different receiving stations.

This method of operation requires two transmitters and thus increases the system physical penalties (power, weight and space). However, the second transmitter enhances the reliability of the system, because provision can be made to switch the delayed information to the second transmitter if the first one fails.

Another operational procedure that might be incorporated involve use of a single transmitter and the switching of the delayed transmission to the transmitter only during post-blackout readout. This method prohibits the collection of any real time data during the readout period and results in system reliability deterioration by requiring switching of two sources and elimination of the redundant transmitter. It has as its single advantage the elimination of the physical penalties of the second transmitter, with attendant power savings.

A third method of operation would employ two transmitters, but the recorder and second transmitters would be actuated only during the required periods. This system has little to recommend it. Its only virtue is a power reduction. The method greatly inhibits the probability of obtaining useful data because the reliability of both the transmitter and recorder functions is reduced.

On the basis of these characteristics of the operational systems, the continuous recording and transmission of both real time and delayed data is recommended for the re-entry flight tests.

AVAILABLE INSTRUMENTATION METHODS

There are a number of instrumentation methods now available which

could be utilized during the capsule separation, reactor breakup, and fuel element ejection phases of the test. However, development of instrumentation methods to indicate fuel element burnup, ablation rates and particle size of the ablated material will extend the state of the art. Event instrumentation and potential sensors are summarized in Table 4.

Instrumentation to indicate separation of instrument capsule from the booster is well within the state of the art. Any item that could indicate a break would be adequate as the transducer in this system. Strain gauges, break-away wires, umbilical-type connectors are all acceptable for this operation. There are no unusual environmental problems associated with the use of this transducer. The break-away of the reflector retaining band can use the same system. The transducer must only indicate a break in the band. This supposes that the band with a weak section is installed on the reactor. If analysis shows that the entire band may disintegrate or that there will be no particular weak area, the break-away transducers can be placed on the beryllium reflectors.

Instrumentation is preferred which will detect the operation in which interest is centered; for example the separation of the beryllium reflector, rather than the retaining band. If sensors are placed on the band, the transducers would have to be protected from the high heat flux which melts the band. A similar situation exists on the reactor vessel lid. High temperatures may require that the transducer be protected. Similar transducers can also be used in this case. Essentially the problem is to measure a break between two pieces of metal. Measurement of fuel element ejection can also use the break-away technique. In this case, small wires can be imbedded in the sample elements. The wire length will be greater than reactor vessel length, the extra length being loosely coiled at the end of the individual fuel elements. As the elements are ejected, the coils will straighten out, placing tension on the wire. The wire will then break, opening the circuit that denotes fuel element clearance of the reactor vessel. Design of such a system is somewhat critical due to environmental conditions. It is important that the on-board instrumentation system and its installation be thoroughly tested under all possible environmental conditions of proposed use in order to prove the acceptability for flight test during the actual test operation. Systems which may be used to circumvent some of the environmental problems are described in a following section. The data required to verify fuel element burnup can be obtained by two types of flight test experiments. First, captive fuel element tests represent a controlled experiment where the fuel elements are mounted on the vehicle and present various aspects to the re-entry path. Second, free-flight tests offer data opportunities during re-entry where the fuel elements are ejected from the instrumentation vehicle into a free-flight trajectory path, the ejection may be controlled or may occur during reactor breakup. Both kinds of experiment are considered

Table 4. Event Instrumentation

Event	Sensor Used	State-of-Art	Fuel Element Test Requirement			Possible Weight Of Sensor
			Free-Falling	Captive	Scaled Up	
Capsule Separation from Booster	Umbilical Connector Breakaway wiring	Available Available	(1)	(1)	(1)	6 oz
Reflector Band Disintegration	Thermocouples Breakaway wiring	Available Available	Yes	(2)	(2)	3 oz ea 1 oz
Reflectors Drop Off	Breakaway wiring	Available	Yes	(2)	(2)	8 oz
Reactor Can Lid Drop Off	Thermocouples Breakaway wiring	Available Available	Yes	(2)	(2)	3 oz 1 oz
Ejection of Fuel Elements	Breakaway wiring Reactance-reluctance methods	Available Available Laboratory experiment required	Yes (3)	No	Yes (3)	1 oz ea 8 oz ea
Ablation of Fuel Elements	Thermocouples Resistance measurements	Available Exp required	Yes	Yes	Yes	3 oz ea 8 oz
Particle Size and Dispersion	Impingement devices Radar Infrared Optics	Available Not on range Development Development	Yes	Yes	Yes	Ground Ground Ground

(1) Capsule separation from booster may not be required

(2) Not necessarily required, dependent on test

(3) Fuel elements do not necessarily have to be ejected from reactor, they can be ejected from any type of pod as long as they are freed from mother body

(4) If captive fuel elements test item recovered, optical instruments could also be on board

necessary for a flight test program. This approach ensures that maximum re-entry information will be obtained. Table 5 summarizes the two flight experiments. The captive fuel element experiments allow use of instrumentation sensors located within the test specimens. These sensors provide a direct measurement of the fuel element ablation history. The fuel element specimens are mounted to present various attitudes to the re-entry environment and to be free from the shock wave created by the parent vehicle. Fuel element specimens are rigidly mounted to the instrumentation unit. One is mounted with the element axis parallel to the flight path, a second test element is mounted with its axis perpendicular to the re-entry path. A third fuel element could be mounted to allow free rotation about an axis perpendicular to the flight path to approximate the tumbling motion of the fuel element during free-flight re-entry. Instrumentation of the captive fuel elements is achieved by imbedding thermocouples in the fuel element cores and along their lengths. These sensors provide the necessary heat transfer data from which the ablation histories can be established. In addition, the loss of signal from a sensor as ablation progresses, yields an indirect measurement of fuel element size. The placement of sensors inside the test specimens must not structurally weaken the elements and cause premature breakup. The advantage of this type of experiment is that it permits direct fuel element measurements during the re-entry phase of flight. Disadvantages are that physical constraints can affect the data and that extreme care must be exercised in evaluation and interpretation of such data.

Table 5. Fuel-Element Burnup Experiments

Experiment	Measurable Parameters	Required Instrumentation	Remarks
Captive	Fuel element temperature history Ablation rate Fuel element size	Thermocouples imbedded in fuel element	Provides direct measurements. Insures data collection. Fuel element constraints limit data applicability
Free-Flight	Temperature Trajectory Ablation spectra Size (indirectly)	Ground and airborne optical and infrared equipment	Simulates re-entry environment. Does not provide ablation rate; difficult to identify fuel element from other re-entry objects

In the free-flight tests, during which the fuel elements are subjected to a re-entry environment more nearly simulating the expected operational one, optical and infrared instrumentation provides the only methods of monitoring the re-entry events without interference. A flare will be released to indicate that fuel elements are ejected and to track rods as soon as possible for controlled ejection tests. The fuel elements will be impregnated with a material possessing an optical emission spectra easily distinguished from the parent vehicle. The characteristic spectra will clearly identify the ablating fuel elements so that they can be tracked independently.

The tracer element should not be lumped at the center of the fuel element. Analysis of lumped alkali metals indicates the metal may vaporize before being heated to a sufficiently high temperature to excite the electronic states. In addition, it is possible that premature fuel element breakup could occur due to internal vapor pressure. For tests where the rods are ejected normally by reactor breakup, it is recommended that extra fuel elements be stored in a pod and mechanically ejected at a pre-selected altitude. This insures collection of re-entry data and makes sure a test flight is not wasted if the fuel elements do not escape the reactor vessel during re-entry breakup. Optical tracking of the re-entering fuel elements provides an indirect, or possibly negative, method for ascertaining burnup. If the fuel elements are tracked below the minimum altitude for melting, reportedly 100,000 feet, it can be assumed that complete burnup has not occurred. Table 6 shows the infrared and optical equipments of the test range that are considered to represent the minimum instrumentation requirements necessary to obtain usable data from the re-entering fuel elements. Ablation particle size measurements could be made by sampling techniques. Particle impingement devices could be mounted on the rear circumference of the instrumentation capsule directly behind the captive test fuel elements. These would collect samples of the particles ablated. Such a technique would give an ablation particle size sampling measurement only. They would not necessarily give information as to the end particle size, unless the samples could be correlated with sampling measurements from other experiments, either laboratory or airborne.

POSSIBLE SYSTEMS

Although possible instrumentation systems acceptable for use during nuclear powerplant re-entry tests were partly discussed in the preceding section, they will be discussed here in greater detail.

Separation Tests

If separation of the instrument capsule from the booster is a requirement, a connector of umbilical type could be used. This connector could have uses other than its action as a transducer. It could be used for transfer of electrical power from the last booster stage into the instrumentation capsule before any instrument capsule electrical power is initiated. It could also be used to transfer the action on command signals into the instrument capsule as a means of beginning any sequence of events such as power initiation, beacon system turn-on, initiation of the separation procedure, etc. Size of the connector would depend on its multiplicity of uses. The size could range from a simple two-pin connector to the larger multi-pin connector. Simple, small strain gauges could also be used. They would serve only to denote strain between the two stages, including the breaking

Table 6. Optical and Infrared Instrumentation Requirement for Free-Flight Burnup Experiments

Instrument	Location	Remarks
Motion Picture Cameras	Ground and/or ship	Used as boresight cameras to monitor the aiming and to record the objects viewed by various instruments
Long Focal Length Motion Picture Camera	Ground and/or ship	Provides a photographic record of the re-entry object at maximum resolution
Two Banks of Staggered Ballistic Cameras	Ground and/or ship Airborne	Each array with approximately 180° view angle; one array chopping and dispersing into a spectrum, with a transmission grating, the incoming radiation; the other array without the grating and not chopped
Two Spectral Sequence Cameras	Ground and/or ship Airborne	Resolve target structure along line of motion. One camera operating in the 3600 Å to 7000 Å region and the other from 5000 Å to 9000 Å
Bank of Photometers	Ground and/or ship Airborne	For measuring target irradiance in several selected narrow wavelength regions
Infrared Radiometers	Ground and/or ship Airborne	Measure target radiation in the 0.7 μ to 5 μ region
Infrared Spectrometer	Ground and/or ship	To record target spectrum in the 0.8 μ to 5 μ region

point. Low-stress, easily-broken conductors could also be used, but these are basically the same as the umbilical connector idea mentioned above. Disintegration of the reflector retaining band presents an instrumentation problem similar to that just discussed; namely, whether one part falls freely away from another part. This can be accomplished by using a break-away wire. The break-away wiring can be connected to thermocouples located on the band to give a time-temperature history of the band. By having a number of thermocouples (with break-away wiring) located around the band, information can also be obtained on the entire band, and it can be determined whether or not the entire band breaks away cleanly or in segments. Measurement of the beryllium reflectors break-away can also be measured by using break-away wiring concepts. Break-away wiring can be attached to each reflector to ascertain that the particular reflector is broken away from the test specimen.

Measuring of the opening of the reactor vessel lid may be accomplished by use of thermocouples and break-away wiring techniques. Thermocouples can supply time-temperature history of the lip or the reactor vessel up to the time the lid is free of the vessel. These thermocouples can be spaced around the lip of the can to obtain data on the total upper portion of the vessel as a means of determining whether the entire lid falls away or just a portion.

Ejection of individual reactor fuel elements presents a unique problem determining whether or not they leave the can. The fuel elements are packed into the can, along with beryllium fillers, in such a manner that they will be acted upon by deceleration forces as the open reactor vessel slows during re-entry into the atmosphere. Whether or not these rather tightly packed elements will actually exit from the can is arguable. If they do fall out and drop away from the can, break-away wire circuitry may be used, providing there is enough force to break the wire. Break-away wiring with small breaking forces may rupture due to vibration and therefore present a false sensing signal. Alternatively, the fuel elements may be instrumented for use with a linear transducer. For example, wire (or rope, or similar item) can be imbedded in one end of the fuel element. The other end of the fuel element can be wrapped around a small pulley, which can be attached to the shaft of a low-torque multi-turn potentiometer mounted on (or in) the back of the can. As the element exits, the wire is pulled off the pulley, causing the potentiometer to change resistance. This denotes the distance the fuel element has exited. The wire length can be equal to or slightly longer than can length. When wire is fully extended, it will be broken to allow the fuel element to fall free. The resistance value can be telemetered to a data station where it can be compared with a laboratory measurement. If potentiometers are not desired, inductance units might be used or electro-mechanical relays, operated by the turning of a pulley. These units would be mounted in the relatively cool "back-end" of the can, where environmental problems would be less severe.

Captive Tests

For captive fuel elements, volumetric resistance measurements might be made (pre-test laboratory experiments would be necessary). In this case a low-temperature (in relation to melting temperature of Zr-H) insulated wires could be imbedded in the center of the fuel element, the two wires entering the fuel element midway between the ends (at the mount) then extending to where bare wire will adhere to the zirconium elements near each end. As the element melts away the insulation and wire should also melt to give a temperature measurement of the material remaining. As an alternative, thermocouples could be imbedded in the fuel element to provide a time-temperature history which could be compared with experimental rod burning to give an ablation rate.

To give an indication of the size of the fragments ablating from the captive fuel elements, impingement devices may be mounted on the aft end of the instrument capsule. These devices essentially collect the fragments and process them through a series of funnel-shaped sampling elements, each successive element decreasing in size. The number of fragments impinging on each sampling element is counted. This counting could be telemetered back to the data station or the test capsule could be recovered from the ocean. The particles could then be counted and the captive rods examined. The particular problem area with the impingement devices is that it would require additional data reduction instrumentation in the test capsule.

If the test capsule is recoverable after flight, it may be possible to use cameras to take pictures of the captive rods. Cameras would give a good picture of ablation progress. It might also be possible to ascertain fragment sizes, at least down to a particular size, depending on camera capabilities.

Radar Techniques

The size of residue particles may be determined by radar techniques without directly sampling of the residue cloud. The scattered rf signal received at the radar site can be directly associated with particles of average size.

The average received power from a cloud of particles which fills the beam cross-section is given by:

$$\bar{P}_r = \frac{P_t G^2 \lambda^2 \theta \Phi r C \eta}{2(4\pi)^3 R^2} \quad (\text{Reference 3})$$

where:

\bar{P}_r = average received power	r = pulse length
P_t = peak transmitted power	C = speed of light
G = antenna gain	η = radar cross section per unit volume
λ = wavelength	R = range
$\theta = \Phi$ = half-power beamwidths of the antenna	

* The radar cross-section-per-unit volume is given by

$$\eta = N \bar{\sigma} \quad (2)$$

where

N = Total number of scatterers per unit volume
 $\bar{\sigma}$ = average cross section $\cong 4\pi\alpha^2 (2\pi\alpha/\lambda)^4$

Note that it varies as the sixth power of the radius. The AVCO report reference indicates that the residue droplets will be in the form of spheres. The radar cross-section per unit volume of conducting spheres is given by:

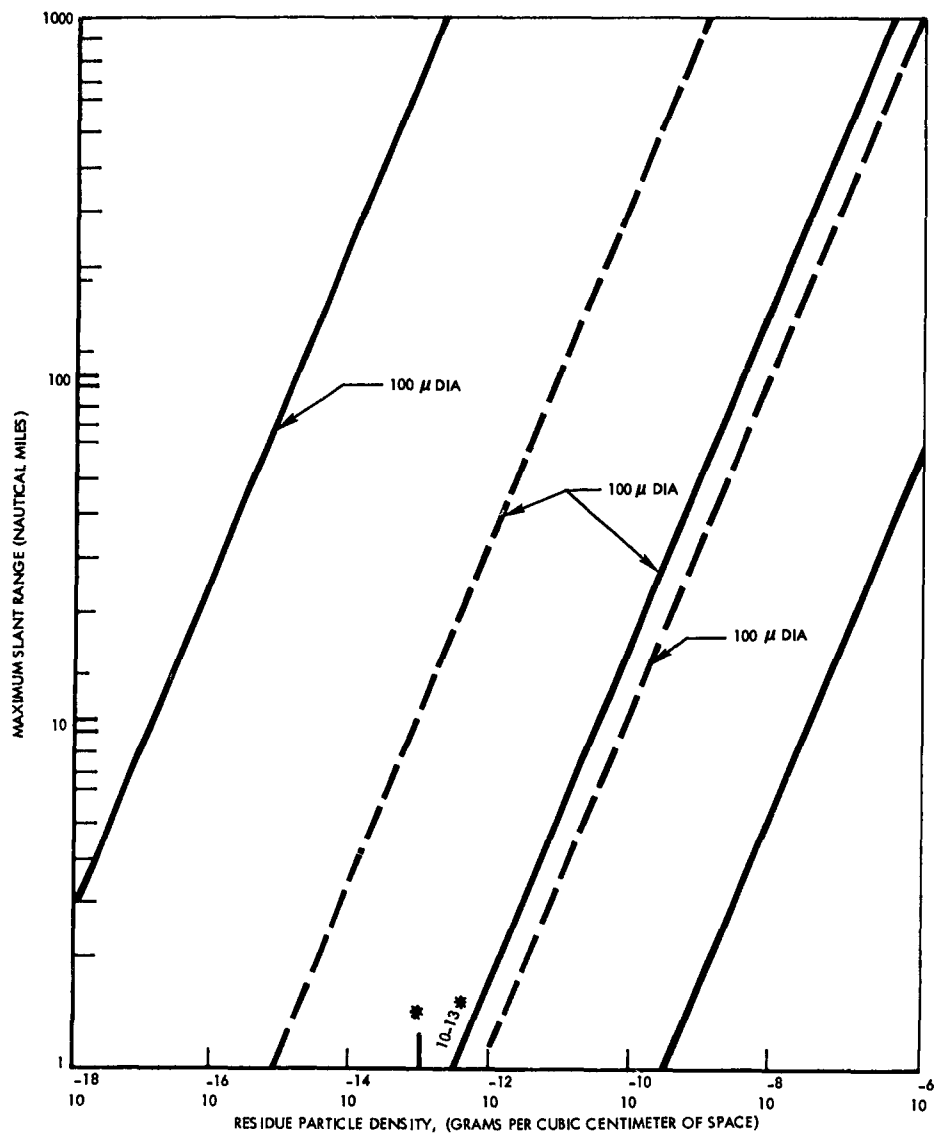
$$\eta = 6\pi \frac{\mu}{\rho\lambda} \left(\frac{2\pi\tilde{\alpha}}{\lambda} \right)^3 \quad (3)$$

where:

M = total mass of residue cloud per unit volume
 ρ = mass density of residue particle
 $\tilde{\alpha}$ = mean particle radius

Assuming a mean radius, $\tilde{\alpha} = 50\mu$ and 500μ , a calculation was made to determine maximum range at which a radar could detect the residue cloud. Figure 48 is a plot of the calculated range versus particle density for three C-band radars along the re-entry path.

The limitations of the radar technique are fairly obvious. First, accurate data must be known concerning the location of the residue cloud to reduce the search volumes. Second, more severe, the radar cannot distinguish between fuel element particles and ablated particles from other portions of the re-entry vehicle. Third, the particle number density along the re-entry path must be known accurately in order to evaluate radius of



NOTE
 VALUES AT DIFFERENT RANGES ASSUME THAT THE
 PARTICLE CLOUD FILLS THE AREA OF THE RADAR BEAM
 *REFERENCE 2

Figure 48. Residue Particle Range and Density

the particles. An error of one magnitude in the number-density calculation could mean an error by a factor of about 10^6 in the particle size.

Laser Technique

Another possible technique is scattering of visible light to determine residue particle dimensions. The method is the same as with radar except in a different frequency domain. The method requires a high intensity light source, possibly a laser, and a sensitive receiving system. The disadvantages are the same as in the case of radar case, i. e., residue cloud location and differentiation between fuel element residue particles and aerosol particles or other re-entry debris. However, further investigation and analysis is necessary to ascertain feasibility and applicability.

The possibility of using a scaled-up fuel element with its own telemetry system does not appear economically feasible in the near future. Miniaturized instrumentation systems capable of withstanding the potential environment are not readily available. Such equipment could be developed in the next two to four years. Novel antenna techniques would have to be developed. Materials would have to be found capable of withstanding the high heat while still remaining effective electromagnetic radiators. Microminiaturized instrumentation systems would not be available until the last half of the 1960 decade, if development were to begin now.

GOSS REQUIREMENTS

Regardless of the booster used, certain range considerations must be met. Launch sites must be heavily instrumented with the normal complement of ground test and checkout equipment as well as the various radio frequency links, optical equipment, and range safety equipment. All launch sites likely to be designated have the usual heavy complement of support equipment. Since the main interest is in the re-entry instrumentation systems, there is no need to discuss launch site instrumentation.

Along the trajectory path of the booster vehicle there should be a sufficient number of tracking stations to effect a good track of the trajectory for accurate prediction of the re-entry area. Small errors in the booster guidance system can widely affect the re-entry point. The vehicle's position in space, its velocity, altitude and attitude should be known at the beginning of the re-entry experiment. This tracking capability of the ascent portion of the trajectory is readily available at the Atlantic Missile Range. Downrange tracking for a Wallops Island range must be provided by Bermuda and by appropriately positioned ships. At PMR, offshore islands may be used to track initial launch trajectory.

The re-entry portion of the trajectory must be adequately instrumented with radar to track the entire length of the re-entry path under study. If land is not situated along the range to allow land-based radar installations, radar equipped surface ships must be stationed in the re-entry area to provide this instrumentation coverage.

All downrange stations (including ships) should be well-instrumented. In addition to the instrumentation systems already discussed optical, infrared, and possibly special radar systems will be required. Optical and infrared techniques will be heavily utilized to provide spectral information on the free-falling fuel elements. Special, low-noise-figure radar systems may be utilized to track particulate clouds during their existence. These radars will have to be orders of magnitude improved over the standard range FPS-16 radars now in use. As mentioned previously, telemetry receiving stations will have to be provided in the re-entrant area. These stations may be on board the downrange ships as well as on aircraft flying in the area. It is recommended that two such aircraft be available and utilized during re-entry experiments. Besides telemetry, these aircraft may also carry optical and infrared equipment capable of tracking the re-entering objects. Preliminary re-entry body track information would have to be furnished to the aircraft. Range timing signals would also have to be furnished for use with all the aircraft's recording equipment.

area to take high-altitude air samples; these samples could give an indication of any of the ablated fuel element material which re-enters the upper atmosphere. This type of flight measurement is within the capability of the U-2 aircraft, and these craft have flown similar missions. Since the U-2 can be guided and accurately positioned in space, any measurements made could be of positive value in determination of nuclear reactor hazards.

The general flight test range instrumentation support requirements are shown in Figure 49.

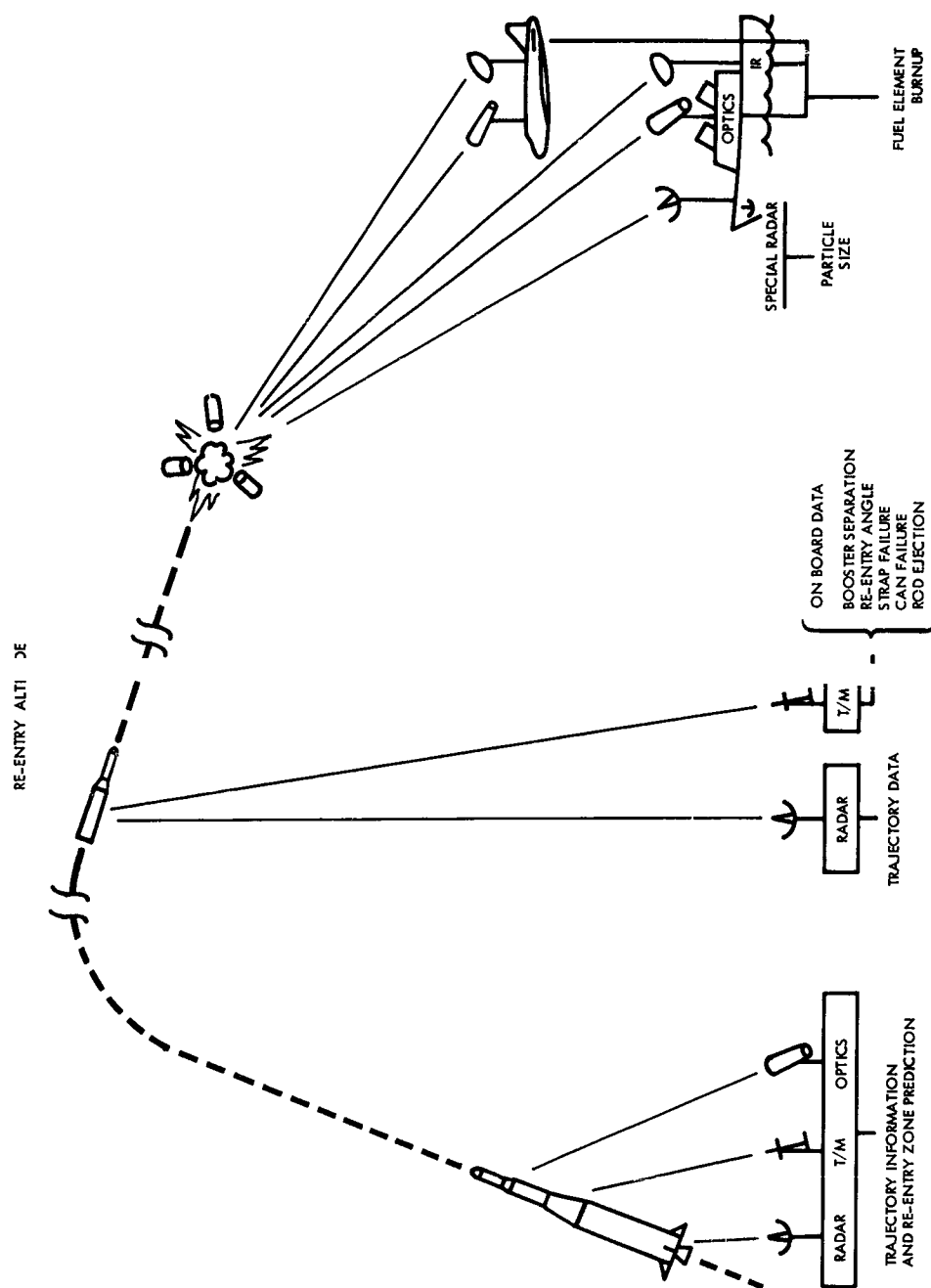


Figure 49. Instrumentation-System Test Range-Support Requirements

LAUNCH VEHICLES

A study of presently available booster systems was made to determine those vehicles which would provide a practical low-cost simulation of the orbital decay heating environment.

Two possibilities for obtaining low-cost flight tests exist. One scheme is to use a presently available booster which has the capability of providing the desired flight-test objectives. The other is to use piggyback pods on a test of some other vehicle such as Atlas, Titan, or the X-15.

Several problems are encountered in the second method. The vehicles being tested would not give the desired NAP re-entry conditions, and would necessitate the use of a velocity package with guidance capability; however, it may be found that primary mission requirements would not permit an additional pyrotechnic device aboard. Downrange facilities would provide primary support to the main test; thus, adequate support of the NAP experiments might not be available. Since the pod experiments must not interfere with the primary vehicle tests, support for the NAP experiment might be withdrawn at any time.

For these reasons, attention during the study was focused on those vehicles which would provide the desired conditions for the NAP flight test.

POSSIBLE BOOSTER SYSTEMS

A summary of the payload capability of some of the launch vehicles considered is presented in Figure 50. It can be seen from this figure that, from payload requirements, the vehicles of interest for the NAP flight test mission are of the Scout, Minuteman, Thor/Able-Star and Delta category. The ideal velocity shown in Figure 50 is the minimum theoretical velocity increment required to perform the given mission, assuming the propulsion system is capable of instantaneous velocity changes. In the calculation of the booster performance presented in this figure, Hohmann transfer maneuvers from the surface of the earth with instantaneous velocity changes were assumed. Thus, drag and gravity losses were not considered. The Blue Scout and Thor/Able-Star are representative of the range of performance capability (payload and guidance) required for the NAP tests, hence, they were selected for a detailed performance and cost analysis.

Payload capability for the range of re-entry conditions of interest is 200 plus pounds for Blue Scout and 500 plus pounds for Thor/Able-Star.

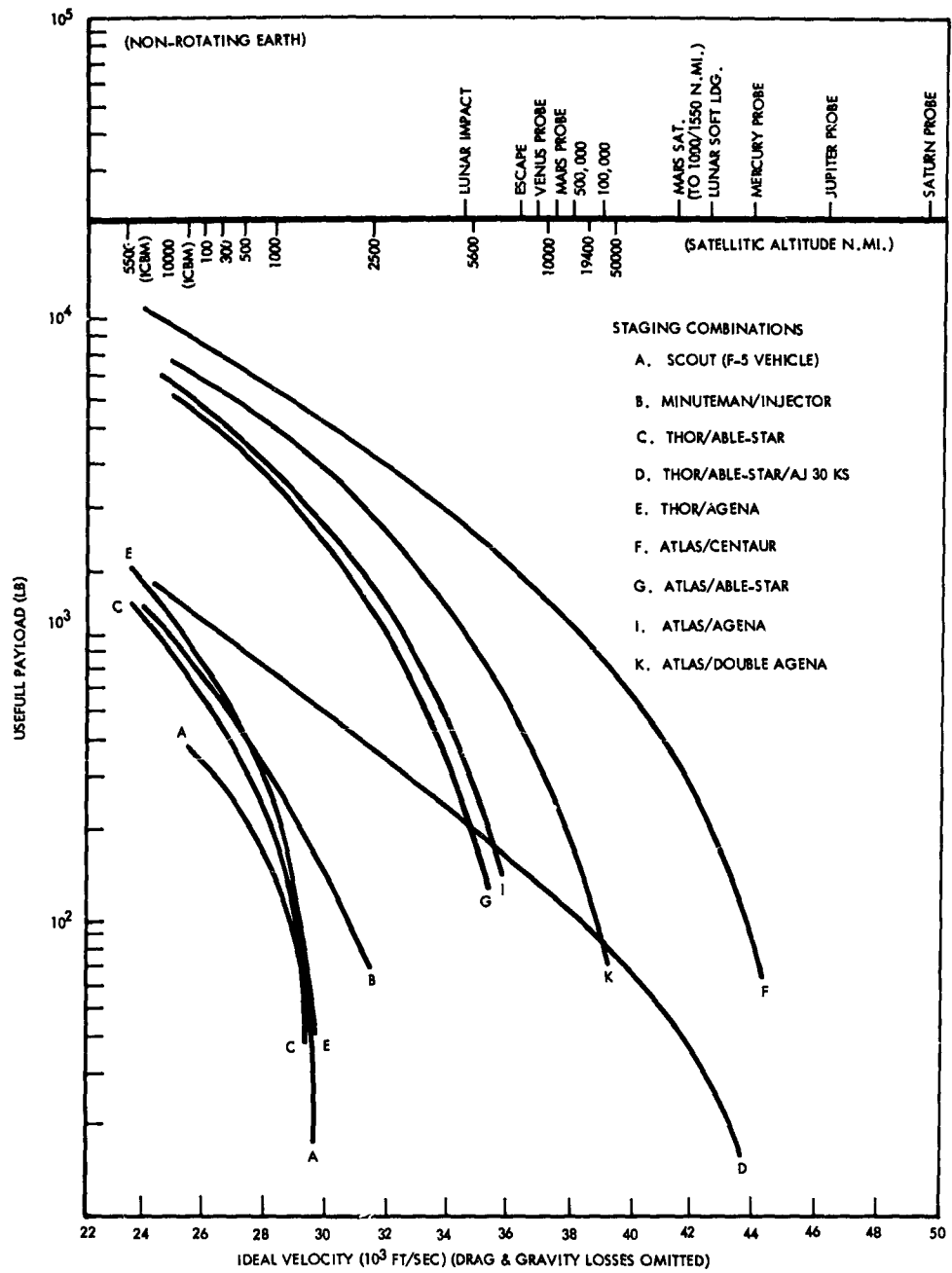


Figure 50. Comparison of Booster Payload Capability

The strong influence on maximum payload of re-entry flight-path angle, velocity, and altitude should be considered in selecting a combination of re-entry trajectory parameters for simulation of the orbital decay heating environment. For a particular booster, minimum payload requirements would establish an upper limit on these initial re-entry conditions. However, time limitations and the unavailability of latest motor performance estimates precluded a definition of this bound for the launch vehicles considered.

GUIDANCE AND CONTROL REQUIREMENTS

It is essential that test specimen burnup be accurately located for telemetry, optical observation, and residue sampling. The effect of errors in re-entry flight path angle on the location of a tumbling fuel element for a re-entry altitude of 400,000 feet is presented in Figure 51. It can be seen that for a re-entry angle of -8 degrees, and $V_E/V_C = 1.2$, an error of ± 1 degree will cause the test article to arrive at an altitude of 150,000 feet at any point along a line approximately 150 nautical miles long. A re-entry error of ± 2 degrees increases this dispersion to a line approximately 300 nautical miles long. In terms of altitude, for a re-entry flight path angle of -8 degrees at an altitude of 400,000 feet, an error of ± 1 degree in re-entry flight path angle means the test specimen may be approximately 130,000 feet from the predicted altitude at a distance of 300 nautical miles from the re-entry point.

The Blue Scout contractor has indicated guidance accuracy on flight path angle to be ± 0.75 degrees. Tolerance of the Thor/Able-Star is not known; however, it is felt to be very accurate.

PAYLOAD REQUIREMENTS

Representative Configurations

Figure 52 shows a representative telemetry and radar beacon module, and Figure 53 shows representative launch-vehicle and payload combinations. Sizes and weights of components are indicated, and suitable arrangements are depicted. The purpose of presenting these representative configurations is to establish a convenient reference guide for the design and evaluation of particular flight test programs.

Telemetry and Radar Beacon Module

In establishing a representative telemetry and radar beacon module primary consideration was given to provision of as complete a list as possible of required system components, indication of representative state-of-the-art sizes and weights of the required components, and illustration with particular solutions of the main installation and operational

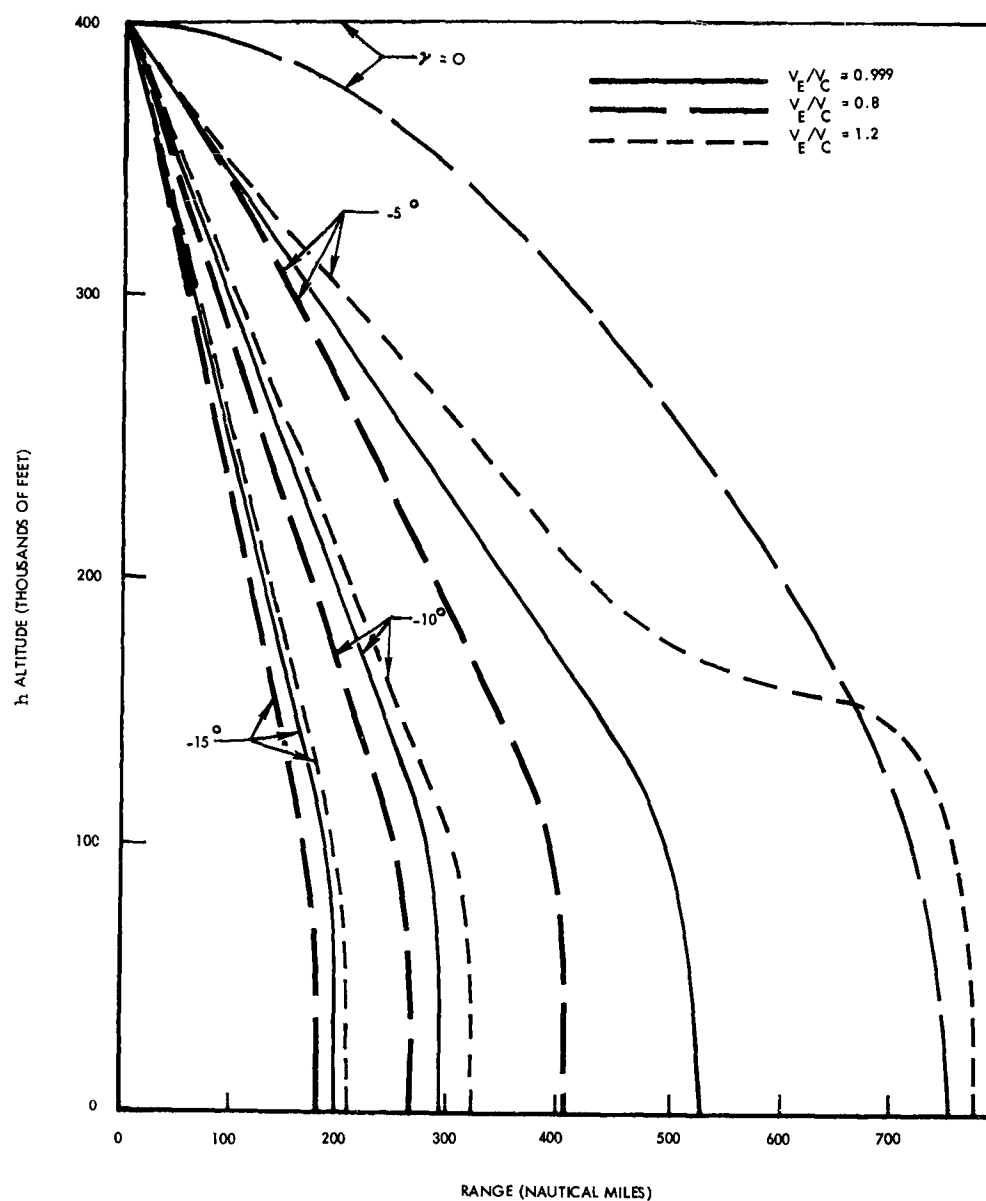
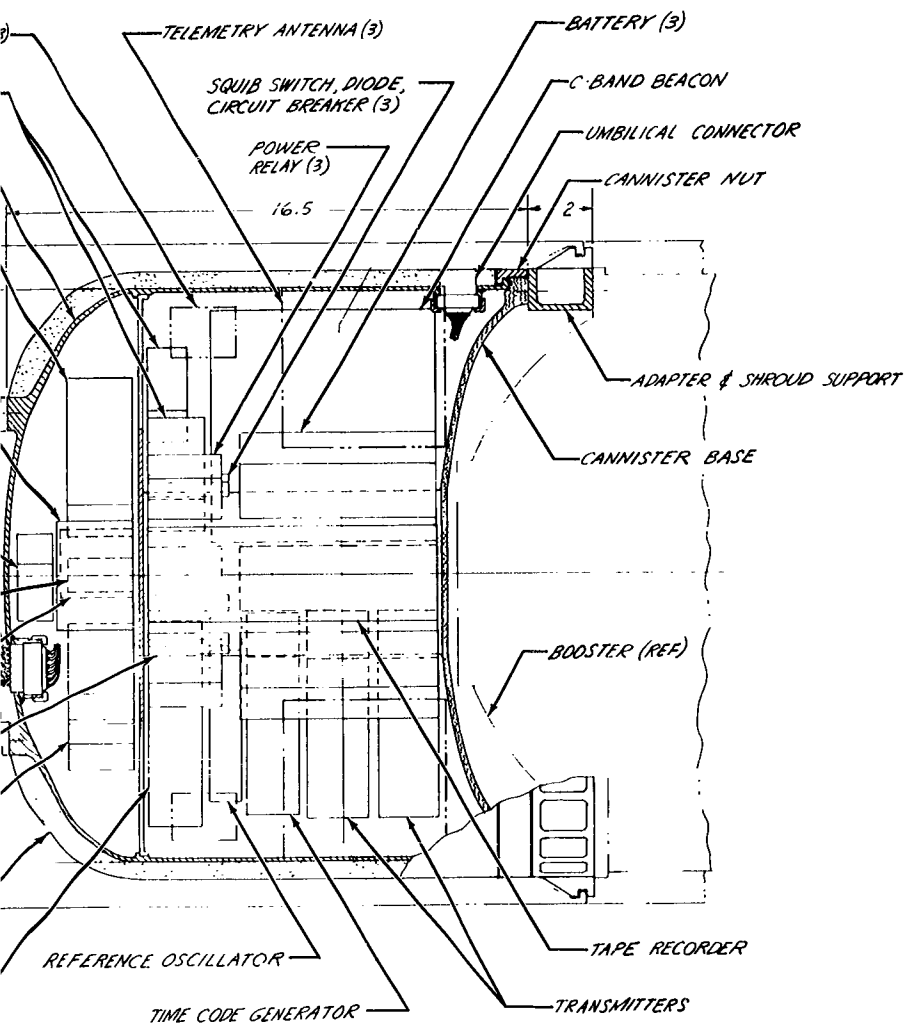


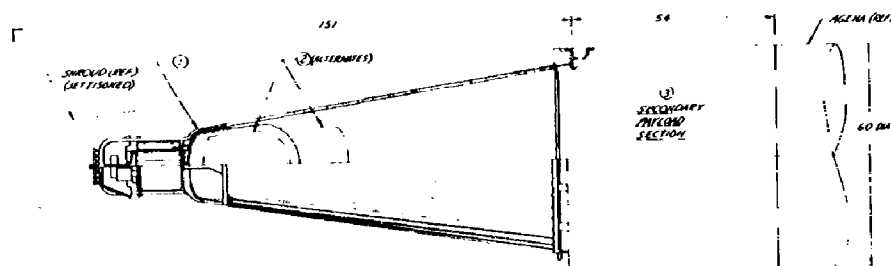
Figure 51. Variation of Altitude and Range With Re-Entry Velocity and Flight-Path Angle



COMPONENT SUMMARY LIST

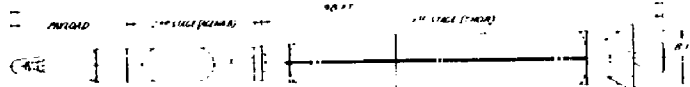
<u>ITEM</u>	<u>WEIGHT (LBS)</u>
<u>POWER SUPPLY</u>	<u>12.7</u>
BATTERIES (3)	4.5
POWER RELAYS (3)	1.5
SQUIB SWITCHES (3)	.5
DIODES (3)	.6
CIRCUIT BREAKERS (3)	.6
TIMER	1.0
VOLTAGE REGULATOR	1.0
WIRING/SUPPORT	3.0
<u>TELEMETRY</u>	<u>35.0</u>
CONVERTER	1.8
COMMUTATORS	2.0
SUB-CARRIER OSCILLATORS (9)	1.5
REFERENCE OSCILLATOR	.3
COMPENSATOR	1.0
SIGNAL CONDITIONER/MIXER	.8
TIME CODE GENERATOR	1.0
TAPE RECORDER	8.5
TRANSMITTERS (2)	3.0
ANTENNA POWER DIVIDER	1.1
ANTENNAS (3)	3.0
WIRING/SUPPORT	5.0
<u>RADAR BEACON</u>	<u>9.4</u>
C-BAND BEACON	5.7
POWER DIVIDER	.3
ANTENNAS (3)	1.8
WIRING/SUPPORT	1.6
<u>MISCELLANEOUS</u>	<u>11.4</u>
COOLER/CHASSIS	5.0
ACCELEROMETERS (3)	1.2
PRESSURE TRANSDUCER	.2
RADIOMETER	2.0
INSTRUMENTATION CONNECTOR	1.0
UMBILICAL CONNECTOR	2.0
<u>STRUCTURE</u>	<u>43.5</u>
CANNISTER DOME	10.0
CANNISTER BASE	5.0
INSULATION	25.0
ADAPTOR	3.5
<u>TOTAL MODULE</u>	<u>112.0</u>

Figure 52. Representative Re-Entry Test
Telemetry and Radar-Beacon Module

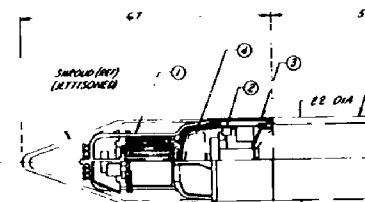


- REPRESENTATIVE PAYLOAD II**
- | | |
|---|-----------------|
| (1) FULL SIZE COMPLETE SHIP ON TEST | 643 LBS |
| INSTRUMENTS, WIRING, PUMP, AIRCRAFT | 395 |
| PAYLOAD AND INSTRUMENTS | 152 |
| SHROUD (WET) TELETYPE/SHROUD (WET) 130 W | |
| STRUCTURE WET | 81 |
| (2) TELETYPE, RADIO BEACON, AIRCRAFT (LESS INSTRUMENTS) 840 W | 840 LBS |
| (3) AVAILABLE FOR INSTRUMENTATION, ADDITIONAL TEST, AND/OR RESERVE DESIGN | 773 LBS |
| TOTAL | 1500 LBS |

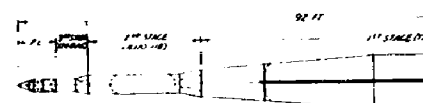
RESERVED WTD IS PARTIALLY SIMULATED
BY T/M - RIB MODULE



THOR AGENA B LAUNCH VEHICLE

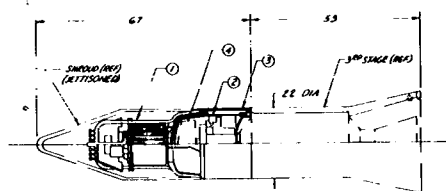


- REPRESENTATIVE PAYLOAD II**
- | | |
|---|-----------------|
| (1) FULL SIZE COMPLETE SHIP ON TEST (WET) | 125 |
| INSTRUMENTS, WIRING, PUMP, AIRCRAFT | 23 |
| SHROUD (WET) TELETYPE/SHROUD (WET) 130 W | 39 |
| STRUCTURE WET | 108 |
| (2) TELETYPE, RADIO BEACON, AIRCRAFT (LESS INSTRUMENTS) 840 W | |
| (3) AVAILABLE FOR INSTRUMENTATION, ADDITIONAL TEST, AND/OR RESERVE DESIGN | 773 LBS |
| TOTAL | 1500 LBS |

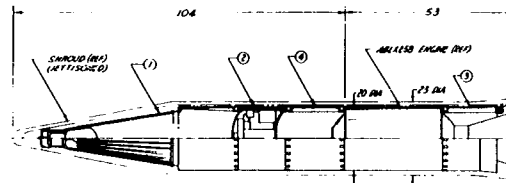


THOR DELTA LAUNCH

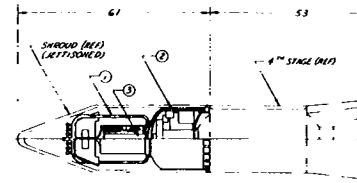
1



- REPRESENTATIVE PAYLOAD II**
- | | |
|---|----------------|
| ① FULL SIZE COMPLETE SHUTTLE RECTOR (MEL) | 295 LBS |
| CORE (MEL) | 125 |
| VEHICLE & GAMES | 23 |
| PUMP, PUMP | 23 |
| REFLECTOR, CONTROLS, STRUCTURE | 108 |
| ② TELEMETRY/RANGE BEACON MODULE | 112 LBS |
| ③ ADAPTOR | 25 LBS |
| ④ AVAILABLE FOR INSTRUMENTATION, FLARES, ETC. | 68 LBS |
| TOTAL | 500 LBS |



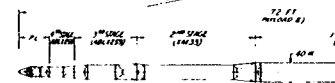
- REPRESENTATIVE PAYLOAD III**
- | | |
|--|----------------|
| ① ONE-TONNED SIZE (22 INCHES) SHUTTLE RECTOR | 76 LBS |
| ② TELEMETRY/RANGE BEACON MODULE | 112 LBS |
| ③ FLARE (UNMANNED AERIAL VEHICLE) OF ONE AND | 50 LBS |
| ④ AVAILABLE FOR ADAPTOR AND INSTRUMENTATION | 62 LBS |
| TOTAL | 300 LBS |



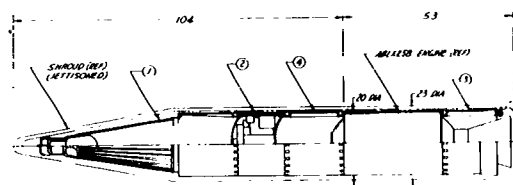
- REPRESENTATIVE PAYLOAD II**
- | | |
|---|----------------|
| ① FULL SIZE SHUTTLE SHUTTLE RECTOR | 133 LBS |
| CORE (MEL) (50 INCHES) OF | 125 |
| VEHICLE (MEL) | 19 |
| PUMP, PUMP | 23 |
| ② TELEMETRY/RANGE BEACON MODULE | 112 LBS |
| ③ AVAILABLE FOR INSTRUMENTATION, FLARES, ETC. | 55 LBS |
| TOTAL | 300 LBS |



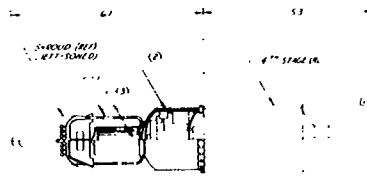
THOR DELTA LAUNCH VEHICLE



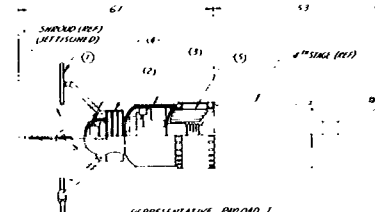
THOR DELTA LAUNCH VEHICLE



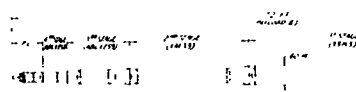
- REPRESENTATIVE PAYLOAD III**
- ① ONE THIRD SIZE (1/3) REENTRY SYSTEM - 74 LBS
 - ② TELEMETRY/RADAR BEACON MODULE - 112 LBS
 - ③ THERMAL CONDUCTED HEAT (1/3) OF 1000 JAW - 50 LBS
 - ④ THERMAL PROTECTION SYSTEM - 62 LBS
- TOTAL 300 LBS



- REPRESENTATIVE PAYLOAD II**
- ① ONE THIRD SIZE (1/3) REENTRY SYSTEM - 74 LBS
 - ② TELEMETRY/RADAR BEACON MODULE - 112 LBS
 - ③ THERMAL CONDUCTED HEAT (1/3) OF 1000 JAW - 50 LBS
 - ④ THERMAL PROTECTION SYSTEM - 62 LBS
- TOTAL 300 LBS



- REPRESENTATIVE PAYLOAD I**
- ① ONE THIRD SIZE (1/3) REENTRY SYSTEM - 74 LBS
 - ② TELEMETRY/RADAR BEACON MODULE - 112 LBS
 - ③ THERMAL CONDUCTED HEAT (1/3) OF 1000 JAW - 50 LBS
 - ④ THERMAL PROTECTION SYSTEM - 62 LBS
- TOTAL 300 LBS



REENTRY AIR FORCE SCOUT LAUNCH VEHICLE

Figure 53. Representative Re-Entry Test Launch Vehicles and Payloads

problems involved. The configuration depicted is to scale, and most of the components and their listed weights represent available "off the shelf" hardware. Arrangement is based on a three-antenna telemetry system. By mounting the antennas on a removable dome, and other components on a central base-mounted chassis, good access to all components is attained. A union-type attach nut provides reliable sealing of the cannister, with rapid servicing on or off the launch vehicle. Environmental control is achieved by means of a combination of external insulation and an evaporation cooler integral with the equipment chassis.

The cannister weights are based on an aluminum dome covered by a non-charring teflon insulation of 75 pounds-per-cubic-foot strength, and a fiberglass base and nut. The resulting total telemetry and radar beacon module weight is 112 pounds. It has a diameter of 19 inches and length of 16.5 inches. Alternate arrangements, such as a two-antenna based concept, might permit somewhat denser packaging with a small reduction in size. However, the weight and size of the configuration shown are believed to be a good average representation of feasible state-of-the-art systems.

Launch Vehicle - Payload Combinations

The launch-vehicle and payload combinations shown in Figure 52 are intended to cover a representative spectrum of launch vehicles and associated payloads. Emphasis is on the inclusion of a broad variety of test concepts rather than on particular test configurations. However, the drawings are to scale and are indicative of feasible hardware. The payload capabilities are upper limits for optimum trajectories, and are consequently subject to reduction for particular test missions. This is especially true of the Scout, which, due to its accuracy limitations, may require steeper re-entry (and consequently higher velocity) missions.

Weights and depiction of the reactor elements are given according to current Atomics International data. The telemetry and radar beacon module sizes and weights are in accordance with Figure 51. Other elements are arbitrarily chosen to illustrate possible allowances within the payload limitations.

Payloads I, II and III depict typical Scout vehicle capabilities. Payload I indicates various fuel-elements-only test concepts. Such tests, either singly, or in various combinations, are evidently well within the Scout capability. Payload recovery in the case of captive fuel element tests is also possible.

Payload II shows one concept of a full-scale reactor test. Partial stripping of the reactor is obviously necessary, as the complete SNAP 10A reactor alone weighs approximately 295 pounds. Omission of the reflector

system and reduction of the rod complement are employed to stay within the payload allowance. Demonstration of reflector shucking would have to be by other means. Presumably, by omitting central fuel elements only, the heat sink characteristics of the vessel lip can be retained for acceptable demonstration of vessel rupture and fuel element expulsion. The space vacated by the omitted elements would ideally house test instrumentation.

An alternate Scout vehicle full-scale reactor test concept (not illustrated) would be to retain the reflector system at the expense of greater reduction of the fuel element complement. The weight breakdown of this concept would be as follows:

Full-size stripped SNAP 10A Reactor	171.0 pounds
Core (fuel elements, 90 percent depleted)	13.5
Vessel (dry)	10.5
Reflector and controls	108.0
Pump, piping	39.0
Telemetry and radar beacon module	112.0 pounds
Available for instrumentation	<u>17.5 pounds</u>
Total	300.0 pounds

It is apparent that this configuration is marginal, only 17.5 pounds being available for instrumentation. Also, the small fuel element complement and resulting alteration of the heat sink characteristics at the vessel lip would make questionable the validity of the vessel-rupture demonstration.

Payload III illustrates a scaled-down complete SNAP 10A system. The one-third size depicted fits well with the Scout geometry and payload capability. By incorporating the Scout fourth stage engine as part of the re-entry body, and utilizing a jettisonable full-length shroud as interstage, complete geometrical simulation of the SNAP 10A - Agena B vehicle is attained. The 300-pound payload capability could accommodate approximately one-ninth of the weight scale of the vehicle system. This allows the drag-to-weight ratio to be properly scaled for a valid re-entry path with associated heat-flux environment. Also, the size and mass of items subject to heating must be duplicated for internal heat transfer to be valid. The considerable latitude available in the telemetry and beacon module location provides for center-of-gravity location simulation. By providing a de-spin and tumble system, complete dynamic simulation of the full scale SNAP 10A system for any re-entry mode appears feasible. Also, because the one-ninth weight scale requirement means one to one thickness scale, thermal simulation of certain characteristics may be possible, such as failure of the radiator to Agena - B joint structure, disintegration of the radiator, or even melting of the reactor vessel lip.

Payload IV illustrates the feasibility of testing a full-scale SNAP 10A reactor, including the support structure and simulated shield nose, within the payload and geometry limitations of the Thor-Delta launch vehicle. No other test concepts appear applicable to this class of booster.

Payload V depicts a representative full scale SNAP 10A test system launched by the Thor-Agena-B vehicle, and indicates the large payload margin (773.0 pounds) available with this type of test concept.

COST ANALYSIS

A cost estimate breakdown of the Blue Scout and Thor/Able-Star launch vehicles is given in Table 7. Data were obtained for the Blue Scout and for the Thor/Able-Star using Reference 6 and other unclassified sources. As can be seen, cost of the basic missiles is \$750,000 for the Blue Scout and \$1,720,000 for the Thor/Able-Star. Contractor overhead for the Scout is approximately \$200,000. Management service and system engineering is \$350,000 for the Thor/Able-Star. Unit-launch cost is estimated to be \$200,000 for the Scout and \$1,370,000 for the Thor/Able-Star. Payload integration is estimated to be \$50,000 for either missile.

Table 7. Launch Vehicle Cost Estimate Breakdown

	Blue Scout (each)	Thor/Able-Star (each)
Basic Launch Vehicle	\$ 750 K	\$1.72 M
Management Service	200 K	350 K
Payload Integration	50 K	50 K
Launch	200 K	1.37 M
Total Cost (per launch)	\$1,200 K	\$3.49 M
Lead Procurement Times	12 months	Unknown

TYPICAL TRAJECTORY FOR BLUE SCOUT AND THOR/ABLE-STAR BOOSTER SYSTEMS

The estimated weights and engine performances of the Blue Scout and Thor/Able-Star vehicles are contained in Tables 8 and 9, respectively. These estimates are known to be conservative and are based on performance

Table 8. Blue Scout Weight and Motor Data
(104-pound payload)

Stages	Weight (pounds)			Thrust (pounds)	I _{sp} (seconds)
	Initial	Propellant	Stage		
First-Argol	37,158	18,997	4,634	103,000 ^(a)	214 ^(a)
Second-Castor	13,527	7,313	2,342 ^(b)	66,000 ^(c)	265 ^(c)
Third-Improved Antares	3,872	2,500	702	19,000 ^(c)	281 ^(c)
Fourth-Improved Altair	670	483	83	5,080 ^(c)	278 ^(c)
<p>(a) Sea-level performance</p> <p>(b) Includes a 160-pound heat shield over the payload</p> <p>(c) Vacuum performance</p>					

Table 9. Thor/Able-Star Weight and Motor Data
(465-pound payload)

Stages	Weight (pounds)			Thrust (pounds)	I _{sp} (seconds)
	Initial	Propellant	Stage		
First-Thor	119,000	101,885	6,890	150,000 ^(a)	250 ^(a)
Second- Able-Star	10,325	8,560	1,300	7,890 ^(b)	278 ^(b)
<p>(a) Sea-level performance</p> <p>(b) Vacuum performance</p>					

data available which may be obsolete. Recent NASA releases (Reference 7) indicate a 67 percent increase in payload capability of the Scout for a 300-nautical-mile orbit incorporating improved first, third, and fourth stage motor performance. For this reason, boost trajectories were not optimized. Trajectories included for the Thor/Able-Star and Blue Scout are thus typical only and do not represent a proposed flight test trajectory.

Figure 19 indicates that an acceptable combination of re-entry conditions for simulation of fuel element heating is a flight-path angle of -7.5 degrees and re-entry velocity of 1.153 of circular at an altitude of $400,000$ feet. Figure 20 shows the resulting re-entry range to be approximately 430 nautical miles. For these re-entry conditions at $400,000$ feet altitude, conditions of the rod at $300,000$ feet altitude are $\gamma = -6.92$ degrees, and $V/V_c = 1.157$.

For the Blue Scout the boost scheme used (Figure 54) consists of a vertical boost for three seconds followed by a programmed turn into a zero-lift trajectory. A coast period of 48 seconds duration following first-stage burnout was incorporated to reduce aerodynamic heating and gain altitude. Optimum steering powered flight occurred for the remainder of the boost trajectory with zero staging time assumed.

Figure 53 shows that for the engine performance assumed and the boost scheme employed, the Blue Scout boosted approximately 104 pounds to the desired re-entry conditions at an altitude of $300,000$ feet. The associated boost range is 210 nautical miles. The re-entry range of a tumbling rod at these initial conditions is approximately 300 nautical miles, resulting in a total range from beginning of boost to impact of 510 nautical miles.

Boost scheme for the Thor/Able-Star consisted of a vertical lift for twenty seconds followed by a zero-lift turn to 150 seconds. Optimum steering with no coast between stages was then utilized for the remainder of boost flight.

Figure 55 shows that the Thor/Able-Star boosted approximately 465 pounds to an altitude of $400,000$ feet with the desired end-boost conditions.

Range during boost of the Thor/Able-Star was found to be 930 nautical miles, resulting in a total range from begin boost to rod impact of 1360 nautical miles.

An altitude-range profile of the Blue Scout and Thor/Able-Star trajectories discussed above is presented in Figure 56.

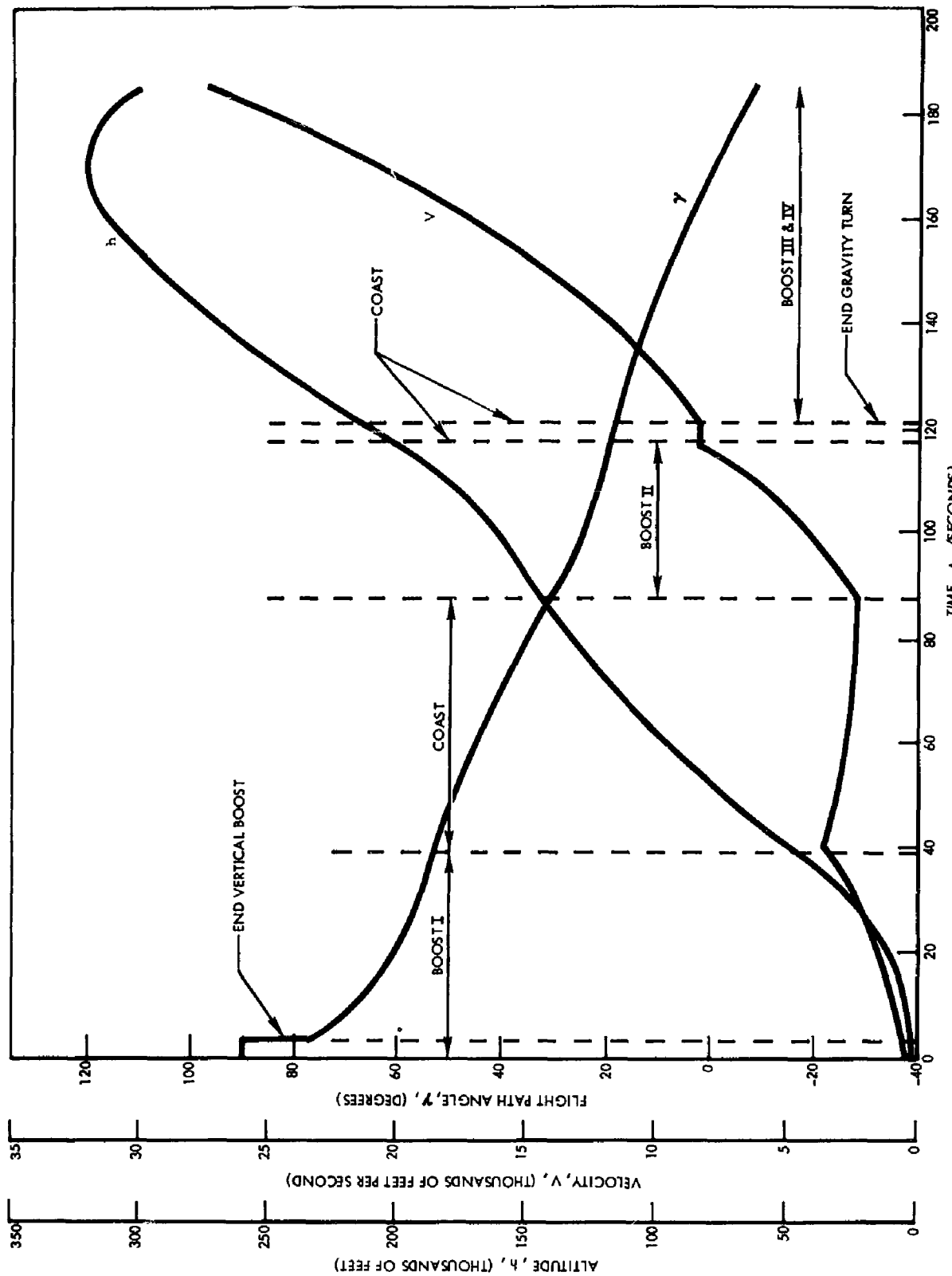


Figure 54. Typical Blue Scout Boost Trajectory

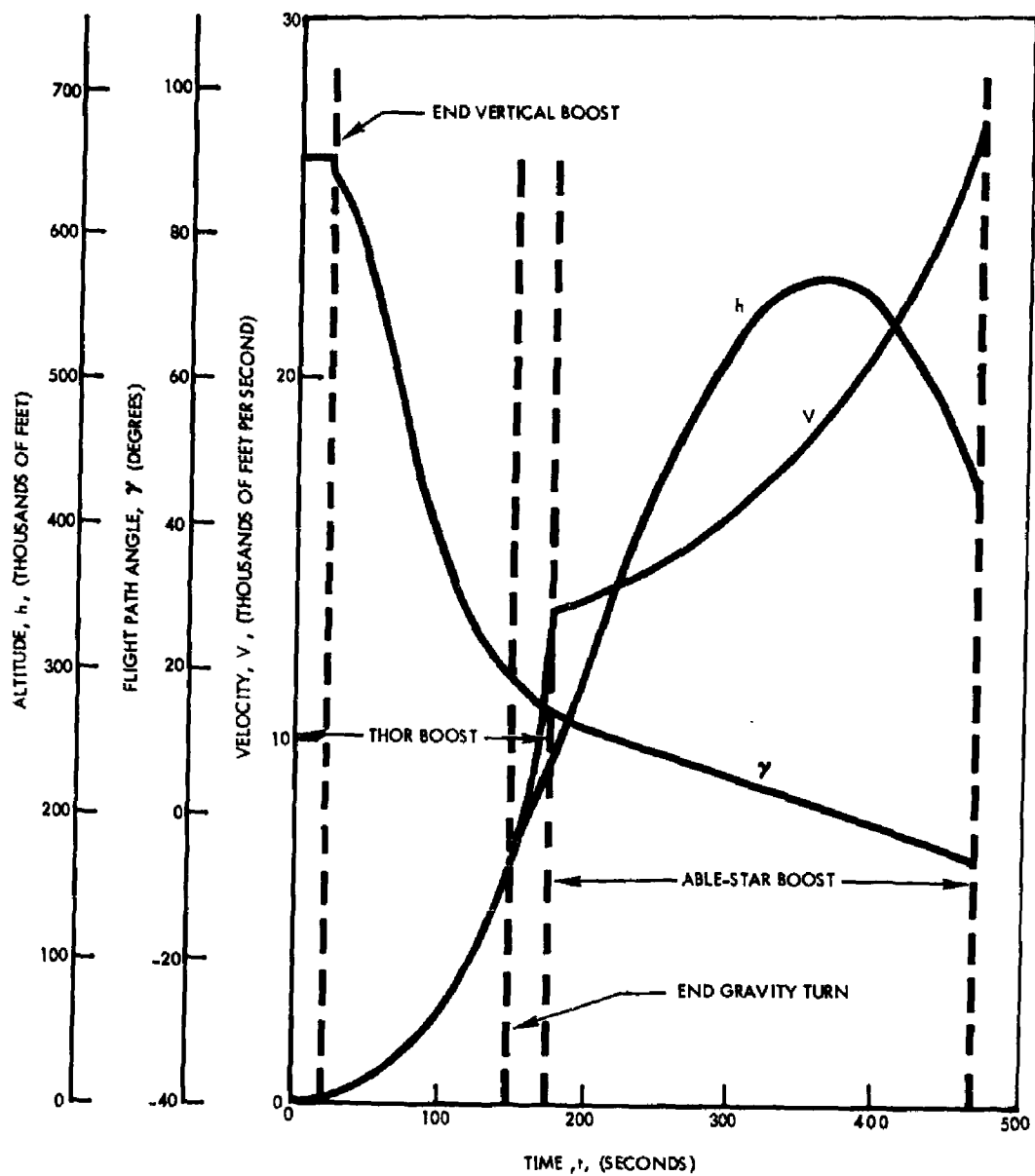


Figure 55. Typical Thor/Able-Star Boost Trajectory

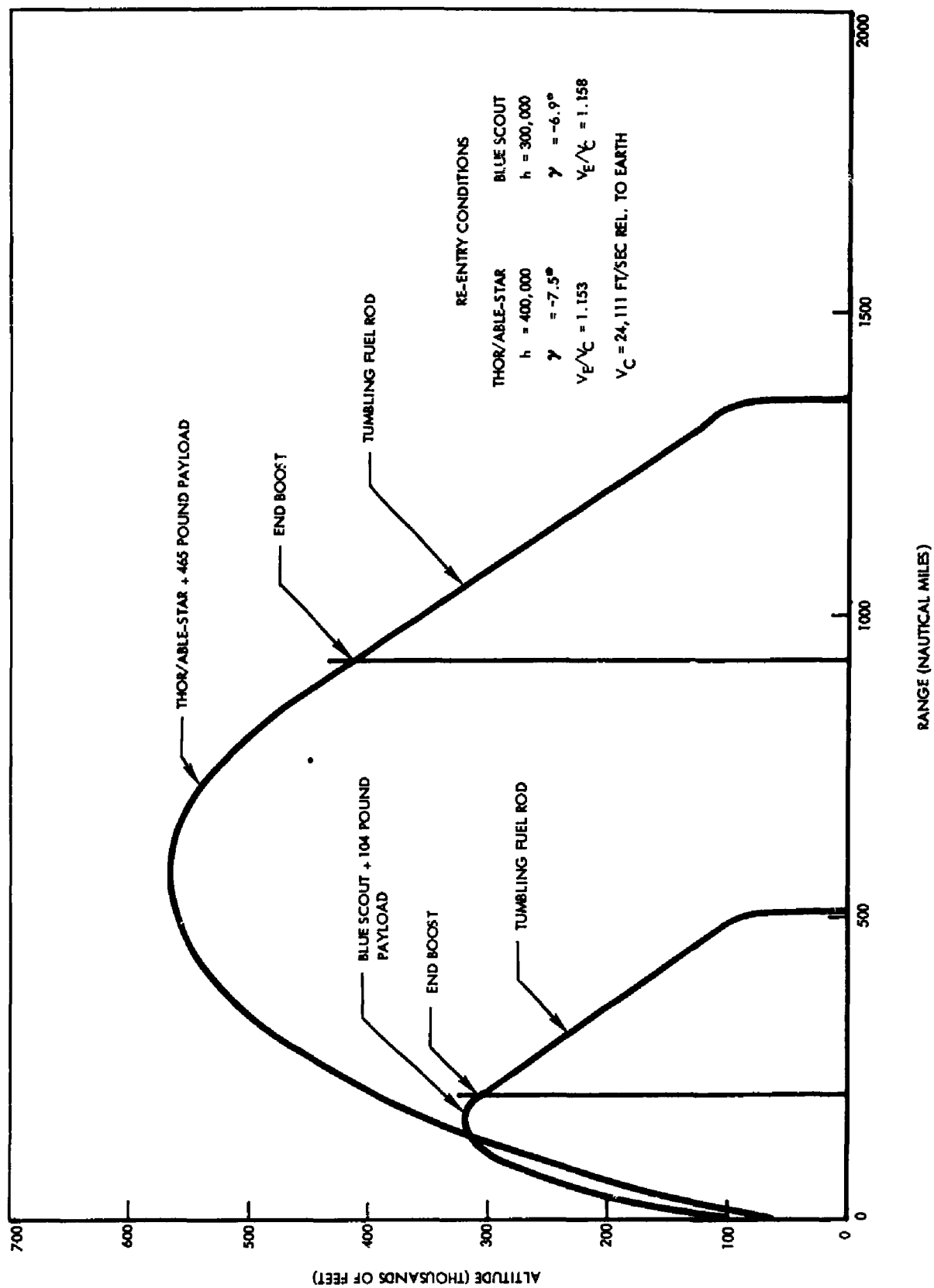


Figure 56. Altitude-Range Profile for Typical Flight Tests

PROPOSED LAUNCH VEHICLE

The Blue Scout vehicle is recommended to be the carrier for NAP flight experiments for the following reasons. Scout payload capability is adequate to provide the necessary redundancy of test items required for reliability. It can accomplish the mission at a relatively low cost. The reliability of the Scout should be well established by the time the NAP tests are conducted.

The errors inherent in the Scout guidance system will make it difficult to obtain optical re-entry observations. The guidance system manufacturer, Minneapolis Honeywell, is conducting studies on methods of increasing guidance accuracy. Results of these studies were not available to S&ID.

LAUNCH SITES

AVAILABLE RANGE SITES

A survey was conducted to determine the capabilities of the various test ranges that might be utilized to fulfill flight test requirements of the re-entry burnup program. The ranges surveyed were the Atlantic Missile Range, Edwards Air Force Base, Eglin Air Force Base, Pacific Missile Range, Wallops Station, Weapons Research Establishment (Adelaide, Australia), and White Sands Missile Range.

Atlantic Missile Range (AMR)

The AMR has launch capabilities for the Blue Scout vehicle at Pad 18A. There appears to be some question regarding the continued use of this pad. A facility to launch the Scout vehicle has been planned for Pad 18B; however, work on this facility has been discontinued due to lack of funds. Capabilities for the launch of Atlas, Thor, and Titan are also maintained at AMR. Several islands down range in the first 1200 miles are utilized as tracking and instrumentation stations. These stations provide a capability for radar tracking, telemeter reception, and optical coverage. Additional land based facilities are located at Ascension Island which is approximately 4400 NM down range. Figure 57 shows a profile of the Atlantic Missile Range. Figure 58 depicts the range as far as Antigua showing the range stations in greater detail. Table 10 shows down-range instrumentation at the various stations as it applies to the NAP re-entry burnup. Advanced Range Instrumentation Ships (ARIS) are being outfitted for addition to the mobile equipment available at AMR. Two of these being completed by the Sperry Company may provide SPG-56 radar facilities. The capabilities of this type of radar would be very important in detection of small particles in the burnup residue. The Project DAMP instrumented ship USAS American Mariner has adequate FPQ-4 tracking radar, FPQ-4 cameras, and radiometers. Some instrumented aircraft attached to AMR have radiometer, cine-spectrometer, optical, and telemeter equipment. Eight additional ships have L, C, and X-band radars, infrared acquisition gear and telemetering equipment. Additional aircraft record telemetry and make photographic records.

Edwards Air Force Base

Edwards has been a center for aircraft flight test programs and has complete capabilities for this type of testing. These facilities were expanded to meet the requirements of the X-15 program by extending the instrumented

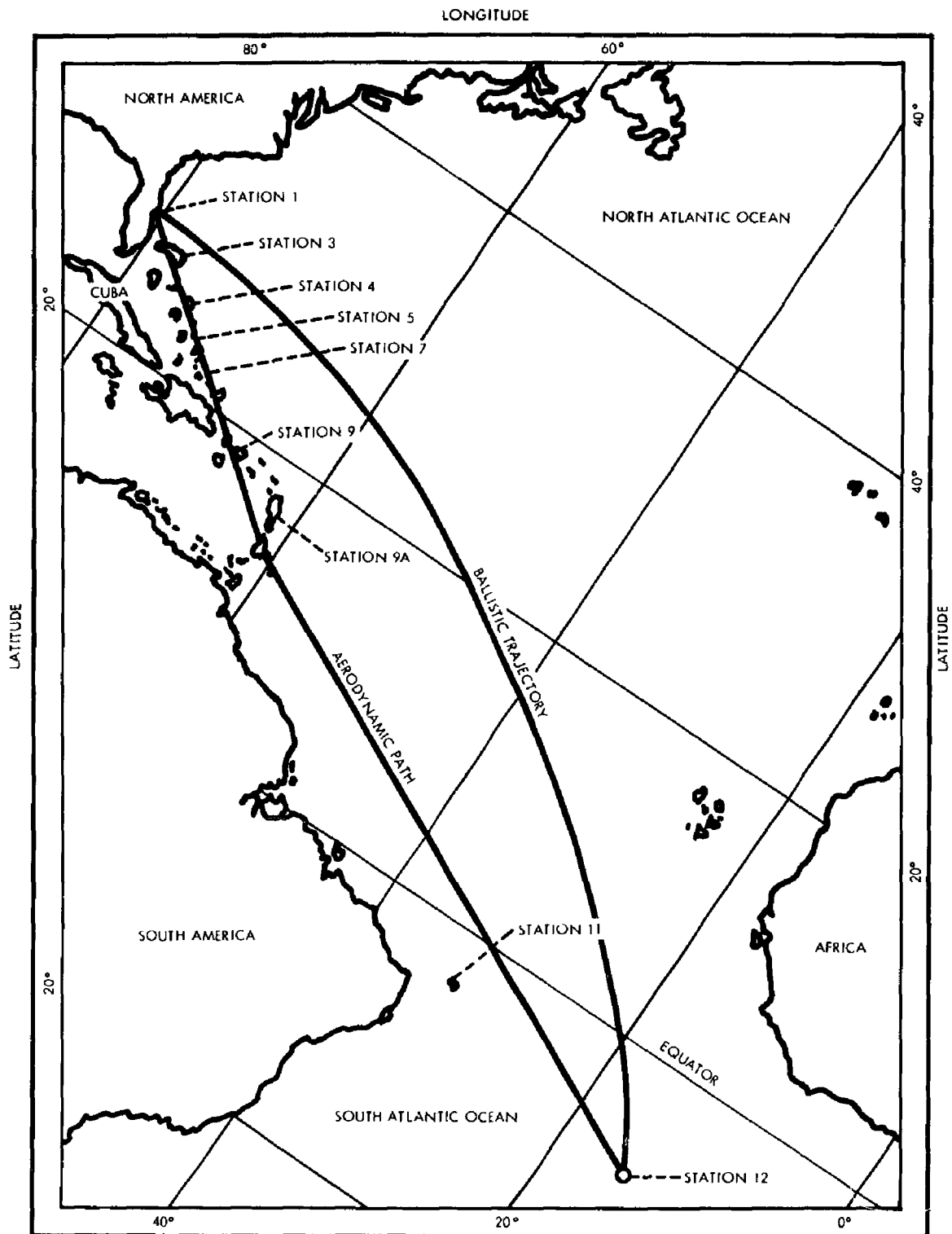
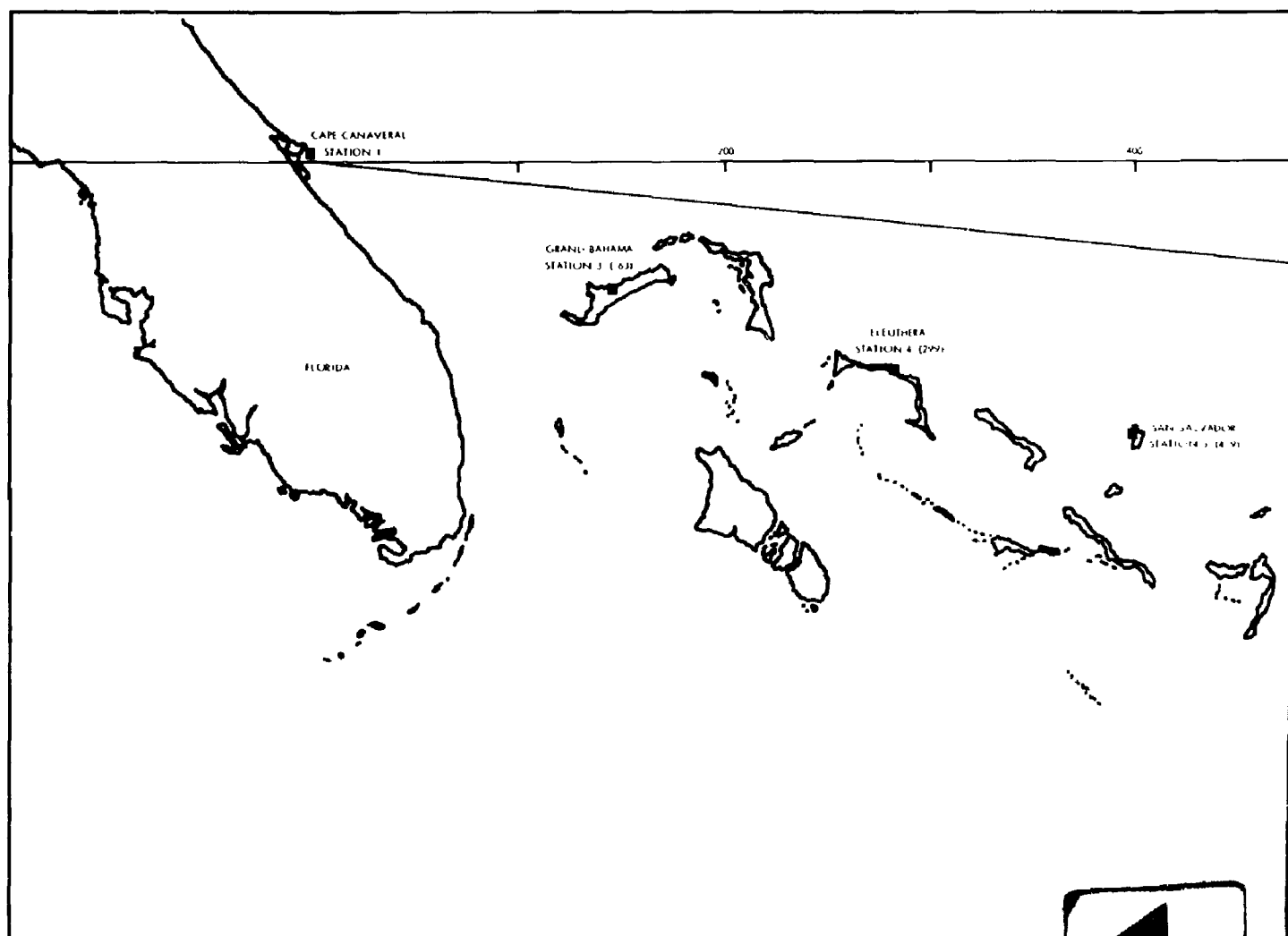


Figure 57. Atlantic Missile Range



1

NAUTICAL MILES

1000

ELEUHERA
STATION 4 (1999)

ATLANTA
STATION 3 (1999)

ATLANTA
STATION 3 (1999)

PUEBLO
STATION 2 (1995)

2

Table 10. Atlantic Missile Range Down-Range Instrumentation

(Limited to Equipment of Special Interest
to the NAP Re-Entry Burnup Tests)

Station	Radar			Ballistic Cameras	Telemetry	Radiometers	Impact Location
	FPS-16	FPQ-4	SPG-56				
Cape Canaveral - 1	X			X	X		
Grand Bahama Island - 3	X			X	X		
Eleuthera Island - 4				X	X		
San Salvador Island - 5	X			X	X		
Grand Turk Island - 7				X	X		X
Puerto Rico - 9					X		
Antigua Island - 9A	X			X	X	X	X
Ascension Island - 12	X			X	X		X
USAS American Mariner		X		X		X	
Advanced Range Instrumentation Ships			X				
Aircraft				X	X	X	

range approximately 455 statute miles northeast. Some proposals have been made to further expand the range north and east to Great Falls, Montana. This would provide an inland range about 1000 statute miles in length. The use of the range would be limited to aircraft-launched vehicles capable of landing on a specific dry lake or similar non-inhabited area. Available impact areas are very limited and would severely restrict re-entry tests. The nature of this range does not lend itself to the requirements of the NAP re-entry tests.

Eglin Air Force Base

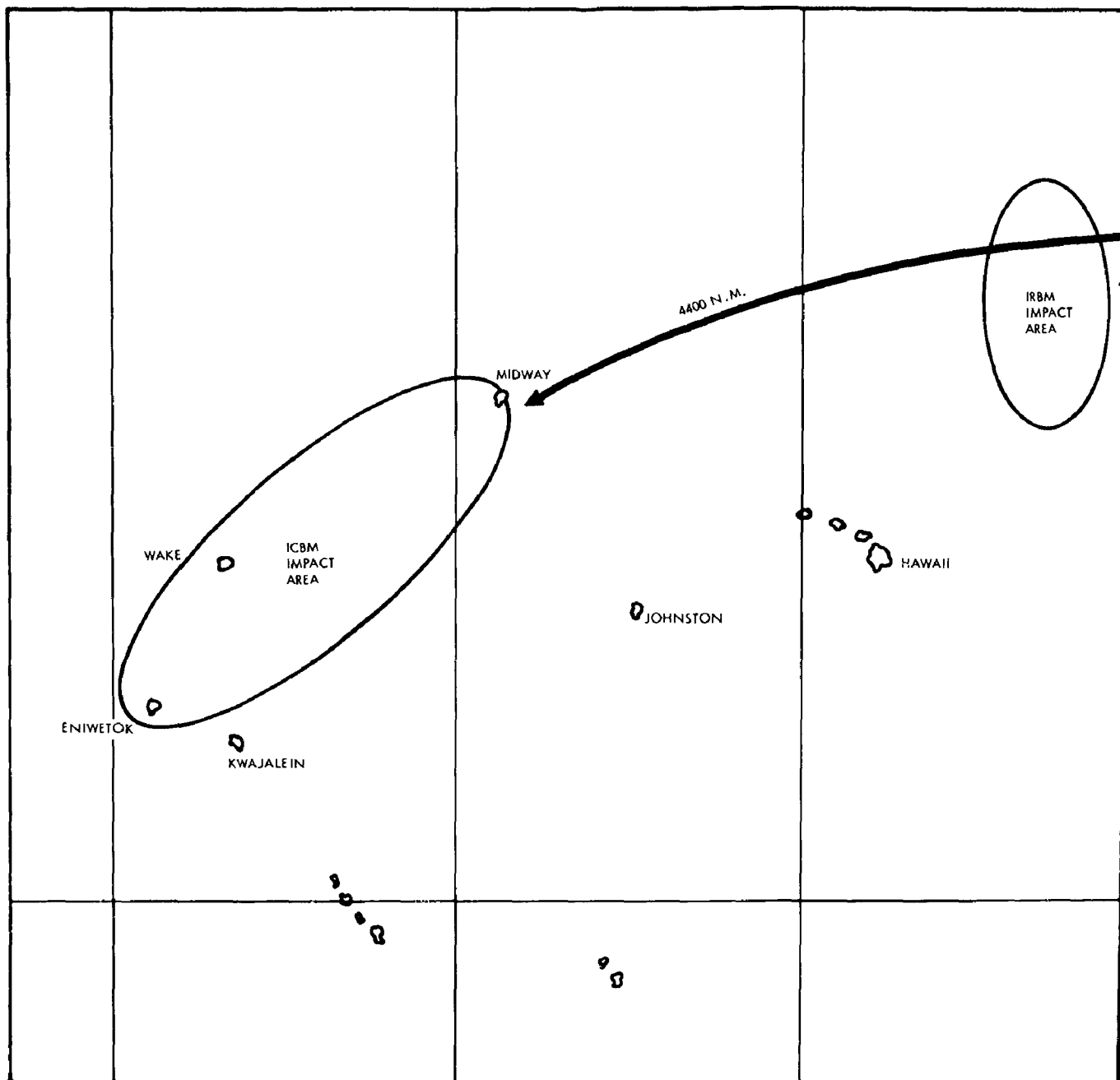
This over-water range utilizes launch facilities at Eglin and down-range tracking facilities along the Florida gulf coast. Such programs as the Bomarc have utilized this range for flight tests. The impact distance from launch is limited to less than 400 nautical miles due to the presence of the Florida Keys. A trajectory which would miss Key West would pass over Cuba at about 80 nautical miles further down range. The limited trajectory range would preclude its use for the re-entry program.

Pacific Missile Range (PMR)

The Pacific Missile Range has launch capabilities for small solid propellant boosters and such boosters as Scout, and Atlas from Pt. Arguello. Vandenberg Air Force Base also has capabilities for Thor, Titan, and Atlas. In general, operational launches are made from Vandenberg, while the test launches for research and development programs are conducted from Pt. Arguello. Two impact areas are frequently utilized. These are in the Kwajalein-Eniwetok area 4400 nautical miles down range, and in the area north and east of Hawaii at 2000 nautical miles down range. The smaller boosters can be launched from Point Mugu making use of down-range facilities on San Nicolas Island, 55 nautical miles down range from Pt. Mugu. Figure 59 shows the ranges used by medium and longer range vehicles.

Down-range facilities in the Kwajalein-Eniwetok area include an extensive radar network and telemeter coverage. These facilities are supplemented by ships and aircraft. Optical equipment is currently installed at Kwajalein, but is not presently available in either the instrumented ships or aircraft. This equipment could be added for specific tests. The PMR operates 6 instrumented ships and 6 instrumented aircraft. Table 11 gives a general review of the optical, radar, and telemetering capabilities.

There is a potential for piggy-back operations on Atlas experimental or development launches from Pt. Arguello. Such operations would require approval and coordination from AF headquarters at Norton Air Force Base. The possibility also exists for conducting flight test piggy-back on an



1

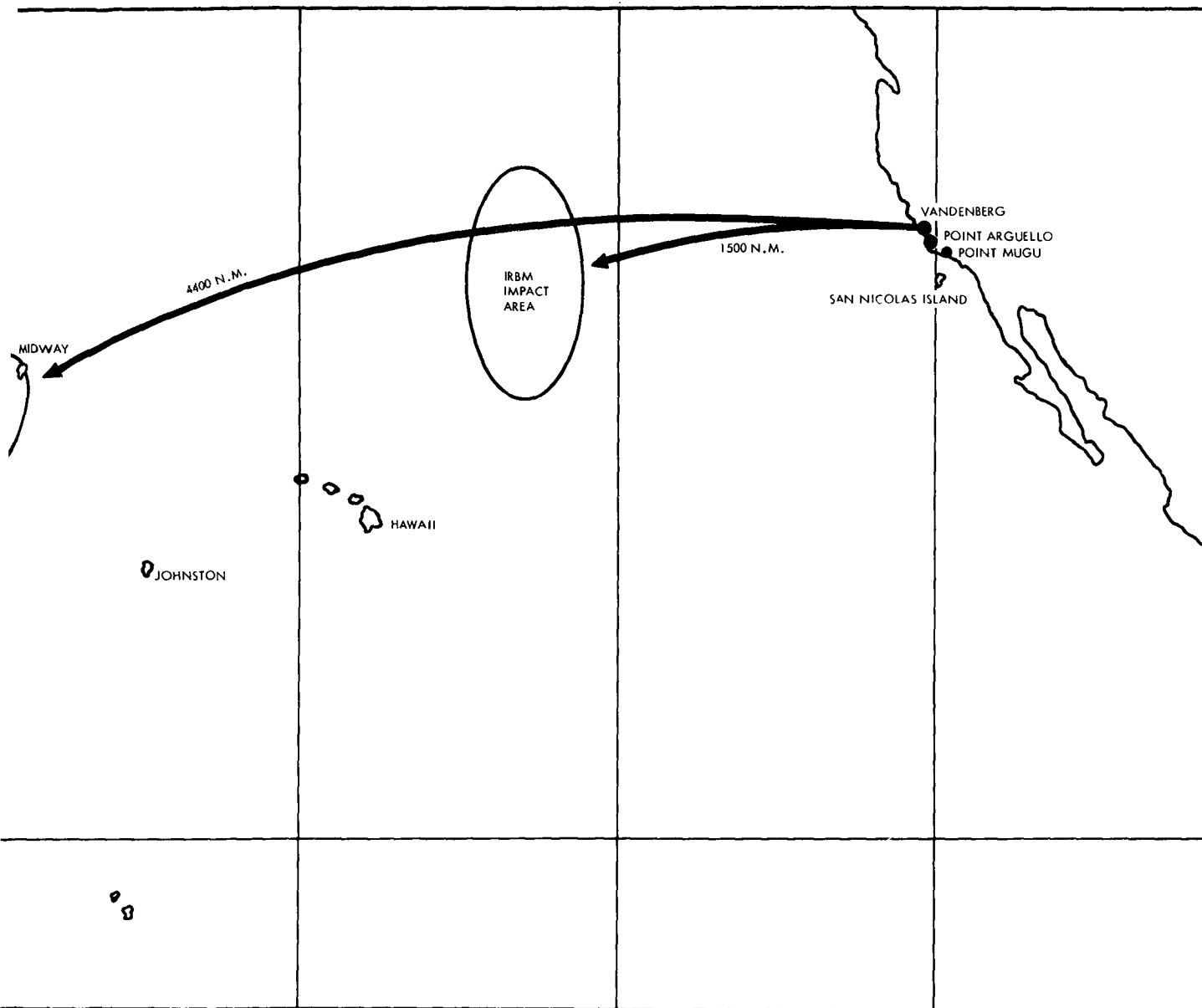


Figure 59. Pacific Missile Range

Table 11. Pacific Missile Range Down-Range Instrumentation

Station	Radar					Telemetering	MILS	Ballistic Cameras
	APS-20E	SPS-29	SPQ-8A	FPS-16	Cubic Agave			
Point Arguello				X		X		X
San Nicholas Island				X		X		X
Kaneohe							X	
Kokee Park, Kauai				X		X		
Barking Sands, Kauai						X		
South Point, Hawaii						X		
Canton Island						X		
Kwajalein*						X		X
Wake Island							X	
Midway Island							X	
Eniwetok							X	X
USNS Range Tracker				X	X	X		
USNS Longview		X	X			X	X	
USNS Richfield					X	X		
USNS Sunnyvale		X				X	X	
USNS Watertown			X		X	X		
USNS Huntsville			X		X	X		
Instr Aircraft (6)	X							
*Zeus Radar System, Target Track Radar, and Tradex.								

operational Atlas or Titan vehicle from Vandenberg; however, scheduling could become a serious problem.

The PMR is located to permit southward polar launches; however, there is no down-range instrumentation which could be utilized for the NAP re-entry tests.

Wallops Station

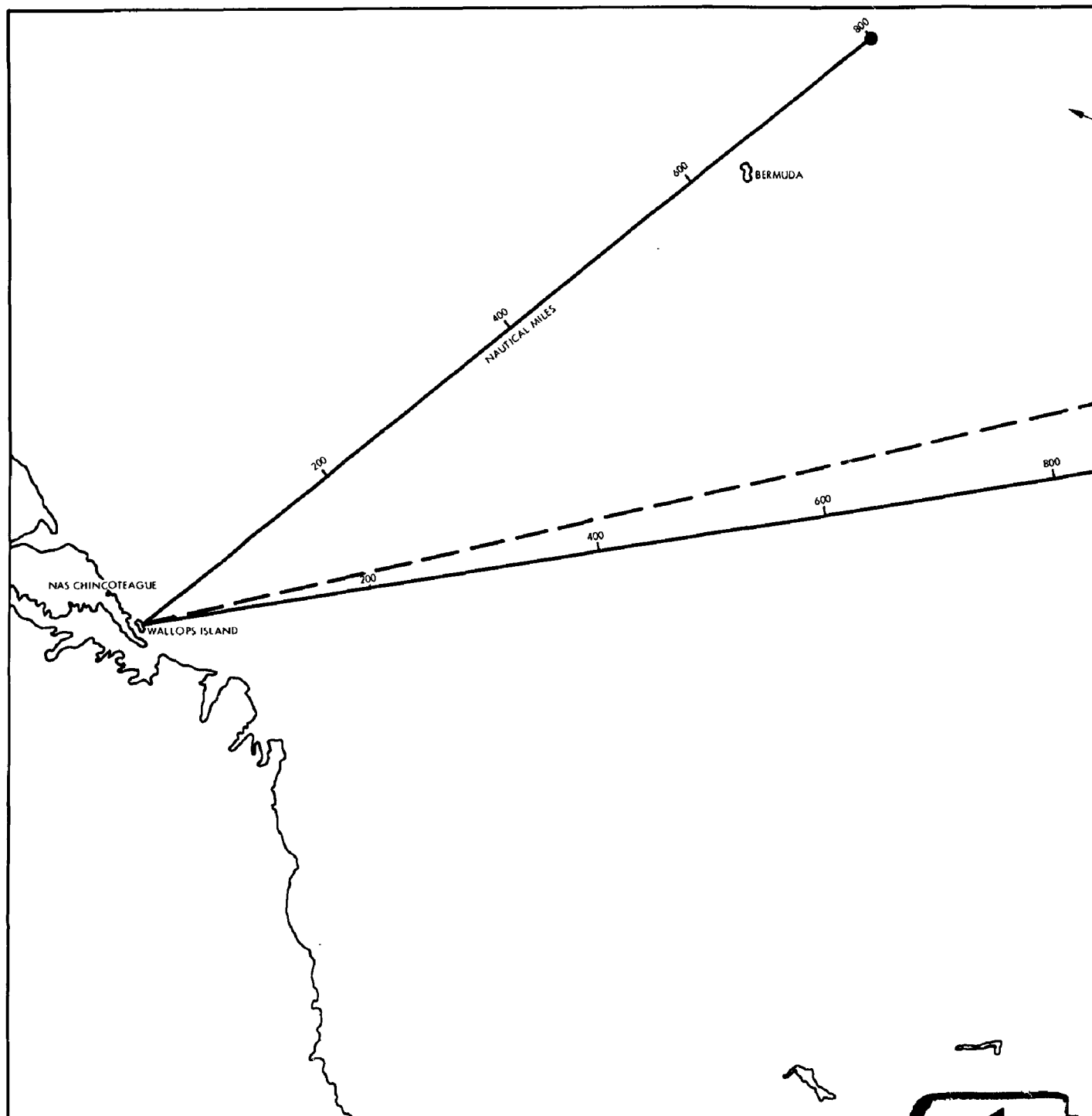
Launch and tracking facilities are maintained at Wallops Station by NASA. These facilities include capability to launch the Scout and Little Joe vehicles. Other launch capabilities do not appear to be applicable to NAP re-entry tests.

The Mercury tracking station located at Bermuda is available for limited support of Wallops Station activities. This station, when not engaged in Project Mercury support, will be able to provide down-range radar, telemetry, command-destruct services, and furnish real-time computing services. The Bermuda station is 625 NM from the launch point at Wallops Island.

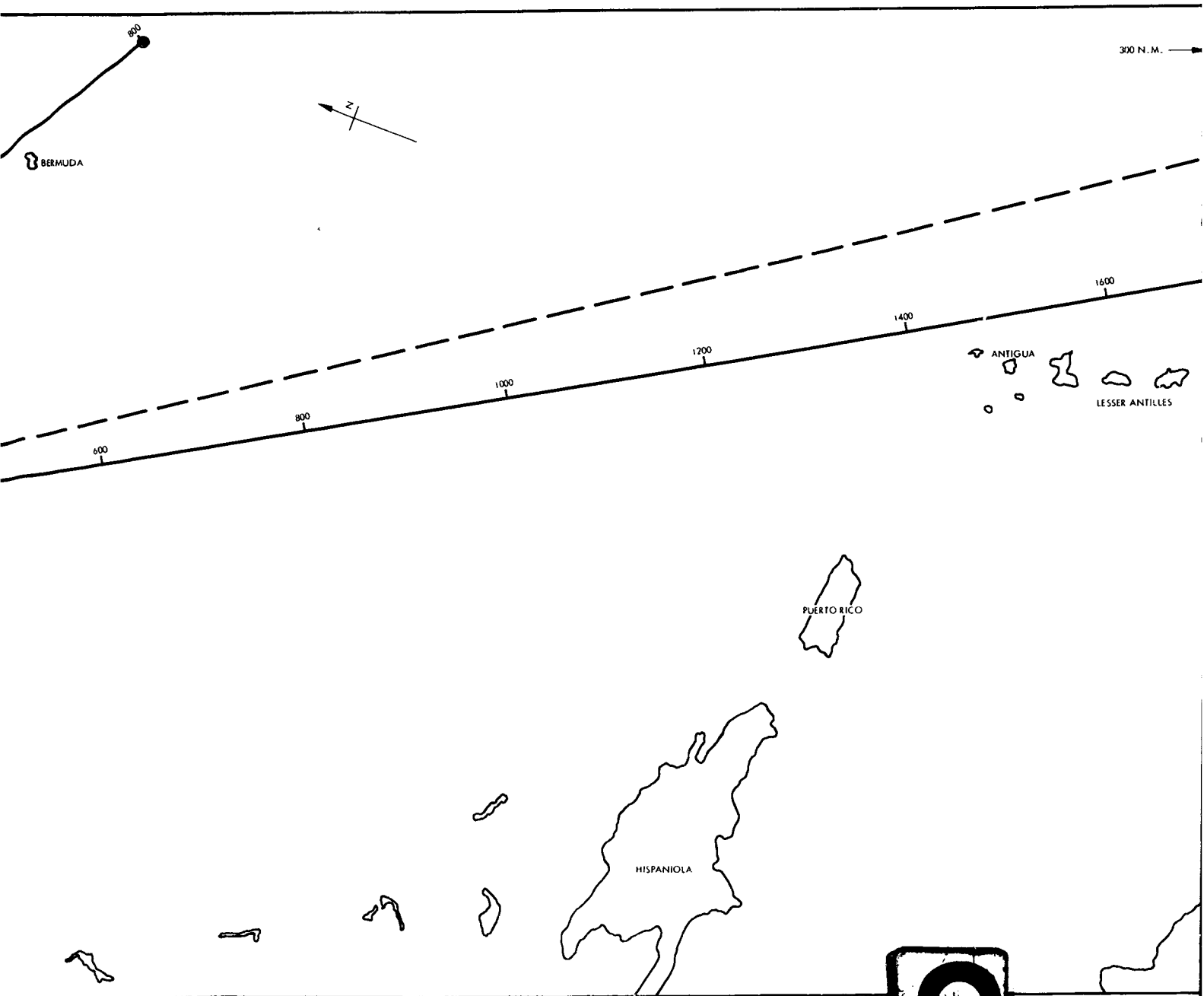
A possible alternate trajectory from Wallops could utilize the AMR down-range facilities located at Antigua. The presence of radiometer equipment, FPS-16 radar and optics, would make Antigua more desirable than Bermuda as a down-range site. The two ranges are shown in Figure 60. A splash area with a 200 nautical mile radius is shown with its center at A. The trajectory with impact at A would bring the flight path close enough to Antigua to utilize its instrumentation effectively. A splash area with a radius of 300 nautical miles is shown with its center at B. A trajectory with impact at B would be approximately 100 nautical miles further from Antigua. This would impose limitations on the usefulness of the facilities there because of instrumentation range limitations. Present indications are that the range and trajectory are feasible with the Scout vehicle from a performance standpoint; however, adequate range safety may require improved guidance capability to avoid possible impact on South America or one of the Caribbean islands.

Weapons Research Establishment (WRE), Adelaide, Australia

The Australian WRE provides a test range overland approximately 1000 nautical miles long. The launch site is located about 26 miles northwest of Woomera. Woomera is also the location of instrumentation facilities including the telemetering receiving station, radio control, and range safety. An FPS-16 radar is located 22 miles northeast of the launch area; a second FPS-16 radar is located about 110 miles down range. A meteorological station is maintained at Giles Station 600 miles down range. An emphasis is placed on optical instrumentation because of the favorable weather conditions. The northwest coast impact zone indicated in Figure 61 was used by the



1



2

Figure

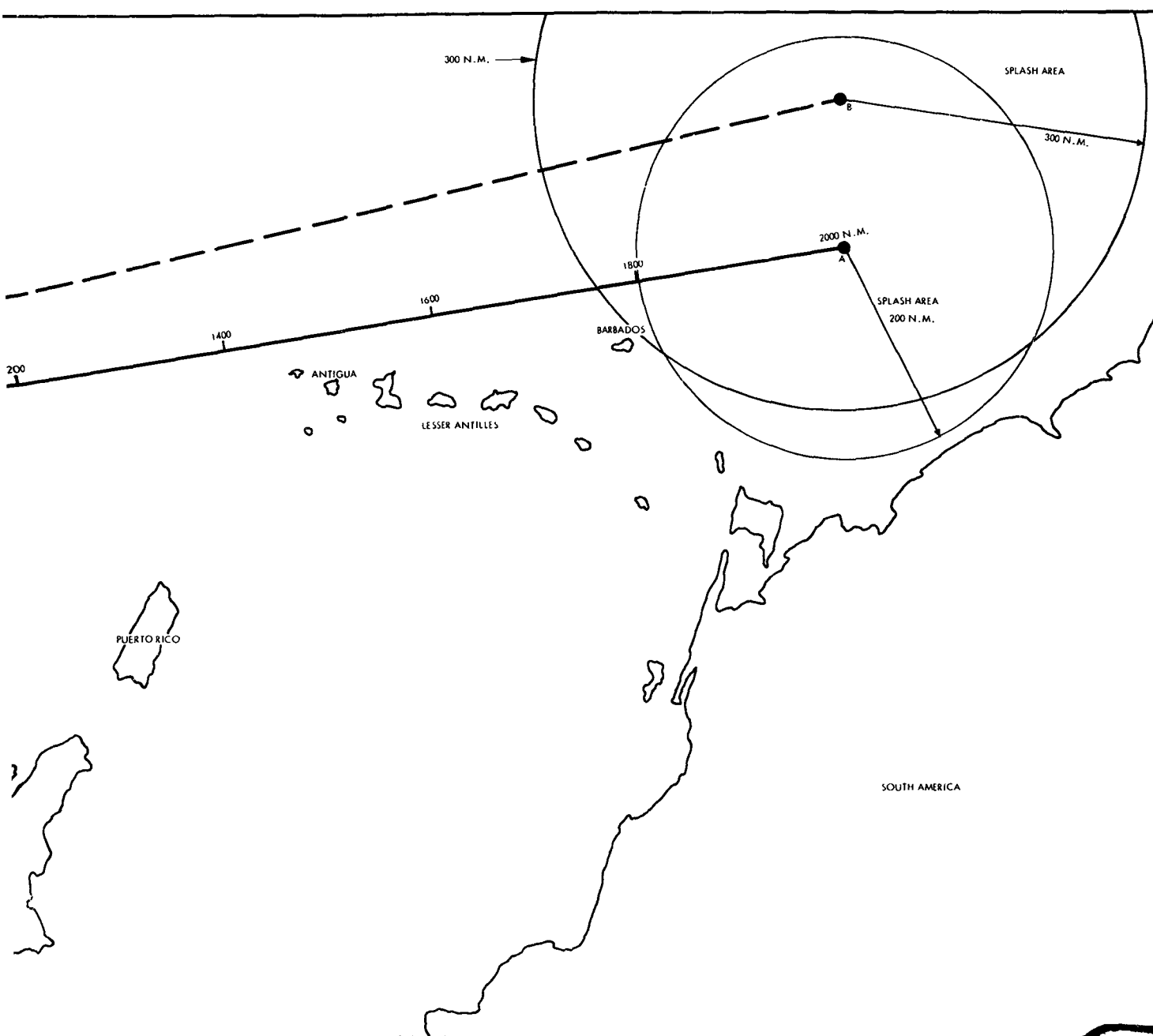
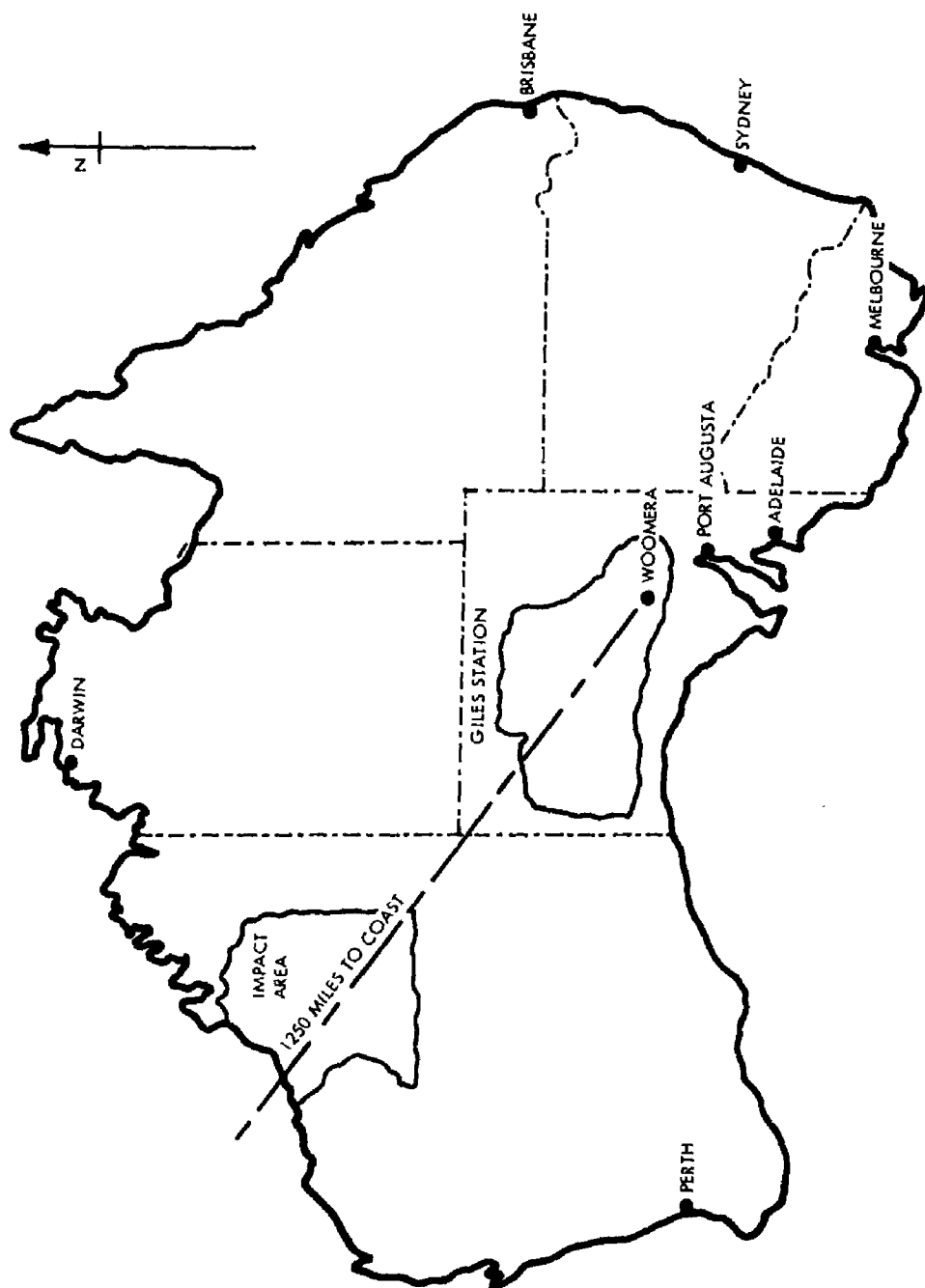


Figure 60. Range Utilization With Wallops Island Launch



British IRBM (Blue Streak). This range does not have capability for Scout launching at the present time.

White Sands Missile Range

The White Sands Range has been utilized for testing of limited-range missiles for some time. The range length is approximately 200 miles and provides limited area for land recovery. The short range precludes its use in the re-entry burnup program.

A summary of suitable flight test range capabilities is shown in Table 12.

RANGE REQUIREMENTS FOR TESTS

There will be requirements for receiving and recording the transmitted telemetering signal during the re-entry. This will include the playback portion at the end of the re-entry trajectory following the black-out period. The range of the telemetering receivers is 300 nautical miles. For practical considerations, this means these receivers can be up to 600 nautical miles apart with the exception of the impact area where the range becomes more limited.

Each station with ballistic cameras BC-4 or equivalent, Model R12-H2 radiometers or equivalent can cover a radius of 150 nautical miles. This requires that this equipment be located at approximately 300 nautical mile intervals. FPS-16 or equivalent radar has a range up to 500 miles. Representative radar coverage for the re-entry portion of the flight is shown in Figure 62. The range of the SPG-56 radar used for particle measurements will have a range which is dependent upon the actual size of particle measured and the density of the particles. These ranges are indicated in Figure 47. Representative radar coverage for the re-entry of the flight is shown in Figure 62. As an example for a particle size of 100-micron diameter and a particle-cloud density of 10^{-8} gm/cc, the range is 100 nautical miles.

The range of required coverage for the various types of instrumentation is shown in Figure 63 as a function of re-entry altitude. Complete coverage by all types of instrumentation for the re-entry phase (300,000 feet and below) is not required. Radiometer equipment coverage is required only for that portion of the re-entry where sufficient aerodynamic heating is present to result in detectable radiation. A similar situation exists for the optical and particle measurements. The actual horizontal distance will differ depending on the re-entry angle.

Table 12. Range Capabilities

Range	Launch Site	Launch* Capability	Instrumentation Range Length	Down Range Instrumentation	Remarks
Atlantic Missile Range	Cape Canaveral	Atlas Thor Titan Blue Scout	1200 NM to Antigua 4400 NM to Ascension	Excellent coverage by fixed stations to Antigua and at Ascension supplemented by ships with instrumentation meeting requirements, also aircraft with optical capabilities.	Crowded schedule; good coverage first 1200 to 1500 NM, and at 4400 NM
Pacific Missile Range	Point Arguello	Atlas Scout	2000 NM to Hawaii 4000 NM to Eniwetok-Kwajalein	Existing impact area near Hawaii would require mobile instrumentation. Available mobile equipment has limited capabilities.	Long range only
Wallops Station	Vandenberg Air Force Base	Atlas Thor Titan		Impact in Eniwetok-Kwajalein area covered with some optical equipment and extensive radar system.	
	Wallops Island	Scout Little Joe	625 NM to Bermuda 1400 NM to Antigua	Trajectory over Bermuda would allow use of Mercury station there. Most data would require ARIS from AMR. Trajectory over Antigua would make use of facilities there and would also require ARIS from AMR.	Good for 500 to 800 NM or possible 1400-1900 NM
Weapons Research Establishment	Woomera Australia	No Facilities for Scout	Approximately 1000 NM over land	Tracking stations first 600 miles. Emphasis on optical tracking systems.	Logistics difficult
*Includes only boosters considered for NAP re-entry tests.					

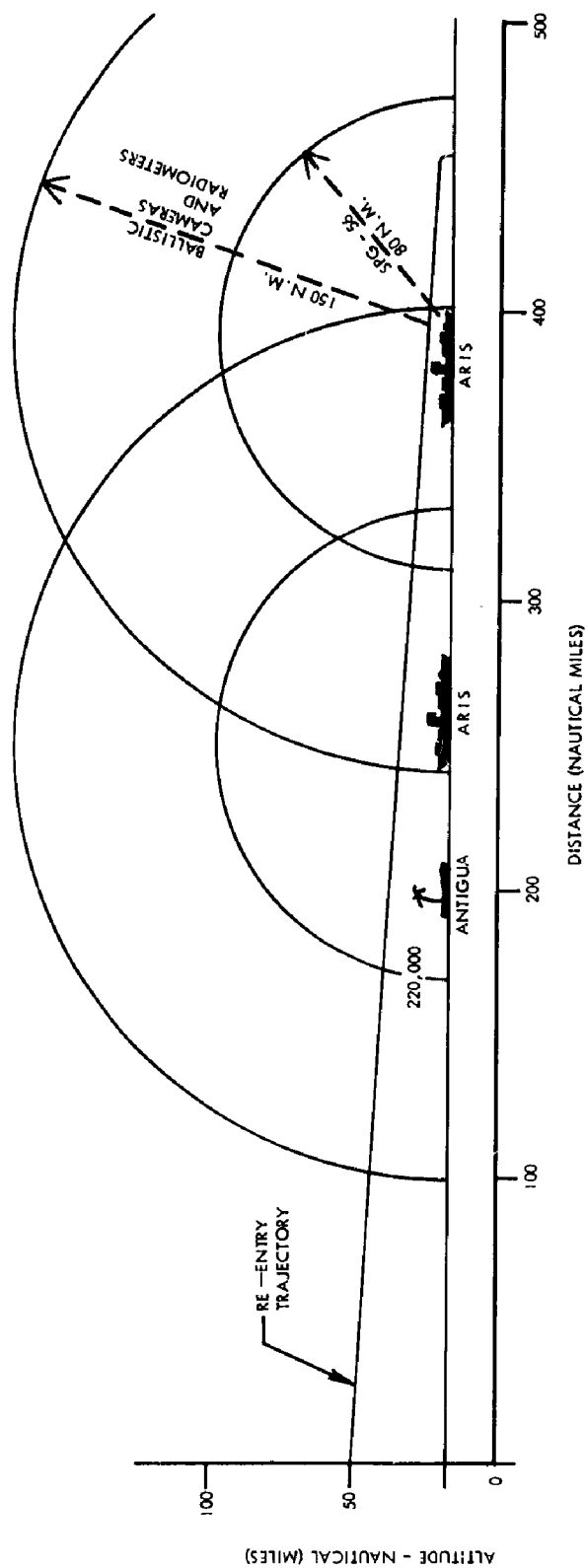


Figure 62. Horizontal Distance Travelled
from 300,000-Foot Re-entry

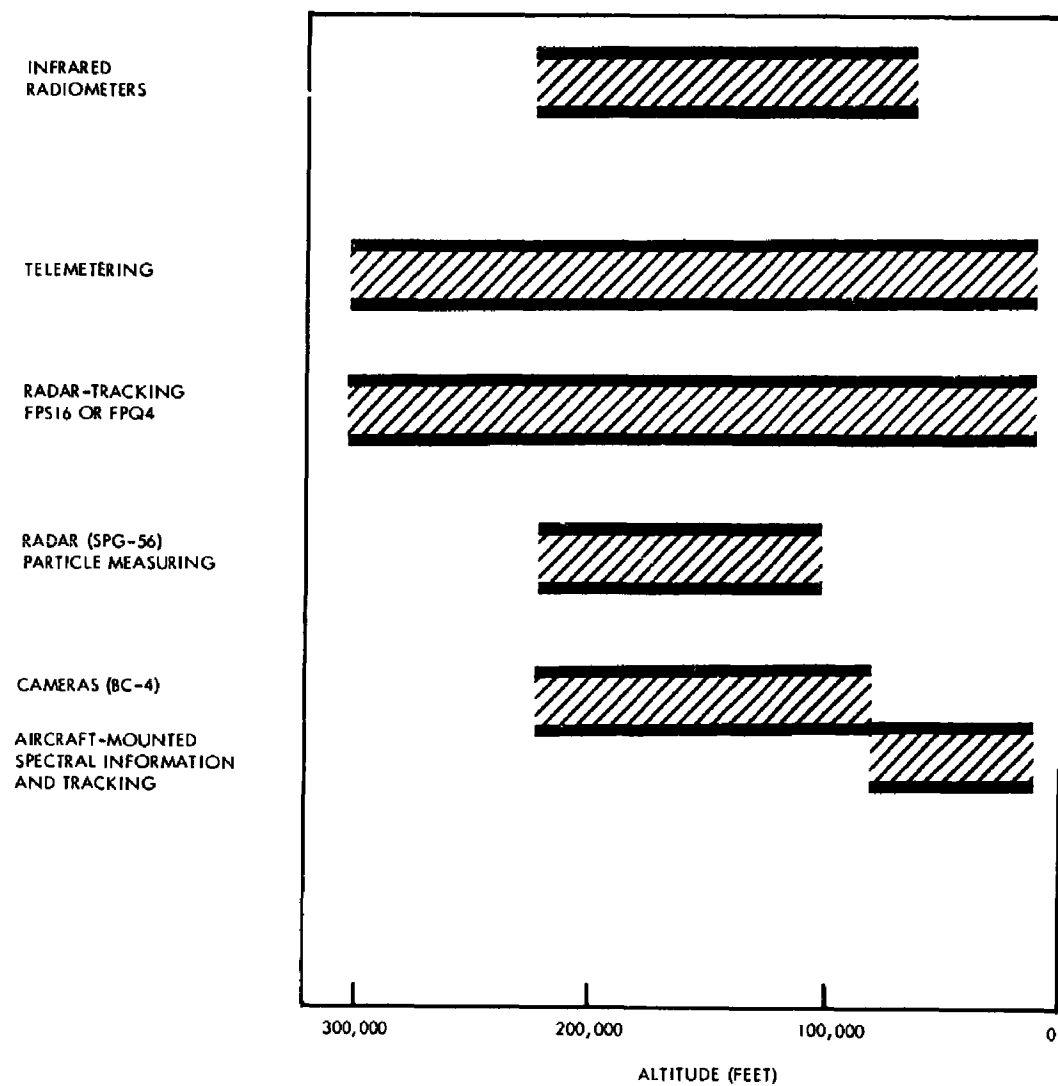


Figure 63. Required Instrumentation Coverage During Re-entry

POSSIBLE RANGE UTILIZATION

The requirements for the SPG-56 and FPS-16 radars (or equivalent), and optical equipments used for particle measurements and tracking place restrictions on the use of the PMR as the test range when utilizing the Scout as the launch vehicle. This range does not have land-based coverage in the Scout impact area, and the mobile equipment does not meet the requirements indicated by Table 10.

The availability of Advanced Range Instrumentation Ships would be an important factor in satisfying the instrumentation requirements. The availability of ships and aircraft with optical, radiometer as well as telemetering equipment at AMR is also an important consideration.

The Scout vehicle will be adaptable to range lengths from a minimum of about 700 nautical miles up to 2000 nautical miles. The programming of the boost phases will depend upon the availability or placement of downrange instrumentation. Figure 64 shows three possible ranges as well as launch and re-entry capabilities. The actual distance requiring instrumentation coverage will depend upon re-entry angle and velocity. In the case of a trajectory over Bermuda, it would be important to keep this distance at a minimum because of the lack of land-based facilities except for one point. Bermuda presnets the only down-range impact safety considerations. The trajectory must be chosen to preclude either the test package or booster stages impacting on the island.

A launch from Wallops over Antigua must utilize a re-entry angle which would give a re-entry phase range length of 550 nautical miles to make use of the facilities at Antigua and also give an impact south of Barbados (1900-2000 nautical miles down range from launch). The feasibility of this trajectory would depend upon the ability to meet range safety requirements with regard to the impact point. As previously pointed out in Figure 60, the advantages of this range (with regard to using land based instrumentation) will depend upon the splash area required.

A launch from Cape Canaveral will be limited to use of down-range facilities at Antigua as far as down-range data acquisition is concerned. A splash area with a 200 nautical mile radius places the optimum splash point 200 nautical miles east and slightly south of Antigua. This would place the trajectory approximately 80 to 100 nautical miles from Antigua at the closest point. Re-entry angles and velocities giving a minimum re-entry phase distance of 400-450 miles would effectively utilize the Antigua facilities and result in reducing the requirements for mobile instrumentation.

The impact points for each of the booster stages must be considered for all launches. Safety requirements dictate that all expended booster stages,

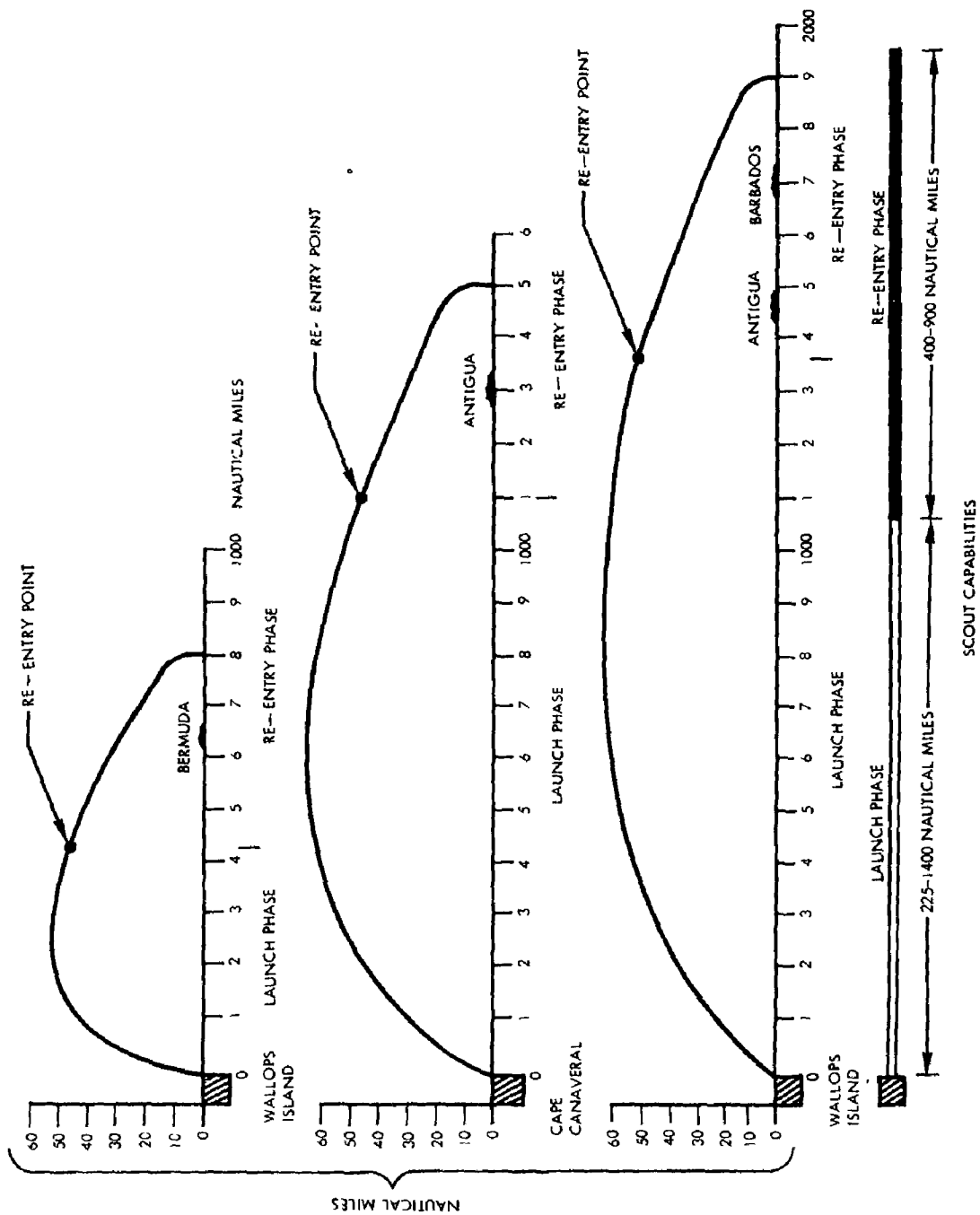


Figure 64. Possible Range Profiles

shrouds, and debris fall into uninhabited areas. This normally requires a sea impact point for each item. Due to the wide tolerance of predicted impact points of falling objects, this fallout clearance requirement can impose range restrictions.

RELIABILITY OF TEST RESULTS

OVERALL RELIABILITY

The test results obtained from any flight test operation must be carefully reviewed to determine what reliance can be placed on their validity and applicability to the NAP re-entry and disposal phenomena. The reliability analysis must include consideration of data in at least three categories:

Analysis Factors Affecting Experiment Design

Certain confidence can be placed in the results from flight tests under review, based on the accuracy of basic data and the analytical methods employed for the design of these experiments. Most of these factors are ones affecting the thermodynamic analysis.

Flight-Test Factors Affecting Experiment Performance

A particular degree of confidence can be estimated for the test results based on the effect that various parameters have on the data obtained during flight tests. These parameters are primarily ones related to the aerodynamic characteristics of the test trajectory.

Test Operation Factors Affecting Event Sequence and Test Data Acquisition

This is the normal mission-reliability analysis for the system used and the operation exercised during the flight test.

The overall reliability of the test results will be the combined effect of all these factors. Thus a reliability value may be predicted for any test flight operation under review and in addition, an estimate for the confidence in the data which may be obtained from these experiments. The values for both confidence and reliability are comparative in nature and offer a means to judge the validity of test results.

CONFIDENCE OF DESIGN ANALYSIS

Fuel Element

Information currently available on the physical constants of the fuel element materials is questionable. A study is now being conducted by Armour Research Foundation to evaluate properties in the range of temperatures above about 1200 F.

The data used in the S&ID studies were obtained from Atomics International and from the manufacturer, in the case of the cladding material. Extrapolation of data to the high temperatures of melting and ablation was necessary for this analysis, and was done according to best judgment.

The values shown in Table 13 were used in the computations.

Table 13. Material Properties of Fuel Elements

Symbol	ZrH Rod	Hastelloy N Cladding	Units
K Conductivity	0.301×10^{-3}	0.13×10^{-3}	BTU/In./ Sec/ °F
C Specific Heat	0.18	0.095	BTU/Lb/ °F
ρ Density	0.2168	0.317	LB/In. ³
Ta Ablation Temp	4000	2900	Deg Fahrenheit
Qa Heat of Ablation	540	1500	BTU/Lb
ϵ Emissivity	0.6	0.6	

The values of specific heat, conductivity and density of the cladding represent the only data which were available; it is not known for which temperature range these values are valid. Additional data were received on the properties of the fuel element after the computations were completed. These data show the variation in material properties as a function of temperature and Zr-H ratio, up to about 900 C. The values given in the table lie within the range of variation.

A value of 0.3 was given for the emissivity of the fuel element but, in view of experience with other materials, it was felt that this was the low temperature value. As emissivity generally increases with temperature, a value of 0.6 was used. This is certainly not correct since considerations of "poisoning" and structural requirements would be among the primary considerations in designing cladding for various fuel element diameters.

Computer Analysis

The computer program used for the analysis of fuel element heat transfer and ablation does not inherently include a means of accounting for these quantities. A program for two-dimensional heat flow from a distributed source was used for heat conduction up to the melting temperature of the material in question (cladding or fuel element), and these solutions were then the input for a one-dimensional heat flow program including heat of ablation. Actually, two-dimensional heat flow continues during fusion and ablation and would yield a larger value of temperature difference between leading and trailing edge of the rod than obtained with a one-dimensional solution. Judgment was exercised in estimating a temperature difference between that obtained by the combined solution described above and the two-dimensional solution without including ablation factors. This result is shown in Figure 65.

Simplifying Assumptions

Certain simplifying assumptions were made in adapting the heat transfer problems to the computer programs. Radiant heat transfer to space was assumed, i.e. the effect of decreased radiant interchange with the earth was neglected. Heat flux values were based on a constant wall temperature of 4000 R. Actual temperature varies from some value above 200 F at entry.

The most uncertainty lies in the values selected for the heat and temperature of ablation. These were arbitrarily assumed to lie between the heats, and temperature, of fusion and vaporization. It appears that this is a fair approximation as, in the absence of viscosity data, it cannot be assumed that the material will be swept away immediately upon the change-of-state.

Cladding

The thickness of cladding which would be used in reactor design for fuel elements of various diameters is unknown. The material and thickness used in computations concerning the nominal 1 1/4 inch fuel elements was obtained from drawings originated by Atomics International. Extrapolation of results to other fuel element diameters was made on the basis of physical

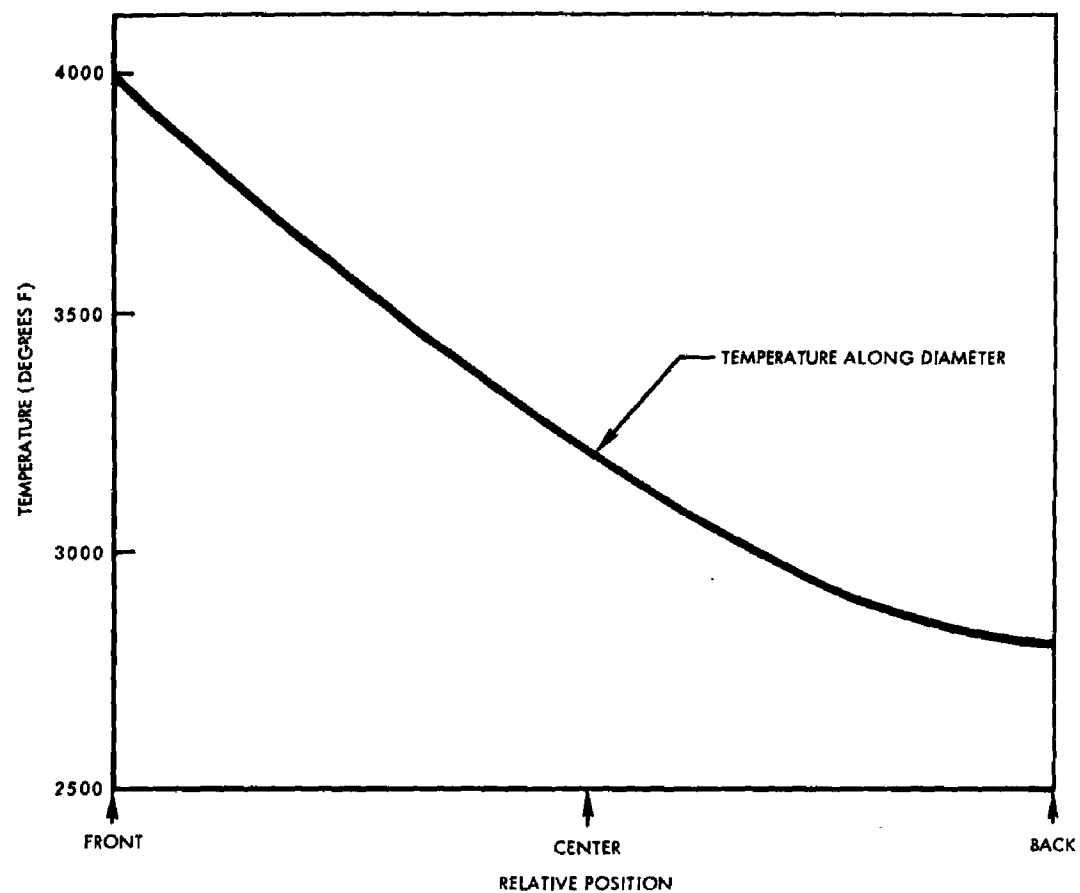


Figure 65. Fuel Element Temperature Distribution With Front Surface at Ablation Temperature

dimensions alone, which would give the same relative importance to cladding regardless of diameter. Analysis indicates that input heat flux is insensitive to a wide range of wall temperature for the conditions of this problem. Surface emissivity was assumed constant at 0.6. Actually at temperatures below about 1500 F this value is 0.3. Emissivity of metals usually increases markedly with temperature, however, so the above value was used in the absence of more precise data. Laminar flow was assumed in determining input heat flux. The precise determination of flow regime in re-entry flow is not possible at this time; however, if flow were actually turbulent, the input heat flux would increase many fold.

TRAJECTORY PARAMETERS

Trajectory parameters affect both the test-article heating characteristics and the ability of the range facilities to measure test results. These parameters and their relative importance are given below.

Re-entry Flight-Path Angle

The effect of deviations in re-entry flight path angle on the heating environment and measurement capabilities is shown in Figures 14 and 38. From Figure 14 it can be seen that an error of ± 1 degree in flight-path angle for a fixed velocity does not significantly alter the integrated heating. However, Figure 38 indicates a considerable effect on range for a given altitude or in altitude for a given range.

Re-entry Velocity

Figure 14 also shows that small errors in re-entry velocity do not have a significant effect on heating characteristics. It was further found from the study that small deviations in re-entry velocity (for example, ± 100 fps) have a negligible influence on the altitude-range profile.

Ballistic Coefficient

It was found that small deviations in $C_D A/m$ did not significantly affect the re-entry trajectory. Hence, the effect on the heating history would also be small.

Test Specimen Attitude

A tumbling attitude of the fuel rods or reactor vessel will reduce the mean heat flux in cross-flow by approximately 40 percent. Therefore, assurance must be given that some fuel elements re-enter in a cross-flow attitude and others in a tumbling attitude. Appropriate identification of attitude will be necessary to interpret data acquired from the test.

Deviations in the atmospheric composition in the re-entry corridor during tests are likely and must be determined for a control of the tests being conducted. The normal practice of the AMR is to make measurements to an altitude of 110,000 feet. Data must be obtained to approximately 300,000 feet altitude in the re-entry area to determine vertical distribution of gases during re-entry burnup experiments.

RELIABILITY OF TEST RESULTS

It is essential that the reliability of the test results be ascertained. Test capsule hardware, selected launch vehicle systems, and event control and measurement systems must all be evaluated to determine methods for estimating the overall reliability of the test program. In establishing flight test reliability, consideration must also be given to deviations in trajectory parameters. A discussion of these parameters follows.

CONFIDENCE OF TEST SIMULATION

To obtain a high degree of confidence in the test results, measurements of the important variables governing burn-up and of the important events (altitude and time of burn-up, for example) must be as complete and accurate as possible. Redundancy of information signaling devices should be included where weight limitations allow. In addition, the individual experiments must be repeated a sufficient number of times so that statistical theory can be applied. In this regard it is highly desirable to know the flight attitude of the articles being tested and to test all anticipated attitudes.

SUMMARY

Results achieved during Phase A of this study are reported in the Interim Report and will be reviewed during Phase B. Further study may alter some of the indicated conclusions so that any results or conclusions must be considered preliminary.

INTERIM CONCLUSIONS

The results of the analysis of flight test criteria have indicated the following conclusions.

The total heat input into the fuel element must duplicate the actual case, and the peak heat flux must be at least as high as that occurring during orbital decay.

Combinations of re-entry velocity and re-entry flight-path angle have been determined to duplicate total heat input of an orbital decay. It will be necessary to achieve supercircular velocities (above 24,000 feet per second) for negative re-entry angles. Higher velocities are required for larger negative re-entry angles.

A 300,000 foot re-entry altitude can be used. Exposure above 300,000 feet is not necessary since the total heat input is less than 10 percent greater for exposure at 400,000 feet than for exposure at 300,000 feet. If exposed at higher altitudes, re-entering bodies that have initial temperatures of more than 1000°F may cool before reaching 300,000 feet.

A full-scale fuel element should be used as a test specimen. The total heat required for burnup is proportional to rod diameter so that fuel elements of less than full scale will not demonstrate burnup of the actual fuel element. Specimens of larger diameter require more heat for burnup which may not be available. Any scaled fuel element specimen (larger or smaller) will present a different condition for internal heat transfer not representative of the actual fuel element.

Instrumentation system requirements for NAP re-entry tests are well within the present state-of-the-art, except for fuel-element ablation determination and particle-size measurements during free flight experiments. For these exceptions, available instrumentation is of very limited capability. Considerable research and development of equipment will be needed to meet these requirements adequately.

FLIGHT-TEST CONSIDERATIONS

The analysis conducted using the SNAP 10A system and a re-entering spacecraft with the Agena B indicates that fuel-rod burnup is unlikely. A study of the altitudes at which initial burnup is likely to start for each of the sequential events preceding fuel-element burnup shows the maximum altitude for fuel element exposure to be below 250,000 ft. A study of the minimum altitude of fuel element exposure for fuel rod burnup shows that the fuel elements must be exposed at 300,000 feet. Thus, there is a deficiency in the expected available exposure time to destroy the fuel rod. Since the fuel-element exposure at sufficiently high altitude is unlikely, the method of exposure is likely to be revised. Any test of system breakup and exposure of a particular element must necessarily be performed using that design in the test specimen. The internal heat transfer within the fuel element presents a complicated problem due to the rod shape and the change of state of the material during ablation. For these reasons it is recommended that testing be concentrated if possible on the fuel elements to verify the minimum altitude of exposure to insure fuel-rod burnup.

REFERENCES

1. W. L. Hankey, Jr., R. D. Neumann, and E. H. Flinn, "Design Procedures for Computing Aerodynamic Heating at Hypersonic Speeds," WADC Technical Report 59-610, June 1960.
2. AVCO Corporation, "Investigation of Re-entry Destruction of Nuclear Auxiliary Powerplant," AFSWC-TR-61-69, October 1961.
3. Olsen, D. C., and H. G. Webb, Jr., "Stability and Control Manual," North American Aviation Report SID 61-236, 28 August 1961.
4. F. L. Pugh, "Description of Minimum IBM-704 Mass Point Trajectory Program," AFSWC-TN-60-1, January 1960.
5. Handbook of Chemistry and Physics - Chemical Rubber Publishing Company.
6. Aeronautics and Astronautics Coordinating Board, Washington, "National Launch Vehicle Program Summary," ASTIA AD322990, 14 February 1961.
7. Senate Committee on Aeronautical and Space Sciences, "NASA Authorization for Fiscal Year 1963" H. R. 11737, June 13, 14, 15, 1962.
8. Kerr, D. E., Propagation of Short Radio Waves, McGraw-Hill, New York, Vol. 13 of Radiation Lab Series, 1951.

BIBLIOGRAPHY

Pirsa, E. F., "The Telemetry and Communication Problem of Re-entrant Space Vehicles," Proceedings of the IRE, Vol. 48, No. 4 April 1960.

Row, R. V., "Effects of Re-entry Ionization on Electromagnetic Propagation," Transactions of the National Symposium 1960 on Space Electronics and Telemetry, IRE, 1960.

Whitner, R. F., Electromagnetic Effects Associated with Hypersonic Re-entry Vehicles, Sylvania Electric Products Inc., Microwave Physics Laboratory, Palo Alto, Calif.

Technical Proposal Fire, NAA-S&ID, S&ID-62-287-1, 9 March 1962.

APPENDIX A - SYMBOLS

Except as identified otherwise, symbols used in the text mean the following:

A	Reference area for drag coefficient; also, fuel element surface or cross section
C	Specific heat (BTU/lb/°F)
C_D	Drag coefficient, $\frac{D}{qA}$
°C	Degrees Centigrade
D	Drag
°F	Degrees Farenheit
g	Gravitational acceleration
g_o	Standard gravitational acceleration, 32.174 feet/second ²
h	Geometric altitude
I_{sp}	Specific impulse
k	Proportionality factor in equation for heat transfer rate (See Equation 9)
L, l	Length
m, n, p	Constants in equation for heat transfer rate (See Equation 9)
M	Mass
p	Pressure
q	Dynamic pressure
\dot{q}	Heat transfer rate
Q	Integrated heat transfer

$^{\circ}\text{R}$	Degrees Rankine
R, r	Radius
T	Temperature
t	Time
V	Velocity
W	Weight
β	Constant used to describe variation of density with altitude in isothermal atmosphere (See Equation 4)
ρ_o	Gamma function
γ	Flight path angle
ϵ	Emissivity
λ, ϕ	Integration constants (See Equations 14 and 28)
ρ	Density
ρ	Reference density
τ	Incremental time difference
α	Angle of attack; also indicates proportionality
θ	Angle from stagnation point
σ	Stefan-Boltzmann Constant

Subscripts

A	Ablation
C	Circular
E	Re-entry conditions
f	Final
i	Initial

g_{\max}	Maximum gravitational force
L	Laminar flow
T	Turbulent flow
W	Wall

DISTRIBUTION

No. cys

HEADQUARTERS USAF

- 1 Hq USAF (AFRDC) Office, Assistant DCS/Research and Technology/AE, Wash 25, DC
- 1 USAF Dep IG for Insp (AFCDI-B-3), Norton AFB, Calif
- 1 USAF Dep IG for Safety (AFINS), Kirtland AFB, N Mex

MAJOR AIR COMMANDS

- 2 AFSC (SCCP, Director of Programs), Andrews AFB, Wash 25, DC
- 1 AUL, Maxwell AFB, Ala

AFSC ORGANIZATIONS

- 1 ASD (Aeronautical Systems Division), ATTN: ASRMFP, Wright-Patterson AFB, Ohio
- 2 RTD (RTO), Research & Technology Division, Bolling AFB, Wash 25, DC
- SSD (Space Systems Division), AF Unit Post Office, Los Angeles 45, Calif
- 1 SSTRE
- 1 SSZMS

KIRTLAND AFB ORGANIZATIONS

AFSWC, Kirtland AFB, N Mex

- 1 SWEH
- 85 SWOI
- 1 SWRP
- 2 SWVPS
- 2 SWVPF
- 1 US Naval Weapons Evaluation Facility (NWEF) (Code 404), Kirtland AFB, N Mex

OTHER AIR FORCE AGENCIES

- 6 Director, USAF Project RAND, ATTN: Miss Mary Romig, via: Air Force Liaison Office, The RAND Corporation, 1700 Main Street, Santa Monica, Calif

DISTRIBUTION (con't)

No. cys

OTHER DOD ACTIVITIES

Director, Advanced Research Projects Agency, Department
of Defense, The Pentagon, Wash 25, DC

2 Lt Col Roy Weidler
2 James E. Blower
10 ASTIA (TIPDR), Arlington Hall Sta, Arlington 12, Va

AEC ACTIVITIES

US Atomic Energy Commission, Wash 25, DC

4 DRD, Assistant Director for Compact Reactor Systems
4 DRD, Assistant Director for Nuclear Safety
1 DRD, Mr. R. L. Kirk
1 SNPO, Lt Col Ralph Decker
3 Sandia Corporation (Document Control Division for Mr. V. E.
Blake, Department 7110), Sandia Base, N Mex
US Atomic Energy Commission, Canoga Park Area Office,
P.O. Box 591, Canoga Park, Calif
1 Mr. J. Levy, Manager
1 Mr. C. Malstrom
1 University of California Lawrence Radiation Laboratory
(Technical Information Division, ATTN: Mr. Clovis Craig),
P.O. Box 808, Livermore, Calif

OTHER





1 NASA, Lewis Research Center, Cleveland, Ohio. ATTN:
Dr. Bernard Lubarsky
3 Battelle Memorial Institute, ATTN: Mr. E. L. Foster, 505
King Avenue, Columbus, Ohio
1 Institute of the Aerospace Sciences, Inc., 2 East 64th Street,
New York 21, NY
10 General Dynamics/Astronautics, ATTN: Mr. E. J. Philbin,
P. O. Box 1128, Mail Zone 596-2, San Diego 12, Calif
3 Stanford Research Institute, ATTN: Dr. Fred Littman,
Menlo Park, Calif
3 Vidya Research and Development, ATTN: Mr. W. J. Fleming,
2626 Hanover Street, Palo Alto, Calif

DISTRIBUTION (con't)

No. cys

3	Astropower, ATTN: Dr. A. E. Levy-Pascal, 2968 Randolph Avenue, Costa Mesa, Calif
3	Westinghouse Electric Corporation, Astronuclear Laboratory (ATTN: Mr. Alexander L. Feild, Jr., 250 Mt Lebanon Blvd., Pittsburgh, Pa
3	Armour Research Foundation, ATTN: Mr. Alexander Goldsmith, 10 West 35th Street, Chicago 16, Ill.
10	Space Information Systems Div., North American Aviation, Inc. ATTN: Mr. Mark Morris, Department 468, 12214 Lakewood Blvd., Downey, Calif
3	General Technology Corp., ATTN: Mr. J. D. Graves, 2302 Willowood Lane, Alexandria, Va
3	AVCO Corp., ATTN: Dr. J. G. Lundholm, 201 Lowell Street, Wilmington, Mass
6	Aerospace Corp., (Library Tech Documents Group, ATD 61-5720 Technical Information Center), P.O. Box 95085, Los Angeles, Calif
6	Atomics International ATTN: Mr. R. L. Determan, 8900 DeSoto Avenue, Canoga Park, Calif
2	Aerojet-General Nucleonics, ATTN: Mr. J. P. Lehman, Fostoria Way, San Ramon, Calif
1	Official Record Copy (SWVPF, Mr. J. J. Ungvarsky)

<p>Air Force Special Weapons Center, Kirtland AF Base, New Mexico Rpt. No. AFSWC-TDR-62-83. FLIGHT TEST CRITERIA FOR RE-ENTERING MAP SYSTEM. Nov 62, p, incl illus., tables, 8 refs.</p> <p>Unclassified Report</p> <p>This interim report covers Phase A of the Flight Test Criteria Study which will determine criteria that can be used as guidelines in setting up a flight test program or in judging one that has been proposed. This study is intended to be universal in application to MAP re-entry phenomena. The SNAP 10A was designated to provide a representative system for study. The various parameters considered and topics discussed in this report include orbital decay and thermodynamic data, scaling, instrumentation, launch vehicles and sites, and reliability. Significant</p>	<ol style="list-style-type: none"> 1. Blackout 2. Blue Scout Junior 3. Flight testing 4. Heat transfer 5. Missile launchers 6. NAP 7. Radiation hazards 8. Re-entry 9. Reliability studies 10. Scaling laws 11. SNAP I. AFSC Project 1831, Task 183103 II. Contract AF 29(601)5104 III. North American Aviation, Inc., Space and Information Systems Div., Downey, Calif IV. In ASTIA collection 	<p>Air Force Special Weapons Center, Kirtland AF Base, New Mexico Rpt. No. AFSWC-TDR-62-83. FLIGHT TEST CRITERIA FOR RE-ENTERING MAP SYSTEM. Nov 62, p, incl illus., tables, 8 refs.</p> <p>Unclassified Report</p> <p>This interim report covers Phase A of the Flight Test Criteria Study which will determine criteria that can be used as guidelines in setting up a flight test program or in judging one that has been proposed. This study is intended to be universal in application to MAP re-entry phenomena. The SNAP 10A was designated to provide a representative system for study. The various parameters considered and topics discussed in this report include orbital decay and thermodynamic data, scaling, instrumentation, launch vehicles and sites, and reliability. Significant</p>	<ol style="list-style-type: none"> 1. Blackout 2. Blue Scout Junior 3. Flight testing 4. Heat transfer 5. Missile launchers 6. NAP 7. Radiation hazards 8. Re-entry 9. Reliability studies 10. Scaling laws 11. SNAP I. AFSC Project 1831, Task 183103 II. Contract AF 29(601)5104 III. North American Aviation, Inc., Space and Information Systems Div., Downey, Calif IV. In ASTIA collection
<p>Air Force Special Weapons Center, Kirtland AF Base, New Mexico Rpt. No. AFSWC-TDR-62-83. FLIGHT TEST CRITERIA FOR RE-ENTERING MAP SYSTEM. Nov 62, p, incl illus., tables, 8 refs.</p> <p>Unclassified Report</p> <p>This interim report covers Phase A of the Flight Test Criteria Study which will determine criteria that can be used as guidelines in setting up a flight test program or in judging one that has been proposed. This study is intended to be universal in application to MAP re-entry phenomena. The SNAP 10A was designated to provide a representative system for study. The various parameters considered and topics discussed in this report include orbital decay and thermodynamic data, scaling, instrumentation, launch vehicles and sites, and reliability. Significant</p>	<ol style="list-style-type: none"> 1. Blackout 2. Blue Scout Junior 3. Flight testing 4. Heat transfer 5. Missile launchers 6. NAP 7. Radiation hazards 8. Re-entry 9. Reliability studies 10. Scaling laws 11. SNAP I. AFSC Project 1831, Task 183103 II. Contract AF 29(601)5104 III. North American Aviation, Inc., Space and Information Systems Div., Downey, Calif IV. In ASTIA collection 	<p>Air Force Special Weapons Center, Kirtland AF Base, New Mexico Rpt. No. AFSWC-TDR-62-83. FLIGHT TEST CRITERIA FOR RE-ENTERING MAP SYSTEM. Nov 62, p, incl illus., tables, 8 refs.</p> <p>Unclassified Report</p> <p>This interim report covers Phase A of the Flight Test Criteria Study which will determine criteria that can be used as guidelines in setting up a flight test program or in judging one that has been proposed. This study is intended to be universal in application to MAP re-entry phenomena. The SNAP 10A was designated to provide a representative system for study. The various parameters considered and topics discussed in this report include orbital decay and thermodynamic data, scaling, instrumentation, launch vehicles and sites, and reliability. Significant</p>	<ol style="list-style-type: none"> 1. Blackout 2. Blue Scout Junior 3. Flight testing 4. Heat transfer 5. Missile launchers 6. NAP 7. Radiation hazards 8. Re-entry 9. Reliability studies 10. Scaling laws 11. SNAP I. AFSC Project 1831, Task 183103 II. Contract AF 29(601)5104 III. North American Aviation, Inc., Space and Information Systems Div., Downey, Calif IV. In ASTIA collection

<p>among the interim conclusions reached is the determination that a 300,000-foot re-entry altitude can be used.</p> 		<p>among the interim conclusions reached is the determination that a 300,000-foot re-entry altitude can be used.</p> 	
<p>among the interim conclusions reached is the determination that a 300,000-foot re-entry altitude can be used.</p> 		<p>among the interim conclusions reached is the determination that a 300,000-foot re-entry altitude can be used.</p> 	

<p>Air Force Special Weapons Center, Kirtland AF Base, New Mexico</p> <p>Rpt. No. AFSCW-TDR-62-83. FLIGHT TEST CRITERIA FOR RE-ENTERING MAP SYSTEM. Nov 62, p, incl illus., tables, 8 refs.</p> <p>Unclassified Report</p> <p>This interim report covers Phase A of the Flight Test Criteria Study which will determine criteria that can be used as guidelines in setting up a flight test program or in judging one that has been proposed. This study is intended to be universal in application to MAP re-entry phenomena. The SNAP 10A was designated to provide a representative system for study. The various parameters considered and topics discussed in this report include orbital decay and thermodynamic data, scaling, instrumentation, launch vehicles and sites, and reliability. Significant</p>	<ol style="list-style-type: none"> 1. Blackout 2. Blue Scout Junior 3. Flight testing 4. Heat transfer 5. Missile launchers 6. MAP 7. Radiation hazards 8. Re-entry 9. Reliability studies 10. Scaling laws 11. SNAP <ol style="list-style-type: none"> I. AFSC Project 1831, Task 183103 II. Contract AF 29(601)5104 III. North American Aviation, Inc., Space and Information Systems Div., Downey, Calif IV. In ASTIA collection
<p>Air Force Special Weapons Center, Kirtland AF Base, New Mexico</p> <p>Rpt. No. AFSCW-TDR-62-83. FLIGHT TEST CRITERIA FOR RE-ENTERING MAP SYSTEM. Nov 62, p, incl illus., tables, 8 refs.</p> <p>Unclassified Report</p> <p>This interim report covers Phase A of the Flight Test Criteria Study which will determine criteria that can be used as guidelines in setting up a flight test program or in judging one that has been proposed. This study is intended to be universal in application to MAP re-entry phenomena. The SNAP 10A was designated to provide a representative system for study. The various parameters considered and topics discussed in this report include orbital decay and thermodynamic data, scaling, instrumentation, launch vehicles and sites, and reliability. Significant</p>	<ol style="list-style-type: none"> 1. Blackout 2. Blue Scout Junior 3. Flight testing 4. Heat transfer 5. Missile launchers 6. MAP 7. Radiation hazards 8. Re-entry 9. Reliability studies 10. Scaling laws 11. SNAP <ol style="list-style-type: none"> I. AFSC Project 1831, Task 183103 II. Contract AF 29(601)5104 III. North American Aviation, Inc., Space and Information Systems Div., Downey, Calif IV. In ASTIA collection

among the interim conclusions reached is the determination that a 300,000-foot re-entry altitude can be used.		among the interim conclusions reached is the determination that a 300,000-foot re-entry altitude can be used.	
among the interim conclusions reached is the determination that a 300,000-foot re-entry altitude can be used.		among the interim conclusions reached is the determination that a 300,000-foot re-entry altitude can be used.	